Fisheries and Oceans Canada | Pêches et Océans Canada
Ecosystems and Oceans Science | Sciences des écosystèmes et des océans

Canadian Science Advisory Secretariat (CSAS)

Research Document 2025/026

Maritimes Region

Calibration of Bottom Trawl Survey Vessels: Re-analysis of Comparative Fishing Experiment Between the CCGS *Alfred Needler* and CCGS *Teleost* on the Scotian Shelf and Bay of Fundy in 2005

Yihao Yin[1], Hugues Benoît[2] and Ryan Martin[3]

Fisheries and Oceans Canada
[1]Bedford Institute of Oceanography
Fisheries and Oceans Canada
1 Challenger Drive
Dartmouth, NS B2Y 4A2

[2]Maurice Lamontagne Institute
Fisheries and Oceans Canada
850 Rte de la Mer
Mont Joli, QC G5H 3Z4

[3]St. Andrews Biological Station
Fisheries and Oceans Canada
125 Marine Science Drive
St. Andrews, NB, E5B 0E4

August 2025

Canada

Foreword

This series documents the scientific basis for the evaluation of aquatic resources and ecosystems in Canada. As such, it addresses the issues of the day in the time frames required and the documents it contains are not intended as definitive statements on the subjects addressed but rather as progress reports on ongoing investigations.

Published by:

Fisheries and Oceans Canada
Canadian Science Advisory Secretariat
200 Kent Street
Ottawa ON K1A 0E6

http://www.dfo-mpo.gc.ca/csas-sccs/
DFO.CSAS-SCAS.MPO@dfo-mpo.gc.ca

ISSN 1919-5044
ISBN 978-0-660-76843-4 Cat. No. Fs70-5/2025-026E-PDF

Correct citation for this publication:

Yin, Y., Benoît, H., and Martin, R. 2025. Calibration of Bottom Trawl Survey Vessels: Re-analysis of Comparative Fishing Experiment Between the CCGS *Alfred Needler* and CCGS *Teleost* on the Scotian Shelf and Bay of Fundy in 2005. DFO Can. Sci. Advis. Sec. Res. Doc. 2025/026. iv + 171 p.

Aussi disponible en français :

Yin, Y., Benoît, H. et Martin, R. 2025. Étalonnage des navires de relevé au chalut de fond : réanalyse de l'expérience de pêche comparative menée entre le NGCC Alfred Needler *et le NGCC* Teleost *sur le plateau néo-écossais et dans la baie de Fundy en 2005. Secr. can. des avis sci. du MPO. Doc. de rech. 2025/026. iv + 171 p*.

TABLE OF CONTENTS

ABSTRACT

Bottom-trawl surveys provide key inputs to stock assessments for groundfish stocks and other taxa, for ecosystem monitoring and reporting, and for research. These surveys can produce annual indices of abundance that are proportional to stock size, provided that the proportionality constant, typically called catchability, does not change over time. This is typically achieved through the use of standardized survey design and procedures. In the Maritimes Region, Fisheries and Oceans Canada (DFO) conducted an annual Summer Ecosystem Research Vessel Survey of the Scotian Shelf and Bay of Fundy employing the Canadian Coast Guard Ship (CCGS) *Alfred Needler* from 1982 to 2023 but due to repairs, the survey was completed by the CCGS *Teleost* instead in 2007, 2018, 2022 and 2023. The two vessels used the same protocol, but there were differences in vessel characteristics. In order to test potential differences between vessel catchabilities for a large number of taxa of interest, a comparative fishing experiment was conducted in the summer of 2005 between the two vessels. Data analysis was conducted in 2009, but ultimately considered unreliable for most species by researchers and assessors in the Region. Upon vessel replacement by the new CCGS *Captain Jacques Cartier* and CCGS *John Cabot*, a second comparative fishing experiment was conducted between *Teleost* and the new vessels. There was a growing interest in a review of both experiments and a re-analysis of the first experiment, such that time series of catch data from the survey across the past four decades employing four different vessels could be consistently maintained and integrated. This document briefly describes the experiment in 2005 and the resulting data, followed by detailed analyses for 60 fish and invertebrate taxa routinely sampled during the survey for which there were sufficient data from the experiment. Recommendations for vessel calibrations of catch numbers based on the results of the analyses were provided for these taxa, where eight taxa had length-dependent conversion factors using length-disaggregated analysis, five taxa had length-independent conversion factors using length-disaggregated analysis, four taxa had length-independent conversion factors using length-aggregated analysis, and calibration of 36 taxa were recommended as not necessary. Results were also provided results from length-aggregated analysis of catch weights to supplement the length-aggregated analysis for catch numbers for 19 taxa.

1. INTRODUCTION

Bottom-trawl surveys provide key inputs to stock assessments for groundfish and some shellfish stocks worldwide. These surveys can produce annual indices of abundance that are proportional to stock size, provided that the proportionality constant, often called catchability, does not change over time. If this consistency is not achieved via proper sampling design and standardization, then there is a risk that changes in abundance will be confounded with changes in catchability. Maintaining consistency in survey protocols, and the survey vessel and gear, is key to maintaining constant catchability. However, periodically it becomes necessary or desirable to change one or more of these aspects and calibration experiments are required to estimate adjustments for possible changes in catchability. The most common and effective form of these experiments is comparative fishing, which usually involves paired trawling of the former and replacement vessel/gear/protocol as close together as safety permits. This design minimizes the difference in fish population densities sampled by the trawls, such that differences in catches over replicates of paired-trawl sampling will reflect the difference in catchability.

From 1982 through 2003, the Maritimes Summer Ecosystem Research Vessel Survey (hereafter referred to as the Summer RV Survey) on the Scotian Shelf and Bay of Fundy (Figure 1) using solely the Canadian Coast Guard Ship (CCGS) Alfred Needler (hereafter referred to as the Needler). In 2003, the Needler was seriously damaged by a fire while at sea and repairs were not completed in time for the 2004 Summer RV Survey. The 2004 survey was instead completed by the CCGS Teleost (hereafter referred to as the Teleost), another stern trawler that used the same gear and protocols as the Needler. The Teleost was required to complete the Summer RV Surveys in 2007, 2018, 2022 and 2023 due to the Needler being unavailable. Compared to the Needler, the Teleost was larger (length: 63 m vs 50 m; beam: 14.2 m vs 11 m; draught: 7.2 m vs 4.9 m; gross tonnage: 2405 t vs 960 t) and was equipped with an auto-trawl system in which trawl geometry is dynamically adjusted during a tow to keep the trawl square to the tow path. In order to test the difference in catch efficiencies between Needler and Teleost and maintain a consistency in annual indices of abundance of important groundfish stocks and other taxa, a comparative fishing experiment between the Needler and Teleost was conducted in the summer of 2005 to quantify relative catchabilities of species between the two vessels. Results of these analyses are presented in Fowler and Showell (2009), while similar analyses were conducted by Benoît (2006) for comparative fishing experiments between the same vessels in the southern Gulf of St. Lawrence. Comparing the results of the two studies showed several inconsistencies and diverging results. Given this, and the fact that no permanent change in the primary vessel was planned at the time, the conversion factors estimated by Fowler and Showell (2009) were largely disregarded by researchers and assessors in the Region. It was decided that the unconverted data be used until a more thorough analysis and review were conducted (especially given similar protocols and same gear employed). As a result, survey data collected by the Teleost have been considered comparable to the historical Needler time series when included in stock assessments and analysis alike.

In 2019, the CCGS Captain Jacques Cartier (hereafter referred to as “Cartier”) and CCGS John Cabot (hereafter referred to as “Cabot”), new offshore fisheries science vessels (OFSV) and sister ships of equal design, were introduced to the Canadian Coast Guard fleet. As the Needler was scheduled to be decommissioned, a comparative fishing experiment between the Needler and Cartier was scheduled for Summer 2021 on the Scotian Shelf. However, the Needler experienced mechanical issues at the beginning of the survey and was not available for comparative fishing, and as such, the 2021 Summer RV Survey was only partially completed by the Cartier alone. In Summer 2022, both the Needler and Cartier were unavailable for

comparative fishing, and in February 2023, the Needler was officially decommissioned. In the absence of the Needler, the Teleost completed the Summer RV Surveys in 2022 and 2023, while also conducting comparative fishing with the Cabot (2022) and Cartier (2023). To maintain the continuity of the Summer RV Survey time series , analyses of the 2022 and 2023 comparative fishing data were undertaken (Yin et al., 2023). However, in order to appropriately link the historical survey data collected by the Needler to calibrations estimated between the Teleost and OFSVs, the 2005 comparative fishing data was re-examined and analyzed using the same methods by Yin et al. (2023).

This document briefly describes the methods used for processing, validating, and subsequently, analyzing the comparative fishing data. These methods have been employed by the Gulf, Québec, Newfoundland, and Maritimes regions to analyze current comparative fishing experiments from 2021 to 2023 (Benoît et al. 2024 for the Québec Region in the northern Gulf of St. Lawrence, Benoît and Yin 2023 for the Gulf Region in the southern Gulf of St. Lawrence, and Trueman et al. 2023 for the Newfoundland Region). Methods for validation of paired comparative fishing sets are detailed in Ricard et al. 2023. Methods for analyses of paired sets include contemporary statistical models used previously in extended comparative fishing analyses in the eastern United States (Miller et al. 2010, Miller 2013), and applied recently to analyses of past comparative fishing data for some stocks in the Gulf of St. Lawrence (Yin and Benoît 2022a, Benoît et al. 2022). These models were extensively tested in a simulation study and were confirmed appropriate for analyses (Yin and Benoît 2022b). Since the vessels employed the same protocols, with the exception of the use of auto-trawl by the Teleost, and the same fishing gear, a substantial difference in catchabilities is not expected for this comparative fishing experiment. Nevertheless, the re-analysis can provide confidence in the consistency of survey indices as the time series combined multiple vessels across the past four decades.

2. METHODS

2.1. COMPARATIVE FISHING

2.1.1. Data correction and validation

Comparative fishing between the Teleost and Needler was conducted between July 1 and July 26, 2005. A total of 170 comparative fishing sets were completed covering the Northwest Atlantic Fisheries Organization (NAFO) Divisions 4VWX5Y (Tables 1 and 2, Figure 2). More details of the comparative fishing data can be found in the past analysis report (Fowler and Showell 2009).

Upon examining the 2005 comparative fishing data, it was determined, and since confirmed by the Chief Scientist at the time, that the Teleost used non-offset measuring boards which resulted in length measurements approximately 1 cm greater than expected. The reason for this is in how length is recorded. Under normal protocols, specimens are measured on a board that is offset by 0.5 cm from the headboard, and the length recorded is the first whole centimeter visible after the tail. Thus, a length of 30 cm includes, as nearly as can be judged visually, all fish between 29.5 and 30.5 cm. It is believed that non-offset measuring boards were used on the Teleost, and the practice of recording the first whole centimeter visible after the tail was followed. This would add approximately 1 cm on the length of a specimen compared to normal protocols, therefore, the decision was made to adjust the lengths for all species that would have been measured on a non-offset board (i.e., all fish and squid species) during the Summer 2005 Teleost missions by 1 cm.

In order to determine the validity of comparative fishing sets, further review of the comparative fishing data was conducted based on a number of criteria as listed below (see Ricard et al., 2023 for details of set validation methods and criteria):

1. Timing difference between sets in a pair: the timing difference was calculated as the difference between the starting times of the two paired tows.
2. Distance between vessels: the starting and ending locations were recorded for each tow; assuming the vessels tracked a straight line in each tow, the minimum/maximum distance was calculated as the minimum/ maximum distance between the two tracks.
3. Depth differences between sets: depths were recorded at the start and end of each tow and differences between start and end depths were calculated; average depth was calculated and assumed as the tow depth and the difference between sets in a pair was calculated.
4. Side of vessel: the side on which Teleost fished in each set pair was identified using the method from Ricard et al., 2023 and cross-validated with notes from captains; the sides sequenced with regard to dates and tested for statistical randomness using a Wald–Wolfowitz runs test (Wald and Wolfowitz 1940, Wu and Zhao 2013).
5. Duration of tows: the duration of tows was examined and significant deviation from vessel-specific protocols was identified.

2.2. COMPARATIVE FISHING ANALYSIS MODELS

2.2.1. Binomial models

In the analysis of comparative fishing data, the goal is to estimate the relative fishing efficiency between a pair of vessel-gear combinations (referred to as vessel in this section for simplicity). The expected catch from vessel v ($v \in \{A, B\}$) at length l and at station i is assumed as

$$E[C_{vi}(l)] = q_{vi}(l) D_{vi}(l) f_{vi}$$

where, $q_{vi}(l)$ is the catchability of vessel v, D_{vi} is the underlying population density sampled by vessel v, and f_{vi} is a standardization term which usually includes the swept area of a tow, and if applicable, the proportion of sub-sampling for size measurement on-board. In a binomial model (e.g., Miller 2013), the catch from vessel A at station i, conditioning on the combined catch from both vessels at this station, $C_i(l) = C_{Ai}(l) + C_{Bi}(l)$, is binomial-distributed

$$C_{Ai}(l) \sim BI(C_i(l), p_{Ai}(l))$$

where $p_{Ai}(l)$ is the expected proportion of catch from vessel A. Tows in a pair are generally assumed to fish the same underlying densities at the station, as the paired vessels typically fish within a small distance of each other: $D_{Ai}(l) = D_{Bi}(l) = D_i(l)$. Then the logit-probability of catch by vessel A is

$$logit(p_{Ai}(l)) = log(\frac{E[C_{Ai}(l)]}{E[C_{Bi}(l)]}) = log(\rho_i(l)) + o_i$$

Where $\rho_i(l)$ is the ratio of catchabilities between vessels A and B at length l and at station i, or the conversion factor, the quantity of interest,

$$\rho_i(l) = q_{Ai}(l)/q_{Bi}(l)$$

and $o_i = log(f_{Ai}/f_{Bi})$ is an offset term derived from known standardization terms for tow length relative to the standard tow lengths and for subsampling.

For a length-based conversion factor, a smooth length effect is assumed, based on a general additive smooth function,

$$log(\rho(l)) = \sum_{k=0}^{K} \beta_k X_k(l) = \mathbf{X}^T\boldsymbol{\beta},$$

where $\boldsymbol{\beta}$ are the coefficient parameters and are estimated, $\mathbf{X}$, or $\{X_k(l), k = 0,1,\cdots,K\}$, are a set of smoothing basis functions, and K is the dimension of the basis that controls the number of coefficient parameters and is usually pre-defined. Here a cubic spline smoother was used (Hastie et al. 2009), with the basis functions and penalty matrices generated by the mgcv (Wood, 2011) R package (R core team 2021).

The estimation of a cubic spline smoother is based on the penalized sum of squares smoothing objective, but in practice, this is usually replaced by a penalized likelihood objective (Green and Silverman 1993):

$$\mathcal{L}(\boldsymbol{\beta}, \lambda) = f(\mathbf{Y}|\mathbf{X}, \boldsymbol{\beta})e^{-\frac{\lambda}{2}\boldsymbol{\beta}^T\mathbf{S}\boldsymbol{\beta}}$$

$\mathcal{L}$ denotes the likelihood objective function. $f(\mathbf{Y}|\mathbf{X}, \boldsymbol{\beta})$ is the joint probability function of the survey data $\mathbf{Y}$ conditional on the basis functions and coefficient parameters. $\mathbf{S}$ is the penalty matrix defined by the smoother and the dimension of the basis, and λ is the smoothness parameter. This smoothness parameter is estimated by maximum likelihood along with other model parameters, but may be sensitive to the data. In such cases, it can be determined by other criteria such as generalized cross-validation (Wood 2000).

The penalized maximum likelihood smoother can also be re-parameterized into a mixed effects model (Verbyla et al. 1999, Wood 2017) to facilitate implementation as well as incorporation of additional random effects:

$$log(\rho_i(l)) = \mathbf{X}_f^T\boldsymbol{\beta}_f + \mathbf{X}_r^T\mathbf{b}$$

where $\boldsymbol{\beta}_f$ are fixed effects and $\mathbf{b}$ are random effects. $\mathbf{X}_f$ and $\mathbf{X}_r$ are transformed from the basis functions $\mathbf{X}$ and an eigen-decomposition of the penalty matrix $\mathbf{S}$, $\mathbf{X}_f = \mathbf{U}_f^T\mathbf{X}$ and $\mathbf{X}_r = \mathbf{U}_r^T\mathbf{X}$, where $\mathbf{U}_f$ and $\mathbf{U}_r$ are the eigenvectors that correspond to the zero and positive eigenvalues of $\mathbf{S}$. The random effects $b \sim \mathrm{N}(0, \mathbf{D}_+^{-\mathbf{1}}/\boldsymbol{\lambda})$ where D_+ is the diagonal matrix of the positive eigenvalues of $\mathbf{S}$. In the mixed effects model representation of the cubic spline smoother, the number of fixed effects is 2 and the number of random effects is bounded by $K - 2$. Smoothing effects are transformed into shrinkage of random effects in the fitting of random deviations, and can be integrated into complex mixed effects models commonly used in fisheries science (Thorson and Minto 2015).

Additional random effects can be incorporated into the mixed effects model to address variations in the relative catch efficiency related to each station,

$$log(\rho_i(l)) = \mathbf{X}_f^T(\boldsymbol{\beta}_f + \boldsymbol{\delta}_i) + \mathbf{X}_r^T(\mathbf{b} + \boldsymbol{\epsilon}_i).$$

where $\boldsymbol{\delta}_i \sim \mathrm{N}(\mathbf{0}, \boldsymbol{\Sigma})$ and $\boldsymbol{\epsilon}_i \sim \mathrm{N}(\mathbf{0}, \mathbf{D}_+^{-1}/\xi)$. From a similar re-parameterization of the cubic spline smoother, these random effects allow for deviations of the length-based conversion at each station. $\boldsymbol{\Sigma}$ is the covariance matrix of the random effects corresponding to the random deviations and contains three parameters. ξ controls the degree of smoothness of the random smoothers and the smoother at each station can differ.

A summary of the above binomial mixed model is as follows,

$$C_i(l) = C_{Ai}(l) + C_{Bi}(l)$$

$$C_{Ai}(l) \sim BI(C_i(l), p_{Ai}(l))$$
$$logit(p_{Ai}(l)) = log(\rho_i(l)) + o_i$$
$$log(\rho_i(l)) = \mathbf{X}_f^T(\boldsymbol{\beta}_f + \boldsymbol{\delta}_i) + \mathbf{X}_r^T(\mathbf{b} + \boldsymbol{\epsilon}_i)$$

The model is estimated via maximum likelihood and the marginal likelihood integrating out random effects is

$$\mathcal{L}(\boldsymbol{\beta}_f, \boldsymbol{\Sigma}, \lambda, \xi) = \int \left(\prod_{i=1}^{m} \int \int f(\mathbf{Y}_i|\mathbf{X}_f, \mathbf{X}_r, \boldsymbol{\beta}_f, \mathbf{b}, \boldsymbol{\delta}_i, \boldsymbol{\epsilon}_i) f(\boldsymbol{\delta}_i|\boldsymbol{\Sigma}) f(\boldsymbol{\epsilon}_i|\xi) \mathrm{d}\boldsymbol{\delta}_i \mathrm{d}\boldsymbol{\epsilon}_i \right) f(\mathbf{b}|\lambda) \mathrm{d}\mathbf{b}$$

The binomial mixed model can be adapted for various assumptions on the smoother and potential station variation to accommodate different underlying density of a species and data limitations especially in length measurements. A set of binomial models considered in the present analyses is provided in Table 3.

2.2.2. Beta-binomial models

The binomial assumption of the catch can be extended to a beta-binomial distribution to explain over-dispersion at the stations (Miller 2013):

$$C_{A,i}(l) \sim BB(C_i(l), p_{A,i}(l), \phi_i(l)).$$

The beta-binomial distribution is a compound of the binomial distribution and a beta distribution. More specifically, it assumes a beta-distributed random effect in the expected proportion of catch from vessel A across stations. As a result, the expected catch by vessel A has a variance of

$$var(C_{A,i}) = C_i p_i (1 - p_i) \frac{\phi_i + C_i}{\phi_i + 1}$$

where ϕ is the over-dispersion parameter that captures the extra-binomial variation.

The same smoothing length effect can be applied to the over-dispersion parameter,

$$log(\phi_i(l)) = \mathbf{X}_f^T \boldsymbol{\gamma} + \mathbf{X}_r^T \mathbf{g}$$

where $\boldsymbol{\gamma}$ are fixed effects and $\mathbf{g}$ are random effects, $\mathbf{g} \sim \mathrm{N}(0, \mathbf{D}_+^{-1}/\tau)$. This length effect models the variance heterogeneity and is particularly useful for projecting uncertainty to poorly sampled lengths. However, estimation of a length-based variance parameter typically requires sufficient catch at length data, which is usually not available for less abundant species.

A summary of the beta-binomial mixed model is as follows,

$$C_i(l) = C_{Ai}(l) + C_{Bi}(l)$$
$$C_{Ai}(l) \sim BB(C_i(l), p_{Ai}(l), \phi_i(l))$$
$$logit(p_{Ai}(l)) = log(\rho_i(l)) + o_i$$
$$log(\rho_i(l)) = \mathbf{X}_f^T(\boldsymbol{\beta}_f + \boldsymbol{\delta}_i) + \mathbf{X}_r^T(\mathbf{b} + \boldsymbol{\epsilon}_i)$$
$$log(\phi_i(l)) = \mathbf{X}_f^T \boldsymbol{\gamma} + \mathbf{X}_r^T \mathbf{g}$$

The marginal likelihood is

$$\mathcal{L}(\boldsymbol{\beta}_f, \boldsymbol{\gamma}, \boldsymbol{\Sigma}, \lambda, \xi, \tau)$$
$$= \int\int \left(\prod_{i=1}^{m} \int\int f(\mathbf{Y}_i|\mathbf{X}_f, \mathbf{X}_r, \boldsymbol{\beta}_f, \mathbf{b}, \boldsymbol{\gamma}, \mathbf{g}, \boldsymbol{\delta}_i, \boldsymbol{\epsilon}_i) f(\boldsymbol{\delta}_i|\boldsymbol{\Sigma}) f(\boldsymbol{\epsilon}_i|\xi) \mathrm{d}\boldsymbol{\delta}_i \mathrm{d}\boldsymbol{\epsilon}_i \right) f(\mathbf{b}|\lambda) f(\mathbf{g}|\tau) \mathrm{d}\mathbf{b} \mathrm{d}\mathbf{g}$$

Likewise, various smoothing assumptions can be applied to the variance parameter. Table 4 presents a set of beta-binomial mixed models.

2.2.3. Tweedie model for biomass data

The binomial and beta-binomial models are appropriate for data constituted of catch counts, but are not appropriate for catch weight or biomass. Biomass indices are routinely derived from survey data for population trend monitoring. For taxa that are measured, biomass values adjusted for the change in relative catchability are most reliably derived by applying the results of the analyses described above to length specific catch numbers and employing a length-weight conversion. However, individual measurements are not made for numerous invertebrate taxa, and were not made for some years or some specific survey hauls for many of the remaining taxa. Estimates of relative catchabilities were therefore required for size-aggregated catch weights for all taxa.

The analysis of catch weights required a probability distribution with a mass at zero, but that is otherwise continuous and can accommodate some overdispersion in catch weights. Unlike the models for catch counts, it was not possible to condition model estimates on the total catch. The following model was employed, which assumed Tweedie (TW) distributed error:

$$W_{i,v} \sim TW(\mu_{i,v}, \varphi, \rho)$$
$$E[W_{i,v}] = \mu_{i,v} = \exp(v + S_i + o_{i,v})$$
$$\varepsilon_{i,v} \sim TW(0, Var[W_{i,v}])$$
$$Var[Y_{i,v}] = \varphi(\mu_{i,v})^{\tau}$$

where $W_{i,v}$ is the catch weight at station *i* by vessel *v*, $\mu_{i,v}$ is the expected catch weight at station *i* for vessel *v*, φ is the dispersion parameter of the Tweedie distribution, τ is a power parameter, restricted to the interval 1< τ <2 (Dunn and Smyth 2005), *v* is the fixed vessel effect, where *exp*(*v*) = ρ, S_i is a fixed effect that accounts for the biomass at station *i*, and $o_{i,v}$ is the offset. Unlike the model for catch numbers in which the offset term was the log of the ratio of sampling effort (tow distance and catch sampling fraction), the offset term in the Tweedie model is the log of sampling effort at station *i* for vessel *v*, relative to the standard effort for that vessel.

A version of the model in which the station effect was treated as a random effect of the following form was initially investigated:

$$E[W_{i,v}] = \mu_{i,v} = \exp(v + \delta_i + o_{i,v})$$
$$\delta_i \sim N(0, \sigma^2)$$

However, the assumed normal distribution for the random effect in the linear predictor was found to be inappropriate.

2.2.4. Model fitting, selection, and validation

The binomial and beta-binomial models in Tables 3 and 4 for analyses of length-disaggregated catches were implemented using the Template Model Builder (TMB) package (Kristensen et al. 2016). TMB uses the Laplace approximation to integrate the joint negative loglikelihood (nll)

over the random effects to calculate the marginal nll (mnll). Optimization of the mnll is then undertaken in R using the *nlminb()* function. The basis functions for the cubic smoothing spline and the corresponding penalty matrices were generated using the R package mgcv (Wood 2011) based on 10 equally-spaced knots ($K = 9$) within the pre-specified length range depending on the range of lengths observed proper to each taxon. TMB automatically calculates a standard error for the maximum likelihood estimation of the conversion factor via the delta method (Kristensen et al. 2016).

Analyses were also undertaken for length-aggregated catch numbers, for those taxa or instances where length-aggregated conversion factors are required. Contrary to the analyses described above that treat the catch of a taxon at a station and in a length class as the basic datum, these length-aggregated analyses model the total catch numbers at each station. For simplicity, these analyses were implemented using the glmmTMB function from the homonymous R package (Brooks et al. 2017). Models BI0, BI1, BB0 and BB1 (Table 2 and 3) were fitted by specifying family=binomial(link = "logit") or family=betabinomial(link = "logit"), as appropriate. Note that conversion factor estimates for these four models obtained from the length-disaggregated analyses are likely to differ from those obtained from the length-aggregated analyses when there are strong underlying length-dependent effects on relative catchability between the two vessels.

The analyses of catch weights were also implemented using the glmmTMB function. The option family="tweedie" was specified.

Length-disaggregated models were fitted only for taxa for which there were data for, (1) at least 10 relevant set pairs (i.e., where each vessel within the pair had at least one catch), (2) at least 30 catches from each vessel, and (3) an observed length range spanning at least 10 cm (or mm depending on the measuring unit in record). Length-aggregated models were fitted for taxa for which there were data for, (1) at least 5 relevant set pairs, and (2) at least 15 catches from each vessel. These criteria were used as minimum requirements to determine a list of taxa to attempt analyses and some taxa did not receive scientific recommendations after further scrutiny of the results. Note that these criteria were updated for this study and thus slightly different from the analyses in other regions (Benoît et al. 2024 for the Québec Region in the northern Gulf of St. Lawrence, Benoît and Yin 2023 for the Gulf Region in the southern Gulf of St. Lawrence, and Trueman et al. 2023 for the Newfoundland Region). Table 5 listed all taxa considered for model-based analyses.

In addition, a ratio estimator (i.e., sample ratio between total catches from paired vessels) was calculated and reported for taxa for which there were data for at least 5 relevant set pairs. The ratio estimator can be used as a reference for comparison with model-estimated conversion factors. However, this sample ratio was not recommended for vessel calibration and therefore its associating confidence interval (CI) was not provided. While these thresholds are somewhat arbitrary, they are reasonable in light of the complexity of the models (number of fixed and random parameters estimated), the total number of taxa, and are consistent with minimum sample size requirements evident from the simulation study of Yin and Benoît (2022b). Table 5 provided a summary of data to illustrate sample sizes available for each taxon. Table 6 provided a summary of spatial distributions and population levels for all encountered taxa in the comparative fishing experiment.

There were in total 13 candidate models of length-disaggregated catches for estimating the conversion factors, although convergence could not be attained for any of the taxa for the most complex model BB7. There were four candidate models for length-aggregated catch numbers. The best model for each set of analyses was selected by BIC (Bayesian information criterion) to maximize model fitting, while avoiding over-fitting of more complicated models, especially in

cases without adequate data. Values were also examined for AIC (Akaike information criterion), which tends to select slightly more complex models compared to BIC. In the present applications AIC largely supported decisions based on BIC.

In each length-disaggregated analysis, the estimated μ function (length-dependent expected proportion of catch by vessel A) from all converged models were compared along with the sample proportions (aggregated by stations and averaged for each length) to provide a more rigorous interpretation of the results. The estimated $\rho(l)$ (expected relative catch efficiency, or conversion factor function) and associated approximate 95% confidence interval (95% CI) from the best model is then shown over the range of lengths contained in the input data. Normalized quantile model residuals (Dunn and Smyth 1996) were produced and plotted using boxplots against length and survey station to visually assess the adequacy of model fit. Finally, model residuals were plotted against depth and the time at which a station was fished, two factors known to affect catchability (e.g., Benoît and Swain 2003), to evaluate whether these effects might interact with the vessel effect under study.

The fit of catch-aggregated analyses for counts and weights was assessed by plotting the conversion factor and associated approximate 95% CI in biplots of the catch of one vessel over the other. Additionally, the scaled quantile residuals obtained using the R package DHARMa (Hartig 2021) were examined. Unlike the normalized quantile residuals used in the length-disaggregated analyses above, which have an expected Gaussian distribution when model fit is adequate, the quantile residuals from DHARMa have an expected uniform distribution. The choice was dictated in part by the fact that it was easier to examine residuals using boxplots in the former case, which has more residual values. Residuals for the catch-aggregated analyses were examined for uniformity and possible overdispersion, and plotted as a function of the fitted values, station depth and time. The evaluation of residuals in size-aggregated analyses was limited to a visual inspection.

2.2.5. Data treatment prior to analysis

Data for some taxa were grouped prior to analysis due to perceived inconsistencies in identification during the surveys or due to small sample sizes amongst related and morphologically similar taxa. *Gadus* sp. (code 251) individuals ≤ 20 cm are processed separately during catch sampling because of difficulties in distinguishing *G. morhua* and *G. ogac* at these sizes in the field. Normally samples are brought back to the laboratory for identification; however, such lab-based identification was not available in time for the comparative fishing data analyses. Given the relative prevalence of Atlantic Cod in the ecosystem, the fact that confirmed catches of *G. ogac* were not sufficiently frequent to include in any of the analyses, and the assumption that the catchability of small *Gadus* sp. should be the same as that of same-sized individuals of the specific species, these data were combined with the catches for *G. morhua*. This and the other taxonomic groupings are outlined in Table 7.

In a very small number of instances, the catch of one or two individuals at the very smallest or very largest lengths had undue influence on the shape of the length-dependent conversion factor function at and around those lengths. This results from the flexibility inherent in the cubic spline functions and is a known problem for these models (Cadigan et al. 2022). Although Cadigan et al. (2022) present an alternative and likely more robust approach, it is only applicable to monotonic length-dependent relative catchability functions and was not appropriate for the results of this comparative fishing where more complex, non-monotonic, functions were prevalent. Instead, the catches for these extreme lengths were excluded from the analysis. These cases are summarized in Table 8.

2.2.6. Interpretation of analysis results and application of conversion factors

Although automatic model selection via BIC was used in the analyses, results were reviewed thoroughly and scrutinized. For a small number of taxa, the best model selected by BIC was rejected and analyses were downgraded from length-disaggregated models to length-aggregated models (i.e., re-analyzed using simpler models). Data and/or results for these taxa were not sufficient to support length-dependency in the conversion factors even though the models could be fit. Similarly, for a small number of taxa where estimated conversion factors are unrealistic (< 0.05 or > 20, i.e., difference between vessels exceeds 20 times), the length-disaggregated models were rejected, and no conversion factors could be estimated or recommended with confidence. These cases usually resulted from lack of effective data for analyses, especially when one vessel had predominantly zero catches compared to the other vessel. For these taxa, the experiment simply did not result in meaningful data to derive a credible relative catch efficiency between the vessels. The taxa where analyses results were rejected for the reasons above are summarized in Table 8. Besides, for both model-based analyses, failure in model convergence or parameter estimation indicates insufficient data and results were not included in this document. However, for taxa where estimated conversion factors did not show significant difference between paired vessels (i.e., the 95% CI encompass a conversion factor of one), result figures were included for reference.

Two general patterns observed in the model selection and model results motivated the adoption of additional screening criteria in determining whether a conversion factor (function) should be applied, and which should be chosen for application in future analyses of the survey data. First, there were some taxa for which the 95% CI for a length-dependent conversion factor function overlapped with a value of one across all lengths, indicating absence of statistical significance for either length-dependency or the difference between vessel catchability, despite a length-dependent model being selected. This likely resulted from the use of marginal AIC and BIC values, for which the effective number of parameters may not be correctly calculated for the model random effects, causing more complex models with smoothed length effects to be favoured. Therefore, adopting conversion factor functions is not recommended when the CI overlaps unity across the range of length. In these cases, the results for non-length dependent analyses were examined; however, it was found that these were not statistically significant either.

As noted above, the estimation of length-specific conversion factor functions can be sensitive to the sparseness of data in the tails of the length frequencies. Despite eliminating some extreme lengths, there were still cases where conversion factor values diverged considerably from the overall length-dependent trend as lengths tended toward the smallest and largest lengths. Therefore the following procedure was adopted. First, lengths were identified that constituted the 0.5^{th} and 99.5^{th} percentiles of the taxon-specific total length frequency distribution for the 2005 experiment for taxa with at least 20 length classes and used the 2.5^{th} and 97.5^{th} percentiles for taxa with fewer classes. Next, the conversions factor function values at these percentiles were identified for each taxon and these values were assumed to be constant for lengths below and above these percentiles, respectively. These constant values were projected respectively to the taxon-specific smallest and largest lengths observed since 1984 in the survey (Ecosystem Research Vessel Surveys).

3. RESULTS

3.1. VALIDATION OF PAIRED SETS

All successful and paired sets in the 2005 comparative fishing experiment (170 pairs in total; Table 2) were validated after pre-processing to fix obvious errors in the data, including correction to length measurements for some taxa. All pairs had a time difference within 10 minutes (Figure 3). There were 10 pairs where depth difference was greater than 20 meters, but as a percentage there was only one pair (station number 109) with a depth difference greater than 20% (Figure 3; percentage calculated using the average depths from both vessels and both starting and ending locations). Upon examining the start depth difference and end depths difference, this pair was trawled at around 100 meters, and paired catches did not seem to affect the results of estimation for most taxa; hence, this pair was retained (Figure 4). Distance between vessels from all but one pair (with a distance < 3 nm (nautical miles)) were within 1 nm, indicating close proximity between tows in a pair (Figures 3). Teleost was on the port side in 82 pairs and the starboard side in 88 pairs (Figure 4). The sequence of sides was tested using a Wald–Wolfowitz runs test and results showed statistical significance for randomness (p-value < 0.001). Durations of tows for the two vessels did not show significant deviations (i.e., under 20 minutes) even though a small number of tows were a few minutes shorter than the standard 30 minutes, though well within the protocol (Figure 4). Overall, no serious concerns were identified and hence all sets were retained for analyses.

3.2. SUMMARY OF RESULTS

In total, the comparative fishing experiment recorded 178 encountered taxa (although some taxa codes were designated to hard-to-identify situations). After data cleaning and grouping of taxa (Table 7), 166 taxa remained but only 60 taxa met the minimum data requirements (> 5 effective paired sets; Section 2.2.4) for analyses. A summary of data availability, sample sizes and the sample conversions (calculated as sample ratio between total catch numbers and biomass) for each taxon were listed in Table 5.

There were 43 taxa that meet the minimum data requirements (Section 2.2.4) for length-disaggregated models (LDM; see Section 2.2 for details). Eight instances were rejected for lack of confidence in estimated length-dependency (Table 8) and results for the remaining 35 taxa were included in this document. Length-dependent conversion factors were estimated for 8 taxa (codes 23, 40, 41, 220, 304, 340, 623, 2526) and length-independent conversion factors for 5 taxa (320, 350, 622, 640, 2520). The remaining 22 taxa showed no significant difference in catchabilities between the vessels. In total, detailed data visualization and results presentation for all 35 taxa were included in Figures 11–46. Model selection and relative evidence based on AIC and BIC values were included in Table 10. BB7 did not converge for any taxon and therefore was not included. Table 5 provides a reference to the result figures for these taxa and the final recommendation of conversion factors for application to vessel calibration and Tables 8 and 9 provide a summary of these results and recommendations.

There were 59 taxa that meet the minimum data requirements (Section 2.2.4) for length-aggregated models (LAM). Taxa with successful model fits were reviewed and five instances with concerns of either data issues or unrealistic results were rejected (Table 9; including those taxa where both LAM and LDM were rejected) for LAM for catch numbers (see Table 9 for details of rejection). LAM for catch weights were also applied to these taxa to supplement LAM for catch numbers. Results for LAM for both catch numbers and weights and for all 60 taxa were listed in Table 11. Excluding the 35 taxa with accepted results from LDM and the 6 taxa with rejected results from LAM, detailed results were presented from LAMs for the remaining 18 taxa

in Figures 46-64. Table 5 provided a reference to these figures for each taxon. Results indicated that among them,14 taxa did not need a calibration for catch numbers.

Overall, estimated conversion factors indicated that the two vessels had similar catchabilities for most taxa of interest, including most groundfish. This result is as expected since the two vessels employed the same gear and same protocol, with the exception of the use of the auto-trawl system by the Teleost. However, for taxa with codes in the 2000s, 4000s, and 6000s (the 2000s represent mostly crabs, lobsters, shrimp and crustaceans; the 4000s represent mostly mollusks, bivalves, and cephalopods; the 6000s include echinoderms such as sea stars, sand dollars, sea urchins, and sea cucumbers), the Teleost tended to catch more (Figure 5). Estimated length-dependent conversion factors (Figure 6) further demonstrated that for some small-sized taxa (or small-size ranges of other taxa), relative catchability had strong and increasing size-dependency.

3.3. PRESENTATION OF RESULTS

Results of the various analyses for the numerous taxa covered in this document are simply too voluminous to interpret in detail. Instead, the detailed results were presented in figures and tables to support decisions for the application of conversion factors and provide some interpretation of results only for key harvested species and species of conservation concern. These are species for which reporting on survey results is likely to be most consequential and frequent, and therefore where the need for careful examination and interpretation of comparative fishing results is arguably greatest. Below is an outline of how the results are summarized and presented, followed by the results for the key species, as well as other cases:

The following tables and figures provide summaries of the results.

- Table 8 includes a summary of special considerations for some taxon, including reasons to reject/downgrade analytical methods.
- Table 9 provides a summary of results of comparative fishing analyses and an overview of recommended approaches to analyses.
- Figure 5 provides an overview of estimated conversion factors from length-disaggregated models for both catch numbers and biomass.
- Figure 6 provides an overview of estimated conversion factors from length-aggregated models for catch numbers.

The following tables and figures provide taxon-specific results:

- Table 5 provides a list of taxa that meet the minimum requirements for analysis, a summary of available data including the sample sizes (including the number of stations where a taxon was encountered by either vessel, the number of stations where a taxon was encountered by Teleost and by Needler, respectively, the number of effective sets where both vessels within the set had at least one catch, and the total number of length measurements) and sample conversions (for both catch numbers and biomass) for these taxa, and finally, an indexing of figures for reference to detailed data and results figures for each taxon. This table also highlights the recommended method for conversion factor for each taxon.
- Table 10 provides details of model selection (ΔAIC and ΔBIC values) for the length-disaggregated analyses.
- Table 11 provides details of the model evidence and selection (AIC and BIC values) for the length-aggregated analyses of catch numbers and biomass, and the estimated conversion factors with 95% confidence intervals from the analyses for taxa that meet the minimum data

requirements. Note that the recommended approach for these taxa is not necessarily the length-aggregated analysis.

- Figures 7 to 9 provide an explanation of the content within each figure for reference to taxon-specific data and results figures in Figures 11–45. Plots for the results of the length-disaggregated analyses are presented in multiple panels across three pages for each taxon. Briefly, the first page (labelled a.) provides a summary of the data from a spatial, size-aggregated and length-specific perspective (details in Figure 7). Results for the size-aggregated analyses are plotted in one of the panels in an effort to reduce the total number of figures contained in this report. The second page (labelled b.) provides a plot of the fit of all converged models and a plot of the selected conversion factor function and 95% confidence interval, along with the projected constant values proposed for the smallest and largest lengths (details in Figure 8). Finally, the third page (labelled c.) provides various boxplots for the normalized quantile residual values for the selected model (details in Figure 9).
- Figure 10 provides an explanation of the content within the figure for reference to taxon-specific data and results figures in Figures 46–64. Plots for the results of the length-aggregated analyses, including the fitted model and model quantile residuals, are presented on a single page for each taxon for the analyses of catch counts (left column) and catch weights (right column) for measured taxa, and catch numbers or weights only (single column) for taxa where analyses of the other failed. Figures are presented only for taxa that were not subjected to length-disaggregated analyses to reduce the total number of figures in this report. Nonetheless, fits of the selected length-aggregated model for catch for the remaining taxa are presented in the plots for length-disaggregated analyses and the estimated conversion factor values are in Table 11.

3.4. TAXON-SPECIFIC RESULTS AND INTERPRETATIONS

3.4.1. *Gadus morhua*

Notably there was one pair where Teleost caught a large number of Atlantic Cod (*Gadus morhua*) while Needler did not catch as many, thus dominating the sample conversion (ratio between total catches numbers was 0.4, Table 5). However, models with a random station effect were able to weight down the contributions from this pair and resulted in estimated conversions factors close to 1, indicating no significant difference between vessel catchabilities (Figure 11). Results from LDM were accepted.

3.4.2. *Sebastes* sp.

Catches of redfish (*Sebastes* sp.) in the summer RV Survey did not distinguish between different redfish species (*Sebastes mentella* and *Sebastes fasciatus*) occupying different depths and the conversion factor derived could be biased when applied to different redfish species separately.

3.4.3. *Leucoraja erinacea, Leucoraja ocellata*

There was difficulty in species identification in the summer RV Survey historically for winter skate and little skate (*Leucoraja erinacea, Leucoraja ocellata*) and they were grouped for analysis after recommendation from the peer review meeting.

3.4.4. *Chionoecetes opilio*

Estimated conversion factor results for snow crab (*Chionoecetes opilio*) were robust after testing a length-grouping of 4–5mm to reduce noise in the data. Results from LDM was accepted. However, the result suggested that it might be important to further investigate potential heterogeneity related to factors such as spatial clustering.

3.4.5. *Placopecten magellanicus, Chlamys islandica*

Analyses were attempted for both Atlantic Sea Scallop and Icelandic Scallop (*Placopecten magellanicus* and *Chlamys islandica*). However, results were rejected with concerns in both data and models suitability: scallop catchability by a trawl can be highly variable and in the comparative fishing experiment, WIIA predominantly caught most of the scallops, resulting in unmeaningful conversion factors. With these concerns and also considering that the scallop assessment typically has limited use of data from the bottom trawl survey, scientific recommendations were not provided for the scallops.

4. DISCUSSION

Overall, the comparative fishing experiment between the Needler and the Teleost in 2005 for the Summer RV Survey in the Maritimes Region was successful. Data from the experiment was sufficient for most taxa of interest for estimating the difference in relative catch efficiencies between old and replacement vessels. Results were also as expected for most taxa and indicated that the two vessels fishing the same protocols had similar catchability. Results were provided for 35 taxa using the length-disaggregated analysis and for 18 taxa using the length-aggregated analysis of catch numbers. As a result of the analyses, estimates and recommendations of length-dependent conversion factors were provided for eight taxa, length-independent conversion factors using length-disaggregated analysis were recommended for five taxa, length-independent conversion factors using length-aggregated analysis were recommended for four taxa, whereas calibration of 36 taxa was recommended as not necessary. Supplementary results were also provided for 19 taxa using length-aggregated analysis of catch weights alongside their length-aggregated analysis of catch numbers.

In practice, in order to apply these conversion factors properly, analysts should carefully examine their interested taxa to avoid misinterpretations. For example, the spatial range of the Summer RV Survey was expanded with the addition of new strata in recent years (i.e., 2011, 2014, and 2016) that were not included in the 2005 summer comparative fishing experiment, and while most habitat types and species commonly encountered in a standard survey were sampled in 2005, any differences in catch efficiencies in these new areas would be unaccounted for in the results. Further analysis was recommended, if applicable to the interested taxa, to explore potential spatial heterogeneity that may further explain variability in the relative catch efficiency and therefore, improve estimation precision. Model estimation uncertainty was also calculated in this study for each accepted conversion factor and analysts are encouraged to consider this uncertainty in their further analysis.

5. ACKNOWLEDGEMENT

We wish to thank Jordan Ouellette-Plante for providing R Markdown code for compiling the numerous figures into the document, to Paul Regular and Andrea Perreault for identifying and correcting an error in the calculation of AIC and BIC values in earlier analyses, to Jamie Emberley, Mike McMahon and Ryan Martin for quality control and guidance for the

interpretation of the data, and to everyone that participated and contributed to discussions on the analyses.

6. REFERENCES CITED

Benoît, H.P., and Swain, D.P. 2003. Accounting for length and depth-dependent diel variation in catchability of fish and invertebrates in an annual bottom-trawl survey. ICES J. Mar. Sci. 60: 1297-1316.

Benoît, H.P. 2006. Standardizing the southern Gulf of St. Lawrence bottom-trawl survey time series: results of the 2004-2005 comparative fishing experiments and other recommendations for the analysis of the survey data. DFO Can. Sci. Adv. Sec. Res. Doc. 2006/008.

Benoît, H.P., Ouellette-Plante, J., Yin, Y, and Brassard, C. 2022. Review of the assessment framework for Atlantic cod in NAFO 3Pn4RS: Fishery independent surveys. DFO Can. Sci. Advis. Sec. Res. Doc. 2022/049. xiii + 130 p.

Benoît, H.P., and Yin, Y. 2023. Results of Comparative Fishing Between the CCGS Teleost Fishing the Western IIA Trawl and CCGS Capt. Jacques Cartier Fishing the NEST Trawl in the Southern Gulf of St. Lawrence in 2021 and 2022. DFO Can. Sci. Advis. Sec. Res. Doc. 2023/083. xiii + 183 p.

Benoît, H.P., Yin, Y, and Bourdages, H. 2024. Results of comparative fishing between the CCGS Teleost and CCGS John Cabot in the Estuary and Northern Gulf of St. Lawrence in 2021 and 2022. DFO Can. Sci. Advis. Sec. Res. Doc. 2024/007. ix + 231 p.

Brooks, M.E., Kristensen, K., van Benthem, K.J., Magnusson, A., Berg, C.W., Nielsen, A., Skaug, H.J., Mächler, M., Bolker, B.M. (2017). glmmTMB balances speed and flexibility among packages for zero-inflated generalized linear mixed modeling. R Journal, 9(2):378-400.

Cadigan, N.G., Yin, Y., Benoît, H.P., and Walsh, S.J. 2022. A nonparametric-monotone regression model and robust estimation for paired-tow bottom-trawl survey comparative fishing data. Fish. Res. 254: 106422.

Dunn, P.K. and Smyth, G.K. 1996. Randomized quantile residuals. J. Comput. Graph. Stat 5: 236-244.

Dunn, P.K., and Smyth, G.K. 2005. Series evaluation of Tweedie exponential dispersion model densities. Statis. Comput. 15:267-280.

Fowler, G.M. and Showell, M.A. 2009. Calibration of bottom trawl survey vessels: comparative fishing between the Alfred Needler and Teleost on the Scotian Shelf during the summer of 2005. Can. Tech. Rep. Fish. Aquat. Sci. 2824: iv + 25 p.

Green, P.J., and Silverman, B.W. 1993. Nonparametric regression and generalized linear models. Chapman and Hall/CRC, 184 p.

Hartig, F. 2021. DHARMs: Residual diagnostics for hierarchical (multi-level.mixed) regression models. R package version 0.4.1

Hastie, T., Tibshirani, R. and Friedman, J., 2009. The elements of statistical learning: data mining, inference, and prediction. Springer Science and Business Media.

Kristensen, K., Nielsen, A., Berg, C.W., Skaug, H., and Bell, B.M. 2016. TMB: Automatic differentiation and Laplace approximation. J. Stat. Softw. 70: 1-21.

Miller, T.J. 2013. A comparison of hierarchical models for relative catch efficiency based on paired-gear data for US Northwest Atlantic fish stocks. Can. J. Fish. Aquat. Sci. 70: 1306-1316.

Miller, T.J., Das, C., Politis, P.J., Miller, A.S., Lucey, S.M., Legault, C.M., Brown, R.W., and Rago, P.J. 2010. Estimation of Albatross IV to Henry B. Bigelow calibration factors. Fish. Sci. Cent. Ref. Doc. 10-05; 233 p.

R Core Team. 2021. R: A language and environment for statistical computing. R Foundation for Statistical Computing, Vienna, Austria.

Ricard, D., Fishman, D., Rolland, N., Sylvain, F.-É., Turcotte, F. and Vergara, P. 2023. Validation of the paired sets from the comparative fishing experiments conducted between CCGS Teleost and CCGS Capt. Jacques Cartier in the southern Gulf of St. Lawrence, September 2021 and 2022. Can. Tech. Rep. Fish. Aquat. Sci. 3547: v + 274 p.

Thorson, J.T. and Minto, C. 2015. Mixed effects: a unifying framework for statistical modelling in fisheries biology. ICES J. Mar. Sci. 72:1245-1256.

Trueman, S., Wheeland, L., Benoît, H., Munro, H. Nguyen, T., Novaczek, E., Skanes, K., and Yin, Y. 2025. Results of comparative fishing between the CCGS Teleost and CCGS Alfred Needler with the CCGS John Cabot and CCGS Capt. Jacques Cartier in the Newfoundland and Labrador Region in 2021 and 2022. DFO. Can. Sci. Advis. Sec. Res. Doc. 2025/021. ix + 229 p.

Verbyla, A.P., Cullis, B.R., Kenward, M.G, and Welham, S.J. 1999. The analysis of designed experiments and longitudinal data by using smoothing splines. J. Royal Stat. Soc. Ser. C 48: 269-311.

Wald, A. and Wolfowitz, J. 1940. On a test whether two samples are from the same population. Ann. Math Statist. 11:147-162.

Wood, S.N. 2000. Modelling and smoothing parameter estimation with multiple quadratic penalties. J. Royal Stat. Soc. Ser. B Stat. Methodol. 62: 413–428.

Wood, S.N. 2011. Fast stable restricted maximum likelihood and marginal likelihood estimation of semiparametric generalized linear models. J. Royal Stat. Soc. Ser. B Stat. Methodol. 73: 3– 36.

Wood, S.N. 2017. Generalized additive models: An introduction with R, 2nd ed. Chapman and Hall/CRC Press, 496 p.

Wu, X. and Zhao, B. 2013. Nonparametric Statistics (Fourth Edition ed). China Statistics Press. pp. 40-42.

Yin, Y. and Benoît, H.P. 2022a. Re-analysis of comparative fishing experiments in the Gulf of St. Lawrence and other analyses to derive stock-wide bottom-trawl survey indices beginning in 1971 for 4RST Greenland halibut, *Reinhardtius hippoglossoides*. DFO Can. Sci. Advis. Sec. Res. Doc. 2022/002. vii + 45 p.

Yin, Y. and Benoît, H.P. 2022b. A Comprehensive Simulation Study of a Class of Analysis Methods for Paired-Tow Comparative Fishing Experiments. Can. Tech. Rep. Fish. Aquat. Sci. 3466: vi + 99 p.

Yin, Y., Benoît, H., and Martin, R. 2025. Calibration of Bottom Trawl Survey Vessels: Results of Comparative Fishing Between the CCGS *Teleost* and CCGS *John Cabot*/ CCGS *Captain Jacques Cartier* on the Scotian Shelf and Bay of Fundy in 2022 and 2023. DFO Can. Sci. Advis. Sec. Res. Doc. 2025/025. iv + 236 p.

7. TABLES

Table 1. Number of comparative fishing sets in 2005 by NAFO Subdivision

Year	4X	4W	4V	5Y	Total
2005	62	45	62	1	170

Table 2. Details for paired comparative fishing sets in 2005, where columns indicated by TEL represent values for the CCGS Teleost and those indicated by NED represent values for the CCGS Alfred Needler. Date is that of the beginning of the tow by the CCGS Alfred Needler, tow start times (Time) are expressed in decimal hours, tow depths (Depth) are in meters and were calculated as the average between start and end depths, Distance values represent the trawled distance for each vessel in nm, longitudes and latitudes are expressed in decimal degrees and were recoded by Alfred Needler in each pair.

Date	Station	Time NED	Time TEL	Depth NED	Depth TEL	Distance NED	Distance TEL	Longitude	Latitude
2005-07-01	1	01:07	01:07	139.5	136	1.8	1.65	-62.94	43.75
2005-07-01	2	06:07	06:07	62	64	1.76	1.7	-63.41	43.64
2005-07-01	3	09:07	09:07	88	86	1.76	1.71	-63.64	43.18
2005-07-01	4	12:07	11:07	80.5	80.5	1.75	1.76	-63.44	43.15
2005-07-01	5	14:07	14:07	91	90.5	1.75	1.78	-63.56	42.9
2005-07-01	6	16:07	16:07	259	230	1.76	1.75	-63.57	42.78
2005-07-01	7	19:07	18:07	115.5	105.5	1.8	1.7	-63.75	42.83
2005-07-01	8	21:07	21:07	262	236	1.8	1.71	-63.91	42.75
2005-07-01	9	23:07	23:07	54	54.5	1.81	1.8	-64.05	42.94
2005-07-02	10	02:07	02:07	46	47	1.77	1.8	-64.15	43.2
2005-07-02	11	04:07	04:07	45.5	45.5	1.7	1.77	-64.19	43.24
2005-07-03	12	16:07	16:07	67.5	64	1.75	1.7	-64.86	43.19
2005-07-03	14	22:07	22:07	49	49	1.75	1.71	-65.88	42.81
2005-07-04	15	00:07	00:07	38.5	40.5	1.78	1.76	-66.01	42.8
2005-07-04	16	04:07	04:07	80.5	77	1.78	1.77	-66.46	42.67

Date	Station	Time NED	Time TEL	Depth NED	Depth TEL	Distance NED	Distance TEL	Longitude	Latitude
2005-07-04	17	06:07	06:07	109.5	108	1.78	1.82	-66.68	42.94
2005-07-04	18	09:07	09:07	91.5	96	1.54	1.7	-66.69	42.78
2005-07-04	19	14:07	14:07	168.5	168.5	1.71	1.77	-66.84	42.34
2005-07-04	20	17:07	17:07	163.5	162.5	1.75	1.65	-67.08	42.59
2005-07-04	21	19:07	19:07	150.5	148	1.75	1.75	-67.16	42.64
2005-07-04	22	21:07	21:07	154.5	149.5	1.75	1.65	-67.28	42.59
2005-07-05	23	03:07	03:07	105	106.5	1.75	1.8	-67.5	43.22
2005-07-05	24	06:07	06:07	113.5	110	1.75	1.78	-67.23	43.45
2005-07-05	25	09:07	09:07	80.5	86	1.75	1.71	-66.91	43.7
2005-07-05	26	13:07	13:07	88.5	84.5	1.59	1.73	-67.03	43.73
2005-07-05	27	16:07	16:07	114	113.5	1.77	1.81	-67.34	43.67
2005-07-05	28	19:07	19:07	89	87.5	1.37	1.54	-67.22	44.03
2005-07-05	29	23:07	23:07	101.5	101.5	1.72	1.76	-66.74	44.26
2005-07-06	30	05:07	05:07	42	39.5	1.23	1.15	-65.89	44.68
2005-07-06	31	09:07	09:07	49	49	1.74	1.71	-65.85	44.94
2005-07-06	32	13:07	13:07	39.5	39.5	1.75	1.79	-65.52	45.17
2005-07-06	33	15:07	15:07	36.5	38.5	1.74	1.76	-65.8	45.16
2005-07-06	34	19:07	19:07	43.5	43.5	1.75	1.7	-66.1	45.08
2005-07-06	35	20:07	20:07	37.5	39.5	1.74	1.71	-66.15	45.11
2005-07-06	36	22:07	22:07	51	50	1.77	1.76	-66.28	45.03
2005-07-07	37	00:07	00:07	64	61	1.73	1.65	-66.06	44.94
2005-07-07	38	03:07	03:07	69.5	69	1.74	1.78	-66.3	44.83
2005-07-07	39	05:07	05:07	70.5	70.5	1.81	1.78	-66.31	44.78
2005-07-07	40	07:07	07:07	72	73.5	1.72	1.73	-66.27	44.63
2005-07-07	41	16:07	16:07	39	38	1.15	1.1	-66.4	44.15

Date	Station	Time NED	Time TEL	Depth NED	Depth TEL	Distance NED	Distance TEL	Longitude	Latitude
2005-07-09	43	00:07	00:07	70.5	65	1.75	1.64	-65.38	43.03
2005-07-09	44	05:07	05:07	71.5	72.5	1.6	1.6	-65.48	42.9
2005-07-09	45	14:07	14:07	59.5	65.5	1.75	1.86	-66.01	42.57
2005-07-09	46	20:07	20:07	119	119.5	1.8	1.6	-65.83	42.26
2005-07-09	47	23:07	23:07	61.5	61	1.75	1.7	-65.47	42.23
2005-07-10	59	23:07	00:07	70.5	71.5	1.75	1.74	-64.77	42.52
2005-07-10	48	01:07	01:07	61.5	62	1.75	1.76	-65.37	42.3
2005-07-10	49	04:07	03:07	53	53	1.75	1.77	-65.44	42.52
2005-07-10	50	05:07	05:07	49	50	1.7	1.77	-65.41	42.66
2005-07-10	51	08:07	08:07	50.5	50.5	1.75	1.8	-65.28	42.66
2005-07-10	52	10:07	10:07	68.5	69.5	1.8	1.77	-65.34	42.83
2005-07-10	53	11:07	12:07	67	68	1.75	1.87	-65.24	42.81
2005-07-10	54	14:07	14:07	56.5	56	1.75	1.78	-64.96	42.77
2005-07-10	55	16:07	16:07	50	50.5	1.75	1.71	-64.98	42.89
2005-07-10	56	17:07	17:07	53	52.5	1.75	1.76	-64.97	42.94
2005-07-10	57	18:07	18:07	47	47.5	1.8	1.76	-64.79	42.93
2005-07-10	58	20:07	20:07	59	60.5	1.72	1.65	-64.84	42.74
2005-07-11	60	02:07	02:07	152.5	125	1.75	1.78	-64.49	42.56
2005-07-11	61	05:07	05:07	60.5	63	1.77	1.75	-64.38	42.76
2005-07-11	62	07:07	07:07	56.5	57	1.8	1.8	-64.21	42.93
2005-07-11	63	12:07	12:07	46	47.5	1.75	1.77	-64.78	43.45
2005-07-11	64	21:07	21:07	86	87	1.8	1.72	-64.06	43.97
2005-07-12	65	00:07	00:07	127.5	125	1.75	1.67	-63.89	43.77
2005-07-12	66	02:07	02:07	107.5	105.5	1.75	1.77	-63.72	43.93
2005-07-13	100	18:07	18:07	59	61	1.4	1.32	-62.81	44.52

Date	Station	Time NED	Time TEL	Depth NED	Depth TEL	Distance NED	Distance TEL	Longitude	Latitude
2005-07-13	101	23:07	23:07	63	63	1.75	1.67	-62.09	44.74
2005-07-14	105	21:07	21:07	81.5	82	1.78	1.75	-60.12	45.6
2005-07-14	106	23:07	23:07	86	88.5	1.75	1.77	-59.94	45.63
2005-07-14	102	14:07	14:07	80.5	91	1.75	1.71	-60.35	45.34
2005-07-14	103	16:07	16:07	73.5	74.5	1.79	1.79	-59.79	45.32
2005-07-14	104	19:07	19:07	88.5	85.5	1.79	1.77	-60.02	45.45
2005-07-15	107	01:07	01:07	52.5	53.5	1.75	1.77	-59.81	45.77
2005-07-15	109	07:07	07:07	106	62	1.75	1.72	-59.47	45.8
2005-07-15	110	12:07	12:07	40	40.5	1.75	1.73	-59.38	46.22
2005-07-15	111	14:07	14:07	60	56	1.75	1.71	-59.47	46.35
2005-07-15	112	16:07	16:07	38.5	40.5	1.82	1.78	-59.72	46.3
2005-07-15	113	18:07	18:07	34	33	1.8	1.77	-59.76	46.5
2005-07-15	114	20:07	20:07	42.5	44.5	1.75	1.82	-59.66	46.55
2005-07-15	115	23:07	23:07	68.5	68.5	1.75	1.73	-59.93	46.78
2005-07-16	116	01:07	01:07	64	63.5	1.75	1.71	-59.98	46.72
2005-07-16	117	03:07	03:07	61	59	1.75	1.52	-60.19	46.56
2005-07-16	118	05:07	05:07	44	47.5	1.77	1.75	-60.29	46.47
2005-07-16	119	07:07	07:07	64	59	1.76	1.81	-60.33	46.55
2005-07-16	120	11:07	11:07	39	42.5	1.75	1.8	-60.17	46.94
2005-07-16	121	12:07	13:07	86.5	79	1.75	1.56	-60.14	47.01
2005-07-16	122	15:07	15:07	122.5	132.5	1.75	1.85	-60.09	47.17
2005-07-16	124	22:07	22:07	174.5	176.5	1.67	1.7	-59.31	46.6
2005-07-17	125	02:07	02:07	50	56.5	1.75	1.76	-59.04	46.13
2005-07-17	126	05:07	05:07	169	162	1.8	1.72	-58.51	46.06
2005-07-17	127	08:07	08:07	155.5	192.5	1.74	1.71	-58.26	45.96

Date	Station	Time NED	Time TEL	Depth NED	Depth TEL	Distance NED	Distance TEL	Longitude	Latitude
2005-07-17	128	11:07	11:07	162.5	156.5	1.75	1.7	-58.56	45.8
2005-07-17	129	12:07	13:07	152.5	138	1.75	1.53	-58.69	45.75
2005-07-17	130	16:07	17:07	63.5	83.5	1.75	1.5	-58.29	45.43
2005-07-17	131	18:07	18:07	46.5	44	1.75	1.72	-58.17	45.43
2005-07-17	132	21:07	21:07	192	180	1.74	1.75	-57.82	45.51
2005-07-18	133	02:07	02:07	78	76.5	1.75	1.82	-58.33	45.18
2005-07-18	134	04:07	04:07	34.5	35	1.8	1.75	-58.06	45.1
2005-07-18	135	07:07	07:07	55.5	62.5	1.72	1.76	-58.2	45.02
2005-07-18	136	09:07	09:07	57.5	78	1.75	1.71	-58.24	44.94
2005-07-18	137	12:07	12:07	25.5	26	1.75	1.76	-57.72	44.96
2005-07-18	138	14:07	14:07	20	21.5	1.75	1.7	-57.66	44.85
2005-07-18	139	16:07	16:07	18	19.5	1.72	1.71	-57.8	44.64
2005-07-18	140	18:07	18:07	45.5	32.5	1.78	1.71	-57.62	44.58
2005-07-18	141	21:07	21:07	180	166	1.73	1.7	-57.26	44.73
2005-07-19	142	01:07	01:07	66	71.5	1.75	1.71	-57.56	44.38
2005-07-19	143	03:07	03:07	362.5	324.5	1.75	1.7	-57.72	44.31
2005-07-19	144	05:07	05:07	51.5	54.5	1.75	1.77	-57.84	44.38
2005-07-19	145	07:07	07:07	48	47	1.75	1.78	-57.89	44.41
2005-07-19	146	14:07	14:07	76.5	81.5	1.75	1.7	-58.46	44.18
2005-07-19	147	19:07	19:07	31	32	1.8	1.76	-58.52	44.28
2005-07-19	148	21:07	21:07	31.5	33	1.77	1.75	-58.28	44.34
2005-07-19	149	23:07	23:07	34	35	1.75	1.76	-58.3	44.4
2005-07-20	150	00:07	00:07	34	35.5	1.75	1.72	-58.34	44.53
2005-07-20	151	02:07	02:07	31	31.5	1.75	1.84	-58.48	44.6
2005-07-20	152	04:07	04:07	48	48	1.86	1.76	-58.47	44.76

Date	Station	Time NED	Time TEL	Depth NED	Depth TEL	Distance NED	Distance TEL	Longitude	Latitude
2005-07-20	153	06:07	06:07	116	118	1.72	1.71	-58.7	44.78
2005-07-20	154	10:07	10:07	46.5	48	1.75	1.76	-58.8	44.7
2005-07-20	155	14:07	14:07	70	57.5	1.75	1.77	-59.07	45.18
2005-07-20	156	17:07	17:07	41	42.5	1.81	1.78	-59.2	44.96
2005-07-20	157	20:07	20:07	127	130	1.67	1.65	-59.38	44.86
2005-07-21	158	15:07	15:07	81.5	95.5	1.75	1.67	-60.25	44.92
2005-07-21	159	18:07	19:07	28	31.5	1.75	1.72	-60.76	44.69
2005-07-21	160	20:07	20:07	29	32	1.72	1.67	-60.72	44.58
2005-07-21	161	21:07	21:07	27.5	28	1.74	1.72	-60.67	44.49
2005-07-22	162	00:07	00:07	45.5	45.5	1.83	1.72	-60.92	44.31
2005-07-22	163	02:07	02:07	29	27.5	1.76	1.74	-60.59	44.39
2005-07-22	164	04:07	04:07	35.5	34.5	1.78	1.8	-60.31	44.54
2005-07-22	165	06:07	06:07	23.5	27	1.76	1.73	-60.39	44.44
2005-07-22	166	07:07	07:07	27.5	29	1.8	1.71	-60.34	44.36
2005-07-22	167	08:07	08:07	81.5	79.5	1.75	1.73	-60.37	44.28
2005-07-22	168	11:07	11:07	35	36	1.79	1.79	-60.52	44.14
2005-07-22	169	12:07	12:07	21.5	24.5	1.75	1.73	-60.46	44.06
2005-07-22	170	15:07	15:07	36.5	37	1.74	1.81	-59.91	44.1
2005-07-22	171	18:07	18:07	85	83	1.72	1.67	-59.7	44.2
2005-07-22	172	21:07	21:07	125.5	131	1.77	1.72	-59.3	44.19
2005-07-23	173	00:07	00:07	72.5	87	1.77	1.87	-59.02	44.28
2005-07-23	174	02:07	02:07	112.5	107	1.82	1.72	-59.17	44.32
2005-07-23	175	04:07	04:07	99.5	94.5	1.83	1.78	-59.25	44.37
2005-07-23	176	06:07	06:07	35.5	39	1.75	1.68	-59.28	44.46
2005-07-23	177	08:07	08:07	27.5	28.5	1.75	1.74	-59.02	44.52

Date	Station	Time NED	Time TEL	Depth NED	Depth TEL	Distance NED	Distance TEL	Longitude	Latitude
2005-07-23	178	10:07	10:07	37	38.5	1.74	1.75	-58.83	44.37
2005-07-23	179	12:07	12:07	33	34	1.79	1.74	-58.81	44.19
2005-07-23	180	15:07	16:07	135.5	154.5	1.74	1.72	-58.47	44.07
2005-07-23	181	18:07	18:07	106.5	101	1.7	1.72	-58.69	43.97
2005-07-24	187	13:07	13:07	129.5	116	1.74	1.76	-60.13	43.46
2005-07-24	188	16:07	16:07	34	36.5	1.81	1.77	-60.46	43.61
2005-07-24	189	18:07	18:07	28.5	29.5	1.82	1.76	-60.64	43.73
2005-07-24	190	20:07	20:07	31	34	1.74	1.74	-60.8	43.62
2005-07-24	191	23:07	23:07	30.5	31	1.77	1.75	-61.37	43.56
2005-07-24	182	02:07	02:07	31.5	33.5	1.76	1.82	-59.28	43.89
2005-07-24	183	04:07	04:07	27.5	27	1.72	1.75	-59.33	43.92
2005-07-24	184	06:07	06:07	57.5	60	1.72	1.74	-59.27	43.76
2005-07-24	185	08:07	08:07	34.5	35	1.74	1.75	-59.54	43.78
2005-07-24	186	10:07	10:07	26	27.5	1.9	1.73	-59.86	43.82
2005-07-25	192	02:07	02:07	69	62.5	1.76	1.67	-61.21	43.29
2005-07-25	193	04:07	04:07	129.5	113.5	1.76	1.68	-61.08	43.26
2005-07-25	194	07:07	07:07	111	133	1.55	1.74	-61.35	43.2
2005-07-25	195	10:07	10:07	46.5	46	1.75	1.71	-61.75	43.34
2005-07-25	196	11:07	12:07	48	48	1.78	1.59	-61.93	43.43
2005-07-25	197	13:07	13:07	49	49.5	1.78	1.76	-61.92	43.32
2005-07-25	198	17:07	17:07	249	268	1.78	1.71	-61.64	42.98
2005-07-25	199	19:07	19:07	145.5	124	1.76	1.77	-61.83	42.98
2005-07-25	200	21:07	21:07	234	242.5	1.75	1.65	-61.96	42.94
2005-07-26	201	01:07	01:07	51	53	1.75	1.71	-62.34	43.14
2005-07-26	202	04:07	04:07	50.5	50	1.81	1.7	-62.34	43.33

Date	Station	Time NED	Time TEL	Depth NED	Depth TEL	Distance NED	Distance TEL	Longitude	Latitude
2005-07-26	203	06:07	06:07	44.5	45	1.78	1.76	-62.42	43.41
2005-07-26	204	08:07	08:07	49	49.5	1.75	1.77	-62.52	43.41
2005-07-26	205	11:07	11:07	122	118	1.76	1.77	-62.84	43.71
2005-07-26	206	13:07	13:07	129.5	131.5	1.74	1.76	-62.79	43.88
2005-07-26	207	16:07	16:07	87.5	91	1.75	1.76	-62.6	43.87

Table 3. A set of binomial models with various assumptions for the length effect and station effect in the relative catch efficiency. A smoothing length effect can be considered, and the station effect can be added to the intercept, without interaction with the length effect, or added to both the intercept and smoother to allow for interaction between the two effects.

Model	$\boldsymbol{log(\rho)}$	Length Effect	Station Effect
$BI0$	β_0	constant	not considered
$BI1$	$\beta_0 + \delta_{0,i}$	constant	intercept
$BI2$	$\boldsymbol{X}_f^T\boldsymbol{\beta}_f + \boldsymbol{X}_r^T\boldsymbol{b}$	smoothing	not considered
$BI3$	$\boldsymbol{X}_f^T\boldsymbol{\beta}_f + \boldsymbol{X}_r^T\boldsymbol{b} + \delta_{0,i}$	smoothing	intercept
$BI4$	$\boldsymbol{X}_f^T(\boldsymbol{\beta}_f + \boldsymbol{\delta}_i) + \boldsymbol{X}_r^T(\boldsymbol{b} + \boldsymbol{\epsilon}_i)$	smoothing	intercept, smoother

Table 4. A set of beta-binomial models with various assumptions for the length effect and station effect in the relative catch efficiency, and the length effect on the variance parameter. A smoothing length effect can be considered in both the conversion factor and the variance parameter. A possible station effect can be added to the intercept, without interaction with the length effect, or added to both the intercept and the smoother to allow for interaction between the two effects.

Model	$\boldsymbol{log(\rho)}$	$\boldsymbol{log(\phi)}$	Length Effects	Station Effect
BB0	β_0	γ_0	constant/constant	not considered
BB1	$\beta_0 + \delta_{0,i}$	γ_0	constant/constant	intercept
BB2	$\boldsymbol{X}_f^T\boldsymbol{\beta}_f + \boldsymbol{X}_r^T\boldsymbol{b}$	γ_0	smoothing/constant	not considered
BB3	$\boldsymbol{X}_f^T\boldsymbol{\beta}_f + \boldsymbol{X}_r^T\boldsymbol{b}$	$\boldsymbol{X}_f^T\boldsymbol{\gamma} + \boldsymbol{X}_r^T\boldsymbol{g}$	smoothing/smoothing	not considered
BB4	$\boldsymbol{X}_f^T\boldsymbol{\beta}_f + \boldsymbol{X}_r^T\boldsymbol{b} + \delta_{0,i}$	γ_0	smoothing/constant	intercept
BB5	$\boldsymbol{X}_f^T\boldsymbol{\beta}_f + \boldsymbol{X}_r^T\boldsymbol{b} + \delta_{0,i}$	$\boldsymbol{X}_f^T\boldsymbol{\gamma} + \boldsymbol{X}_r^T\boldsymbol{g}$	smoothing/smoothing	intercept
BB6	$\boldsymbol{X}_f^T(\boldsymbol{\beta}_f + \boldsymbol{\delta}_i) + \boldsymbol{X}_r^T(\boldsymbol{b} + \boldsymbol{\epsilon}_i)$	γ_0	smoothing/constant	intercept, smoother
BB7	$\boldsymbol{X}_f^T(\boldsymbol{\beta}_f + \boldsymbol{\delta}_i) + \boldsymbol{X}_r^T(\boldsymbol{b} + \boldsymbol{\epsilon}_i)$	$\boldsymbol{X}_f^T\boldsymbol{\gamma} + \boldsymbol{X}_r^T\boldsymbol{g}$	smoothing/smoothing	intercept, smoother

Table 5. Details for data and results of comparative fishing analyses for taxa considered in this study. Taxa not included in the table indicate no recommendations due to lack of data for analyses. The scientific and common names are for taxa after grouping (see Table 5 for details of grouping). Summary of data includes the number of stations where a taxon was encountered (#Stn), the number of stations where a taxon was encountered by Teleost (#TEL) and by Needler (#NED), respectively, the number of effective sets where both vessels within the set pair had at least one catch (#Pair), and the total number of length measurements (#Len). The sample conversion (Sample ratio) was calculated as the ratio between total catches (standardized by tow distances) and was provided for both catch numbers (N) and biomass (B) for reference. The sample conversion is not recommended for application to calibration. Analyses results for length-disaggregated model (LDM) and length-aggregated models (LAM) were provided for each taxon in figure(s) where figure number (Fig. No.LDM, Fig. No. LAM) provides a reference to the figure(s) in the document. Shadings of the Result cells indicates final recommendation for each taxon, where green indicates no calibration is needed for catch numbers, yellow indicates a LAM is recommended, and orange indicates a LDM is recommended. Results for calibration of catch biomass using LAM are found in Table 11. A dash (—) represents taxa without results (and absence of shadings) indicate analyses were attempted but rejected.

Taxon Code	Scientific name	Common name	Summary of data #Stn	Summary of data #TEL	Summary of data #CA	Summary of data #Pair	Summary of data #Len	Sample ratio N	Sample ratio B	Fig. No. LDM	Fig. No. LAM	Result
10	*Gadus morhua*	*Cod(Atlantic)*	105	88	83	66	2206	0.4	0.5	11	—	$\rho=1$
11	*Melanogrammus aeglefinus*	*Haddock*	97	88	87	78	11649	1	1	12	—	$\rho=1$
12	*Urophycis tenuis*	*White Hake*	66	57	52	43	1298	1.1	1.3	13	—	$\rho=1$
13	*Urophycis chuss*	*Squirrel or Red hake*	36	26	31	21	380	1.5	1.2	14	—	$\rho=1$
14	*Merluccius bilinearis*	*Silver Hake*	78	63	70	55	5866	1.1	1	15	—	$\rho=1$
16	*Pollachius virens*	*Pollock*	43	29	34	20	1431	0.8	0.8	16	—	$\rho=1$
23	*Sebastes* sp.	*redfish unseparated*	118	105	101	88	16720	1.5	1.5	17	—	LDM, $\rho(L)$
30	*Hippoglossus hippoglossus*	*Halibut(Atlantic)*	39	28	26	15	141	1	1.1	18	—	$\rho=1$
31	*Reinhardtius hippoglossoides*	*Turbot,Greenland Halibut*	32	27	26	21	1473	1.4	1.4	19	—	$\rho=1$
40	*Hippoglossoides platessoides*	*American Plaice*	139	113	126	100	9683	1.2	1	20	—	LDM, $\rho(L)$
41	*Glyptocephalus cynoglossus*	*Witch Flounder*	97	80	83	66	3094	1.1	1.1	21	—	LDM, $\rho(L)$
42	*Limanda ferruginea*	*Yellowtail Flounder*	71	57	65	51	4705	1.2	1.2	22	—	$\rho=1$
43	*Pseudopleuronectes americanus*	*Winter Flounder*	30	25	25	20	798	1.3	1.2	23	—	$\rho=1$
60	*Clupea harengus*	*Herring(Atlantic)*	100	89	84	73	5876	1	0.9	24	—	$\rho=1$
62	*Alosa pseudoharengus*	*Alewife*	29	23	25	19	353	0.9	0.9	25	—	$\rho=1$
64	*Mallotus villosus*	*Capelin*	28	25	21	18	2040	1.2	0.6	26	—	$\rho=1$
112	*Urophycis chesteri*	*Longfin Hake*	24	22	15	13	502	1	1.1	27	—	$\rho=1$

Taxon Code	Scientific name	Common name	Summary of data #Stn	Summary of data #TEL	Summary of data #CA	Summary of data #Pair	Summary of data #Len	Sample ratio N	Sample ratio B	Fig. No. LDM	Fig. No. LAM	Result
201	*Amblyraja radiata*	*Thorny Skate*	77	59	55	37	675	1.1	3.7	28	—	$\rho = 1$
202	*Malacoraja senta*	*Smooth Skate*	37	24	24	11	135	1.3	1.1	29	—	$\rho = 1$
220	*Squalus acanthias*	*Spiny Dogfish*	32	24	23	15	1715	1.3	1.2	30	—	LDM, $\rho(L)$
300	*Myoxocephalus octodecemspinosus*	*Longhorn Sculpin*	79	69	65	55	1772	0.9	0.9	31	—	$\rho = 1$
304	*Triglops murrayi*	*Mailed Sculpin*	51	38	36	23	645	1	1.2	32	—	LDM, $\rho(L)$
320	*Hemitripterus americanus*	*Sea Raven*	59	43	48	32	406	0.8	0.6	33	—	LDM, $\rho \neq 1$
340	*Aspidophoroides monopterygius*	*Alligatorfish*	53	38	36	21	251	0.8	1	34	—	LDM, $\rho(L)$
350	*Leptagonus decagonus*	*Atlantic Sea Poacher*	22	19	20	17	214	1.7	2.5	35	—	LDM, $\rho \neq 1$
400	*Lophius americanus*	*Monkfish,Goosefish,Angler*	49	31	34	16	153	1.1	1.1	36	—	$\rho = 1$
622	*Lumpenus lumpretaeformis*	*Snake Blenny*	23	19	16	12	229	2.3	2.3	37	—	LDM, $\rho \neq 1$
623	*Lumpenus maculatus*	*Daubed Shanny*	29	27	23	21	1869	1.4	1.5	38	—	LDM, $\rho(L)$
640	*Zoarces americanus*	*Ocean Pout*	28	21	19	12	155	0.6	0.5	39	—	LDM, $\rho \neq 1$
647	*Lycodes vahlii*	*Shorttailed eelpout(vahl)*	28	21	24	17	346	1.8	1.2	40	—	$\rho = 1$
2511	*Cancer borealis*	*Jonah Crab*	64	46	44	26	325	1.1	0.5	41	—	$\rho = 1$
2520	*Hyas* sp.	*toad crab,unident.*	71	57	61	47	1316	1.5	1.4	42	—	LDM, $\rho \neq 1$
2526	*Chionoecetes opilio*	*Snow Crab (queen)*	87	77	77	67	4894	1.6	1.7	43	—	LDM, $\rho(L)$
2550	*Homarus americanus*	*American Lobster*	40	33	31	24	434	0.8	0.9	44	—	$\rho = 1$
4511	*Illex illecebrosus*	*Short-fin Squid*	105	74	88	57	2290	1.3	1.2	45	—	$\rho = 1$
50	*Anarhichas lupus*	*Striped Atlantic Wolffish*	44	29	30	15	153	1.1	1.6	—	46	$\rho = 1$
61	*Alosa sapidissima*	*Shad American*	14	11	10	7	58	1.4	1.3	—	47	$\rho = 1$
114	*Enchelyopus cimbrius*	*Fourbeard Rockling*	24	17	15	8	70	1.6	1.3	—	48	$\rho = 1$
123	*Helicolenus dactylopterus*	*Rosefish(Black Belly)*	23	19	17	13	700	0.9	0.9	—	49	$\rho = 1$
203	*Leucoraja erinacea*	*Little Skate*	32	23	24	15	275	1	1.1	—	50	$\rho = 1$
241	*Myxine glutinosa*	*Northern Hagfish*	30	21	19	10	83	1.4	0.9	—	51	$\rho = 1$
323	*Artediellus* sp.	*hookear sculpin (ns)*	30	22	20	12	185	0.7	0.7	—	52	$\rho = 1$
410	*Nezumia bairdii*	*Marlin-spike Grenadier*	15	9	12	6	81	0.9	1	—	53	$\rho = 1$
502	*Eumicrotremus spinosus*	*Atlantic Spiny Lumpsucker*	25	20	12	7	66	1.7	1.4	—	54	LAM, $\rho \neq 1$

Taxon Code	Scientific name	Common name	Summary of data #Stn	Summary of data #TEL	Summary of data #CA	Summary of data #Pair	Summary of data #Len	Sample ratio N	Sample ratio B	Fig. No. LDM	Fig. No. LAM	Result
610	*Ammodytes dubius*	*Northern Sand Lance*	43	34	30	22	4330	2.2	2.5	—	55	$\rho = 1$
712	*Notolepis rissoi*	*White Barracudina*	12	10	9	7	547	1.5	1.3	—	56	$\rho = 1$
2211	*Pandalus borealis*	*Northern shrimp*	49	33	33	20	0	1	1.2	—	57	$\rho = 1$
2212	*Pandalus montagui*	*Striped shrimp*	104	59	70	27	0	2.7	2.4	—	58	$\rho = 1$
2523	*Lithodes maja*	*Northern Stone Crab*	30	25	20	15	95	1.5	1.9	—	60	LAM, $\rho \neq 1$
2559	Paguridae	*hermit crabs*	69	54	28	19	0	2.9	3.9	—	61	LAM, $\rho \neq 1$
6100	*Asteroidea s.c.*	*Asteroidea*	163	129	116	93	0	0.8	1.7	—	62	$\rho = 1$
6500	Clypeasteroida	*sand dollars*	59	47	22	15	4	1.5	1.7	—	63	LAM, $\rho \neq 1$
6600	Holothuroidea	*holothuroids*	69	44	40	24	0	0.8	1.8	—	64	$\rho = 1$
2416	*Crangon* sp.	*Crangon*	54	22	42	10	0	1	0.8	—	59	—
2532	*Chaceon quinquedens*	*Red Deepsea Crab*	8	6	8	6	118	0.7	0.7	—	—	—
4321	*Placopecten magellanicus*	*Sea Scallop*	40	34	23	17	313	1.2	1.2	—	—	—
4322	*Chlamys islandica*	*Iceland Scallop*	31	24	17	12	385	2.3	2.2	—	—	—
4521	Octopoda	*octopus*	55	39	15	8	1	2.2	2	—	—	—
6400	*Strongylocentrotus* sp.	*sea urchin*	78	33	50	20	22	0.9	2.3	—	—	—

Table 6. Summary of comparative fishing data, i.e., sample size for analyses. Taxa were tallied by the number of stations where they were encountered (i.e., spatial distribution) and the number of total catch numbers (i.e., population level). Each column corresponds to a range of number of effective sets (for example, there were 29 sets that had number of catches within 0–1 AND number of effective sets within 1–5). Most taxa were encountered in the comparative fishing experiment only sporadically and there were not sufficient data for analysis; a few species were both abundant and widely distributed.

Total number of catches	1–5 effective sets	5–50 effective sets	50–100 effective sets	> 100 effective sets
0–1	29	11	4	2
1–10	51	2	2	0
10–100	5	21	1	0
100–1000	1	25	5	0
> 1000	0	6	8	5

Table 7. Taxonomic groupings employed for the analyses of the comparative fishing data. The codes are those used routinely in DFO's Maritimes Region, commonly called RVAN codes.

Taxon	Taxon code	Codes in group
Merluccius bilinearis	14	14, 19
Leucoraja erinacea	203	203, 204
Artediellus sp.	323	323, 306, 880
Liparidae	500	500, 505, 512, 520, 868
Cancer borealis	2511	2511, 2513
Hyas sp.	2520	2520, 2521, 2527
Pagurus sp.	2560	2560, 2561, 2562
Polycheatae	3000	3000 - 3104
Aphrodita hastata	3200	3200, 3210
Buccinum sp.	4210	4209, 4210, 4211, 4212
Nudibranchia	4400	4400. 4410
Pycnogonida	5100	5100, 5101, 5102
Ophiuroidea	6200	6200, 6211, 6213
Euryalida	6300	6300, 6310
Strongylocentrotus sp.	6400	6400, 6411
Holothuroidea	6600	6600, 6601, 6611
Scyphozoa	8500	8500, 8511
Porifera	8600	8600-8612, 8614, 8617-8623, 8628-8632, 8637-8699

Table 8. Summary of data and results treatment for specific taxa, including exclusion of certain lengths from the length-disaggregated analyses, rejection of automatic model selection results.

Taxa	Taxa codes	Special considerations
Myctophidae*, Placopecten magellanicus, Chlamys islandica*	150, 4321, 4322	Both LDM and LAM rejected due to data concerns and model suitability, therefore, no recommendations were provided
Leucoraja erinacea	203	LDM rejected due to small range of length measurements for the majority of effective paired catches data

Taxa	Taxa codes	Special considerations
Artediellus sp.*, Ammodytes dubius*	323, 610	LDM rejected due to data insufficiency
Helicolenus dactylopterus, Notolepis rissoi	123, 712	LDM rejected for wide 95% CI indicating uncertainty in length dependency
Octopoda	4521	LAM was rejected and no conversion could be estimated due to insufficient information in data and/or lack of confidence in results
Strongylocentrotus sp.	6400	LAM rejected due to data concerns (likely corrupted data)
Crangon sp.	2416	LAM for catch numbers rejected due to unrealistic estimates where conversion showing difference greater than 20 times but LAM for catch biomass retained

Table 9. Summary of results of comparative fishing analyses and recommendations for calibration of vessels.

Type of analysis	Number of taxa	Type of recommendations and comments
Length-disaggregated for catch numbers	Results for 35 taxa were provided in figures	22 instances indicated no significant difference in catchabilities 8 instances received length-dependent recommendations based on LDM 5 instances received length-independent recommendations based on LDM
Length-aggregated for catch numbers	Results for 19 taxa were provided in Figures	14 instances indicated no requirement for vessel calibration, i.e., CI covered 1 4 instances received length-independent recommendations based on LAM 1 instance received no recommendation
Length-aggregated for catch biomass	19	Results for biomass were provided as supplementary LAM results for numbers
No recommendations	113	Insufficient data for analyses or analyses rejected due to data insufficiency
Total taxa in analyses (after grouping)	166	See Table 5 for grouping of taxa
Total taxa encountered	178	Total number of species encountered in comparative fishing tows

Table 10. Relative evidence for length-disaggregated binomial and beta-binomial models based on delta values of the Aikaike Information Criterion (ΔAIC) and the Bayesian Information Criterion (ΔBIC) values. Entries with '—' indicate models that did not converge properly. Models BB7 did not converge for any taxon and are not included in the table.

Taxon Code	ΔAIC BI0	ΔAIC BI1	ΔAIC BI2	ΔAIC BI3	ΔAIC BI4	ΔAIC BB0	ΔAIC BB1	ΔAIC BB2	ΔAIC BB3	ΔAIC BB4	ΔAIC BB5	ΔAIC BB6	ΔBIC BI0	ΔBIC BI1	ΔBIC BI2	ΔBIC BI3	ΔBIC BI4	ΔBIC BB0	ΔBIC BB1	ΔBIC BB2	ΔBIC BB3	ΔBIC BB4	ΔBIC BB5	ΔBIC BB6
10	767	0	617	2	—	244	0	234	236	2	5	—	762	0	621	11	—	244	5	243	254	16	28	—
11	619	62	558	63	—	287	8	291	—	11	0	—	600	48	550	60	—	274	0	288	—	13	13	—
12	21	9	19	13	15	6	0	7	8	3	6	—	12	5	19	17	32	2	0	11	21	11	23	—
13	17	0	17	2	—	12	2	14	17	4	—	—	14	0	20	8	—	12	5	20	30	13	—	—
14	278	44	269	27	—	85	9	88	84	0	2	—	261	31	261	23	—	72	0	84	89	0	11	—
16	440	3	412	0	—	221	4	206	206	2	5	—	434	0	413	5	—	218	5	211	218	11	21	—
23	4136	604	3947	480	566	627	35	624	628	13	0	—	4105	579	3927	464	566	601	15	608	623	3	0	—
30	4	0	8	4	—	—	—	—	—	—	—	—	2	0	11	10	—	—	—	—	—	—	—	—
31	111	14	75	5	—	33	0	37	41	0	4	—	103	11	75	8	—	29	0	41	52	8	19	—
40	734	47	684	32	—	387	14	358	345	0	0	—	712	30	673	26	—	370	3	352	351	0	11	—
41	128	19	104	4	68	73	11	62	64	0	4	—	110	6	95	0	78	59	3	58	70	0	13	—
42	164	13	167	14	—	82	0	86	89	2	2	—	154	9	167	19	—	77	0	90	103	11	20	—
43	28	3	28	5	24	17	0	19	21	3	6	—	21	0	29	9	39	14	1	23	32	10	20	—
60	1710	259	1620	240	—	185	7	185	189	0	4	—	1694	247	1613	237	—	173	0	182	195	2	14	—
62	34	3	35	6	—	13	1	14	12	3	0	—	28	0	34	9	—	10	0	17	20	8	11	—
64	1766	125	1055	92	28	42	0	42	45	4	—	—	1761	122	1055	95	39	40	0	44	53	9	—	—
112	113	2	115	0	—	69	3	72	73	2	—	—	108	0	116	4	—	67	3	76	83	9	—	—
123	123	41	116	6	—	35	9	39	40	0	0	—	111	32	110	3	—	26	3	36	43	0	6	—
150	225	69	206	16	—	37	21	34	—	0	—	—	217	63	202	14	—	31	17	32	—	0	—	—
201	10	0	12	4	—	9	1	11	14	5	—	—	6	0	16	12	—	9	5	20	30	17	—	—
202	1	0	5	3	—	3	—	6	10	—	—	—	0	1	9	9	—	4	—	13	22	—	—	—
203	22	0	26	4	—	—	—	28	—	—	—	—	19	0	30	10	—	—	—	35	—	—	—	—
220	33	14	21	0	—	24	12	16	19	2	4	—	22	6	18	0	—	17	9	16	26	5	15	—
300	70	0	68	2	—	43	0	44	47	3	—	—	66	0	73	11	—	43	4	52	64	15	—	—
304	71	19	63	14	—	18	7	11	15	0	2	—	59	10	57	11	—	9	1	8	18	0	9	—

Taxon Code	ΔAIC BI0	ΔAIC BI1	ΔAIC BI2	ΔAIC BI3	ΔAIC BI4	ΔAIC BB0	ΔAIC BB1	ΔAIC BB2	ΔAIC BB3	ΔAIC BB4	ΔAIC BB5	ΔAIC BB6	ΔBIC BI0	ΔBIC BI1	ΔBIC BI2	ΔBIC BI3	ΔBIC BI4	ΔBIC BB0	ΔBIC BB1	ΔBIC BB2	ΔBIC BB3	ΔBIC BB4	ΔBIC BB5	ΔBIC BB6
320	40	6	30	9	—	13	0	12	16	3	6	—	33	2	30	13	—	10	0	16	27	11	21	—
323	38	2	41	0	—	13	1	16	—	1	—	—	34	0	41	2	—	11	0	18	—	5	—	—
340	21	17	1	0	—	17	17	2	6	—	—	—	15	14	0	2	—	14	16	5	14	—	—	—
350	0	2	4	6	—	—	—	—	—	—	—	—	0	5	9	14	—	—	—	—	—	—	—	—
400	0	2	4	6	12	2	4	6	—	—	—	14	0	5	10	14	29	5	10	14	—	—	—	33
610	2572	277	2121	155	—	356	45	333	336	4	0	—	2553	262	2109	147	—	341	33	325	336	0	4	—
622	5	2	4	2	—	2	0	3	5	1	2	—	1	0	5	6	—	1	1	7	15	8	15	—
623	123	34	88	1	—	37	17	28	30	0	—	—	112	27	84	0	—	30	12	27	35	2	—	—
640	1	0	5	3	—	3	2	6	10	5	—	—	0	1	9	10	—	4	6	13	23	15	—	—
647	20	0	18	4	—	20	—	19	—	—	—	—	17	0	21	10	—	20	—	26	—	—	—	—
712	189	17	171	0	—	50	19	46	46	—	—	—	183	13	169	0	—	46	17	46	50	—	—	—
2511	31	1	34	1	—	23	0	26	29	1	3	—	26	0	37	8	—	22	3	33	42	11	20	—
2520	59	0	63	3	—	52	1	55	44	3	3	—	55	0	68	12	—	52	5	64	62	17	26	—
2526	807	43	772	22	287	271	16	250	244	0	0	—	785	26	760	16	298	253	4	244	249	0	11	—
2550	0	1	0	1	—	—	—	2	—	—	—	—	0	4	7	12	—	—	—	13	—	—	—	—
4321	51	0	41	3	—	50	2	43	—	5	—	—	48	0	44	10	—	50	5	49	—	15	—	—
4322	61	3	59	7	—	47	0	48	52	4	8	—	54	0	60	11	—	44	0	51	62	11	21	—
4511	726	35	693	31	—	108	0	112	107	1	0	—	718	31	692	35	—	104	0	116	119	8	16	—

Table 11. Relative evidence for length-aggregated binomial and beta-binomial models for catch numbers based on Aikaike Information Criterion (AIC) and the Bayesian Information Criterion (BIC) values, and estimates of the conversion factor, and approximate 95% confidence intervals, for catches in numbers and in biomass. Results provided included taxa where length-disaggregated analyses were also undertaken. Decisions for recommended conversion factors for each of the taxa are in Table 7. Entries with a dash (—) indicate the model failed to converge.

Taxon Code	AIC BI0	AIC BI1	AIC BB0	AIC BB1	BIC BI0	BIC BI1	BIC BB0	BIC BB1	Numbers Model Conversion	AIC	BIC	Biomass Model Conversion
10	1404	408	406	408	1407	414	411	416	1.02 (0.81,1.29)	1048	1410	0.82 (0.64,1.05)
11	1258	641	638	640	1261	646	643	648	0.89 (0.76,1.04)	1324	1651	0.94 (0.84,1.05)
12	262	251	251	253	264	255	255	259	1.12 (0.93,1.36)	660	858	1.16 (0.94,1.42)
13	139	121	121	123	140	125	124	128	0.98 (0.68,1.41)	173	262	1.06 (0.79,1.44)
14	661	409	406	408	663	414	411	415	0.95 (0.77,1.16)	437	684	0.92 (0.81,1.05)
16	696	192	190	192	698	195	194	197	0.74 (0.47,1.16)	603	716	0.68 (0.48,0.97)
23	6747	861	853	855	6750	867	859	863	1.13 (0.92,1.39)	972	1391	1.23 (0.99,1.52)
30	100	96	95	97	102	99	99	102	1.03 (0.66,1.63)	453	552	1.04 (0.56,1.93)
31	258	151	151	153	260	154	154	157	0.99 (0.72,1.36)	336	412	1.28 (0.99,1.67)
40	1516	765	764	766	1519	771	770	775	1.01 (0.87,1.16)	1023	1538	0.98 (0.87,1.11)
41	531	415	415	417	533	420	420	424	0.96 (0.8,1.15)	572	899	1.03 (0.89,1.18)
42	540	389	389	391	542	394	394	398	1.06 (0.88,1.26)	511	730	1.15 (1.02,1.29)
43	155	131	130	132	157	133	133	136	1.24 (0.89,1.73)	230	299	1.18 (0.93,1.49)
50	118	111	110	112	120	114	113	117	1 (0.64,1.57)	240	357	1.31 (0.71,2.43)
60	2337	605	597	599	2340	610	603	607	1.08 (0.85,1.37)	913	1253	0.99 (0.81,1.21)
61	48	44	44	46	49	45	45	48	1.22 (0.58,2.56)	101	124	1.29 (0.68,2.47)
62	135	105	104	106	137	107	107	110	0.71 (0.47,1.08)	107	173	0.84 (0.61,1.15)
64	4850	173	172	174	4851	175	175	178	1.53 (0.94,2.49)	28	91	1.34 (0.75,2.4)
112	228	117	115	117	229	119	117	120	1.67 (0.93,3)	118	169	1.29 (0.77,2.14)
114	57	59	58	60	58	61	61	64	1.56 (0.96,2.53)	-32	19	1.3 (0.78,2.15)

Taxon Code	AIC BI0	AIC BI1	AIC BB0	AIC BB1	BIC BI0	BIC BI1	BIC BB0	BIC BB1	Numbers Model Conversion	AIC	BIC	Biomass Model Conversion
123	196	114	113	115	197	116	115	119	1.01 (0.61,1.68)	90	137	0.89 (0.6,1.33)
150	267	76	75	77	268	77	76	78	1.21 (0.54,2.71)	-52	-30	0.65 (0.24,1.75)
201	232	223	222	224	235	227	227	231	1.12 (0.91,1.4)	636	879	1.44 (1,2.08)
202	95	94	93	95	97	97	96	100	1.11 (0.68,1.8)	222	314	1.09 (0.7,1.7)
203	134	111	110	112	135	114	113	117	1.06 (0.66,1.71)	284	360	1.2 (0.8,1.8)
220	164	120	120	122	166	123	122	126	1.09 (0.88,1.35)	394	470	1.16 (1.02,1.31)
241	73	73	72	74	74	76	75	79	1.42 (0.91,2.19)	10	80	0.98 (0.62,1.54)
300	404	330	329	331	406	335	334	338	0.86 (0.71,1.04)	466	717	0.88 (0.75,1.04)
304	244	192	191	193	246	196	195	199	1.18 (0.82,1.69)	-173	-32	1.24 (0.95,1.62)
320	220	185	184	186	222	190	188	192	0.74 (0.54,1.01)	484	656	0.63 (0.47,0.85)
323	128	93	91	93	130	95	94	97	0.93 (0.53,1.6)	-212	-143	0.81 (0.52,1.24)
340	148	144	144	146	150	148	148	151	0.91 (0.63,1.33)	-461	-312	1.08 (0.82,1.43)
350	70	72	72	74	71	74	74	77	1.72 (1.3,2.27)	-95	-51	2.08 (1.39,3.13)
400	101	103	103	—	103	107	107	—	1.12 (0.82,1.54)	436	570	1.08 (0.75,1.55)
410	48	50	50	52	49	51	51	54	0.87 (0.56,1.35)	-19	6	0.84 (0.41,1.75)
502	57	57	57	59	58	60	59	62	1.73 (1.05,2.86)	-104	-50	1.62 (0.96,2.75)
610	11685	357	350	352	11687	360	354	357	1.49 (0.93,2.38)	309	418	2.48 (1.72,3.57)
622	86	82	82	84	87	85	85	88	2.02 (1.18,3.49)	-33	15	2.21 (1.59,3.05)
623	256	165	165	167	258	168	168	171	1.47 (1.07,2.01)	-119	-53	1.61 (1.34,1.94)
640	82	81	80	82	84	84	83	86	0.68 (0.41,1.11)	107	170	0.57 (0.4,0.81)
647	133	113	113	115	134	115	115	119	1.42 (0.91,2.24)	79	142	1.49 (0.93,2.38)
712	239	65	65	67	239	66	66	69	1.16 (0.51,2.63)	6	23	1.26 (0.7,2.26)
2211	144329	470	457	454	144330	473	460	460	1.08 (0.33,3.56)	486	609	1.3 (0.88,1.93)

Taxon Code	AIC BI0	AIC BI1	AIC BB0	AIC BB1	BIC BI0	BIC BI1	BIC BB0	BIC BB1	Numbers Model Conversion	AIC	BIC	Biomass Model Conversion
2212	87787	621	600	607	87789	626	605	615	0.82 (0.58,1.16)	526	874	1.54 (1.07,2.21)
2416	4053	199	208	210	4055	203	212	216	0 (0,0)	36	189	0.71 (0.4,1.25)
2511	212	182	181	183	215	187	185	189	1.12 (0.78,1.59)	273	464	0.84 (0.56,1.25)
2520	329	269	268	269	331	274	272	276	1.39 (1.08,1.79)	-122	97	1.47 (1.15,1.87)
2523	68	70	—	—	70	73	—	—	1.53 (1.02,2.32)	133	202	1.72 (1.13,2.62)
2526	1273	509	508	509	1275	514	512	516	1.69 (1.39,2.05)	554	838	1.85 (1.59,2.16)
2550	121	121	121	123	123	125	125	128	0.85 (0.7,1.02)	399	501	0.99 (0.79,1.23)
2559	143	139	138	140	145	143	143	147	2.55 (1.75,3.72)	-57	130	3.02 (2.06,4.43)
4321	149	123	121	123	151	127	125	128	1.7 (1.07,2.72)	147	249	1.47 (1,2.17)
4322	147	110	110	112	149	113	112	116	1.87 (1.08,3.22)	79	145	2.2 (1.51,3.21)
4511	1425	447	440	441	1428	452	445	449	0.9 (0.69,1.18)	340	701	1.13 (0.9,1.41)
4521	135	92	94	96	137	96	98	102	746.63 (15.12,36874.97)	-105	18	2.51 (1.63,3.86)
6100	2492	816	799	800	2495	822	805	809	1.14 (0.91,1.43)	281	857	1.46 (1.25,1.71)
6400	2886	248	238	240	2888	252	243	247	0.55 (0.35,0.85)	164	351	2.3 (1.9,2.79)
6500	268	159	156	158	270	163	160	164	2.59 (1.59,4.21)	4	156	2.28 (1.63,3.17)
6600	552	235	229	231	554	240	233	237	1.03 (0.69,1.54)	428	604	1.72 (1.32,2.25)

8. FIGURES

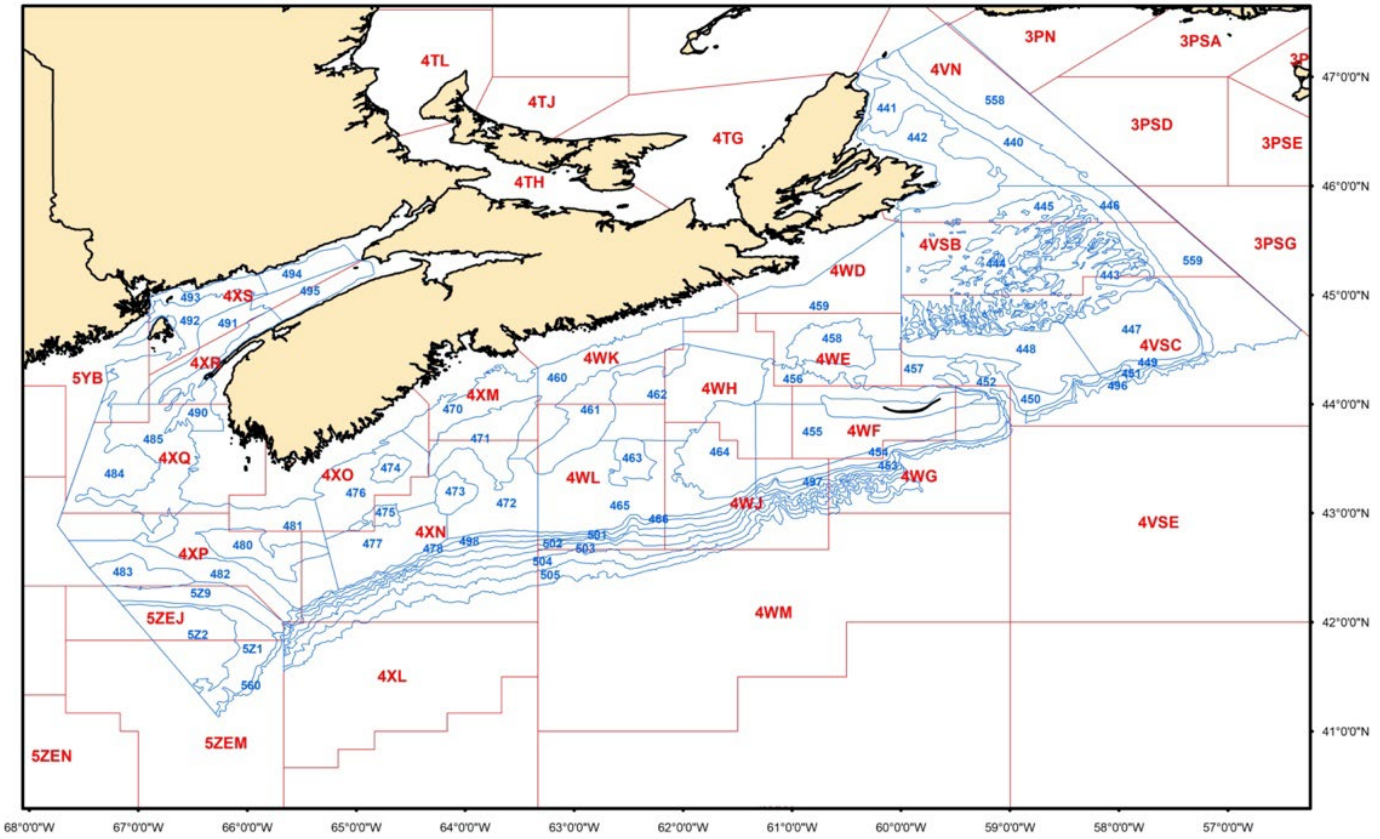

Figure 1. Stratification map for the Summer RV (research vessel) Survey in the Maritimes Region. The strata are labelled in blue and DFO unit areas are labelled in red. The strata design expanded over the years that the Needler was in service. From 1970–1995, sampling concentrated in strata 440–495. Spatial coverage was extended to the Scotian Shelf slope (strata 496–498) in 1996 and the Fundian Channel (5Z1 & 5Z9) in 2011. The sampled area expanded to include strata 558 and 559 in 2014 and strata 5Z2 in 2016.

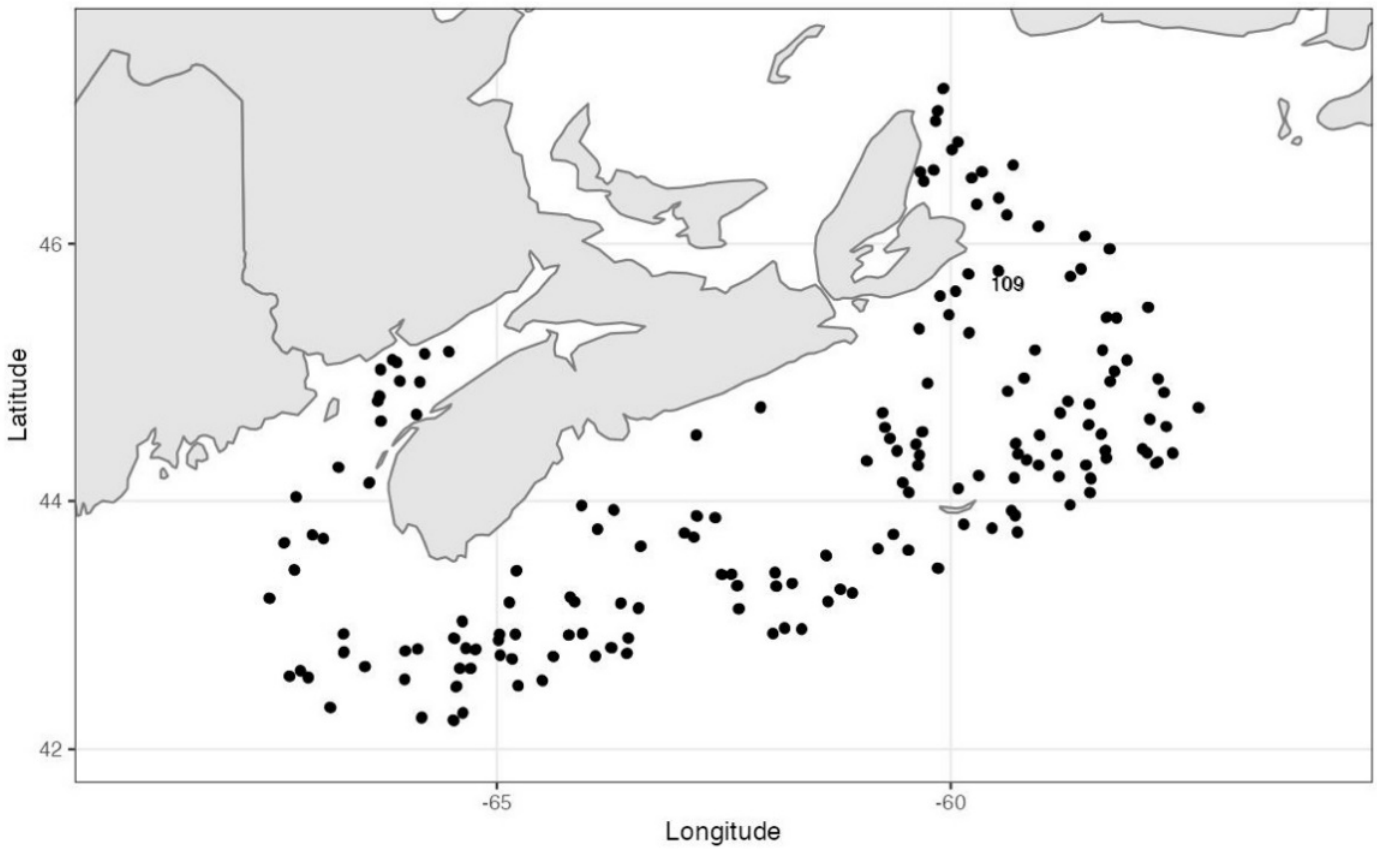

Figure 2. Locations of 2005 comparative fishing sets from the Maritimes Region summer comparative fishing experiment. Station 109 is labelled where paired sets had a depth difference greater than 25%.

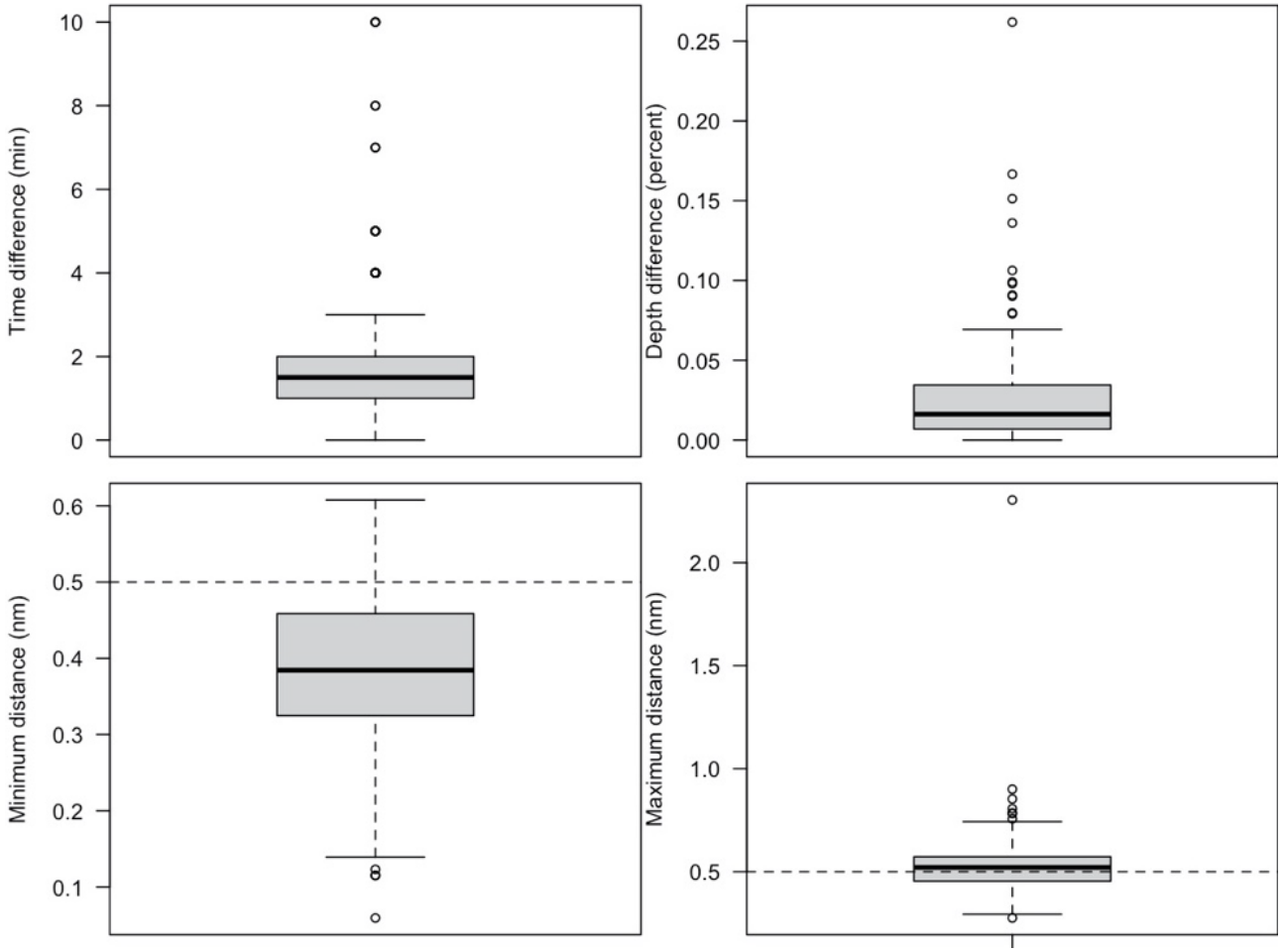

Figure 3. Boxplots showing the amount of time in minutes between the onset of fishing between vessels, the difference in depth in meters between vessels and the minimum and maximum distances between vessels in nautical miles (nm).

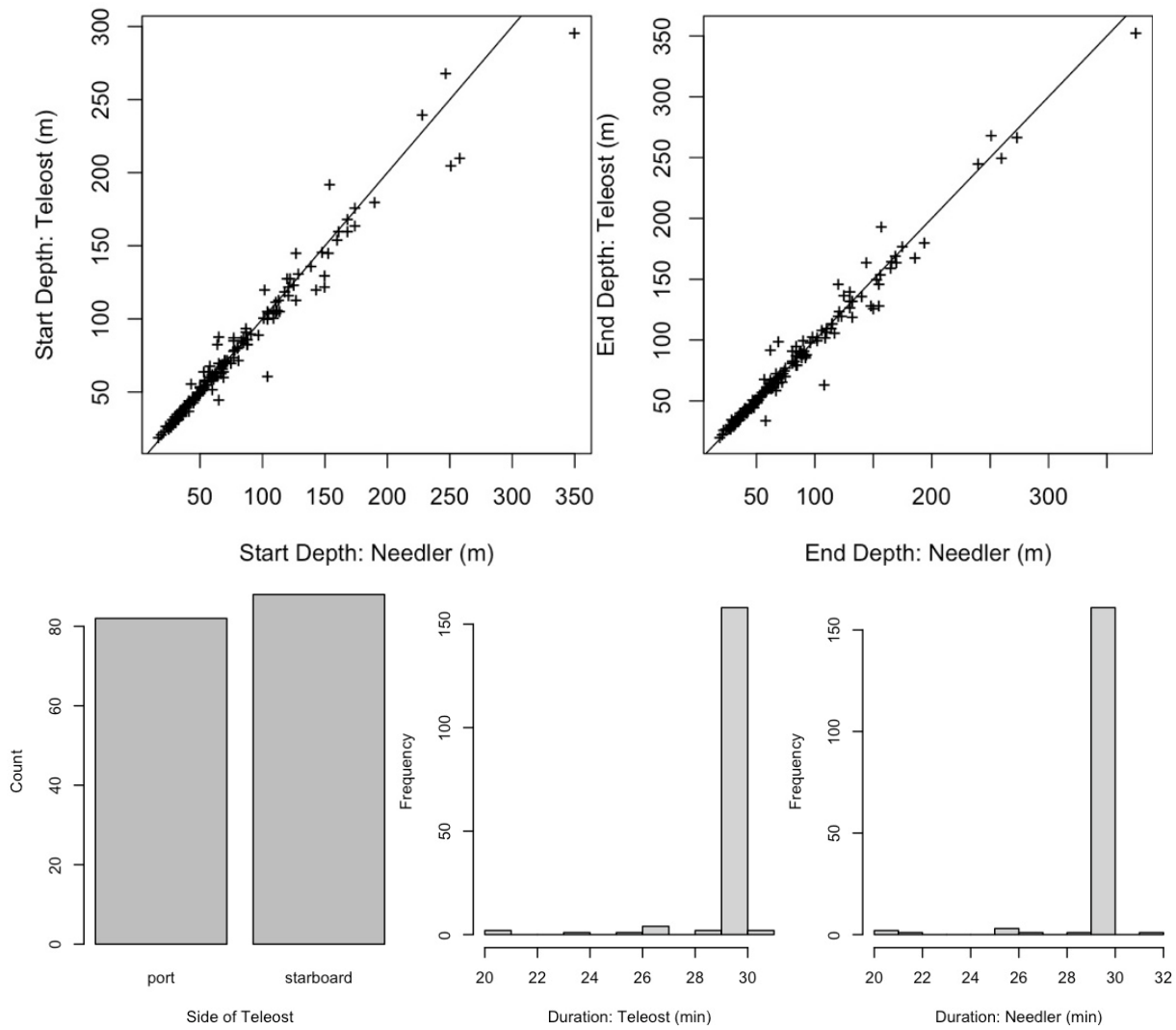

Figure 4. Validation of paired sets. Top two panels plot depths from starting and ending locations from each pair of tows in meters (m). Bottom left panel counts the number of pairs where Teleost fished on each side. The two bottom right panels summarize tow durations in minutes for all tows from the two vessels, respectively.

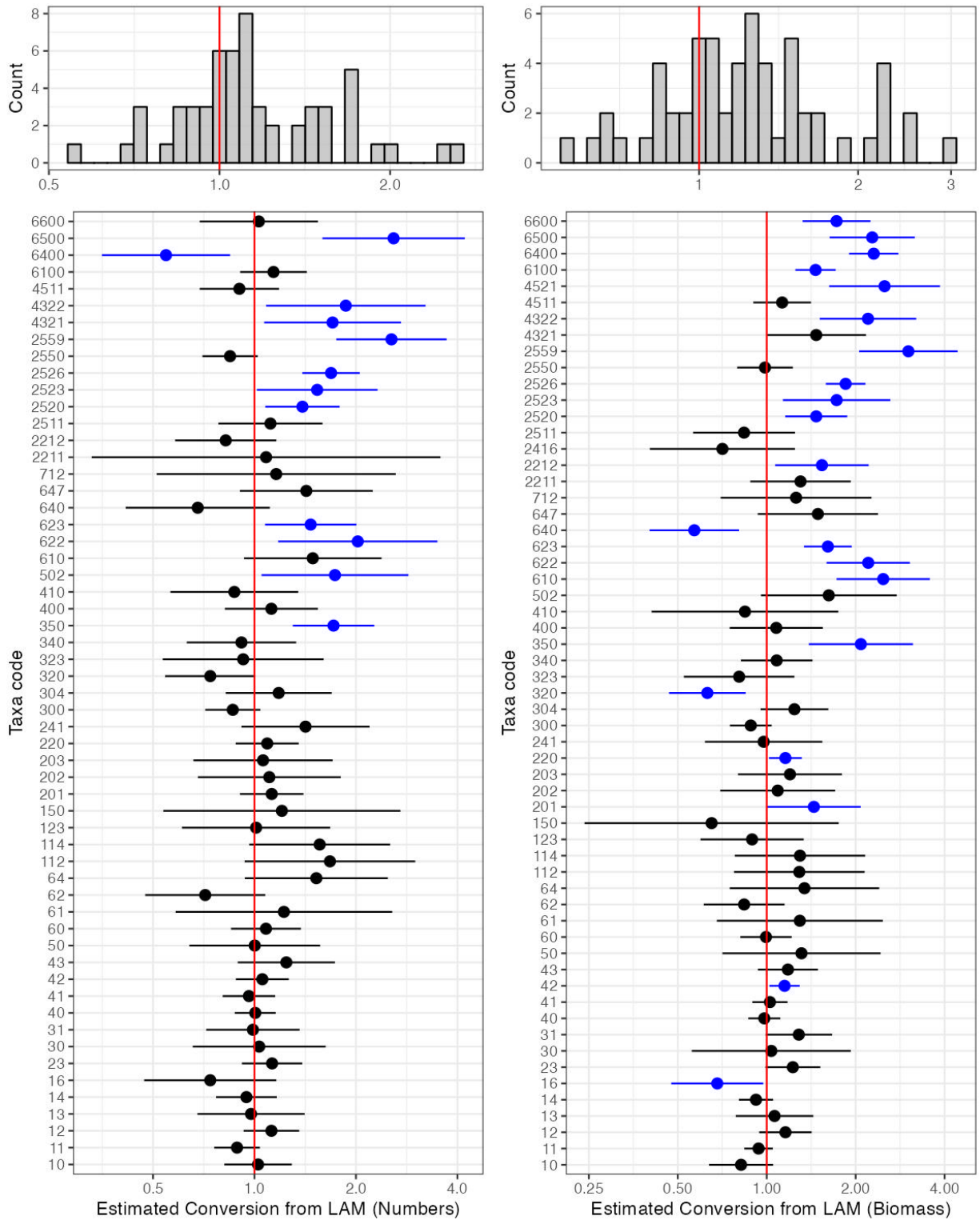

Figure 5. Estimated conversion factors and 95% CI for taxa (see Table 5 for codes) catch numbers and biomass using length-aggregated models (LAM, see Section 2.2 for details) and histogram summaries for estimated conversion factors (taxa whose conversion factors indicated significant vessel difference were noted in blue). Red vertical lines indicate a conversion equal to one.

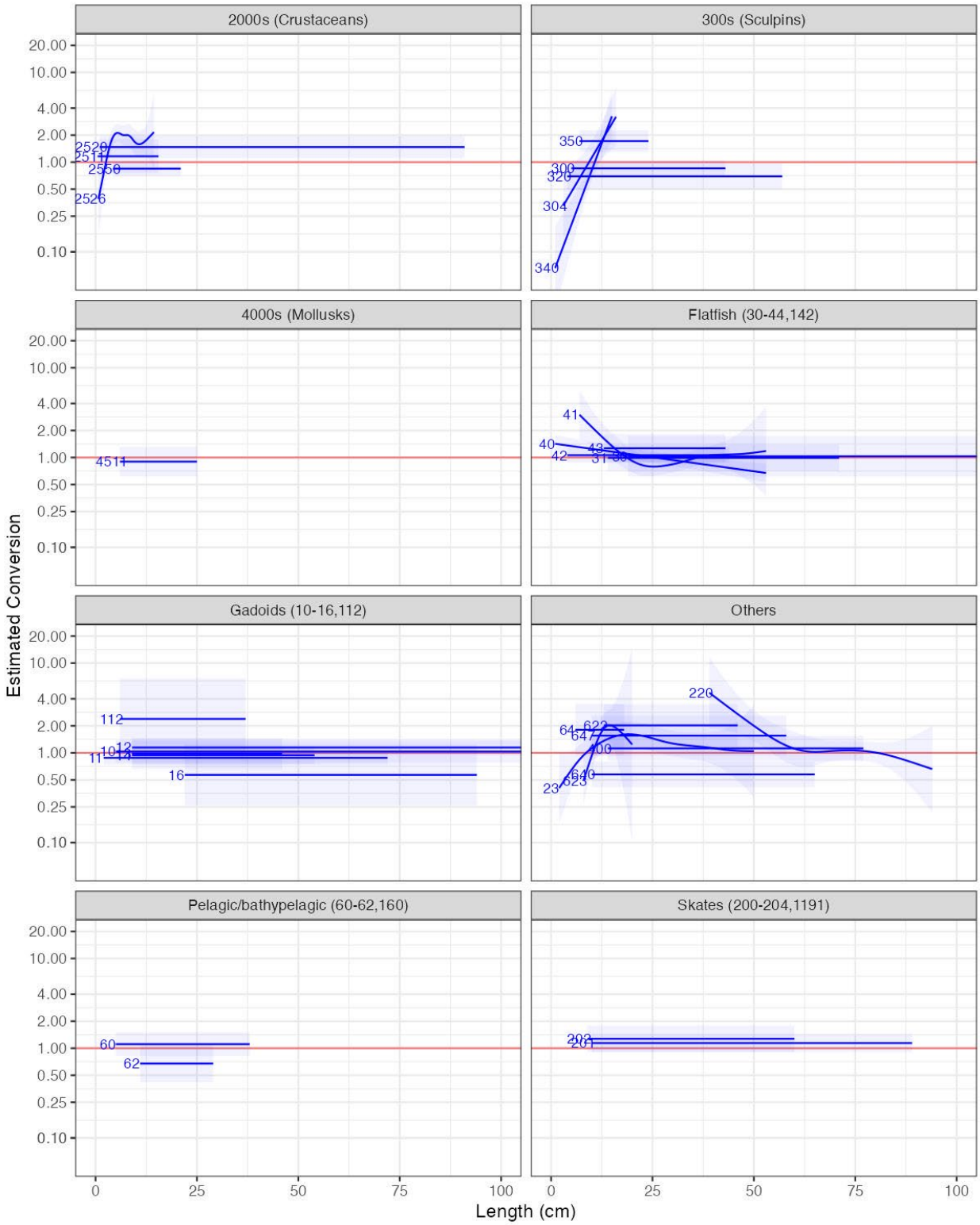

Figure 6. Estimated conversion factors and 95% CI for taxa (see Table 5 for codes) catch numbers using length-disaggregated models (LDM, see Section 2.2 for details). Red horizontal lines indicate a conversion equal to one. Taxa were clustered roughly based on taxonomy (and identified using the taxon codes) in each panel.

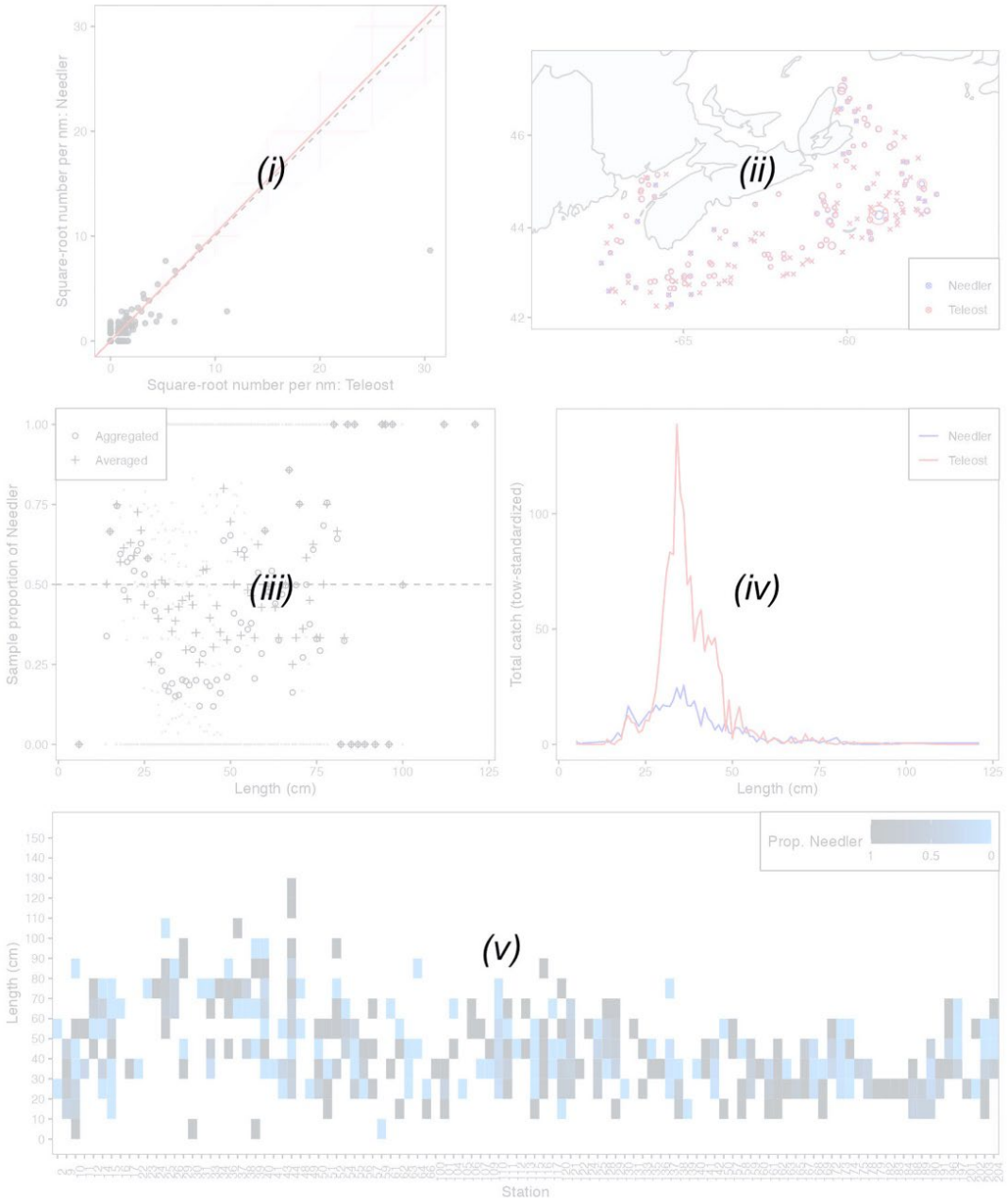

Figure 7.Interpretation for the first of three sets of figures presenting the data and results for taxa for which length-disaggregated analyses were undertaken. (i) Biplot of the square-root of Needler catch numbers against the square-root of Teleost catch, where the red line and shaded interval show the estimated conversion and approximate 95%CI from the best length-aggregated model. (ii) Presents a map of catches by the CCGS Needler (red circles) and by the Teleost (blue circles) in comparative fishing sets, where circle size is proportional to the number caught and nil catches are indicated by x. (iii) Plot of the empirical proportions of catch in a pair made by the Needler as a function of length for each set pair (grey dots), averaged across set pairs in each length interval (black cross) and aggregated across set pairs (black circles). (iv) Total length frequencies for catches made by Needler (blue line) and by Teleost (red line). (v) compositions of catch proportions by Teleost where lengths were aggregated by 10 cm (or mm) intervals.

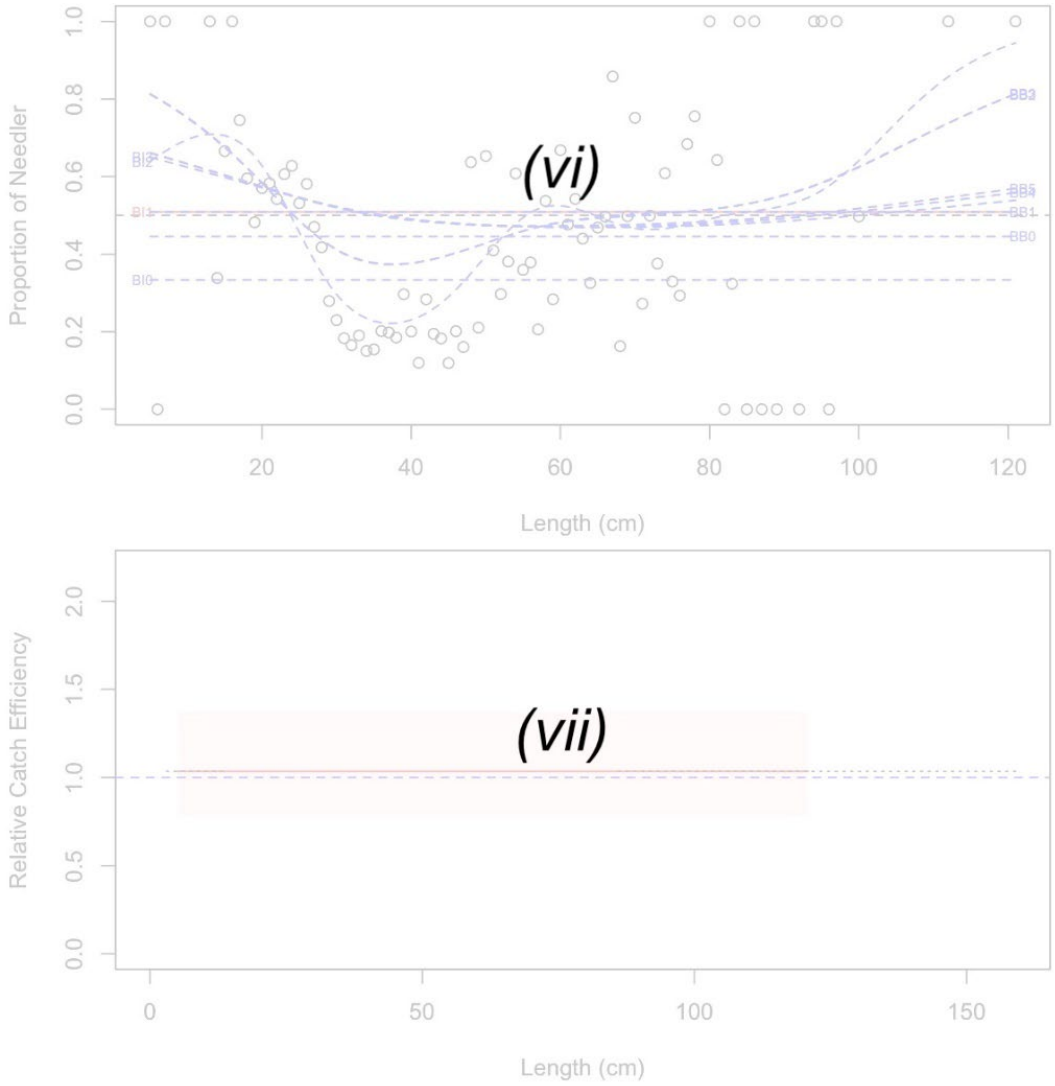

Figure 8. Interpretation for the second of three sets of figures presenting the data and results for taxa for which length-disaggregated analyses were undertaken. (vi) Estimated length-specific catch proportion functions, $logit(p_{Ai}(l))$, for each converged model, with the selected model plotted using a red line along with its approximate 95%CI (shaded area), as well as the length class-specific mean empirical proportion of total catch in a pair made by the CCGS Alfred Needler (black circles). (vii) Estimated relative catch efficiency (conversion factor) function from the best model (with 95% CI). The horizontal dashed red line indicates equivalent efficiency between vessels and the dotted black line indicates the relative catch efficiency function that assumes a constant efficiency at small and large sizes (i.e., extended to minimum and maximum length measurements in the database of historical surveys).

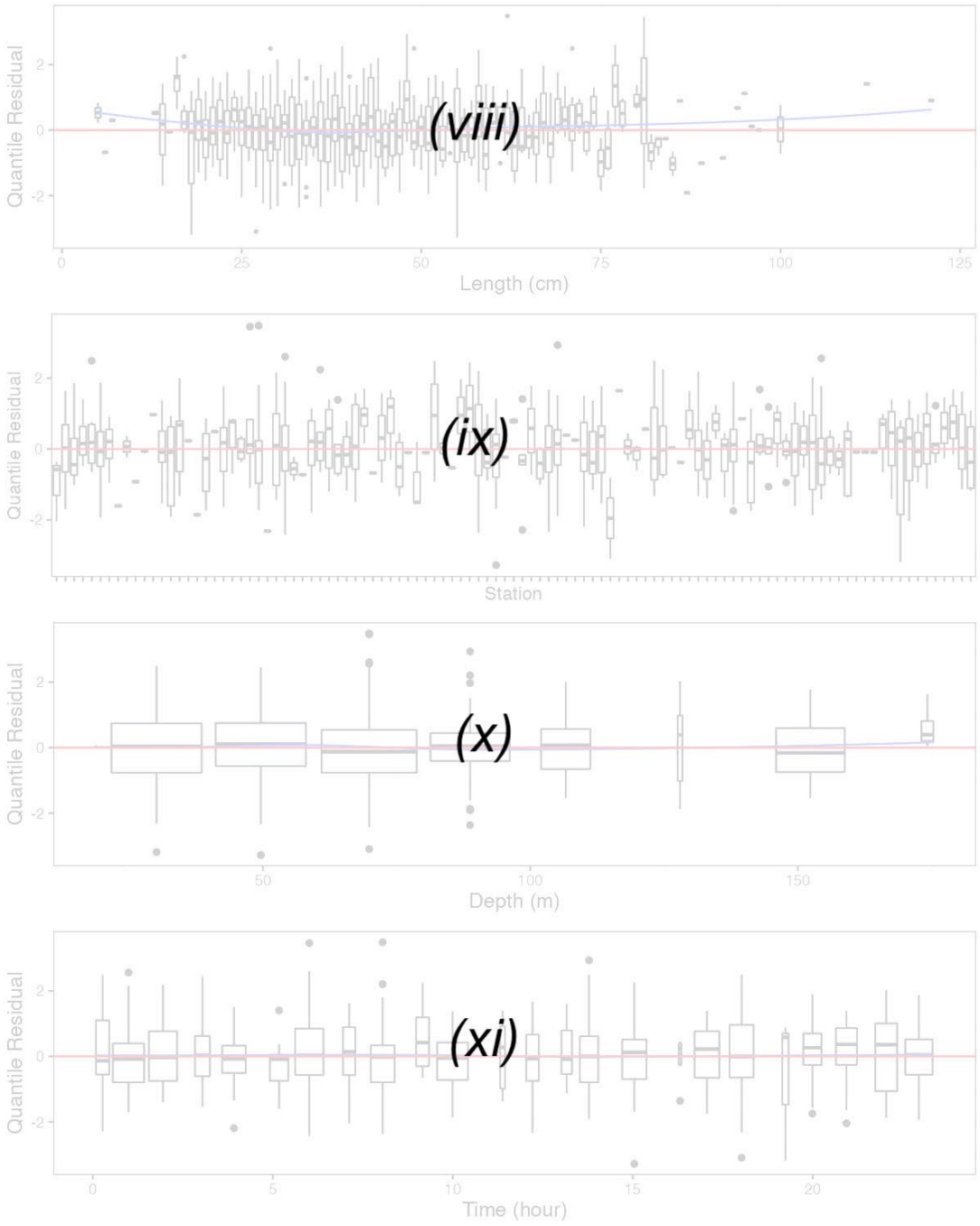

Figure 9. Interpretation for the third of three sets of figures presenting the data and results for taxa for which length-disaggregated analyses were undertaken. Boxplot of normalized quantile residuals as a function of (viii) length, (ix) station, (x) depth class, and (xi) hour. Red horizontal lines indicate zeros and blue lines are smoothers across residuals with a 95% CI in blue shaded area.

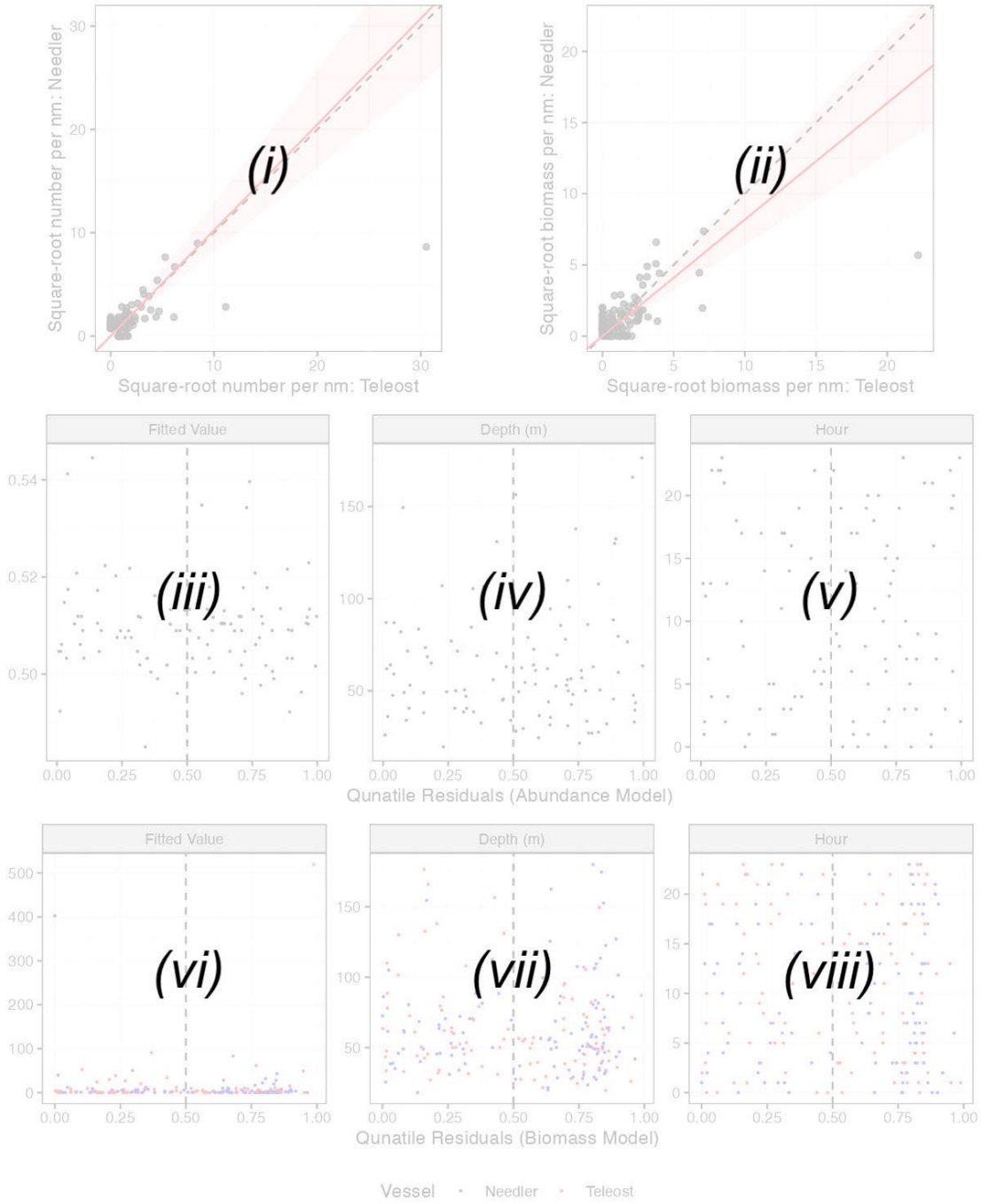

Figure 10. Interpretation for the figures presenting the data and results for taxa for which size-aggregated analyses were undertaken. (i) Biplot of the square-root of Needler catch numbers against the square-root of Teleost catch numbers, where the blue line and shaded interval show the estimated conversion and approximate 95%CI from the best size-aggregated model. (ii) As in (i), except for catch weights. Quantile residuals from the analysis of catch numbers are plotted as a function of (iii) fitted values, and the (v) time and (vii) depth of the paired set (i). Similarly, quantile residuals from the analysis of catch weights are plotted as a function of (iv) fitted values, with values for Needler plotted with blue circles and those for Teleost in red, and the (vi) time and (viii) depth of the paired set. Note that for taxa that are not measured and depending on model conversion, only panels (ii), (iv), (vi) and (viii) are shown.

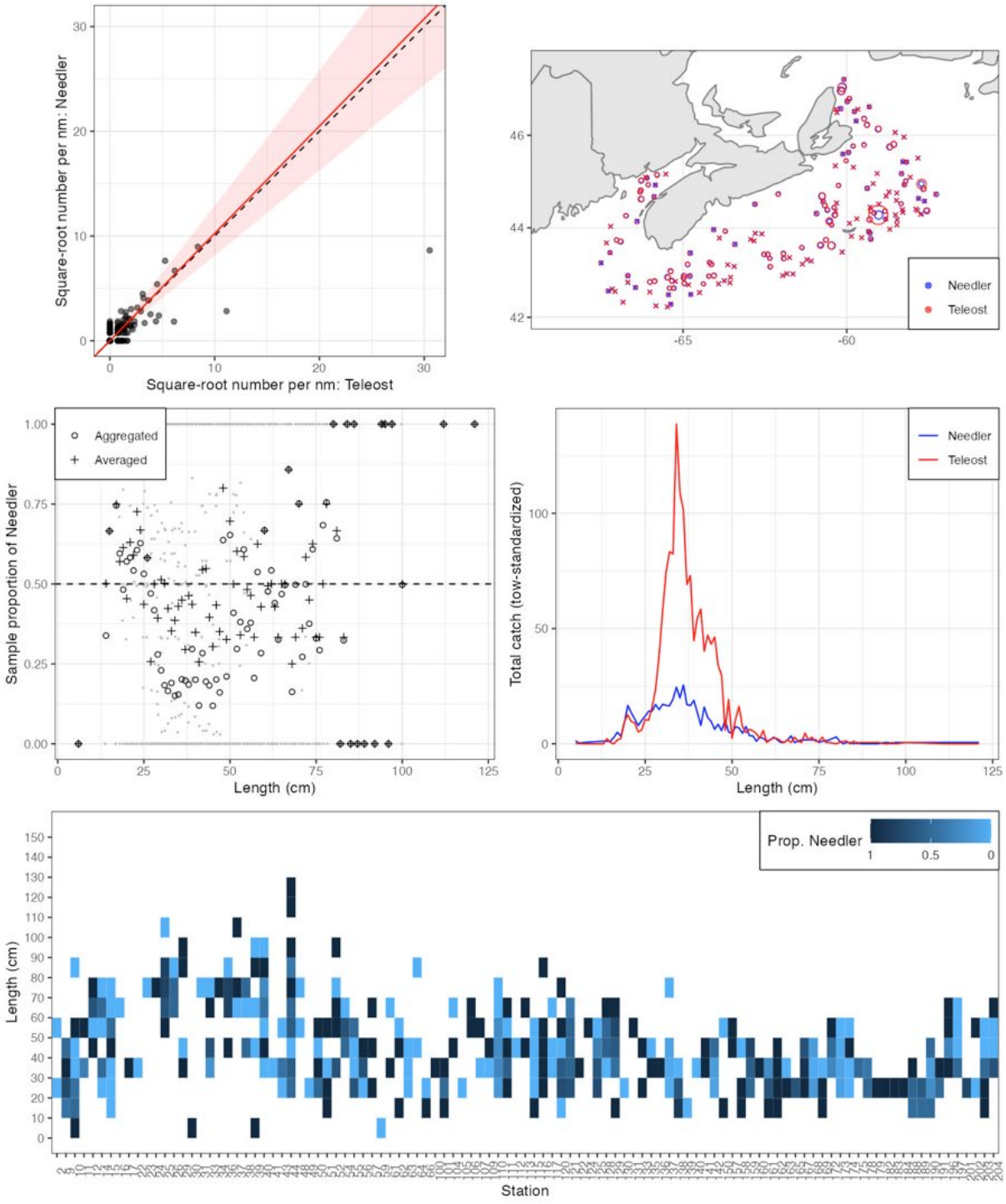

Figure 11a.Visualisation of comparative fishing data and size-aggregated model fit for Gadus morhua (10).

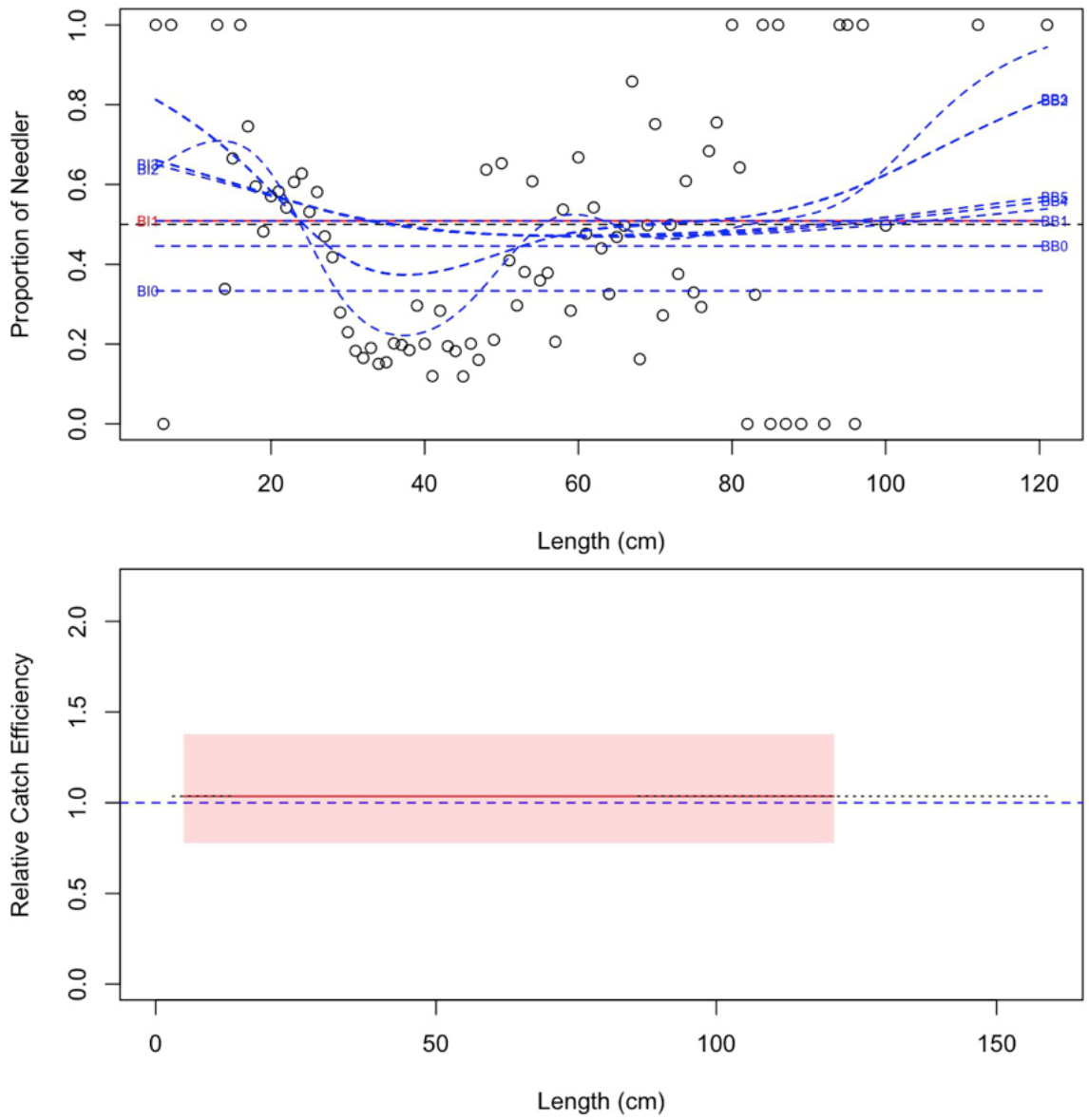

Figure 11b. Model fits and the selected length-based calibration for Gadus morhua (10).

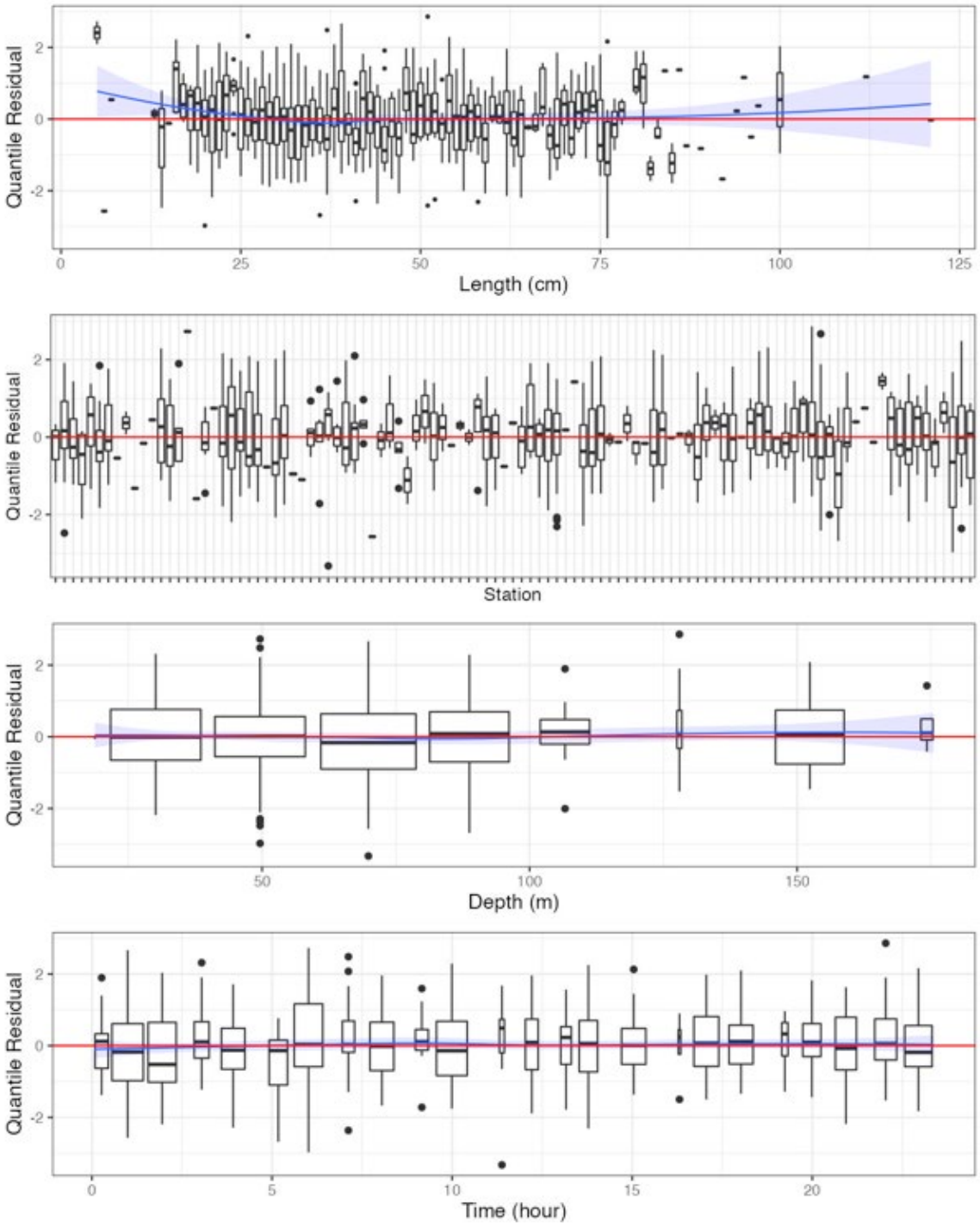

Figure 11c. Randomized and normalized quantile residuals for the selected model for Gadus morhua (10).

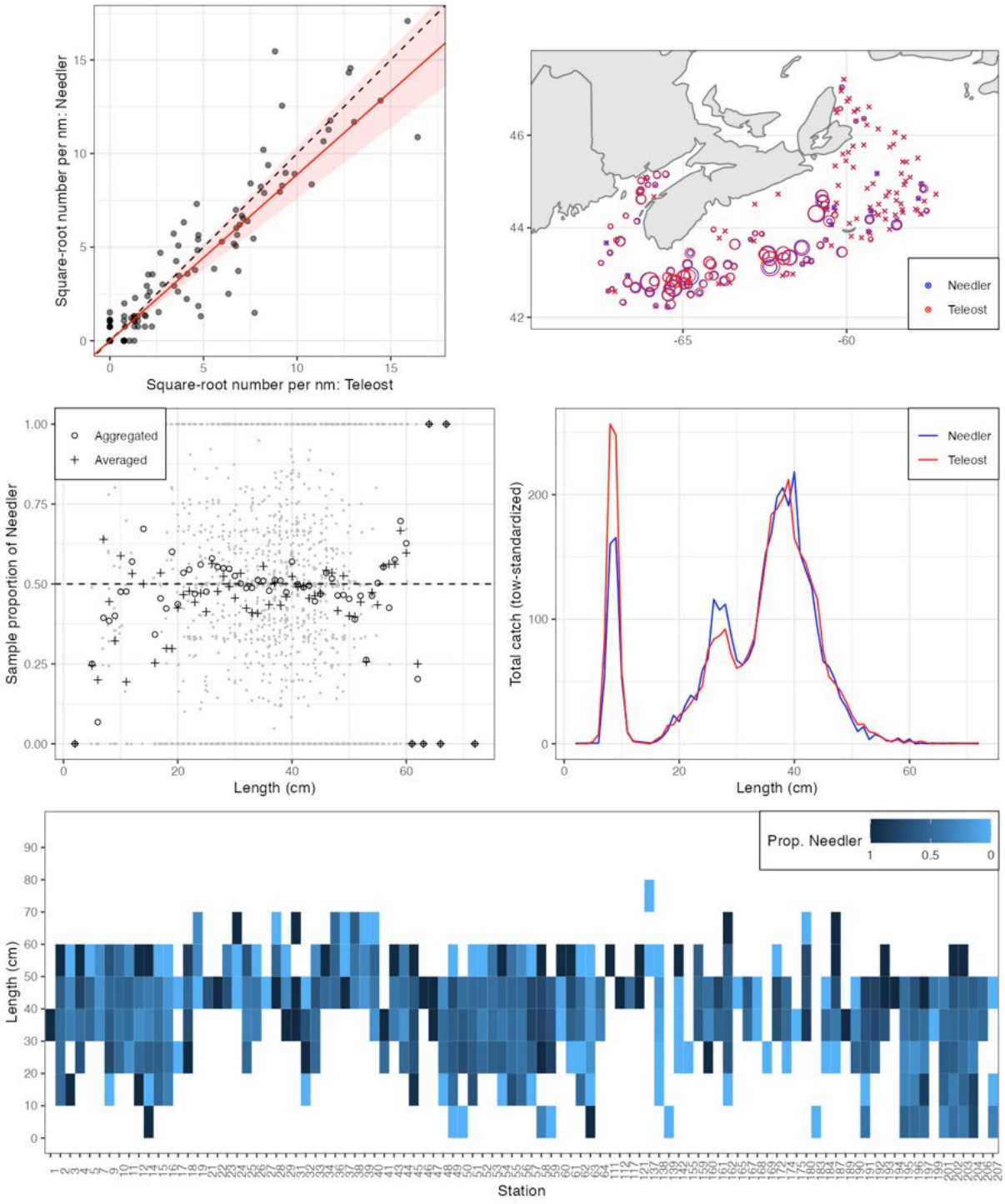

Figure 12a. Visualisation of comparative fishing data and size-aggregated model fit for Melanogrammus aeglefinus (11).

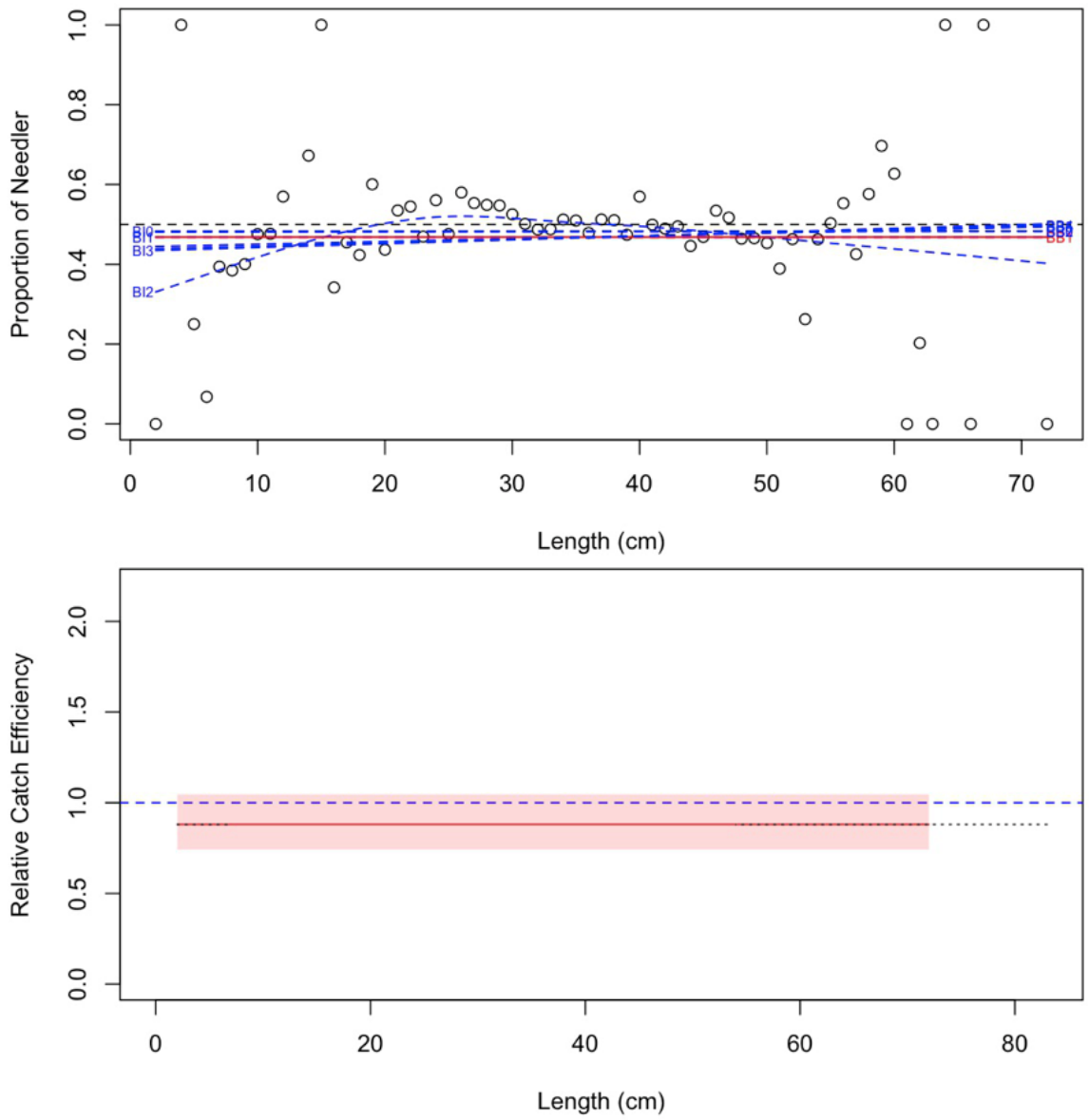

Figure 12b. Model fits and the selected length-based calibration for Melanogrammus aeglefinus (11).

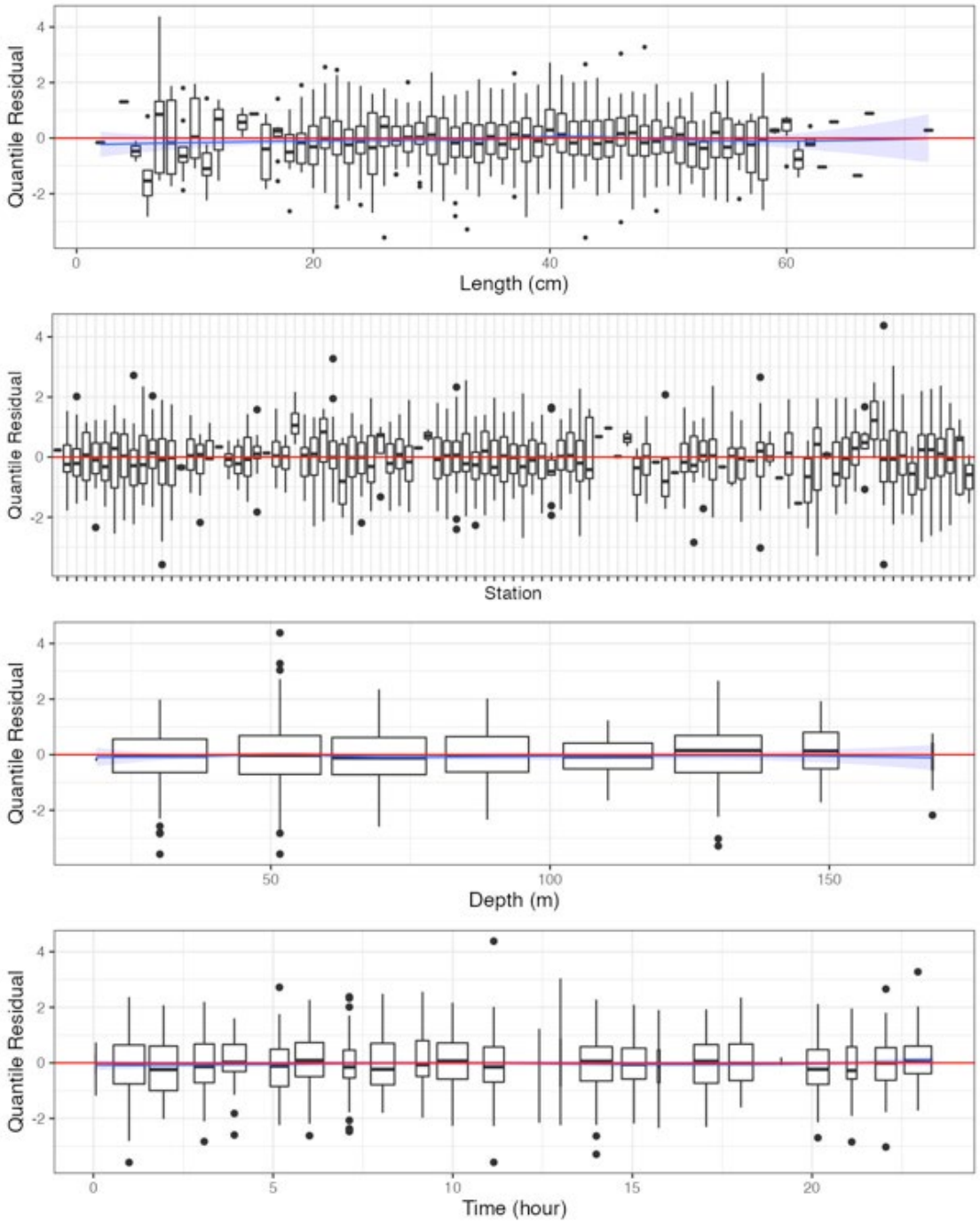

Figure 12c. Randomized and normalized quantile residuals for the selected model for Melanogrammus aeglefinus (11).

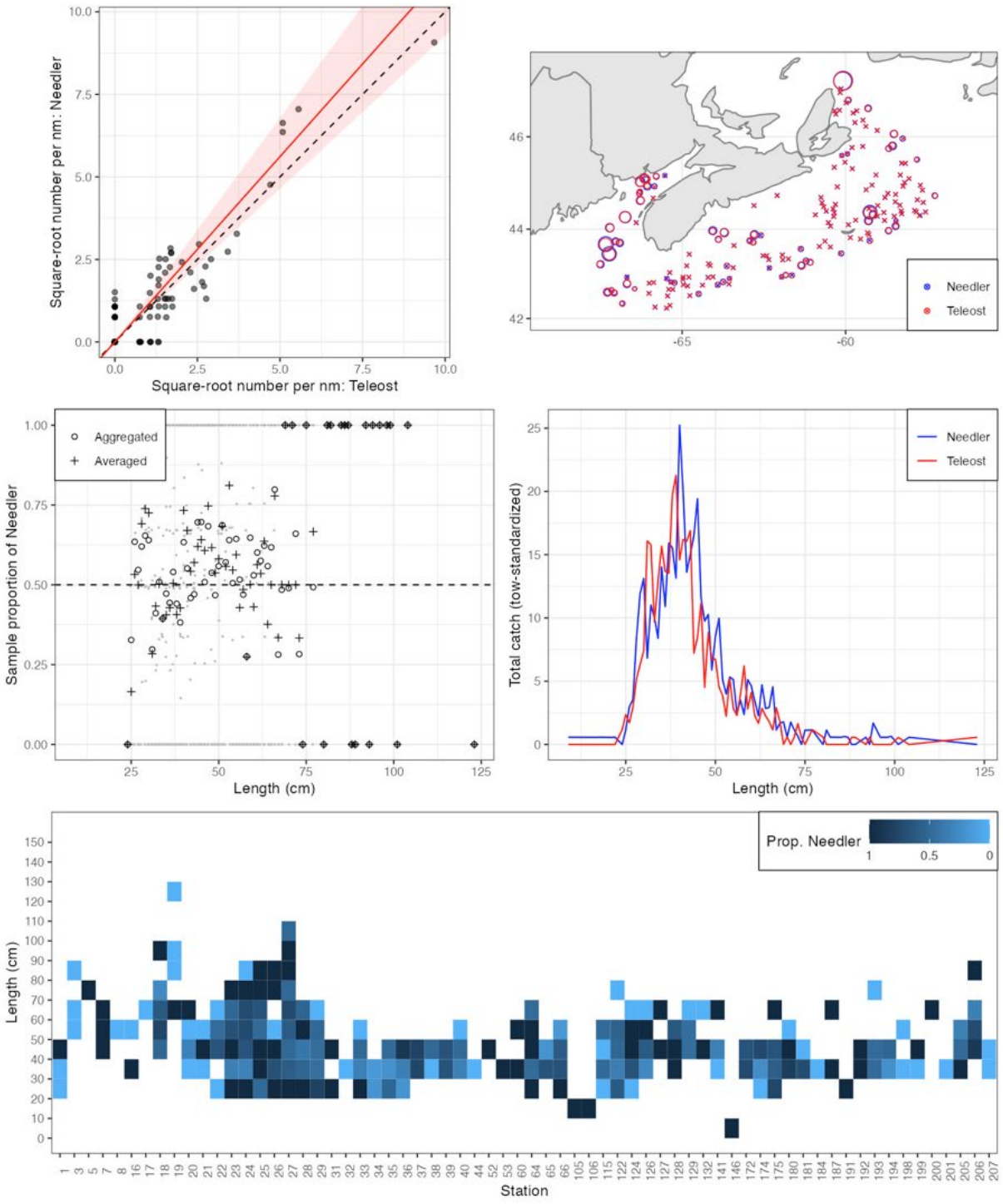

Figure 13a. Visualisation of comparative fishing data and size-aggregated model fit for Urophycis tenuis (12).

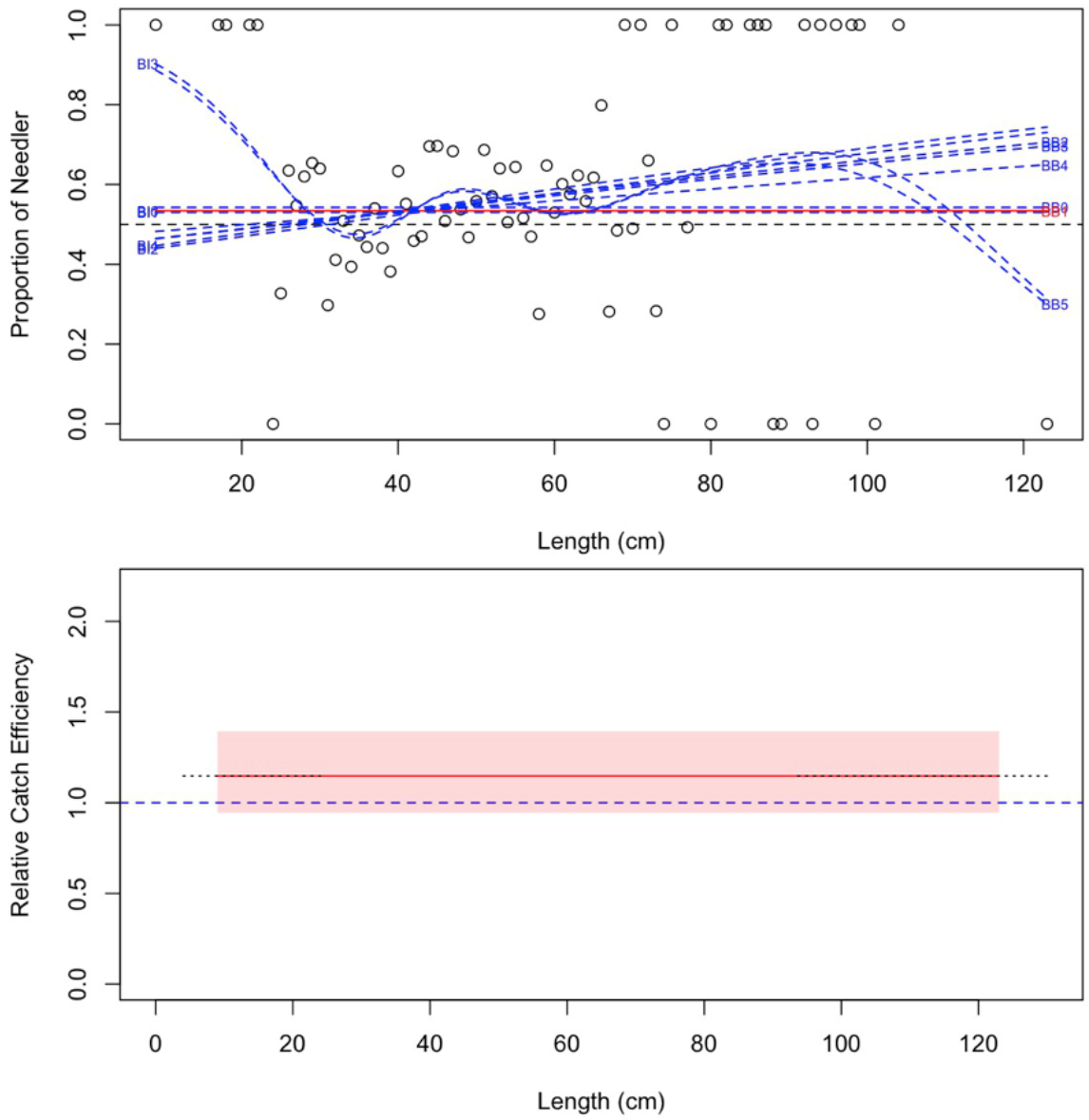

Figure 13b. Model fits and the selected length-based calibration for Urophycis tenuis (12).

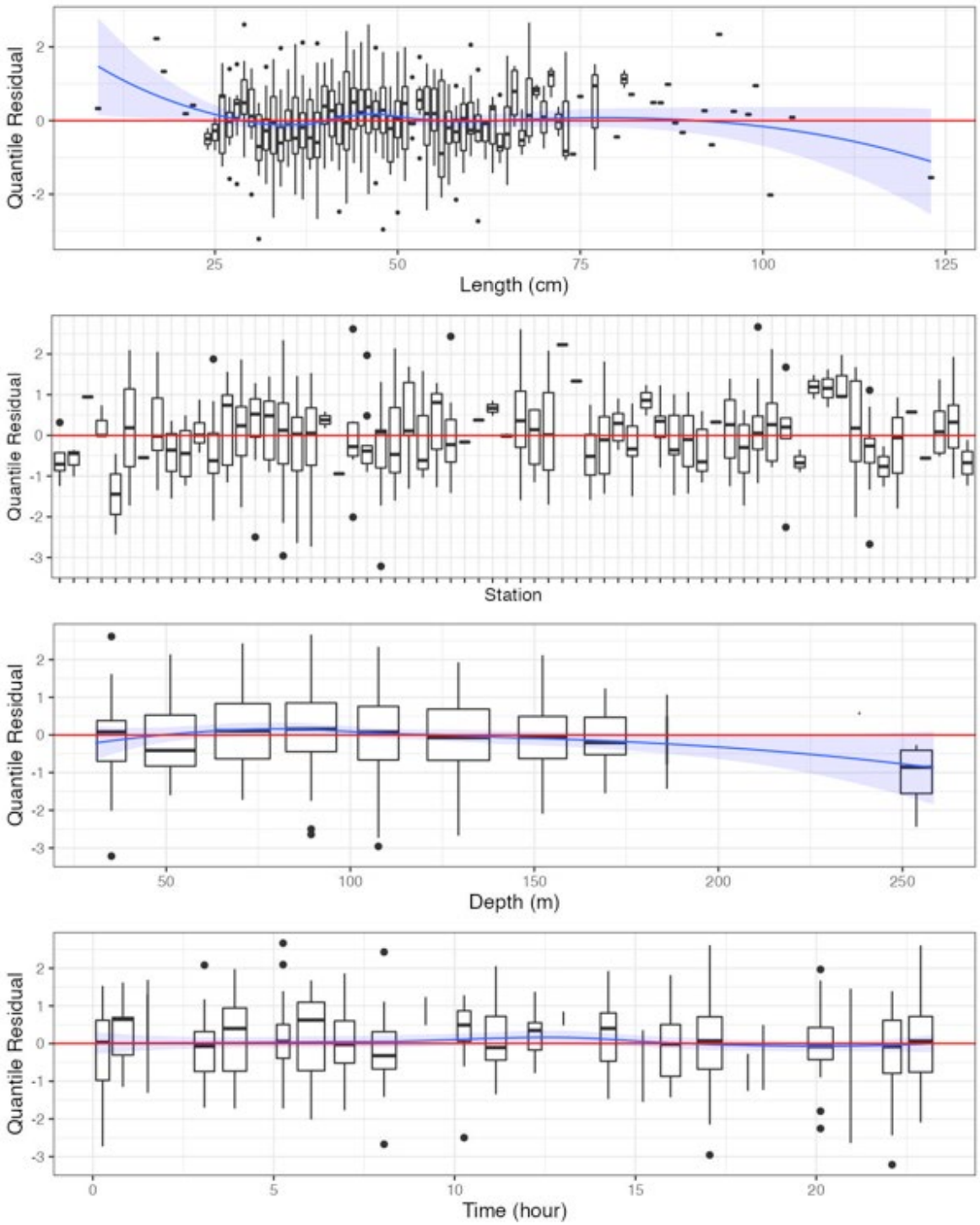

Figure 13c. Randomized and normalized quantile residuals for the selected model for Urophycis tenuis (12).

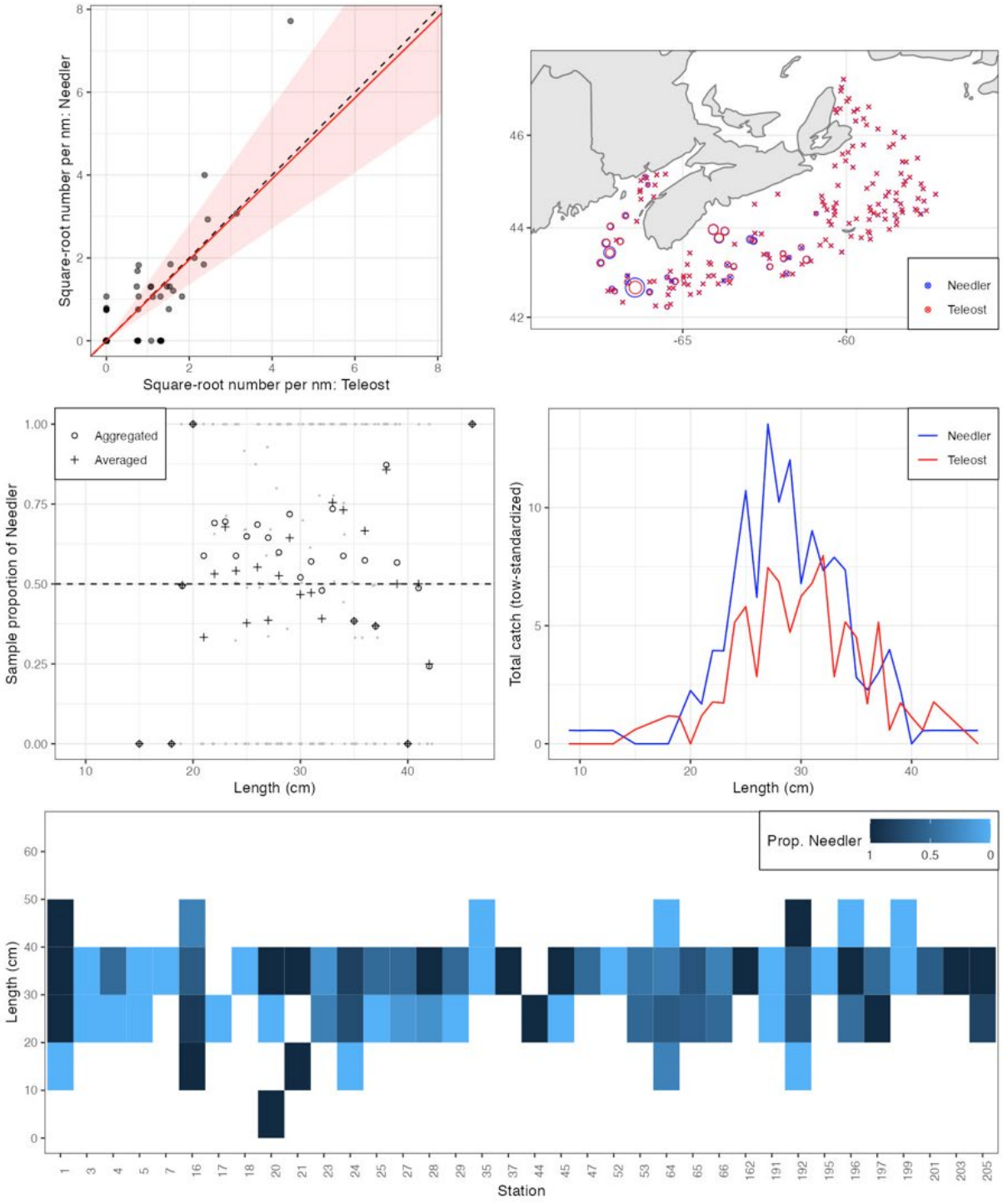

Figure 14a. Visualisation of comparative fishing data and size-aggregated model fit for Urophycis chuss (13).

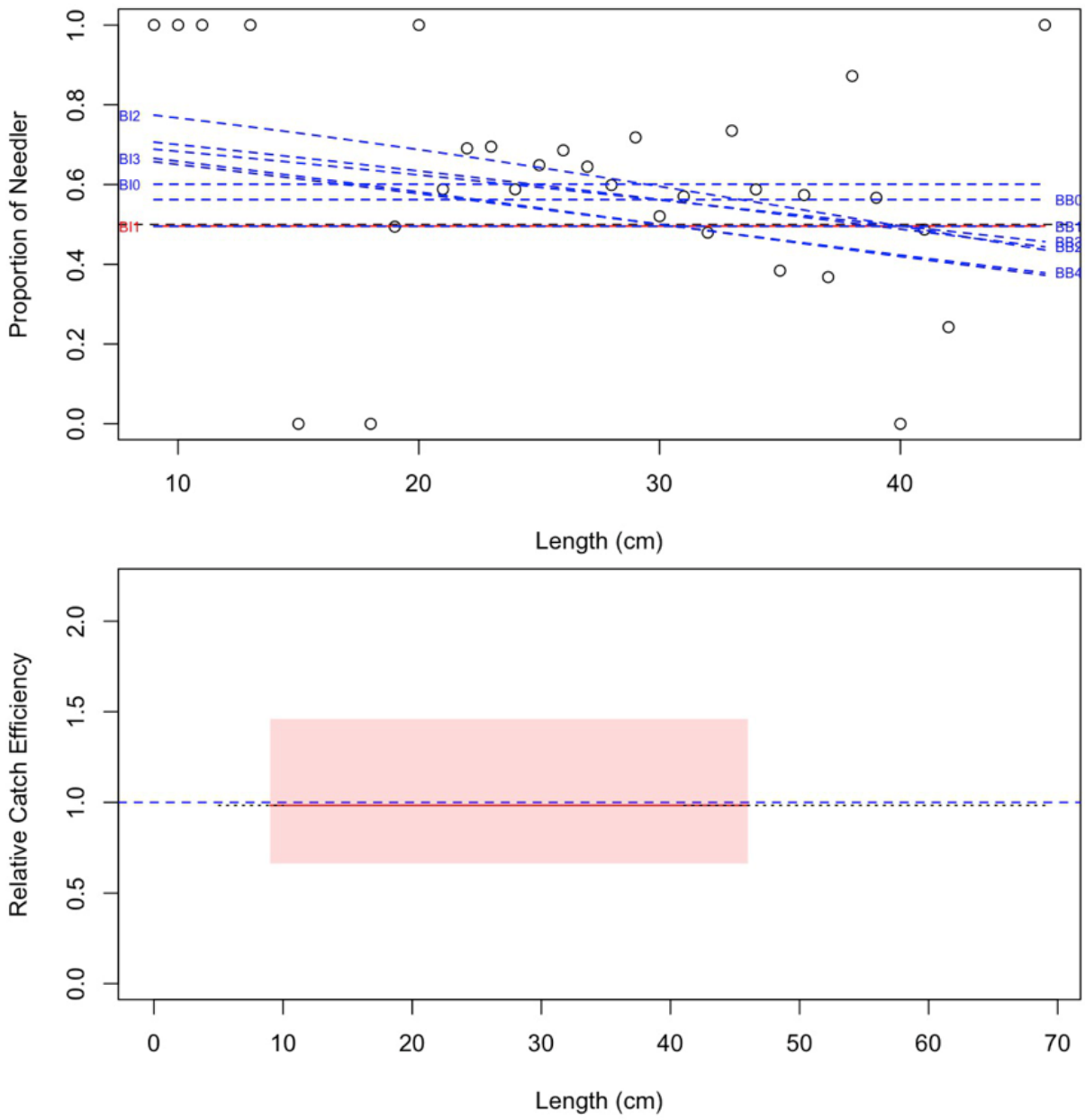

Figure 14b. Model fits and the selected length-based calibration for Urophycis chuss (13).

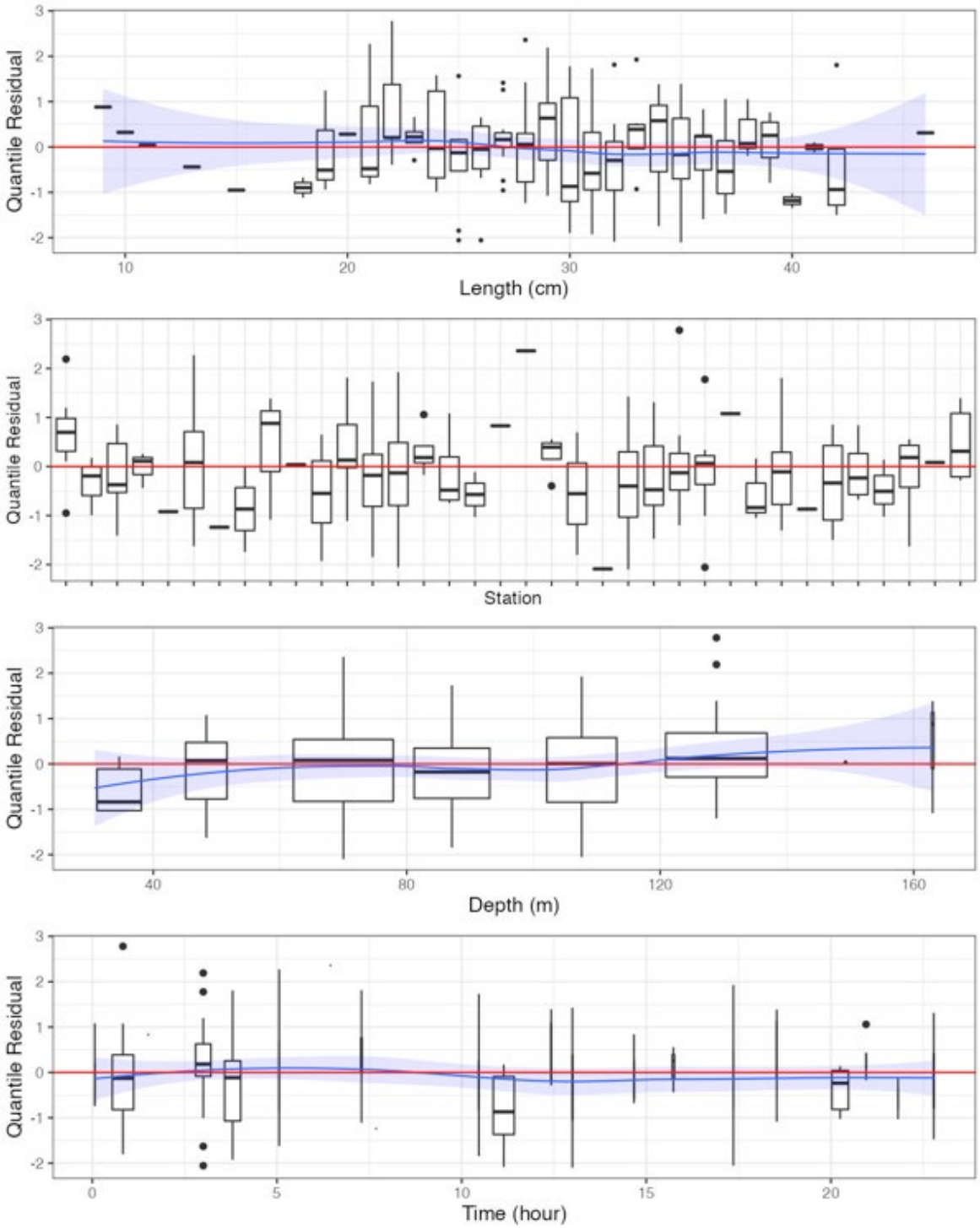

Figure 14c. Randomized and normalized quantile residuals for the selected model for Urophycis chuss (13).

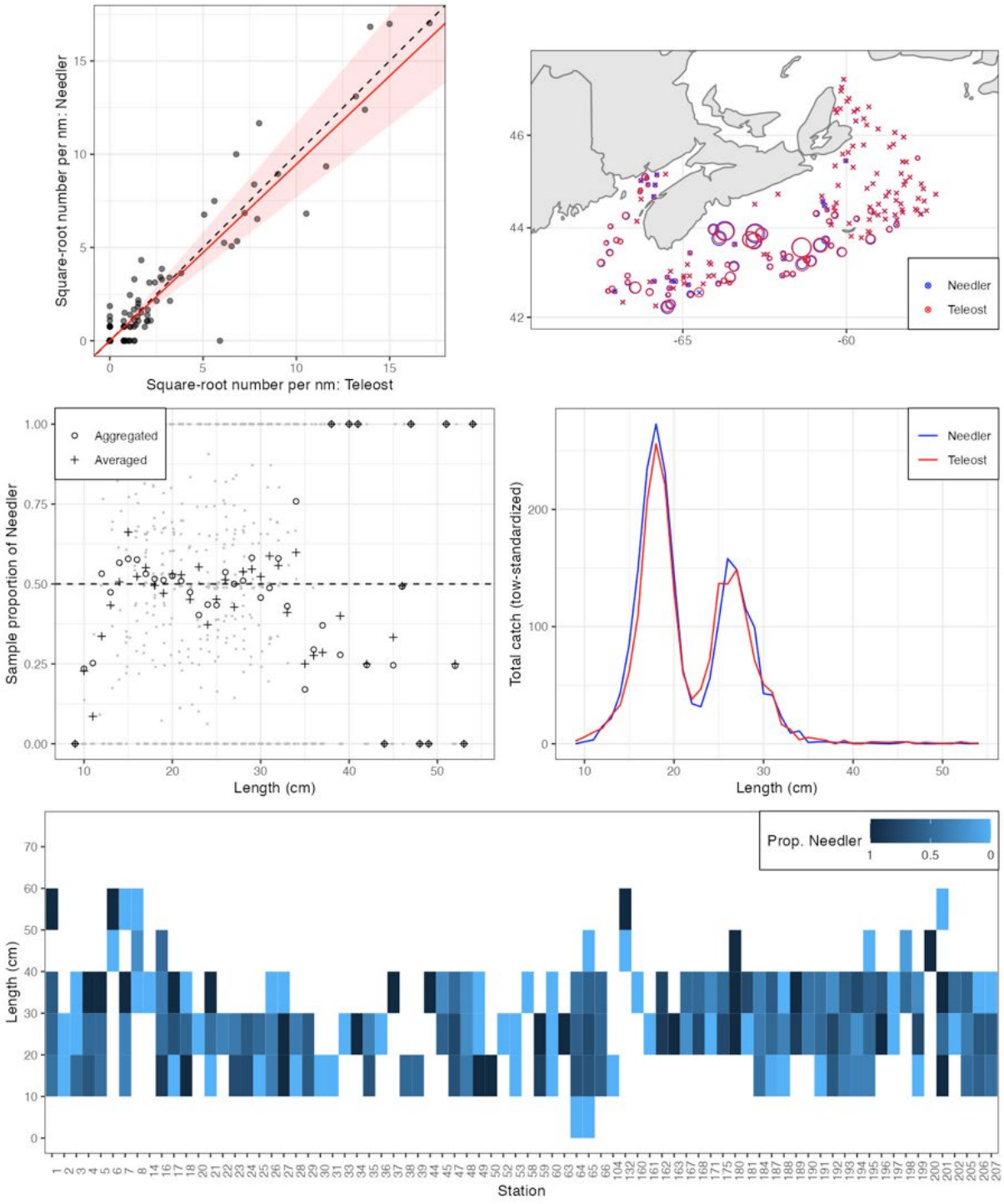

Figure 15a. Visualisation of comparative fishing data and size-aggregated model fit for Merluccius bilinearis (14).

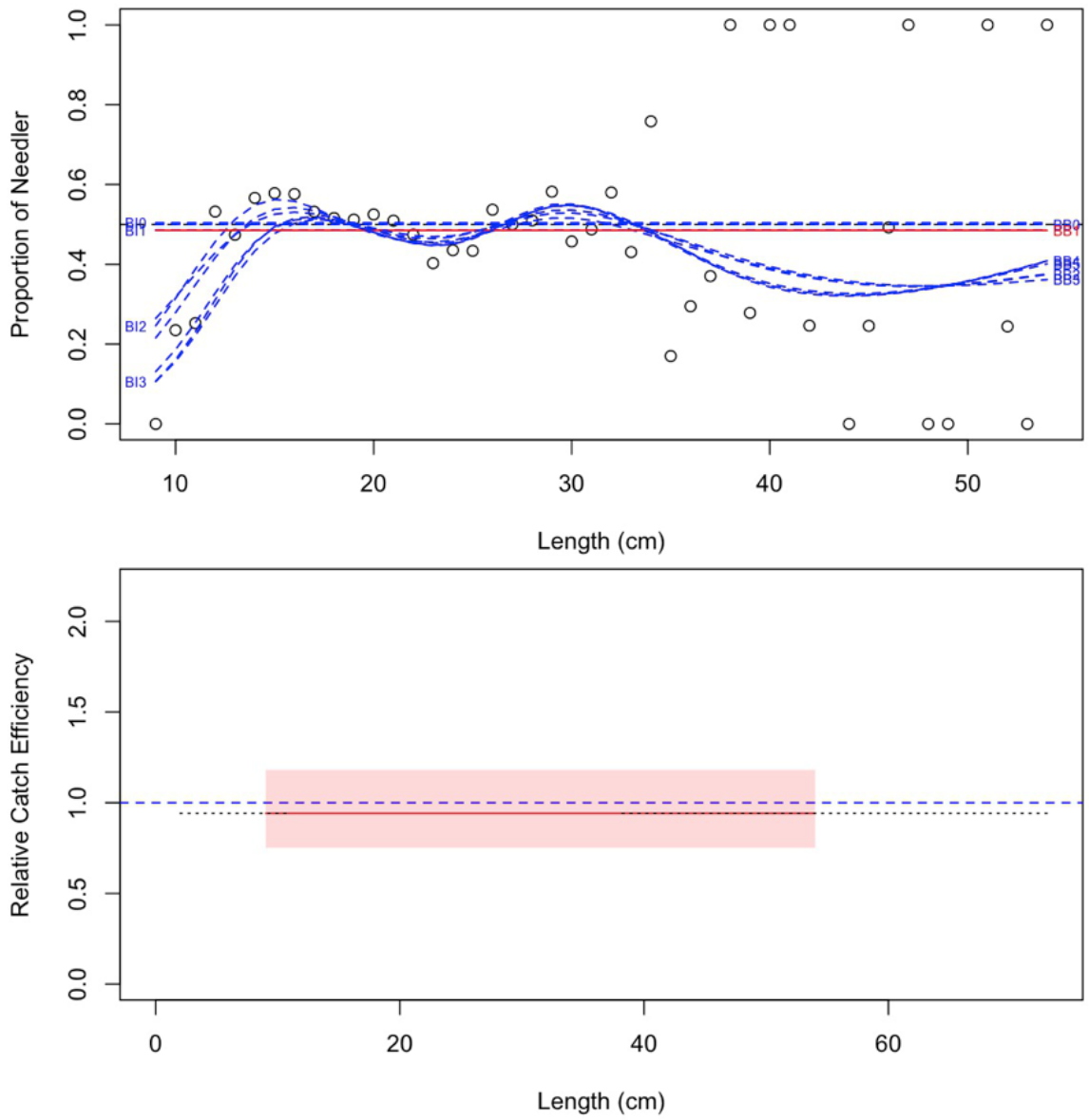

Figure 15b. Model fits and the selected length-based calibration for Merluccius bilinearis (14).

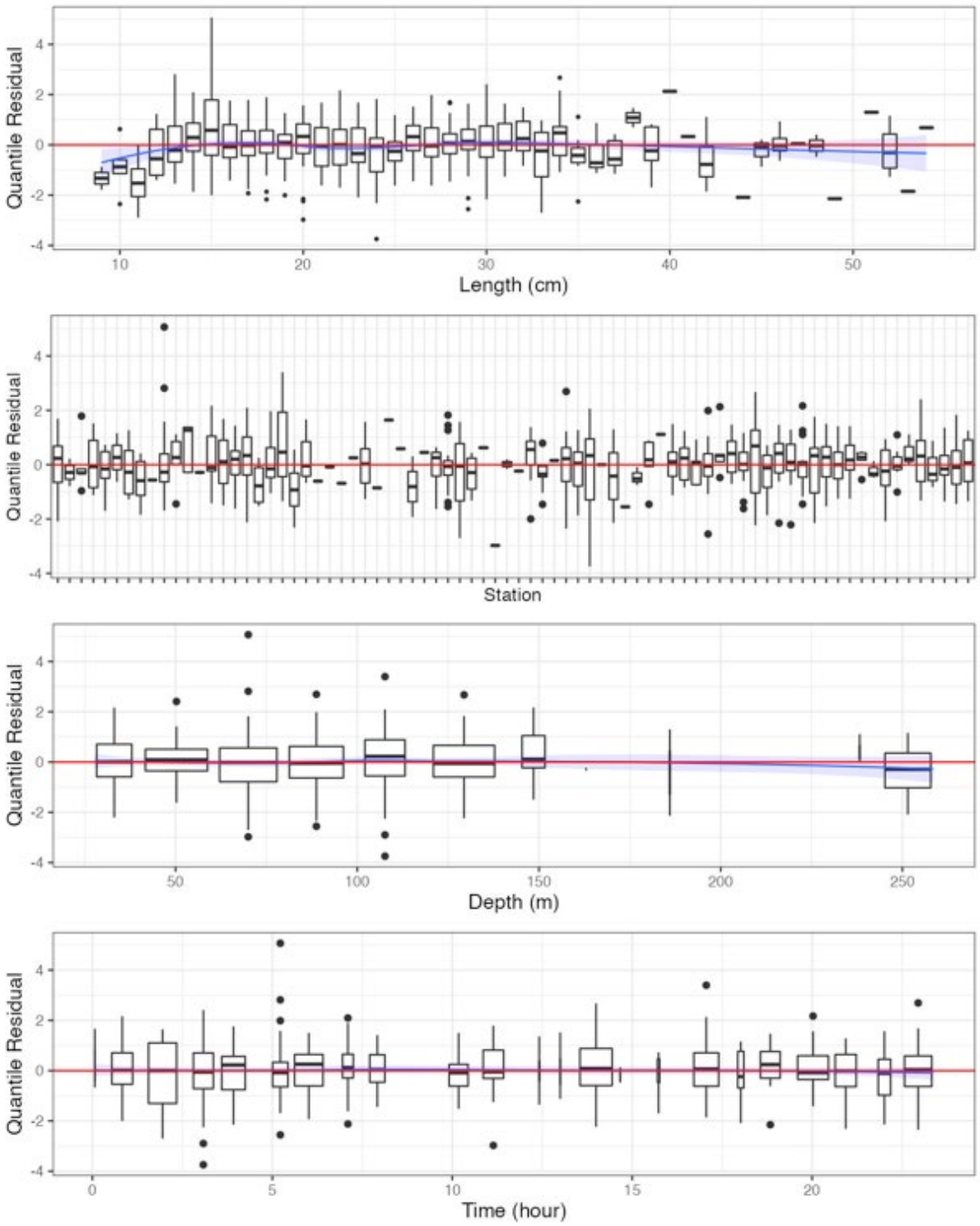

Figure 15c. Randomized and normalized quantile residuals for the selected model for Merluccius bilinearis (14).

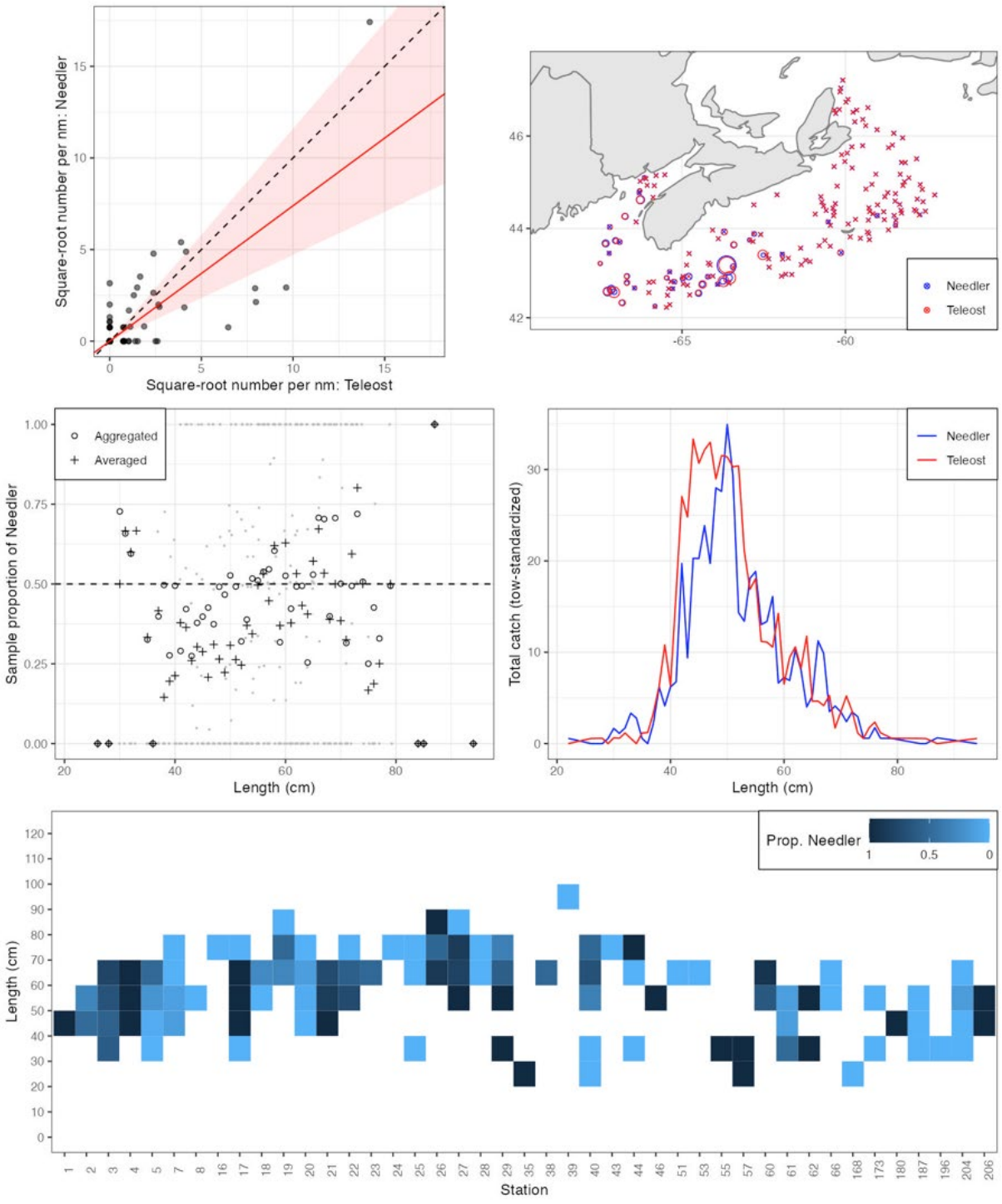

Figure 16a. Visualisation of comparative fishing data and size-aggregated model fit for Pollachius virens (16).

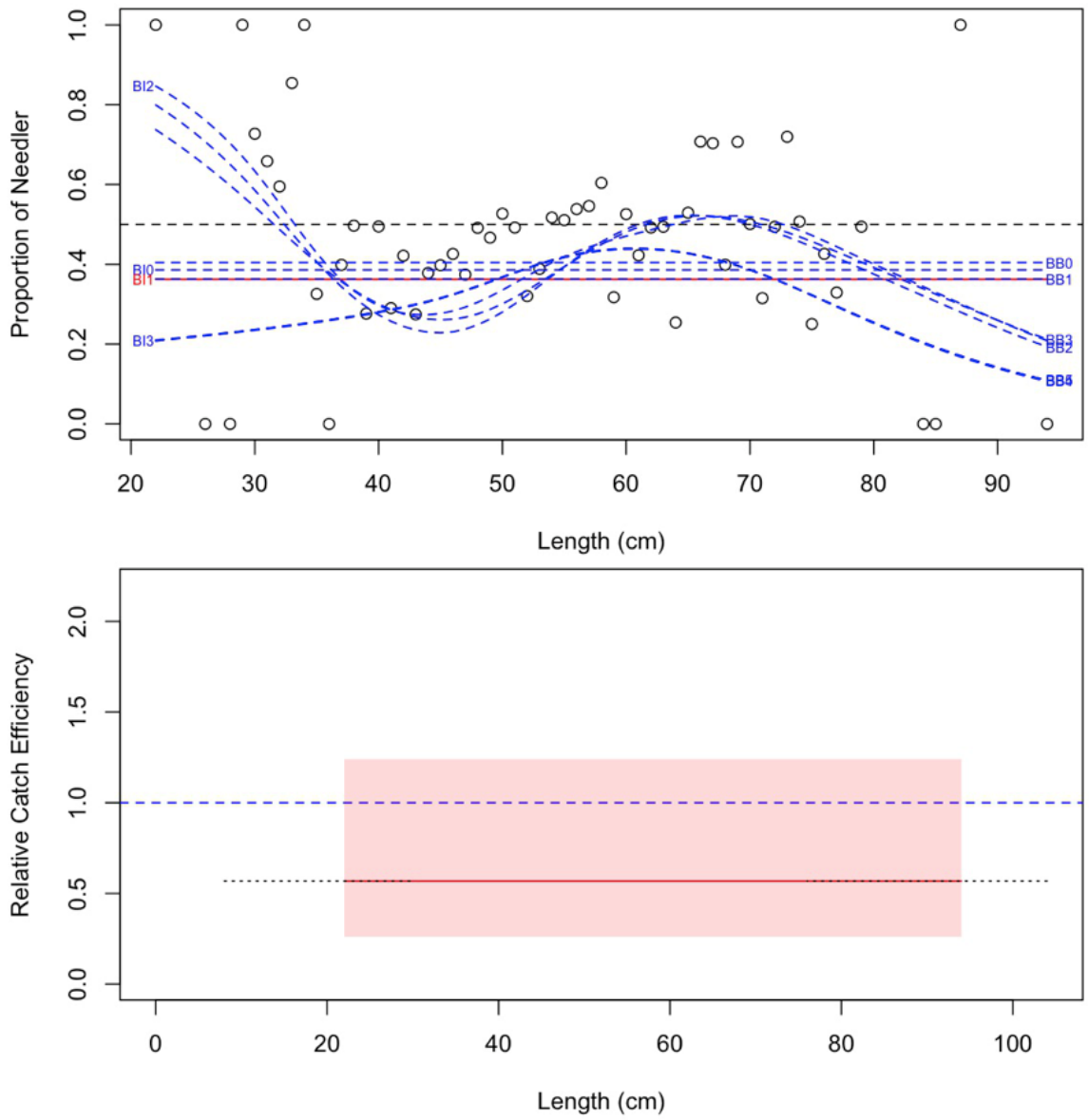

Figure 16b. Model fits and the selected length-based calibration for Pollachius virens (16).

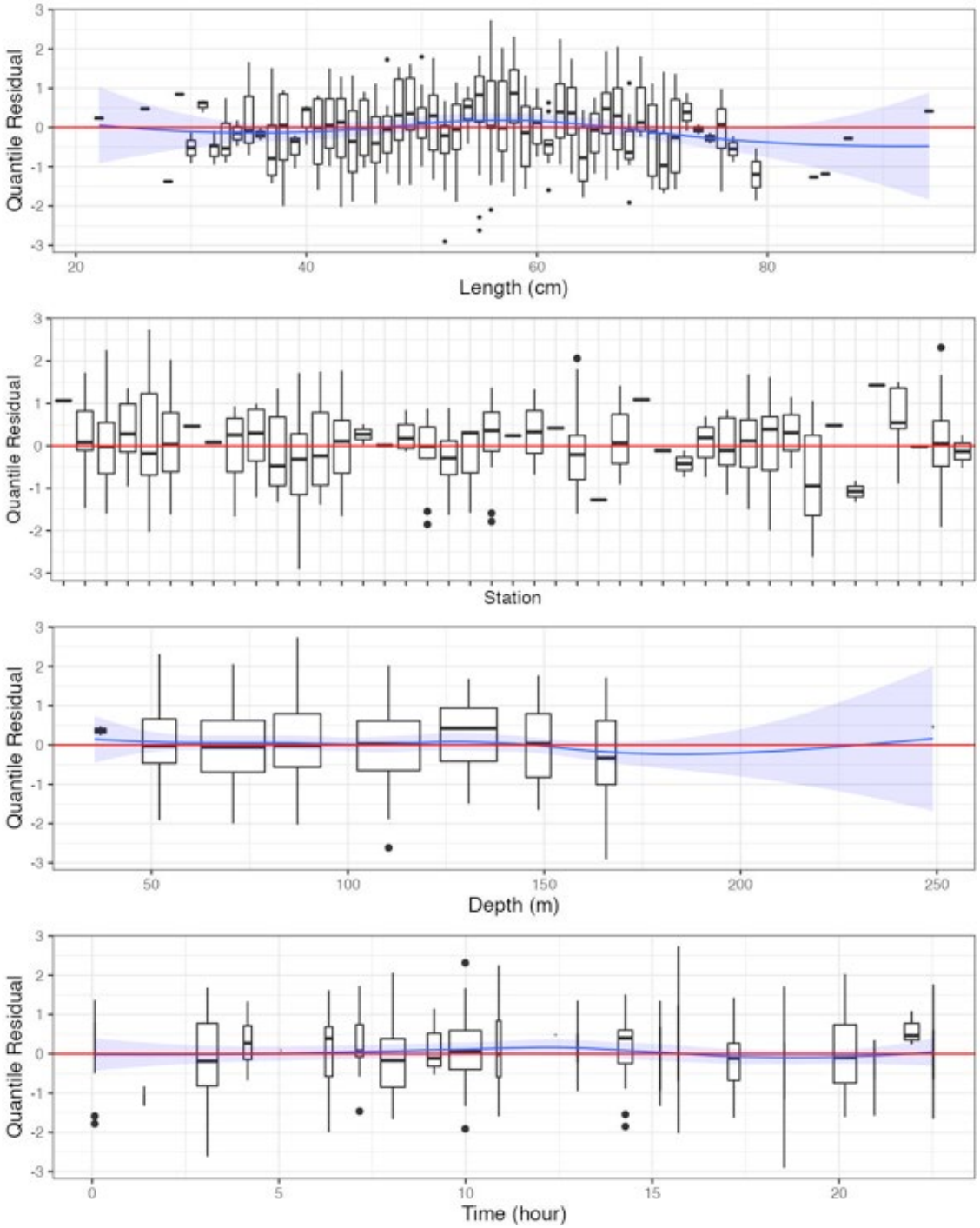

Figure 16c. Randomized and normalized quantile residuals for the selected model for Pollachius virens (16).

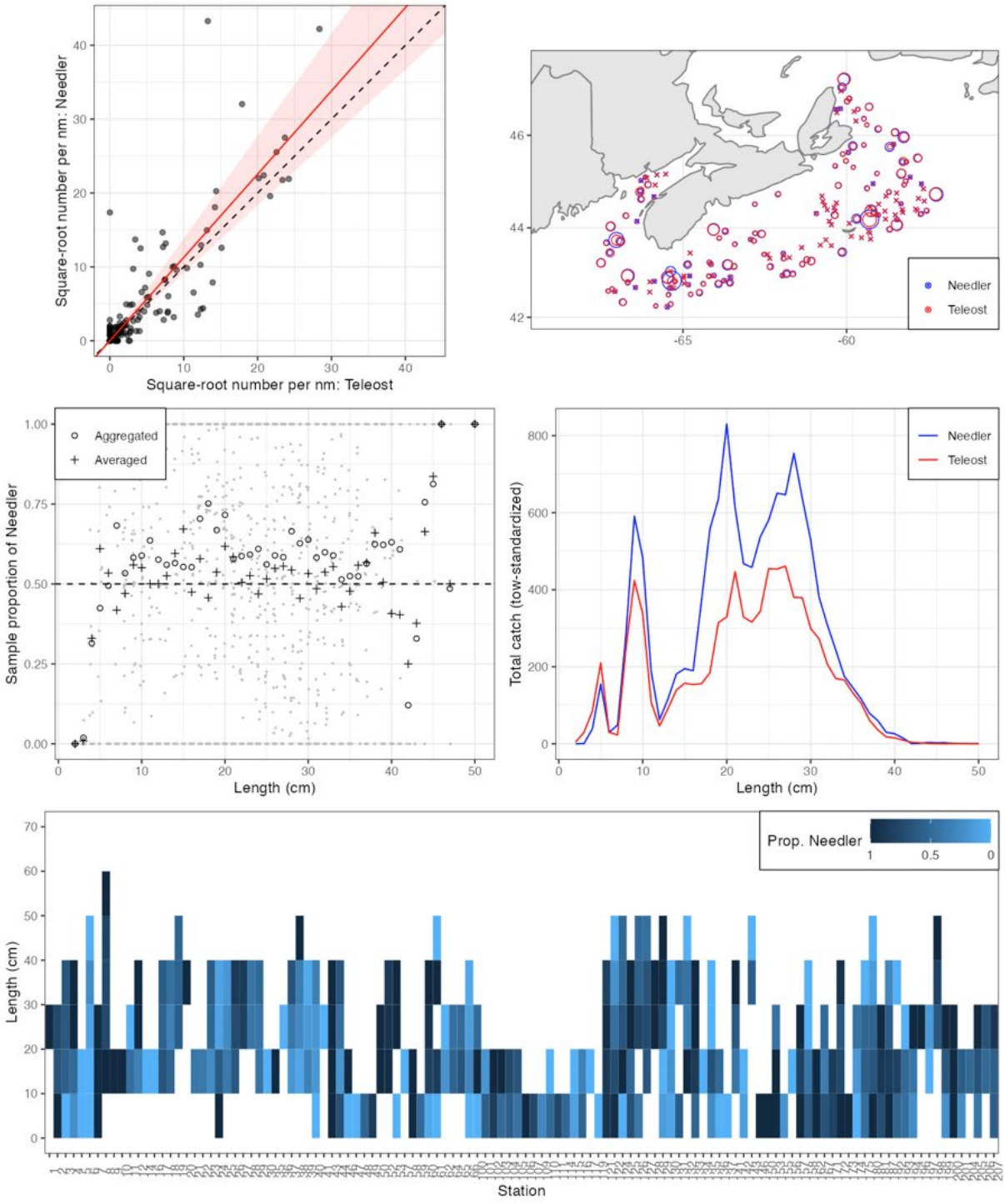

Figure 17a. Visualisation of comparative fishing data and size-aggregated model fit for Sebastes sp. (23).

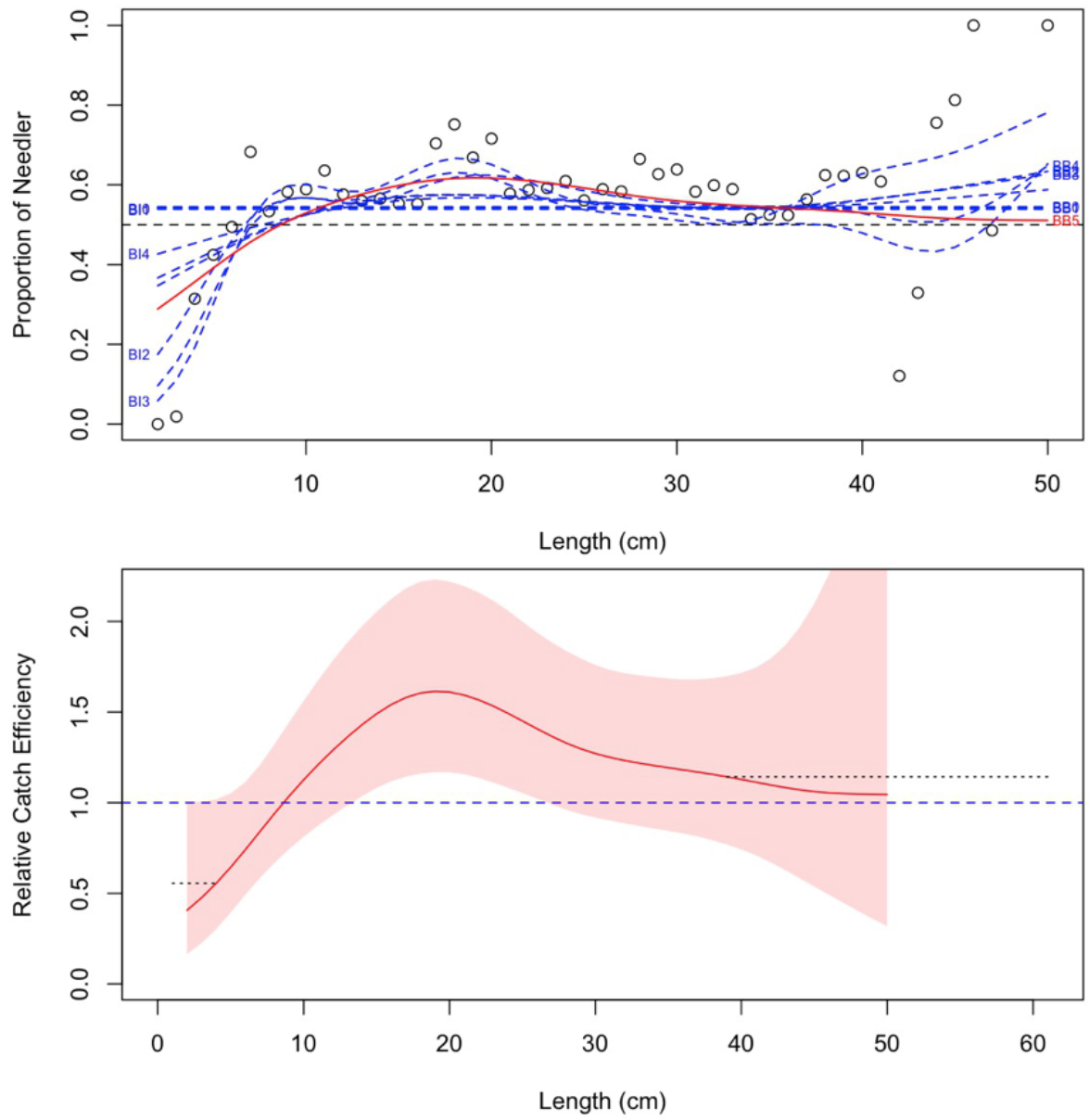

Figure 17b. Model fits and the selected length-based calibration for Sebastes sp. (23).

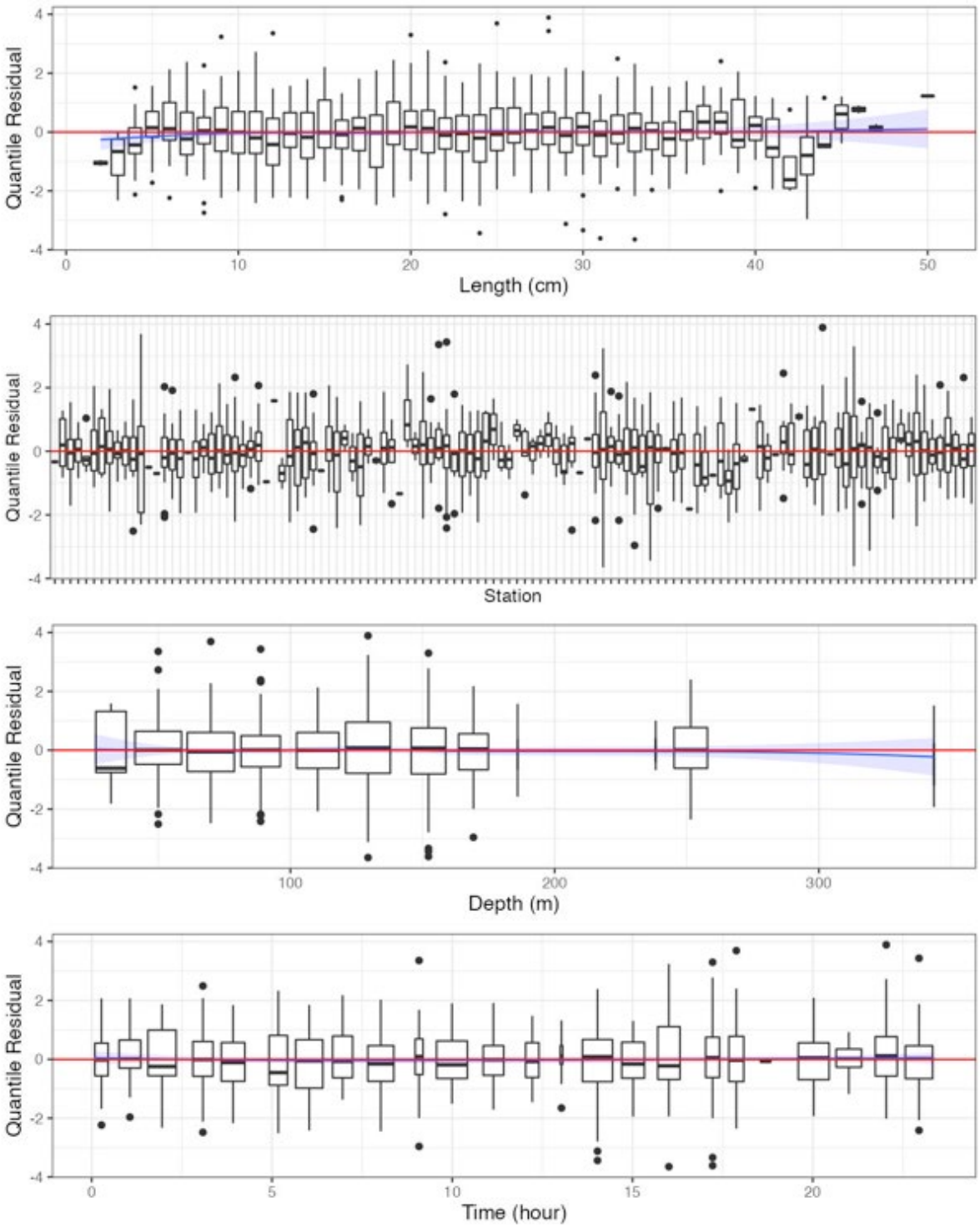

Figure 17c. Randomized and normalized quantile residuals for the selected model for Sebastes sp. (23).

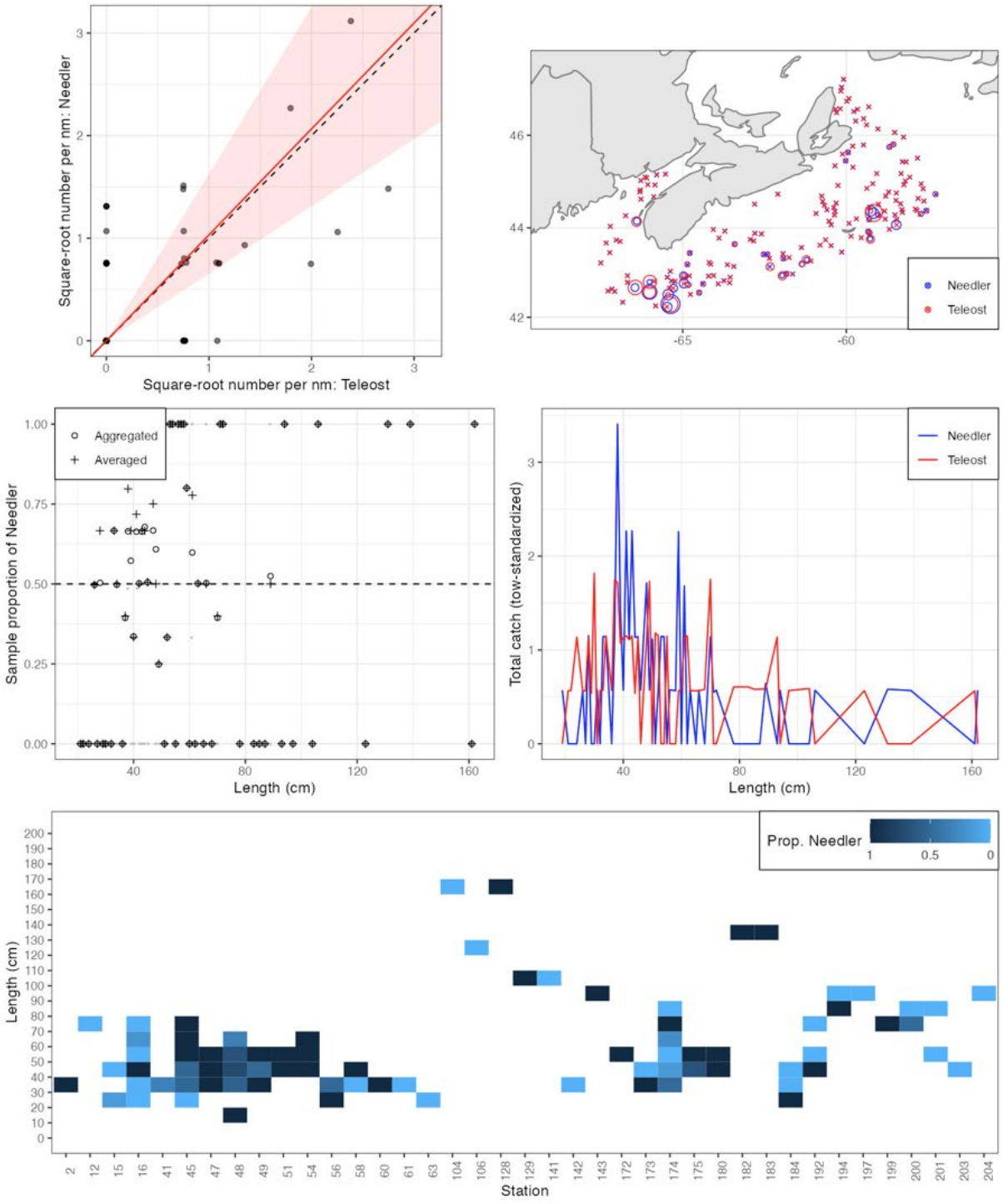

Figure 18a. Visualisation of comparative fishing data and size-aggregated model fit for Hippoglossus hippoglossus (30).

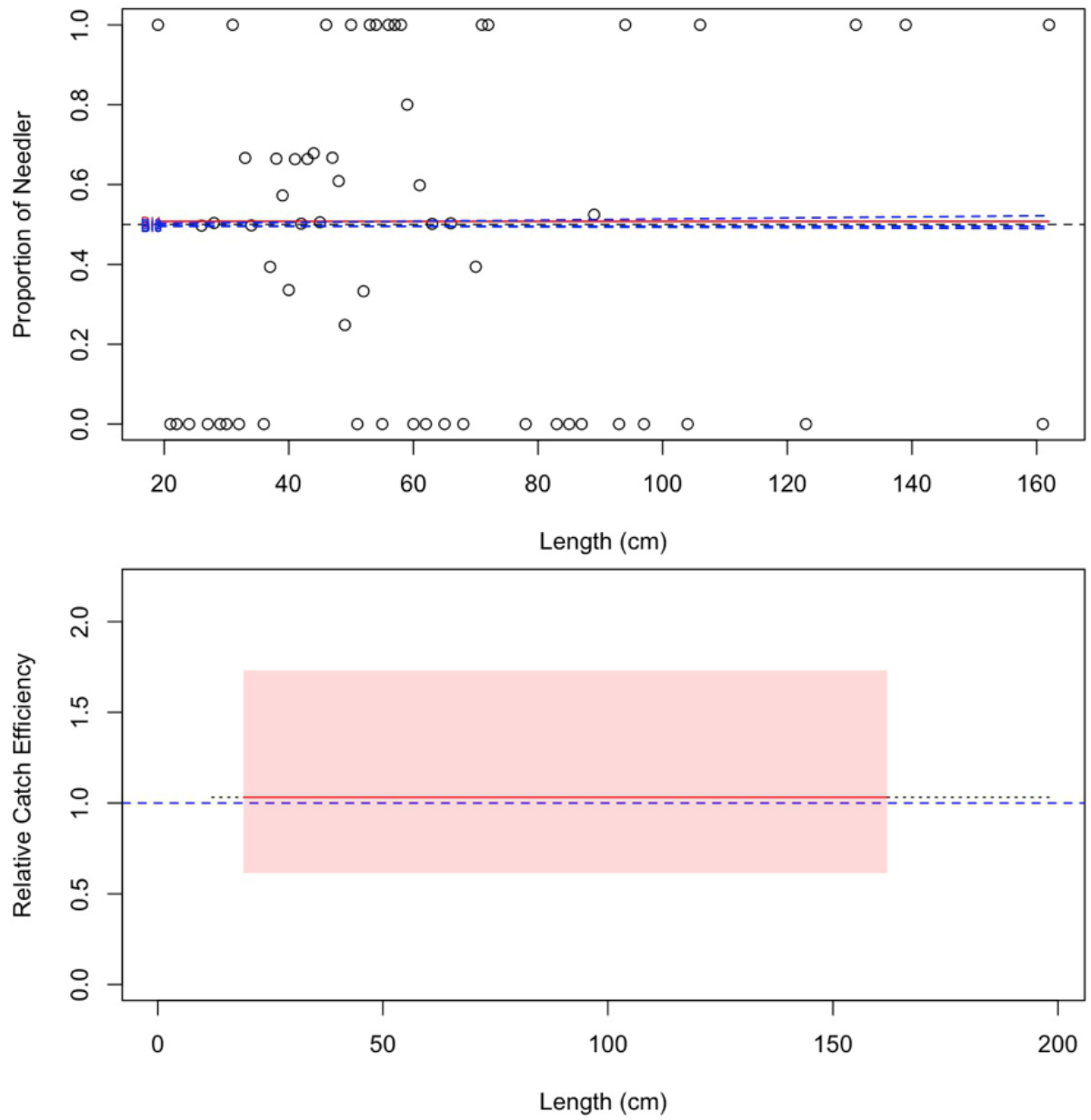

Figure 18b. Model fits and the selected length-based calibration for Hippoglossus hippoglossus (30).

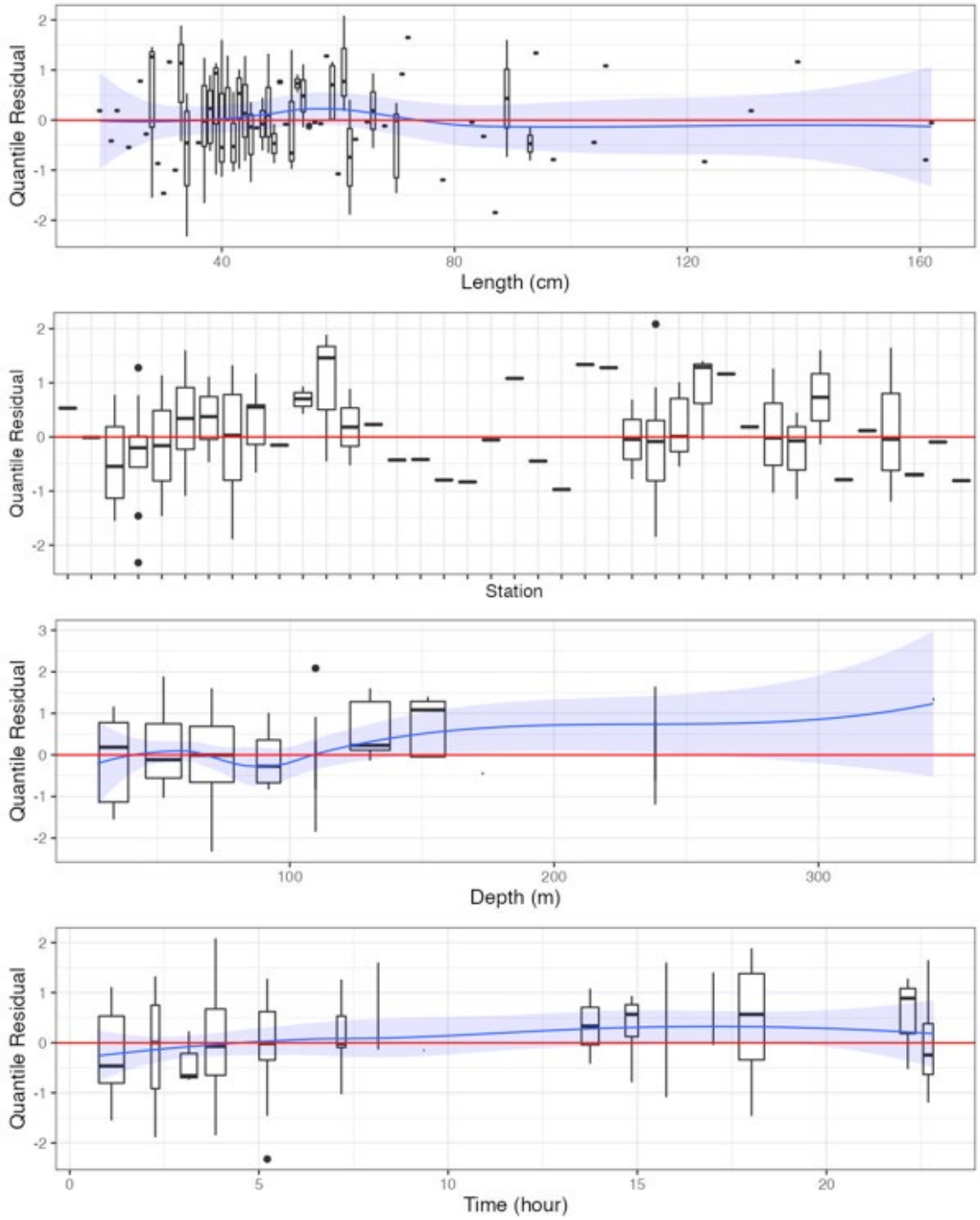

Figure 18c. Randomized and normalized quantile residuals for the selected model for Hippoglossus hippoglossus (30).

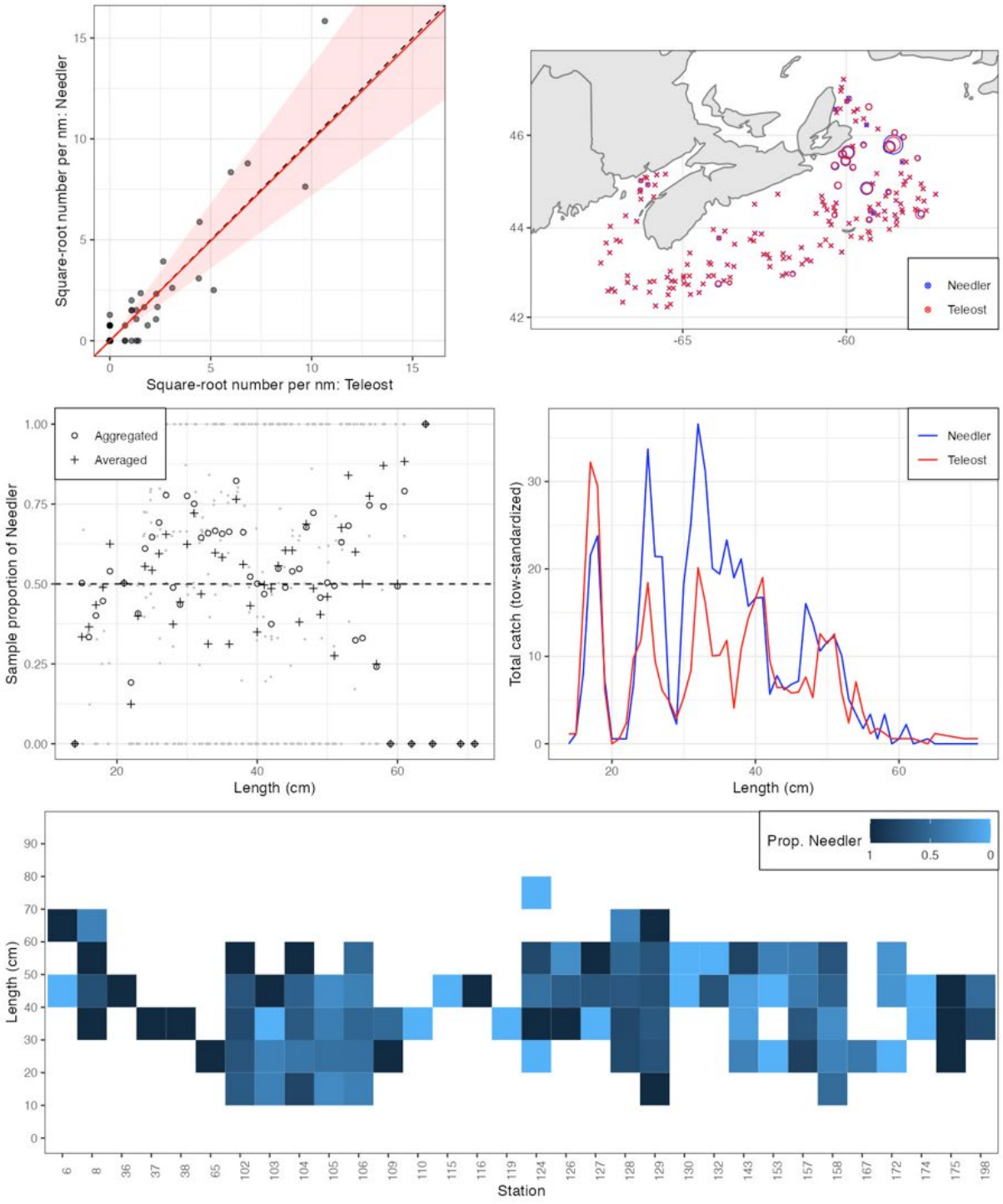

Figure 19a. Visualisation of comparative fishing data and size-aggregated model fit for Reinhardtius hippoglossoides (31).

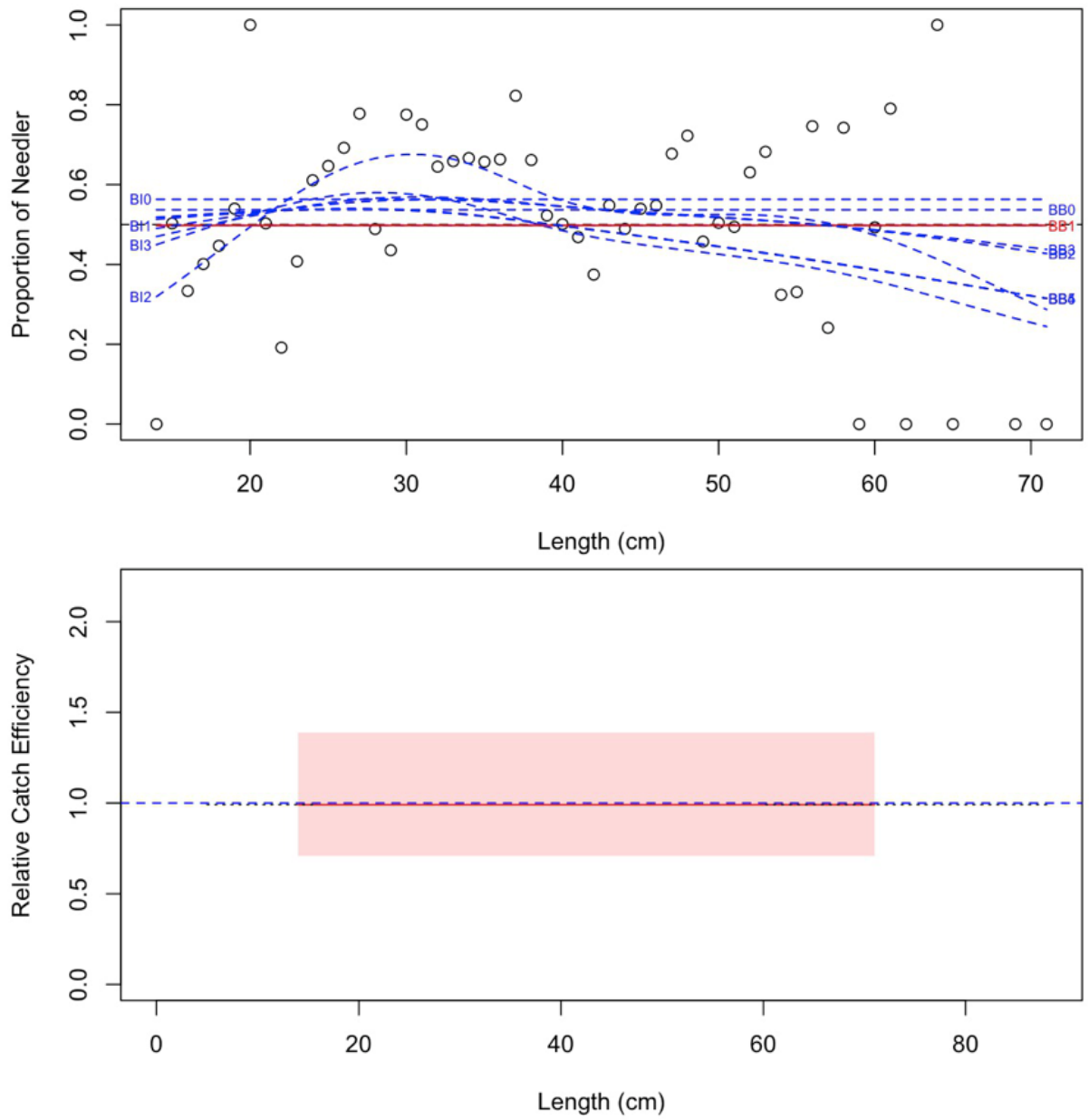

Figure 19b. Model fits and the selected length-based calibration for Reinhardtius hippoglossoides (31).

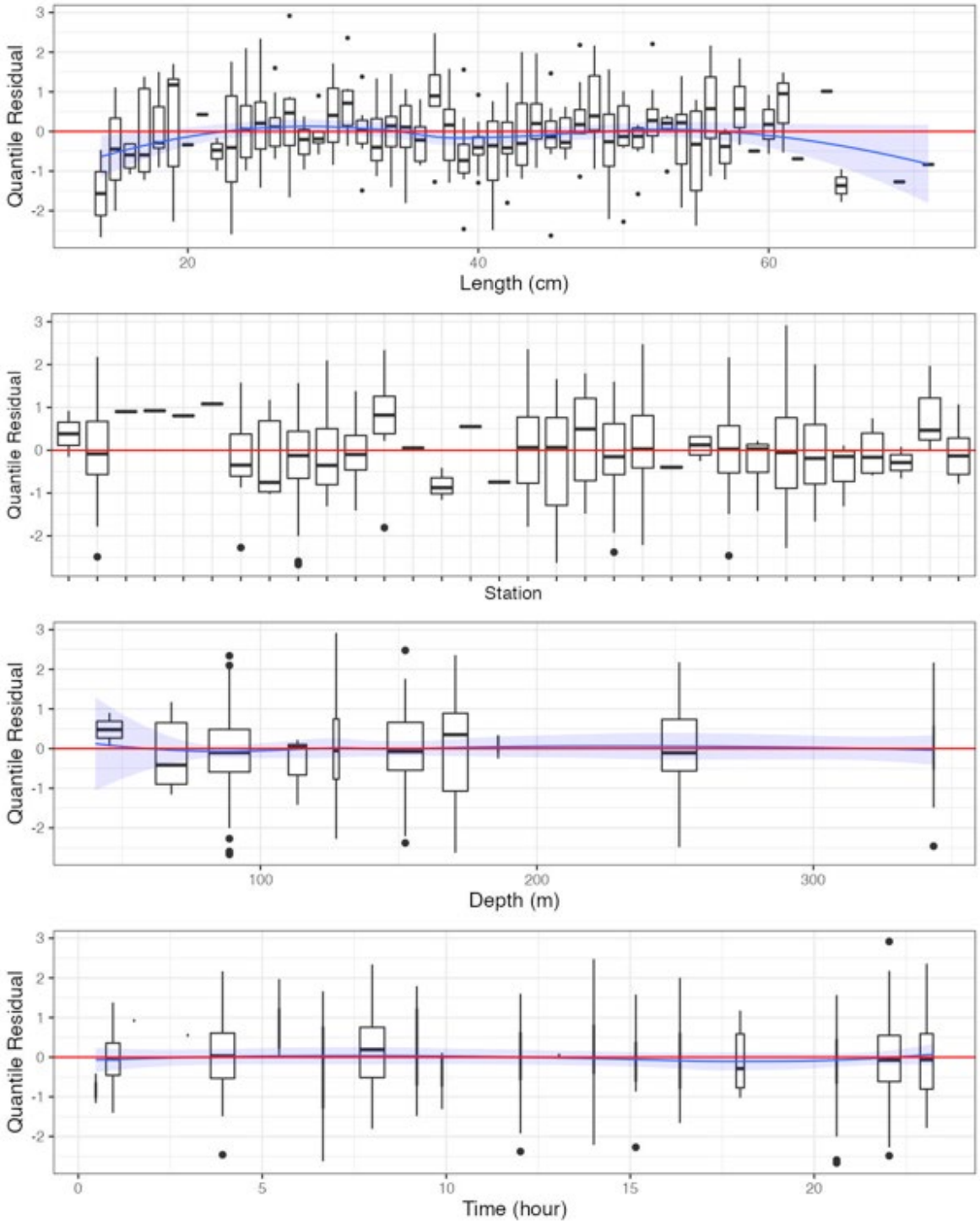

Figure 19c. Randomized and normalized quantile residuals for the selected model for Reinhardtius hippoglossoides (31).

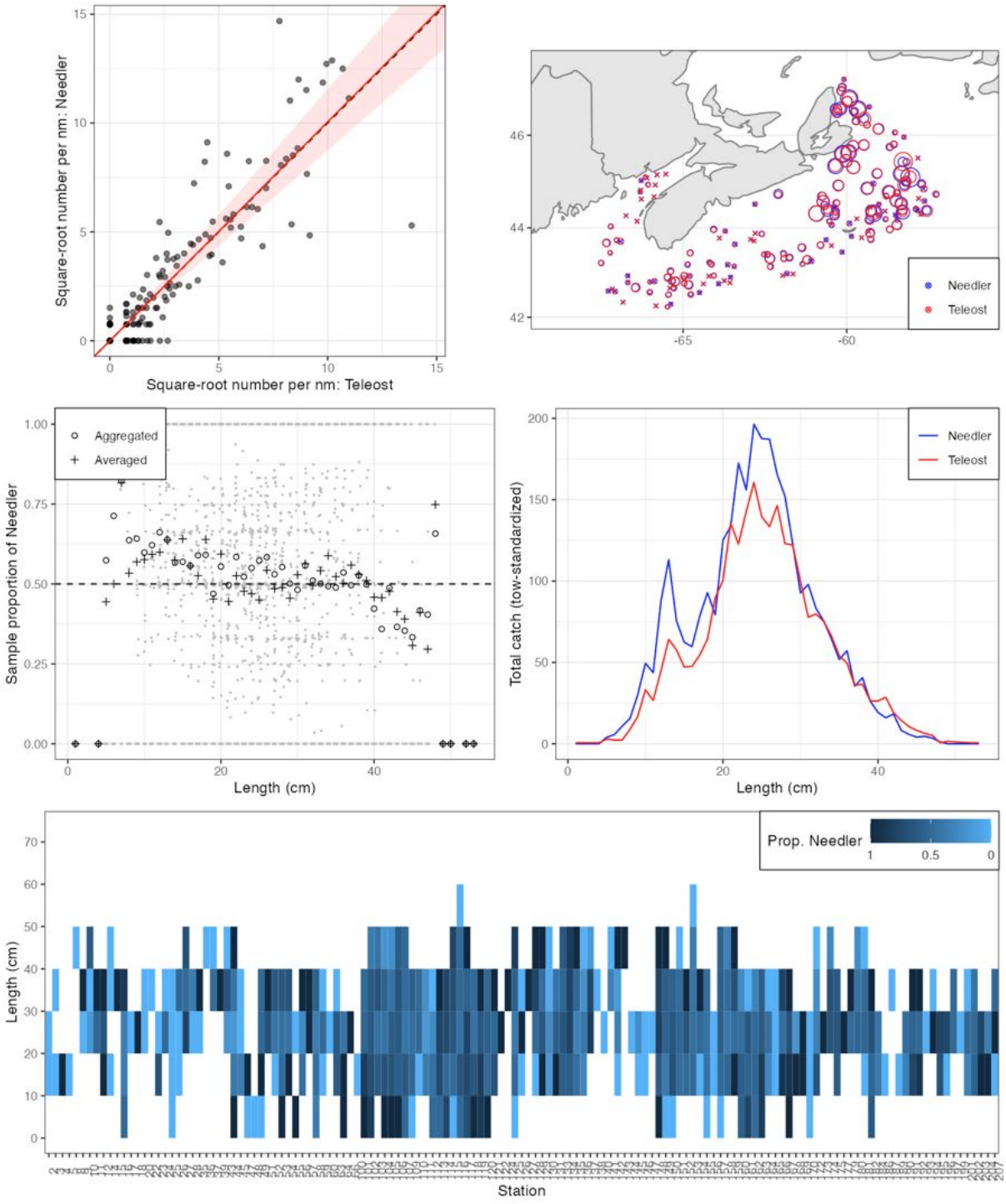

Figure 20a. Visualisation of comparative fishing data and size-aggregated model fit for Hippoglossoides platessoides (40).

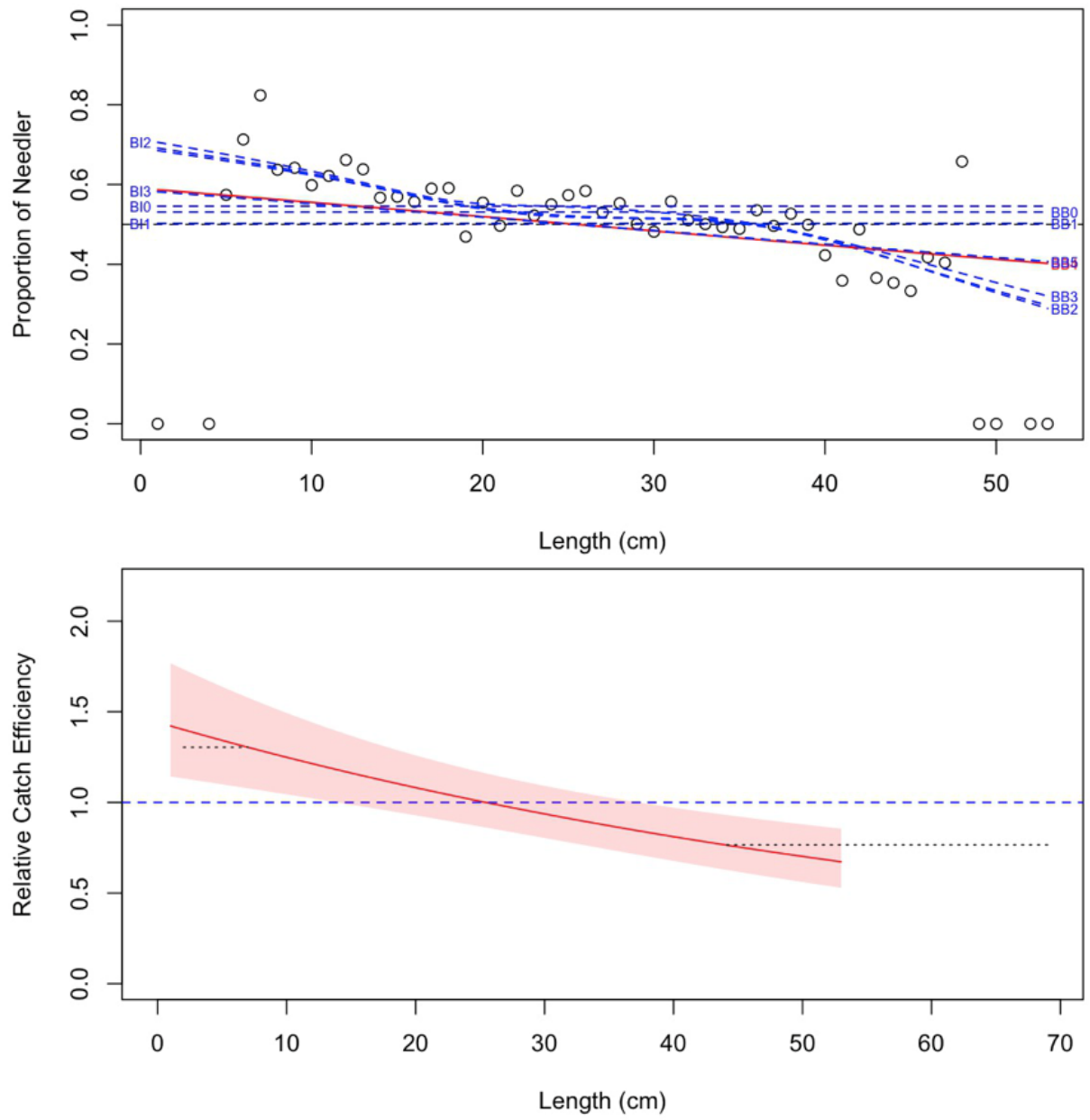

Figure 20b. Model fits and the selected length-based calibration for Hippoglossoides platessoides (40).

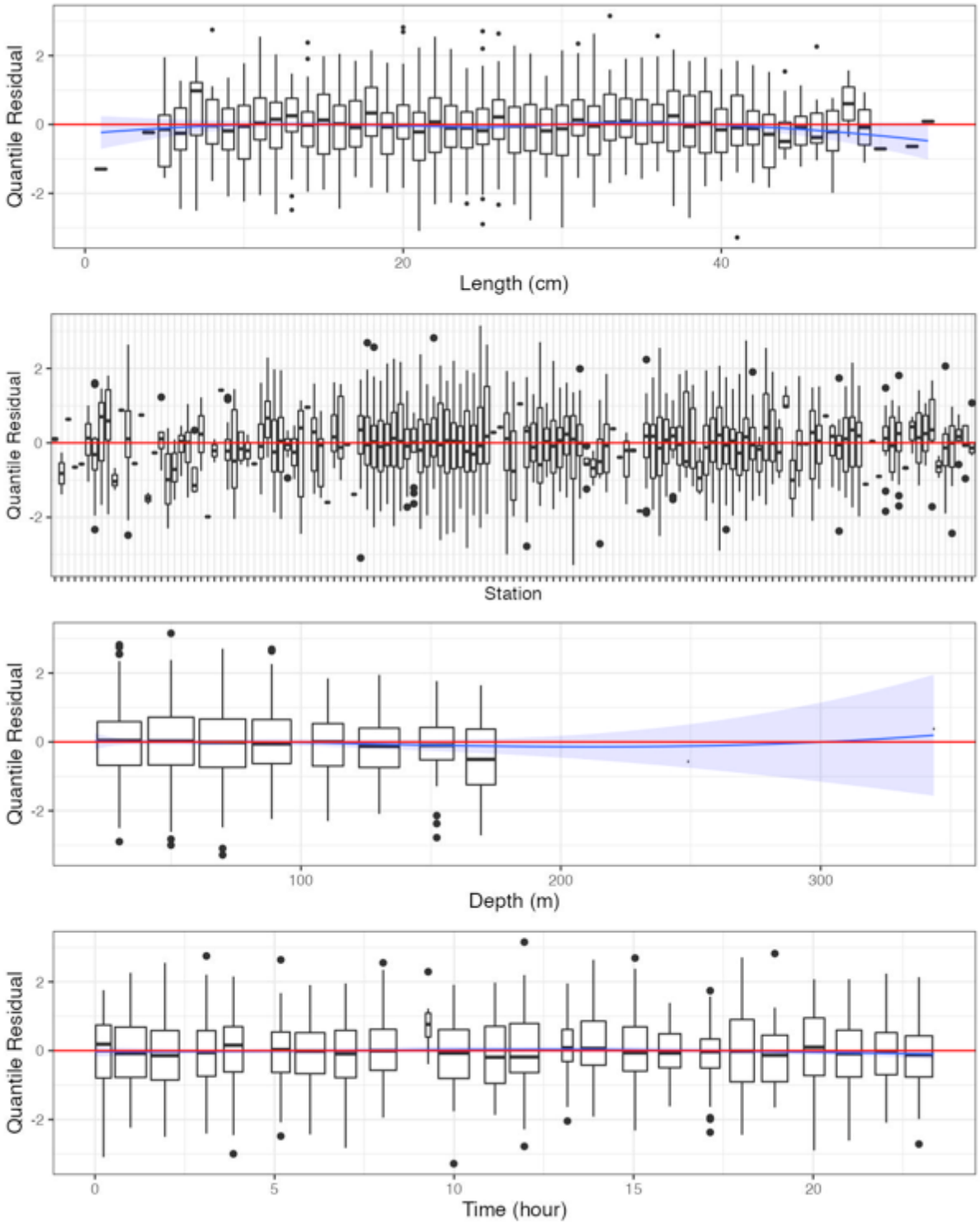

Figure 20c. Randomized and normalized quantile residuals for the selected model for Hippoglossoides platessoides (40).

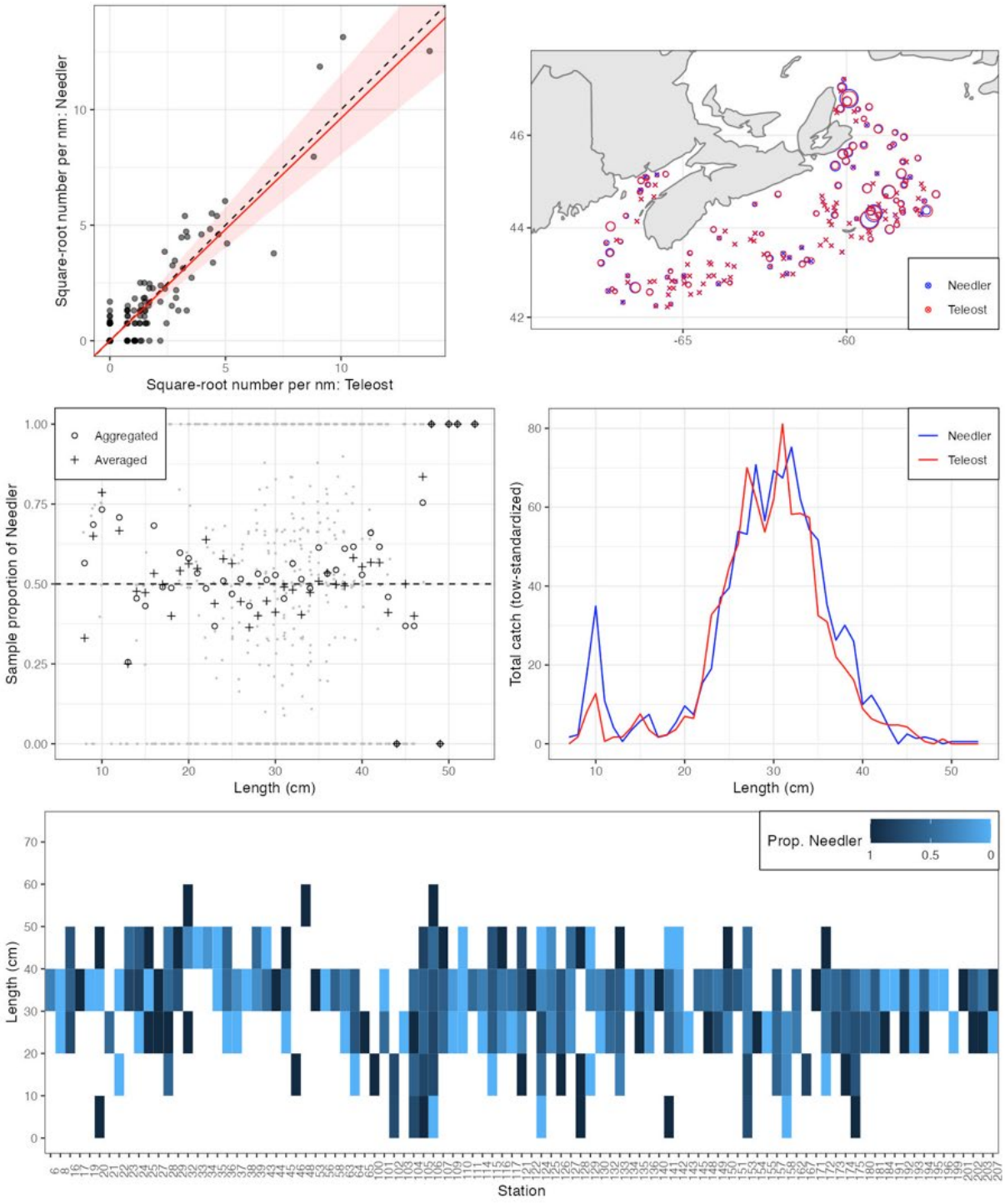

Figure 21a. Visualisation of comparative fishing data and size-aggregated model fit for Glyptocephalus cynoglossus (41).

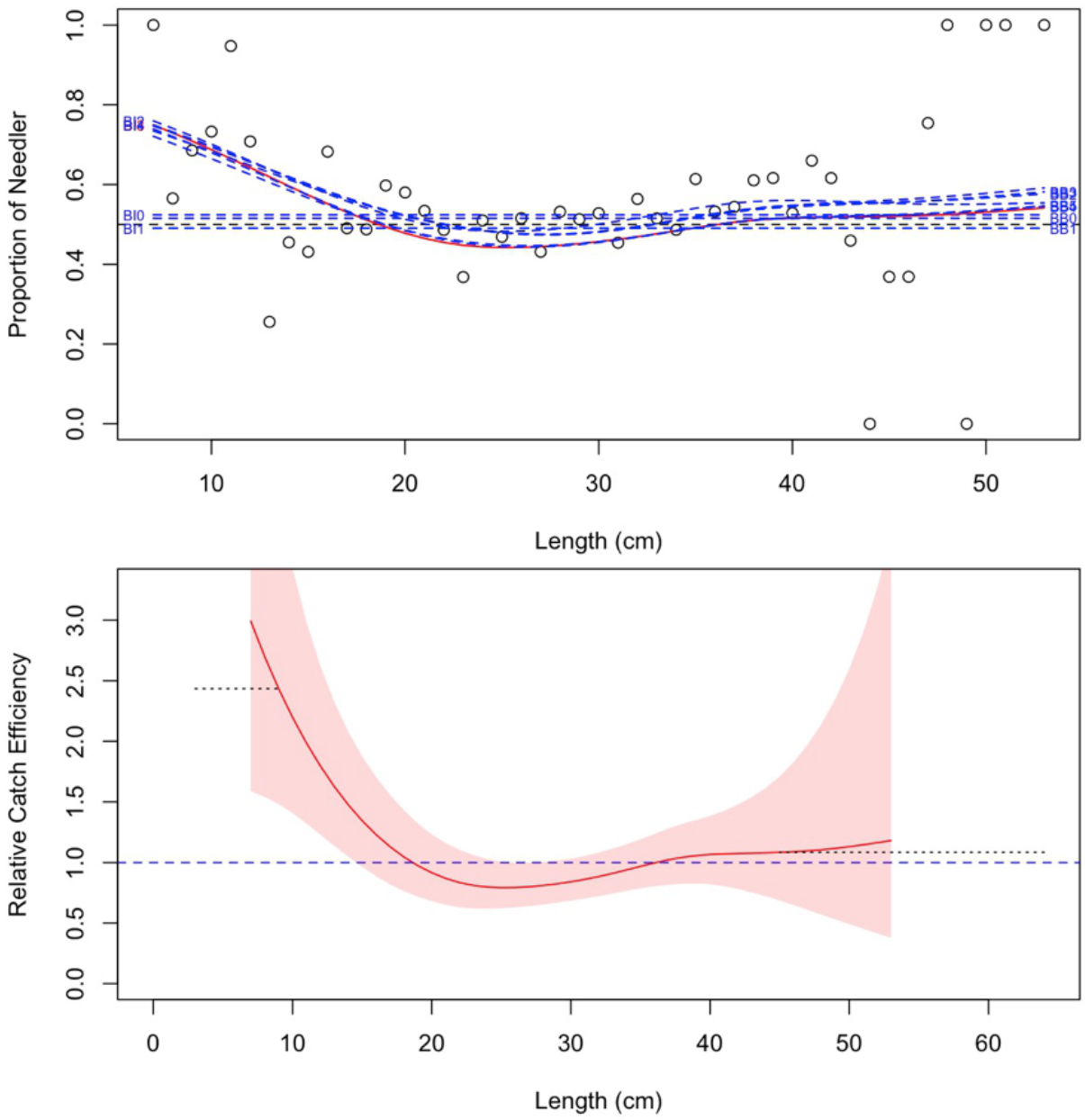

Figure 21b. Model fits and the selected length-based calibration for Glyptocephalus cynoglossus (41).

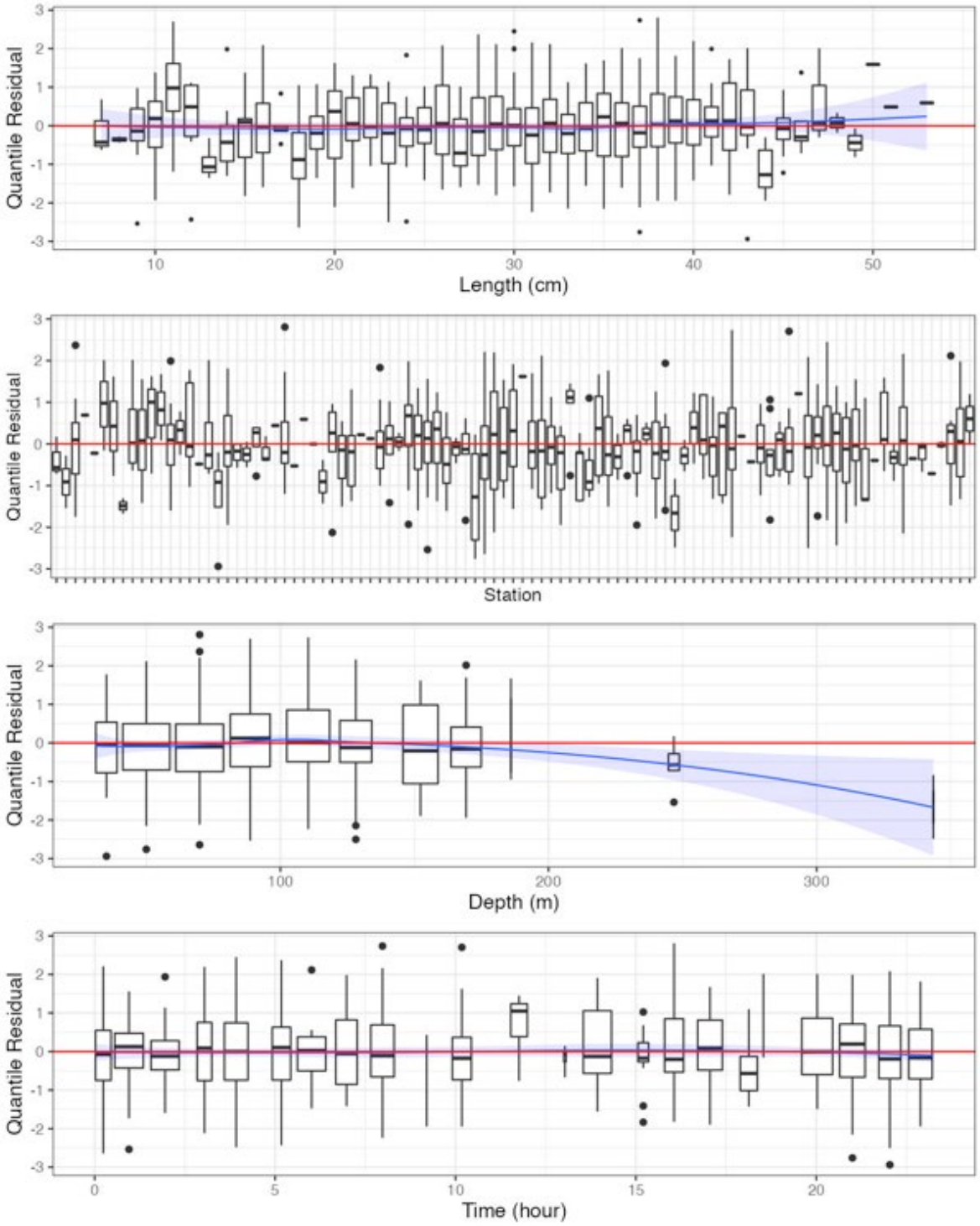

Figure 21c. Randomized and normalized quantile residuals for the selected model for Glyptocephalus cynoglossus (41).

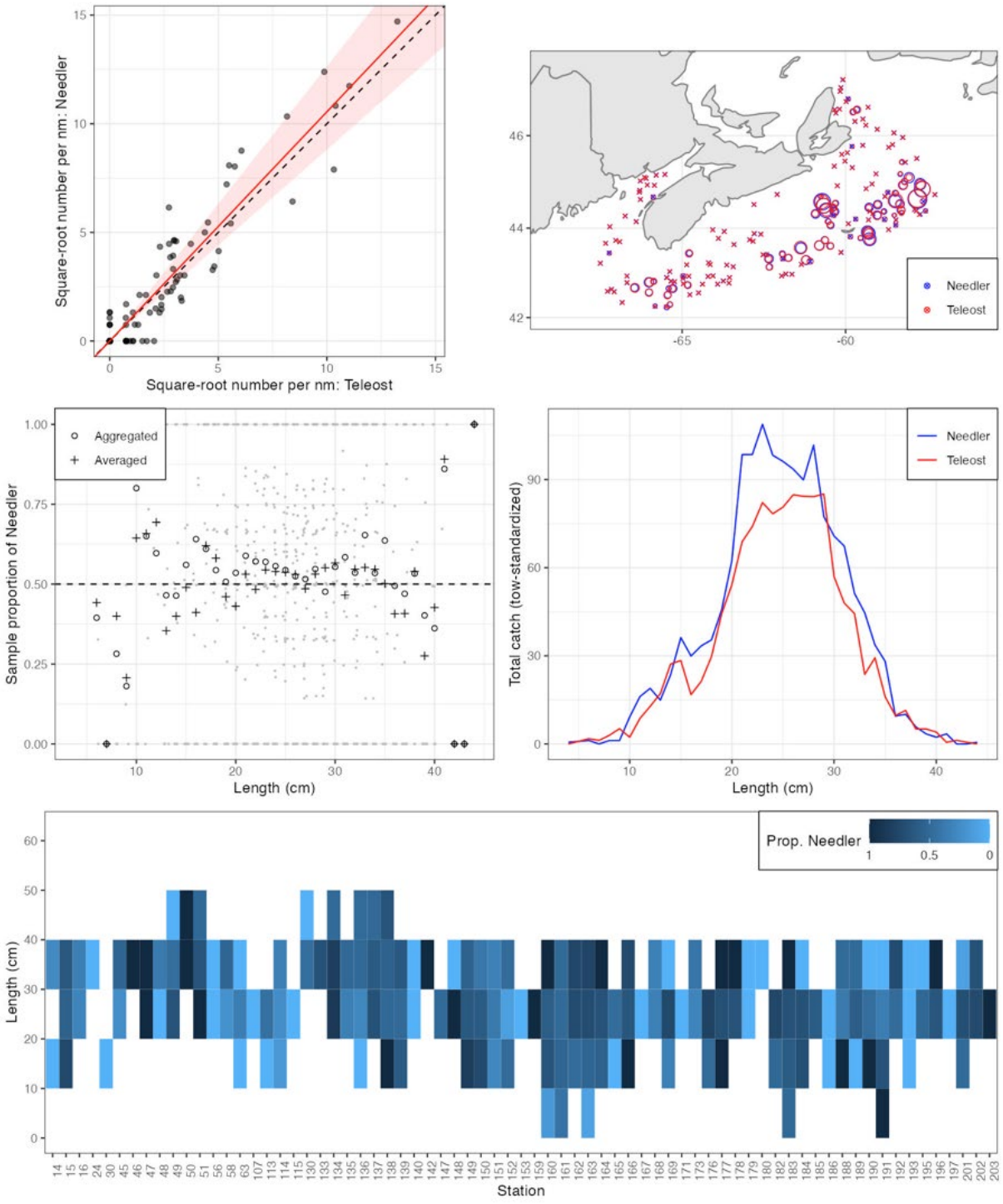

Figure 22a. Visualisation of comparative fishing data and size-aggregated model fit for Limanda ferruginea (42).

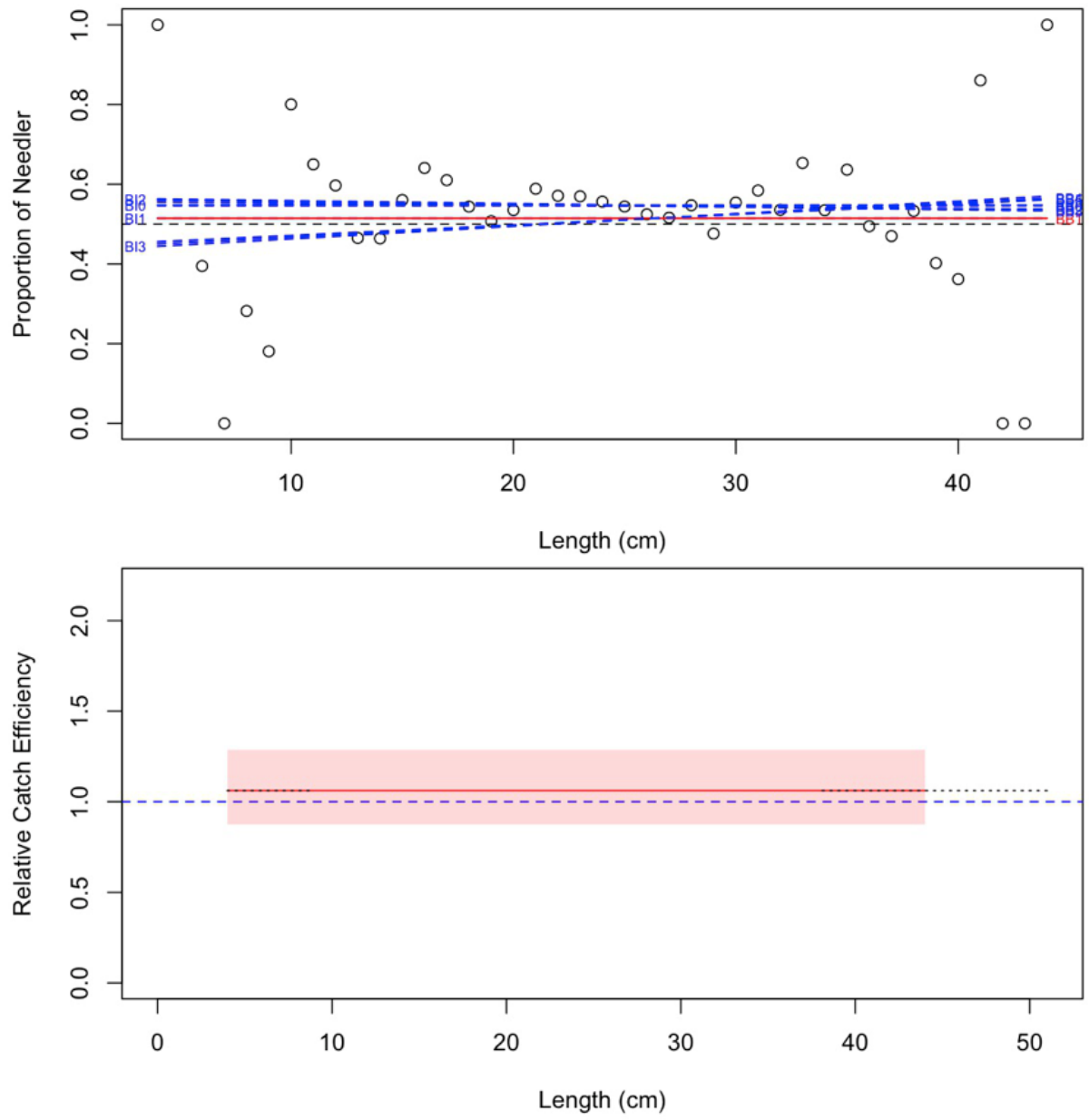

Figure 22b. Model fits and the selected length-based calibration for Limanda ferruginea (42).

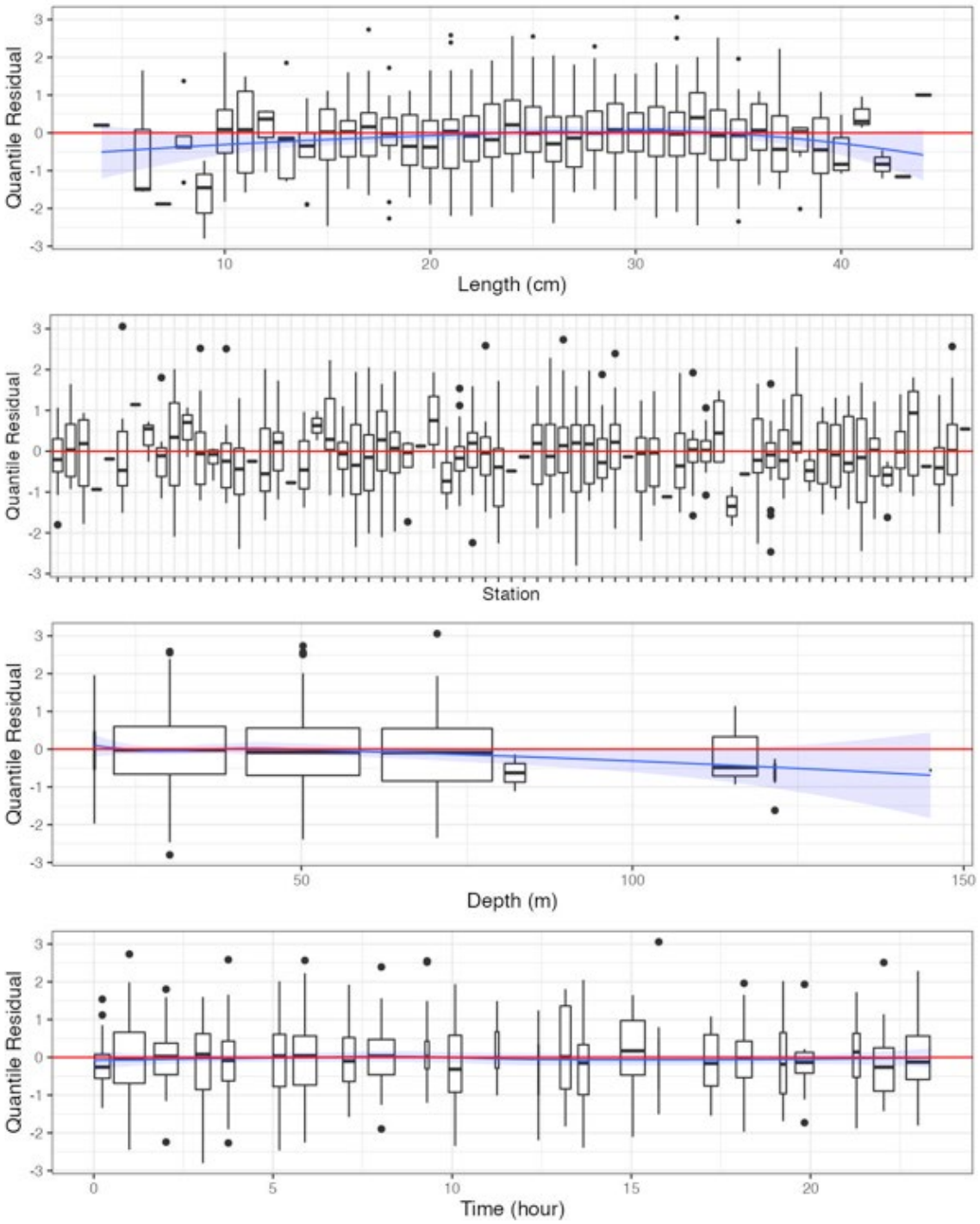

Figure 22c. Randomized and normalized quantile residuals for the selected model for Limanda ferruginea (42).

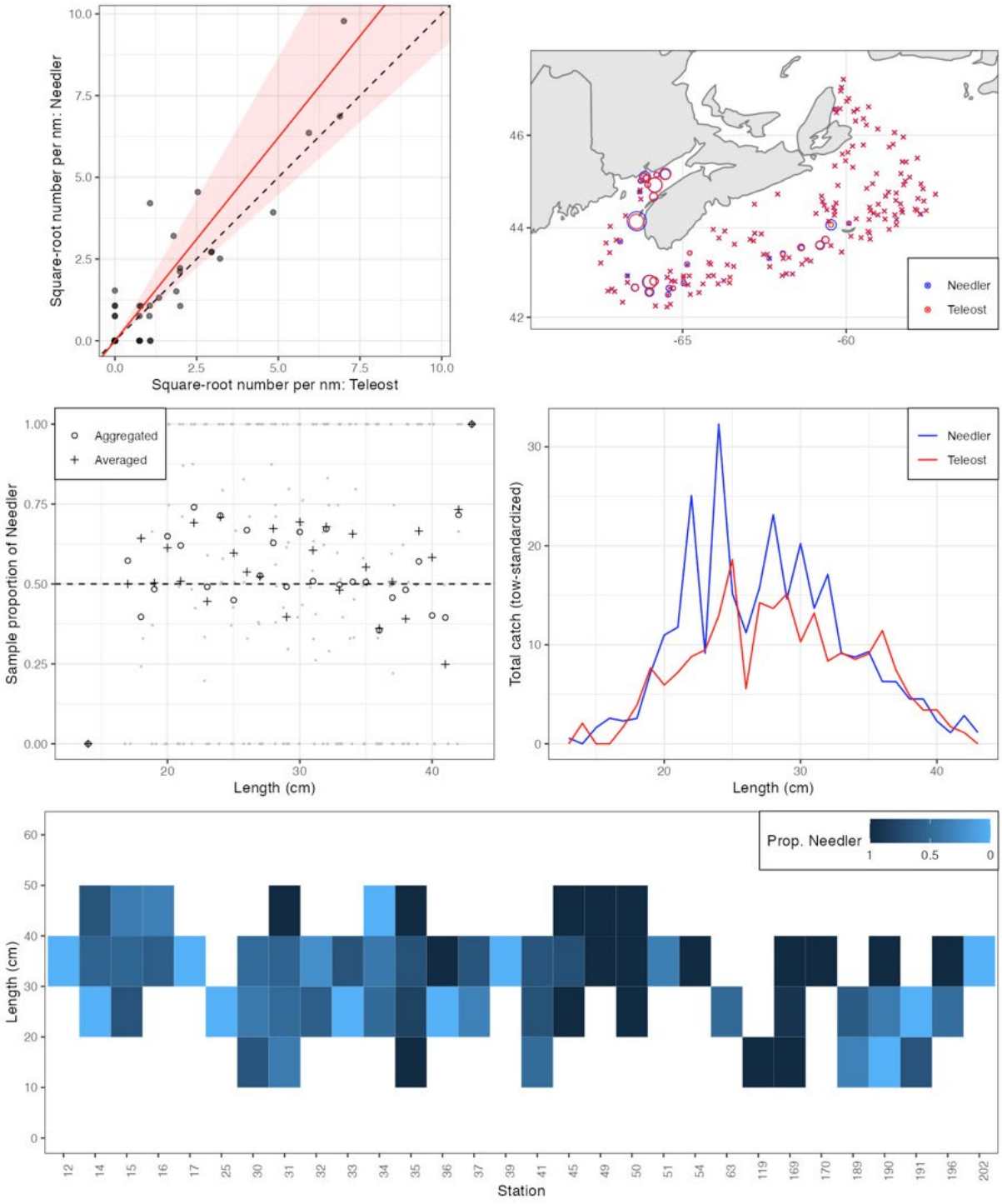

Figure 23a. Visualisation of comparative fishing data and size-aggregated model fit for Pseudopleuronectes americanus (43).

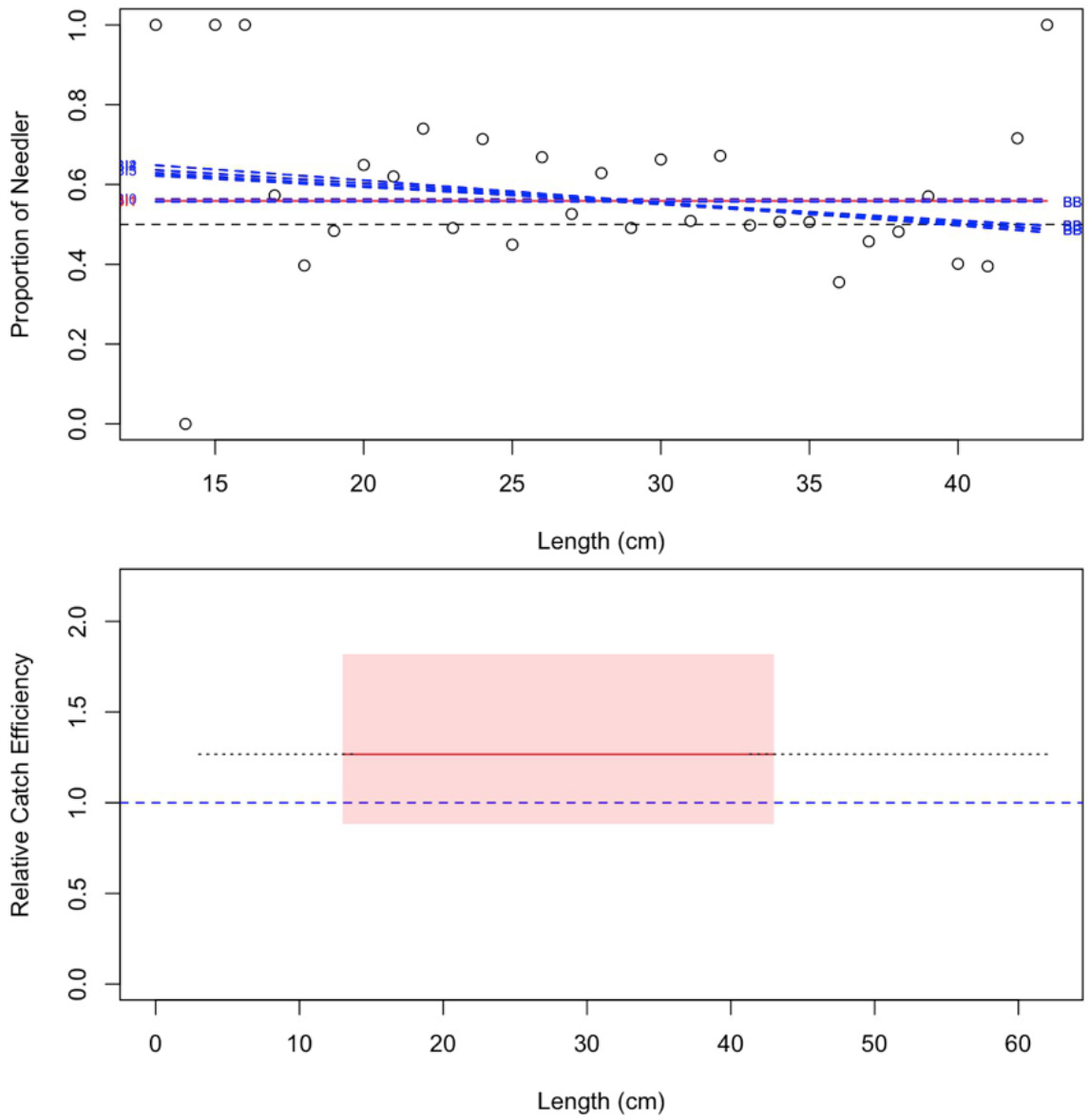

Figure 23b. Model fits and the selected length-based calibration for Pseudopleuronectes americanus (43).

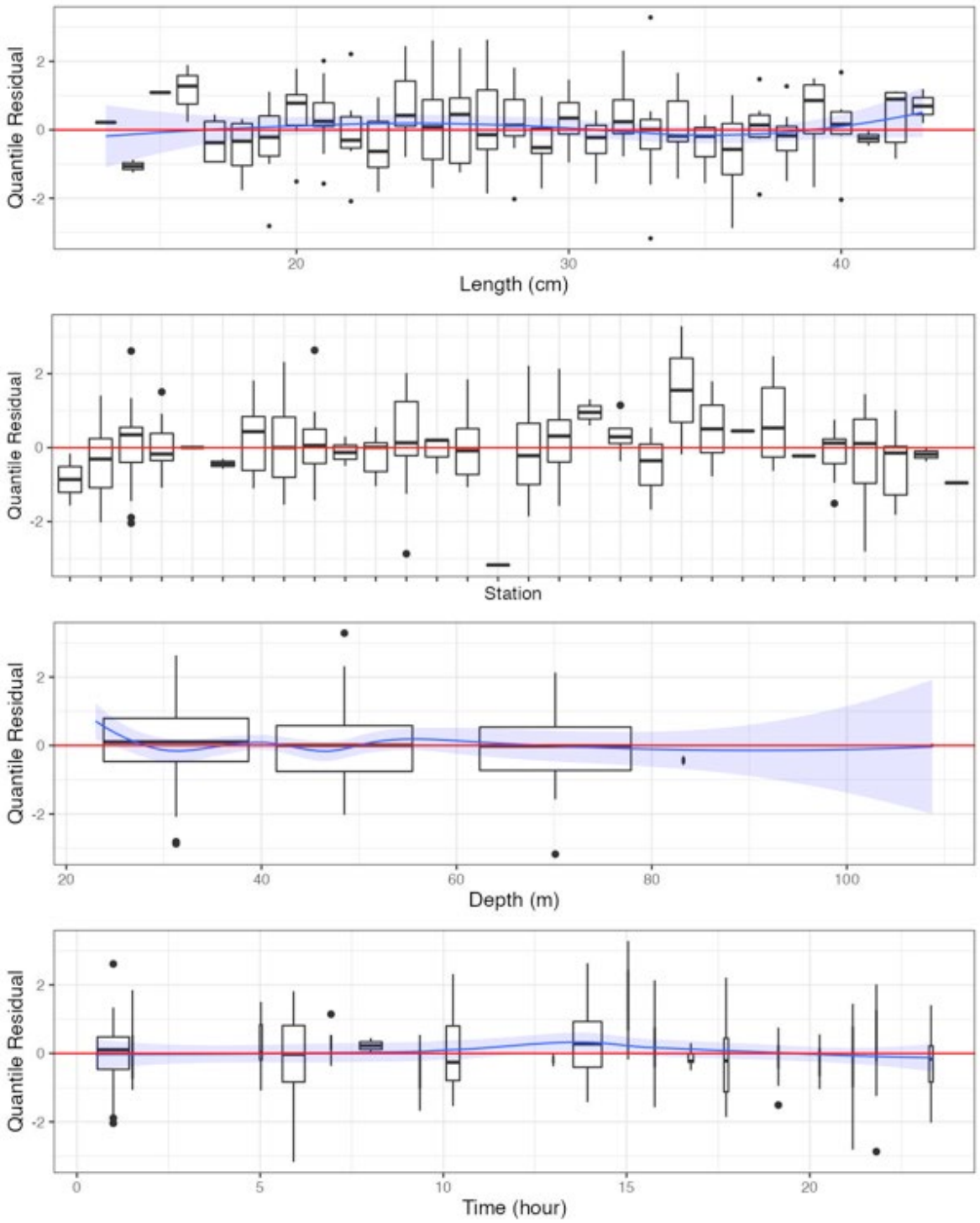

Figure 23c. Randomized and normalized quantile residuals for the selected model for Pseudopleuronectes americanus (43).

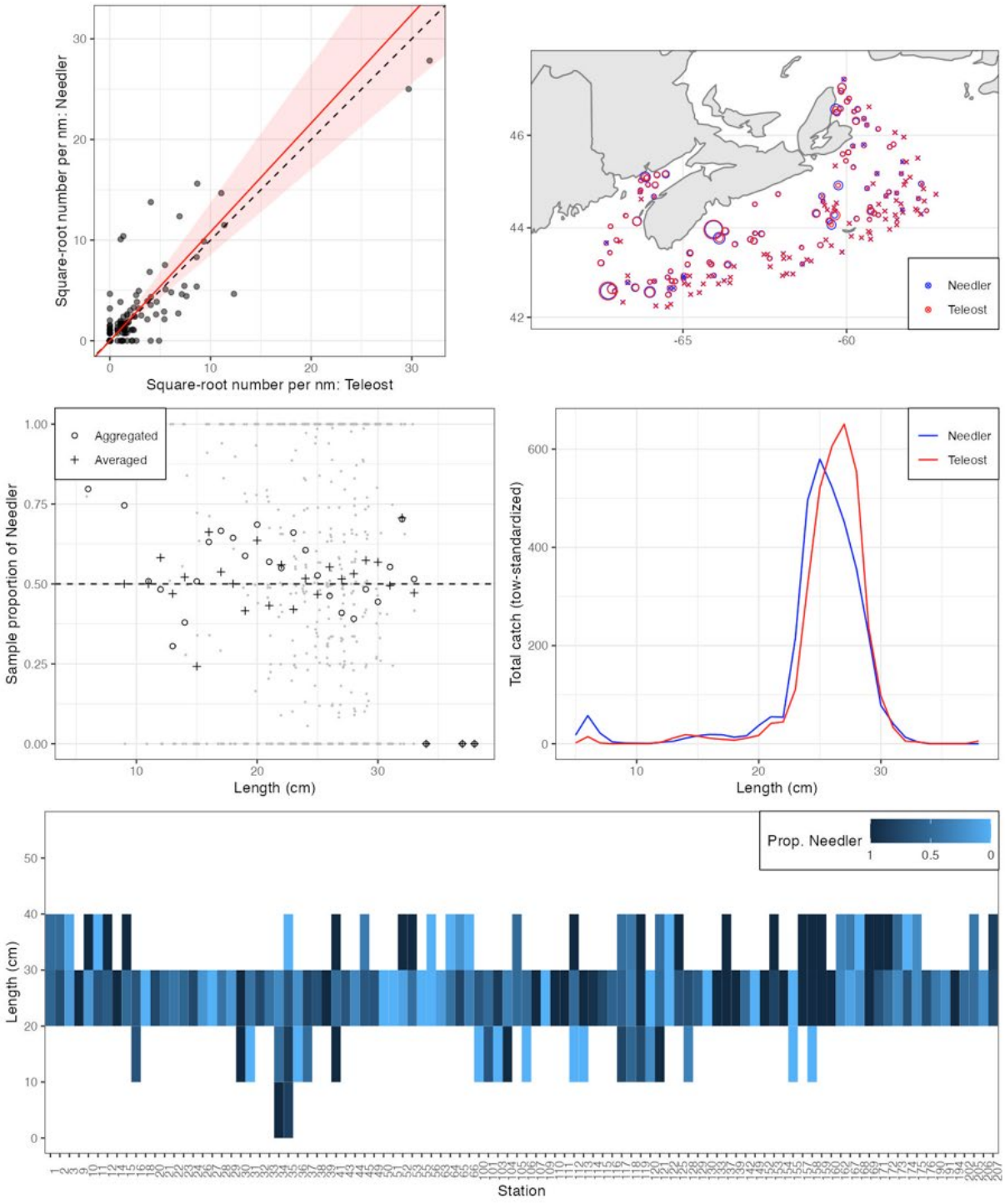

Figure 24a. Visualisation of comparative fishing data and size-aggregated model fit for Clupea harengus (60).

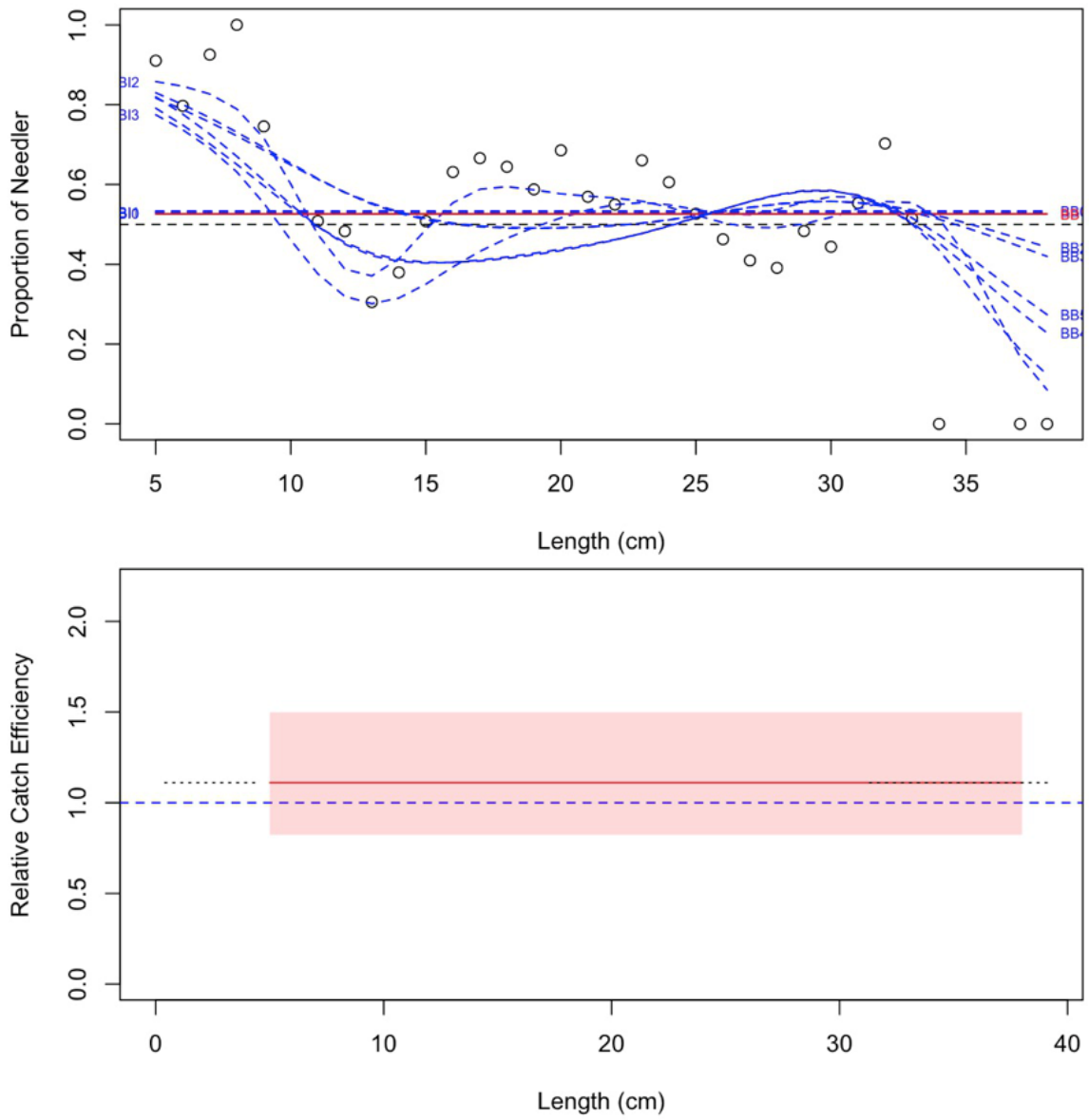

Figure 24b. Model fits and the selected length-based calibration for Clupea harengus (60).

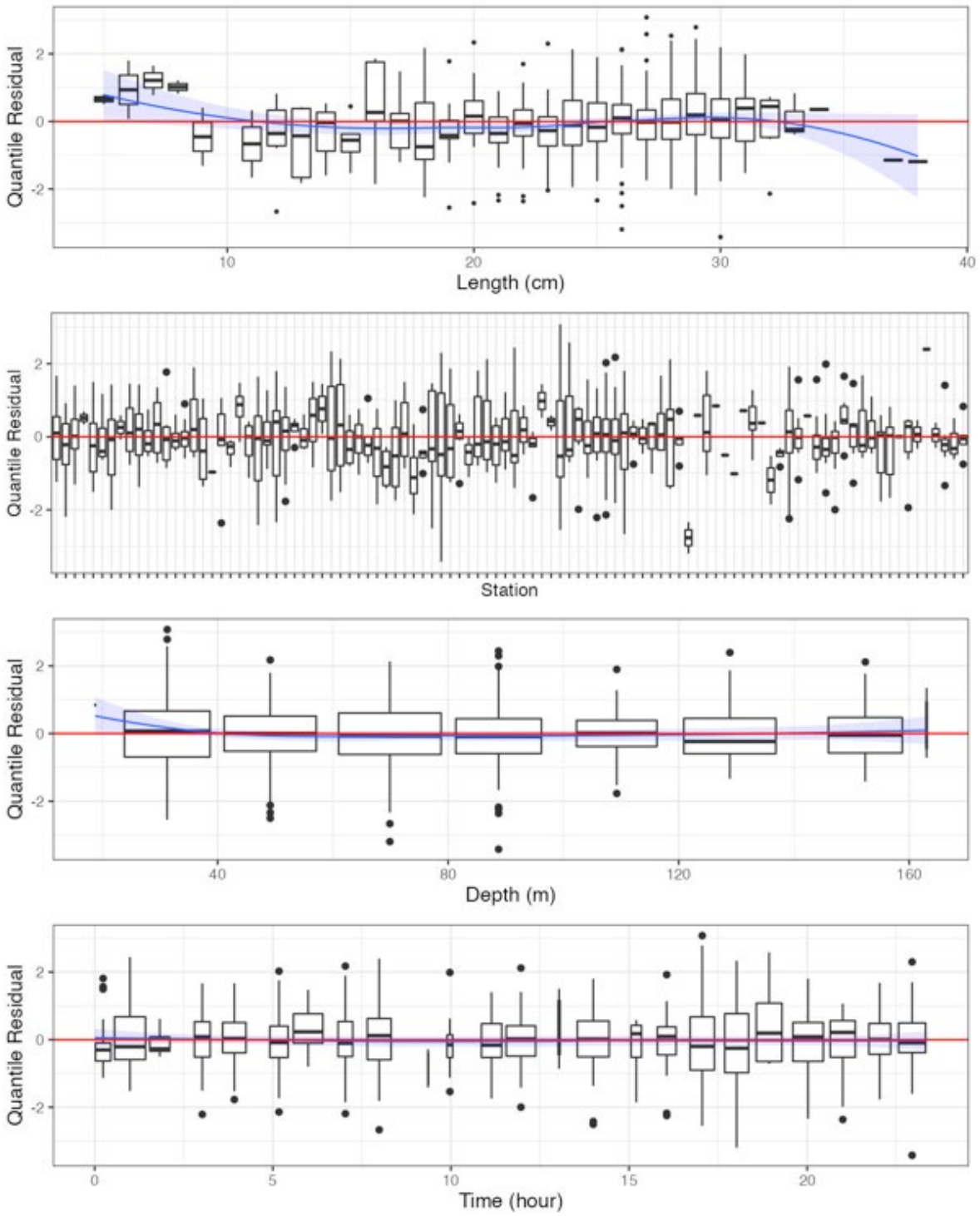

Figure 24c. Randomized and normalized quantile residuals for the selected model for Clupea harengus (60).

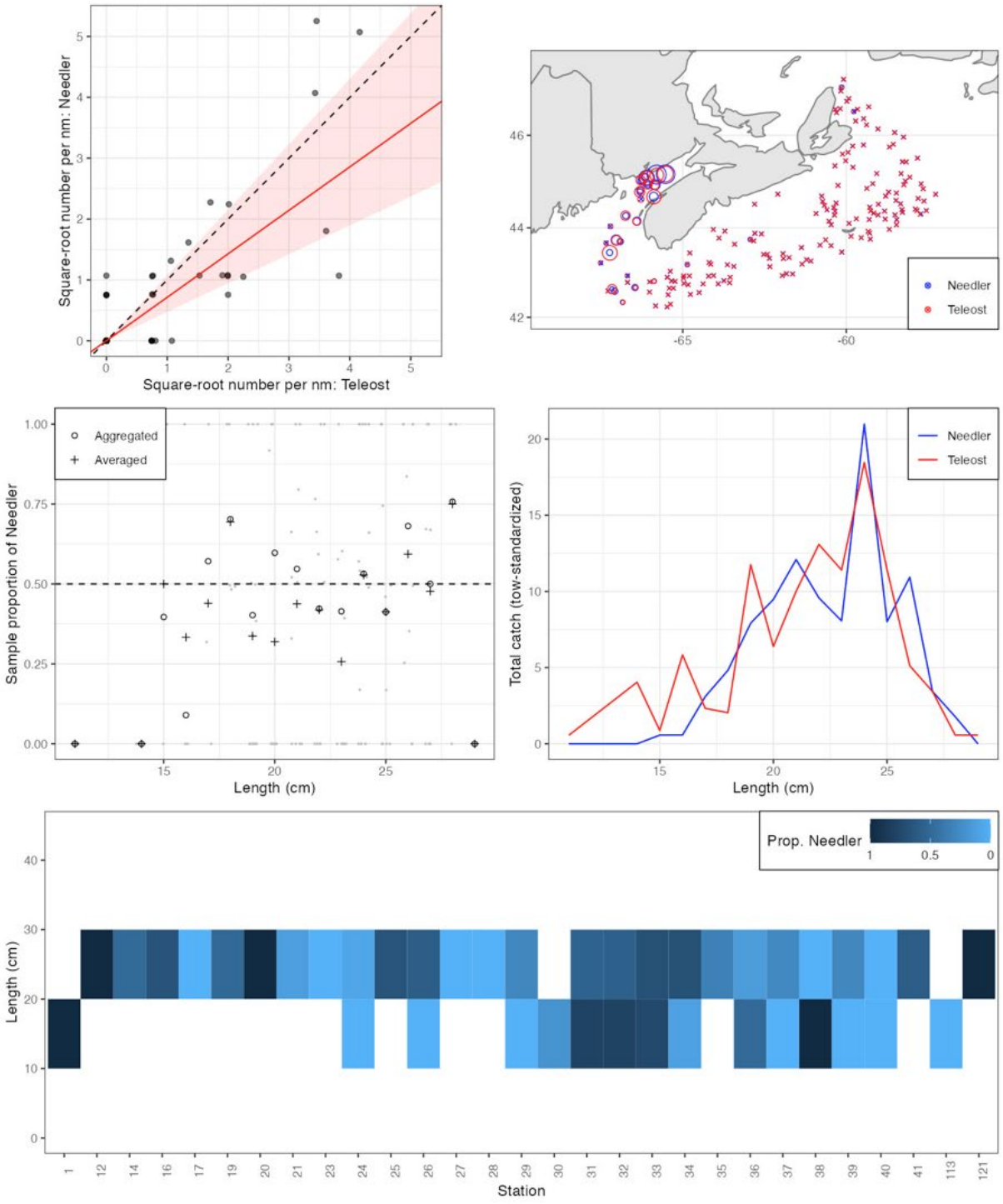

Figure 25a. Visualisation of comparative fishing data and size-aggregated model fit for Alosa pseudoharengus (62).

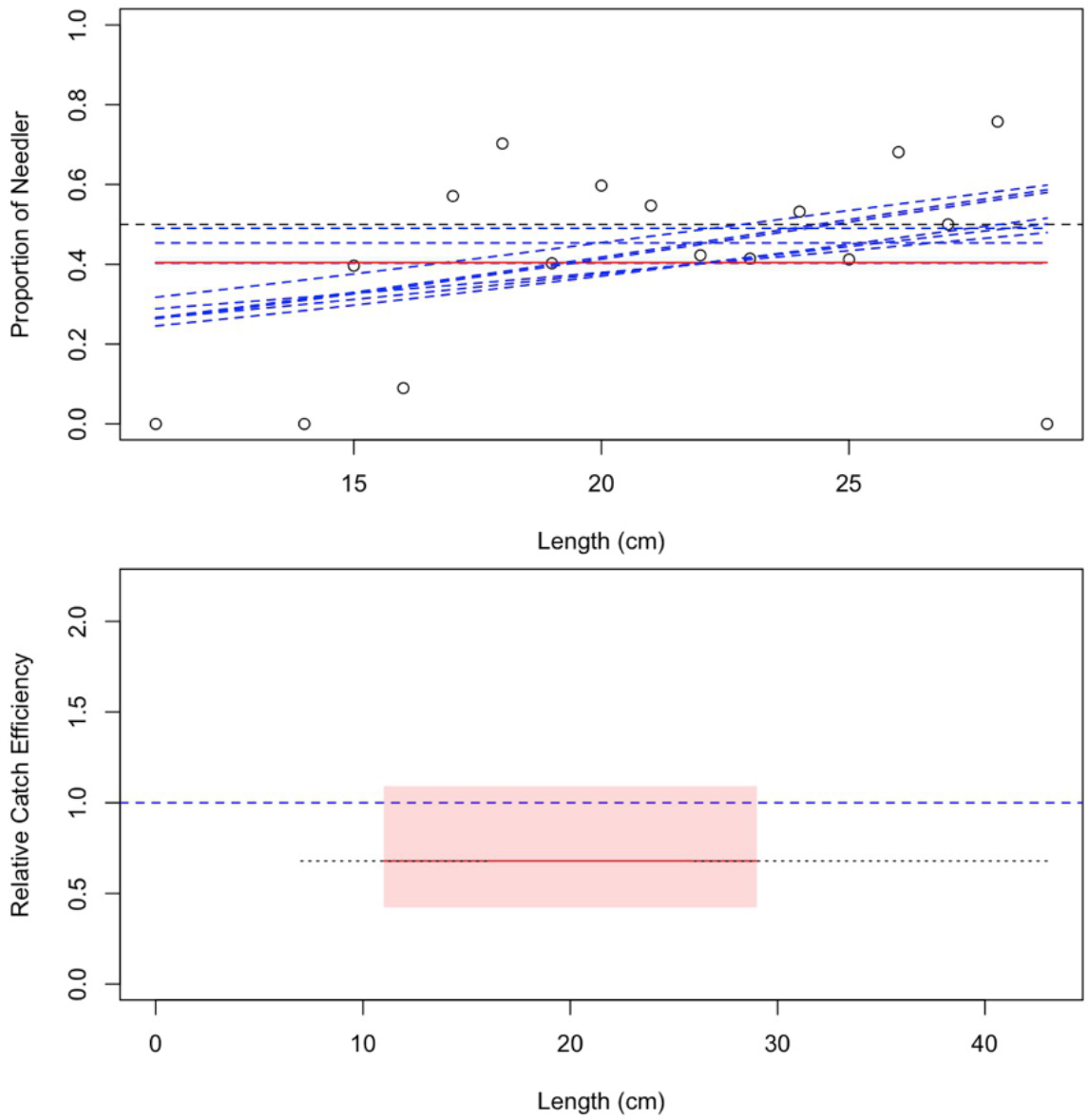

Figure 25b. Model fits and the selected length-based calibration for Alosa pseudoharengus (62).

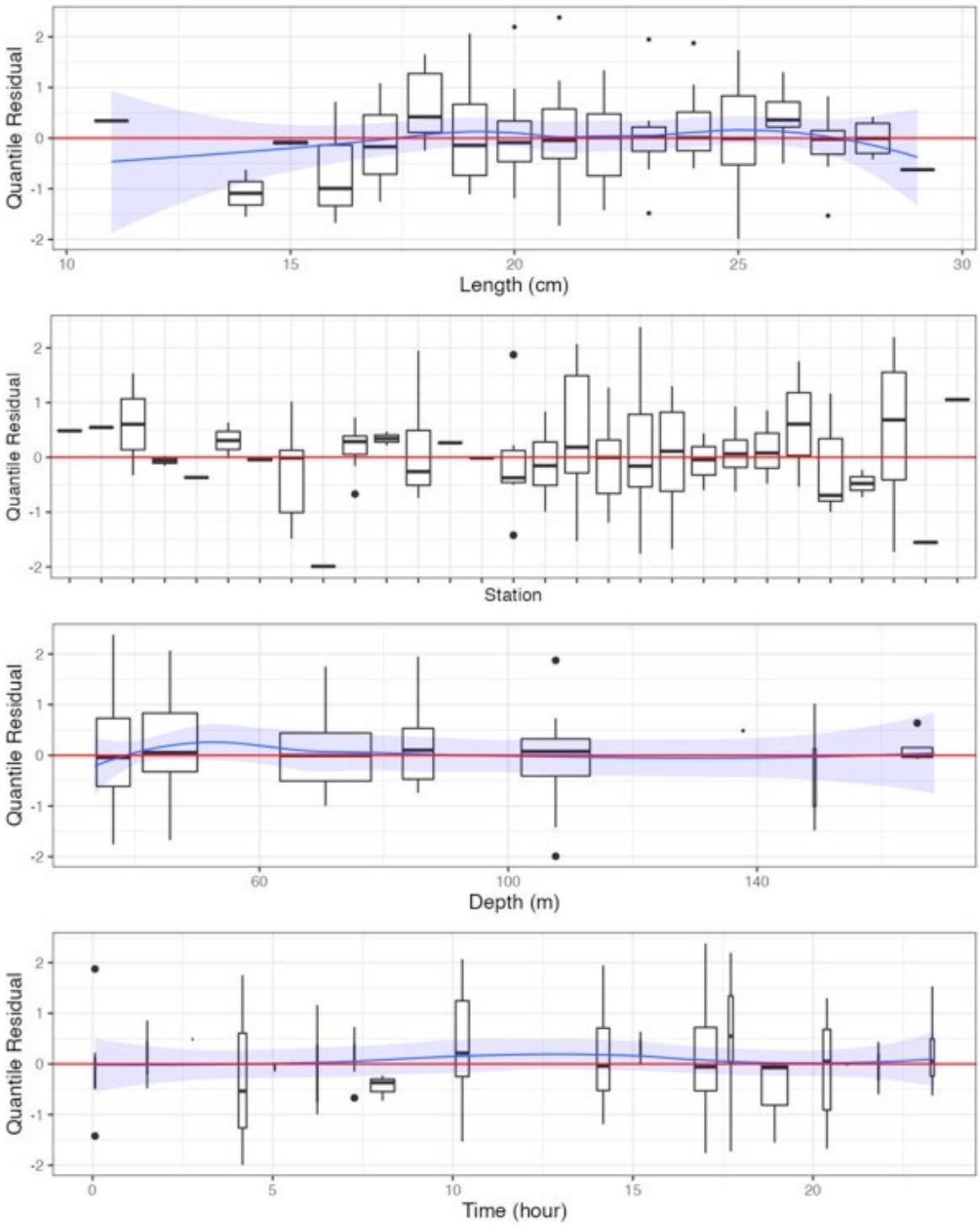

Figure 25c. Randomized and normalized quantile residuals for the selected model for Alosa pseudoharengus (62).

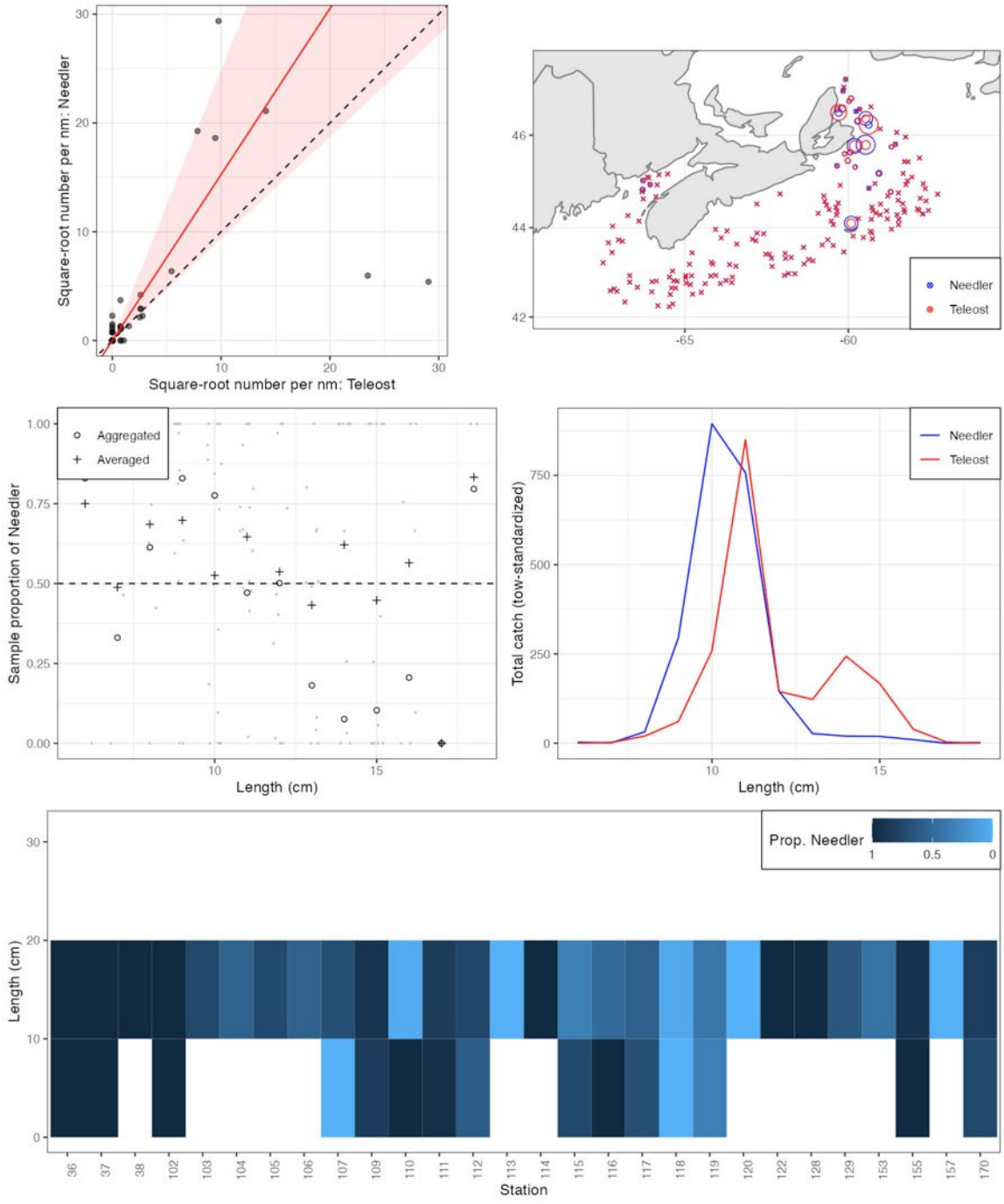

Figure 26a. Visualisation of comparative fishing data and size-aggregated model fit for Mallotus villosus (64).

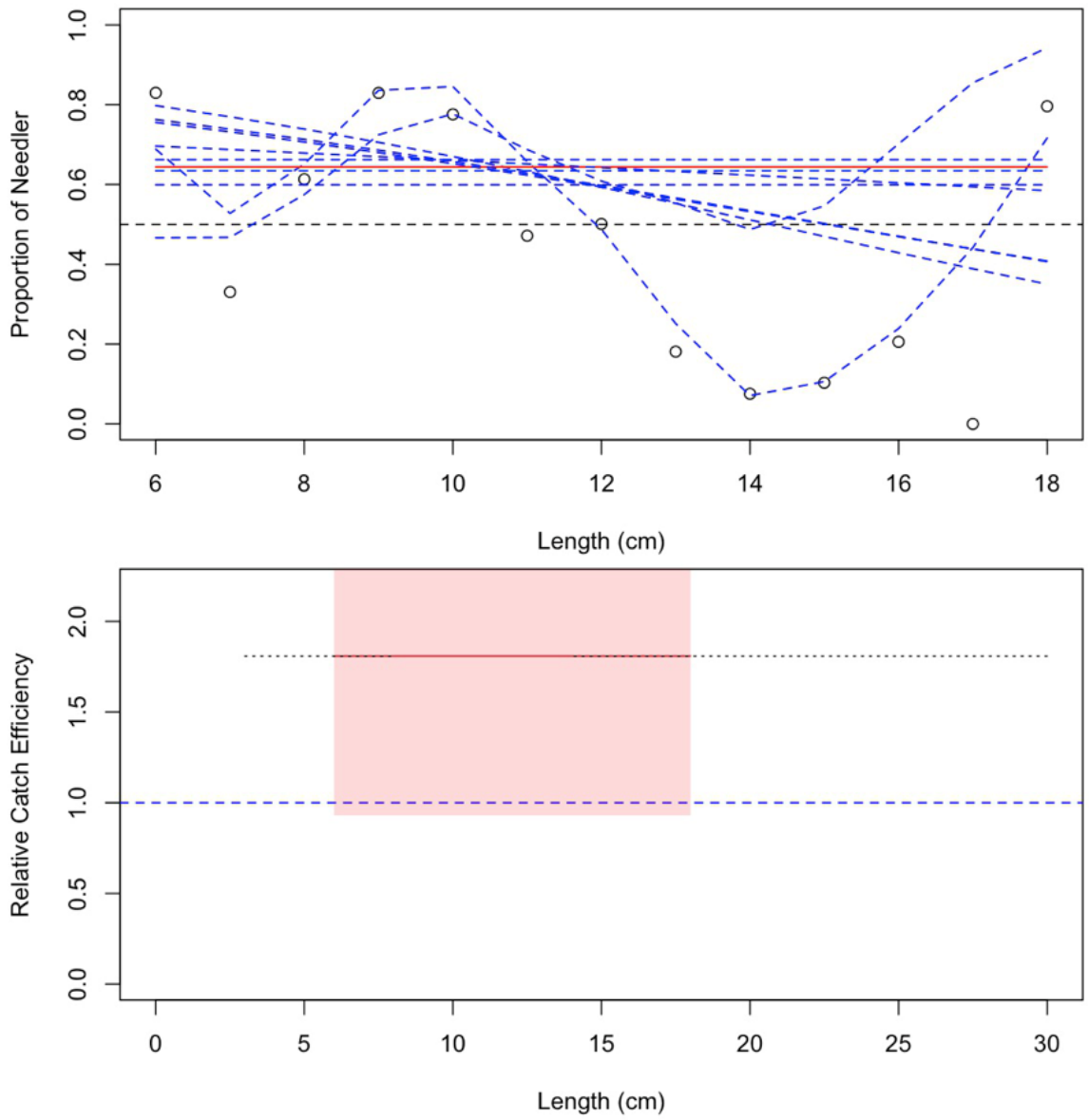

Figure 26b. Model fits and the selected length-based calibration for Mallotus villosus (64).

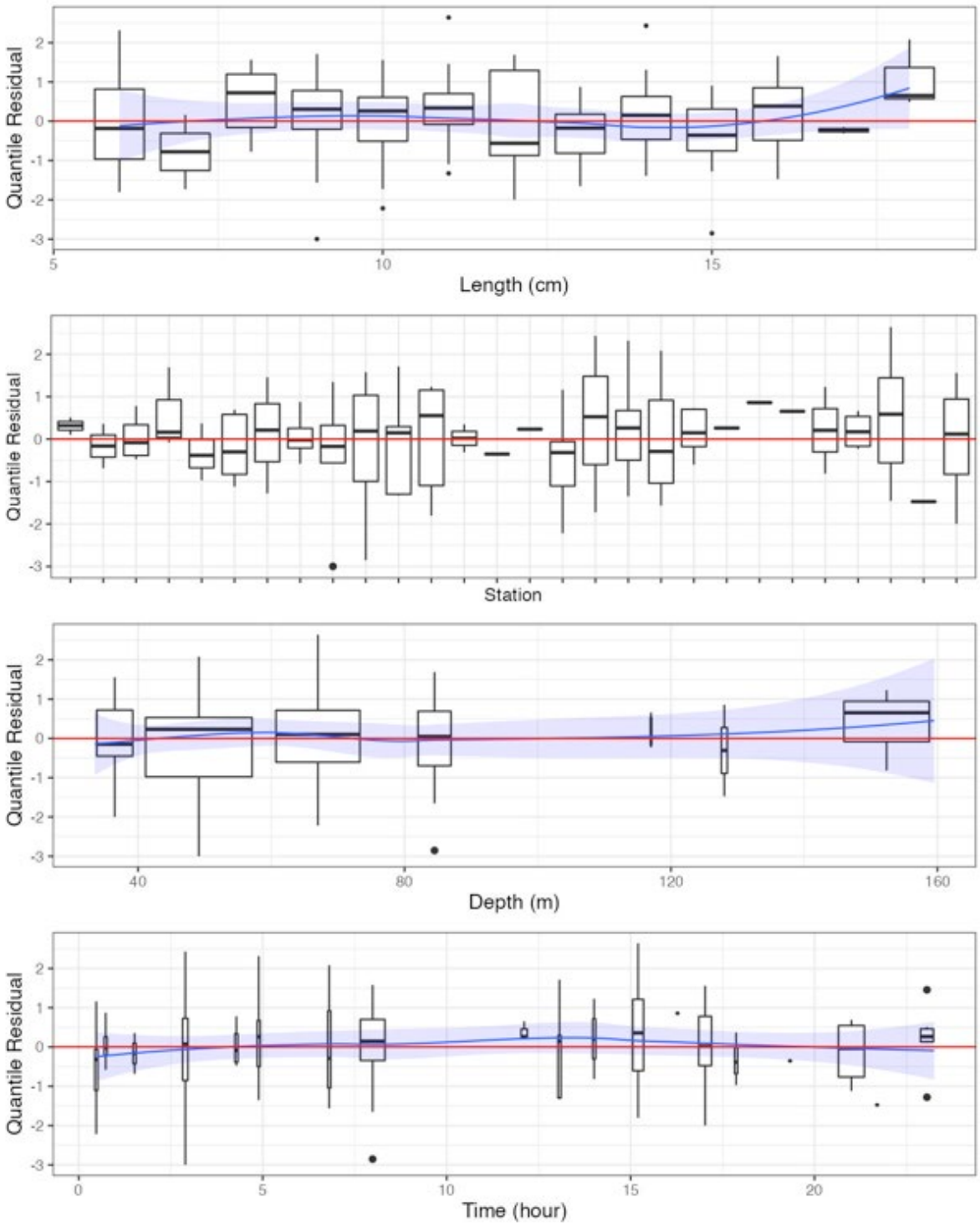

Figure 26c. Randomized and normalized quantile residuals for the selected model for Mallotus villosus (64).

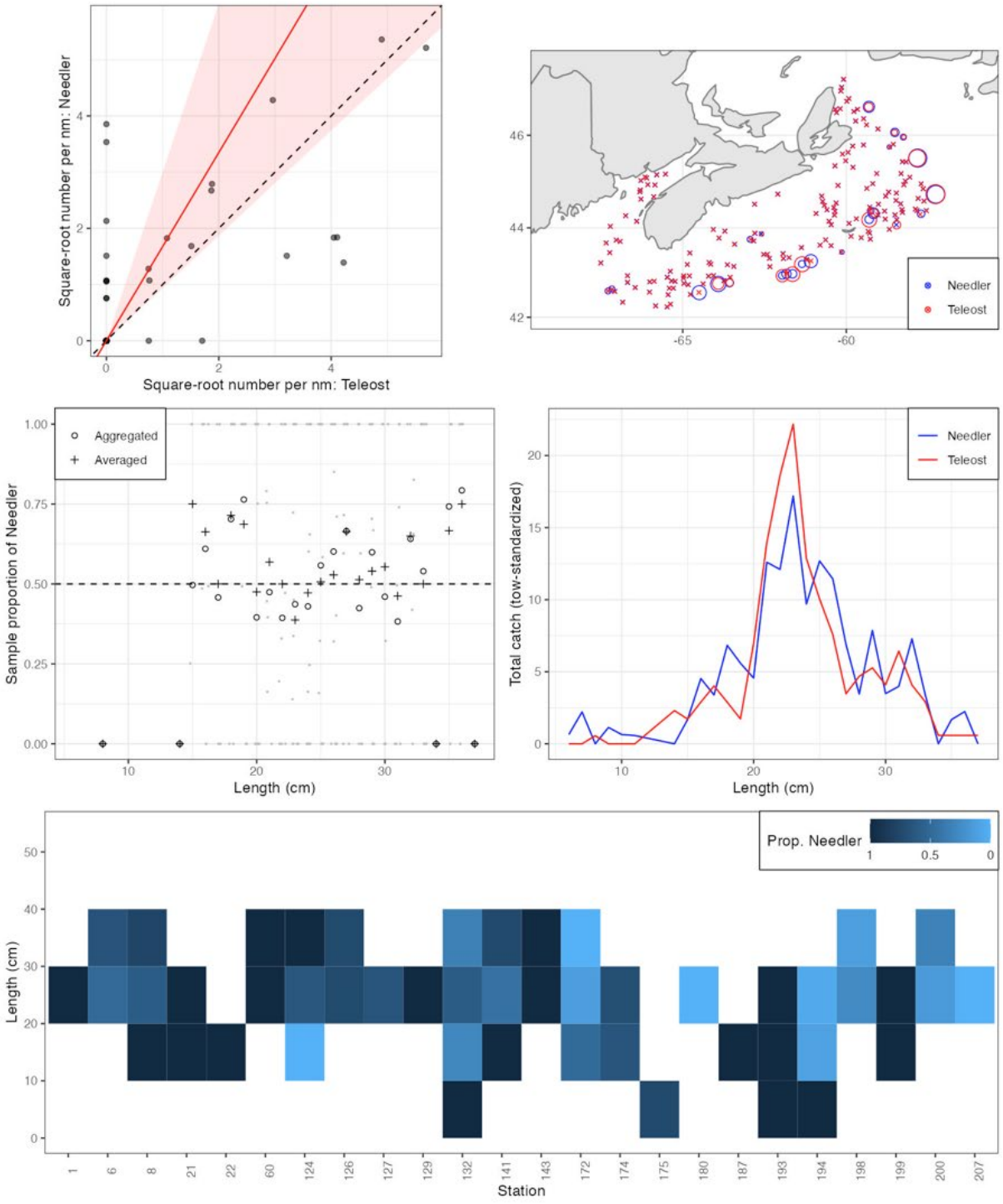

Figure 27a. Visualisation of comparative fishing data and size-aggregated model fit for Urophycis chesteri (112).

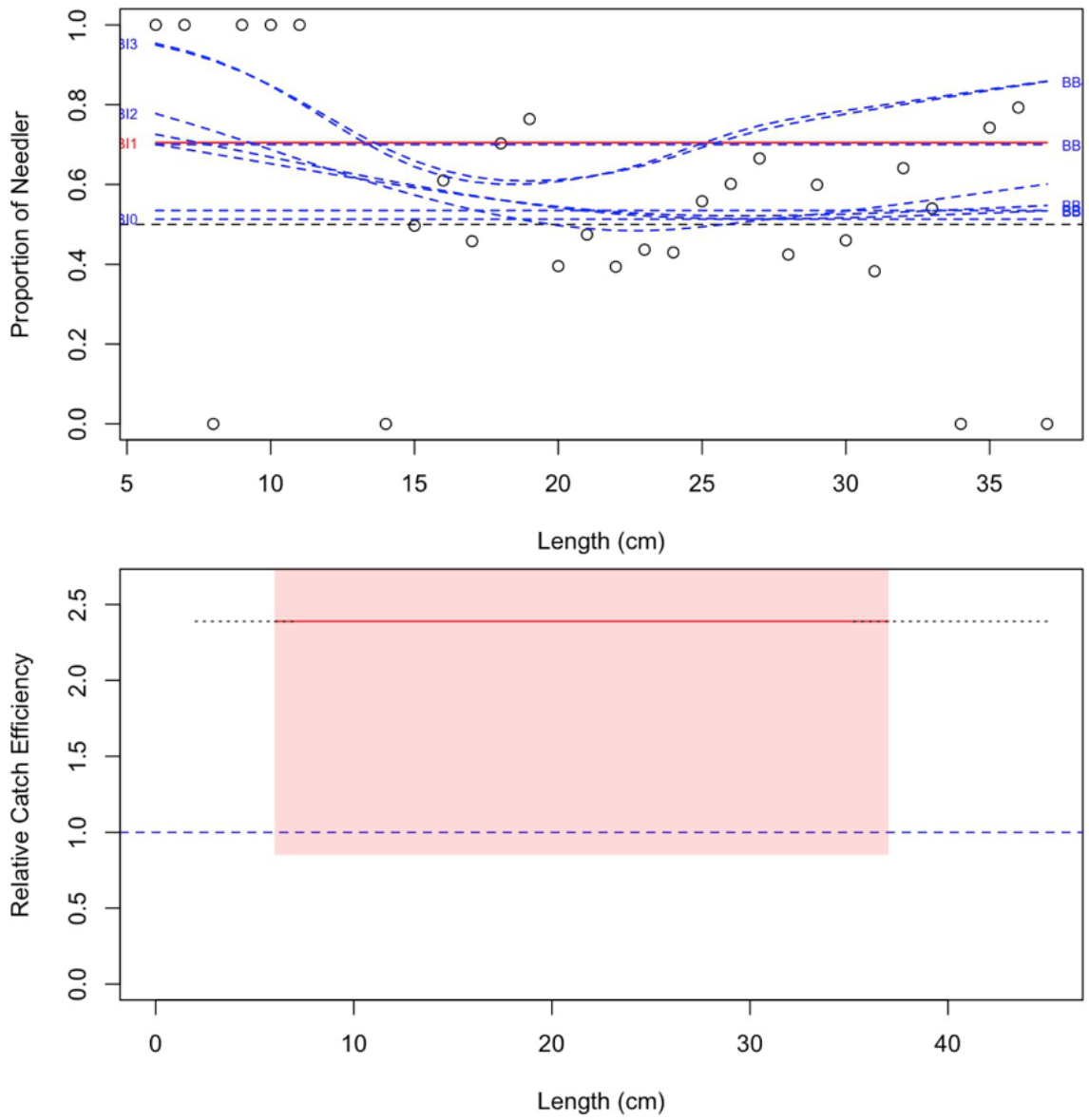

Figure 27b. Model fits and the selected length-based calibration for Urophycis chesteri (112).

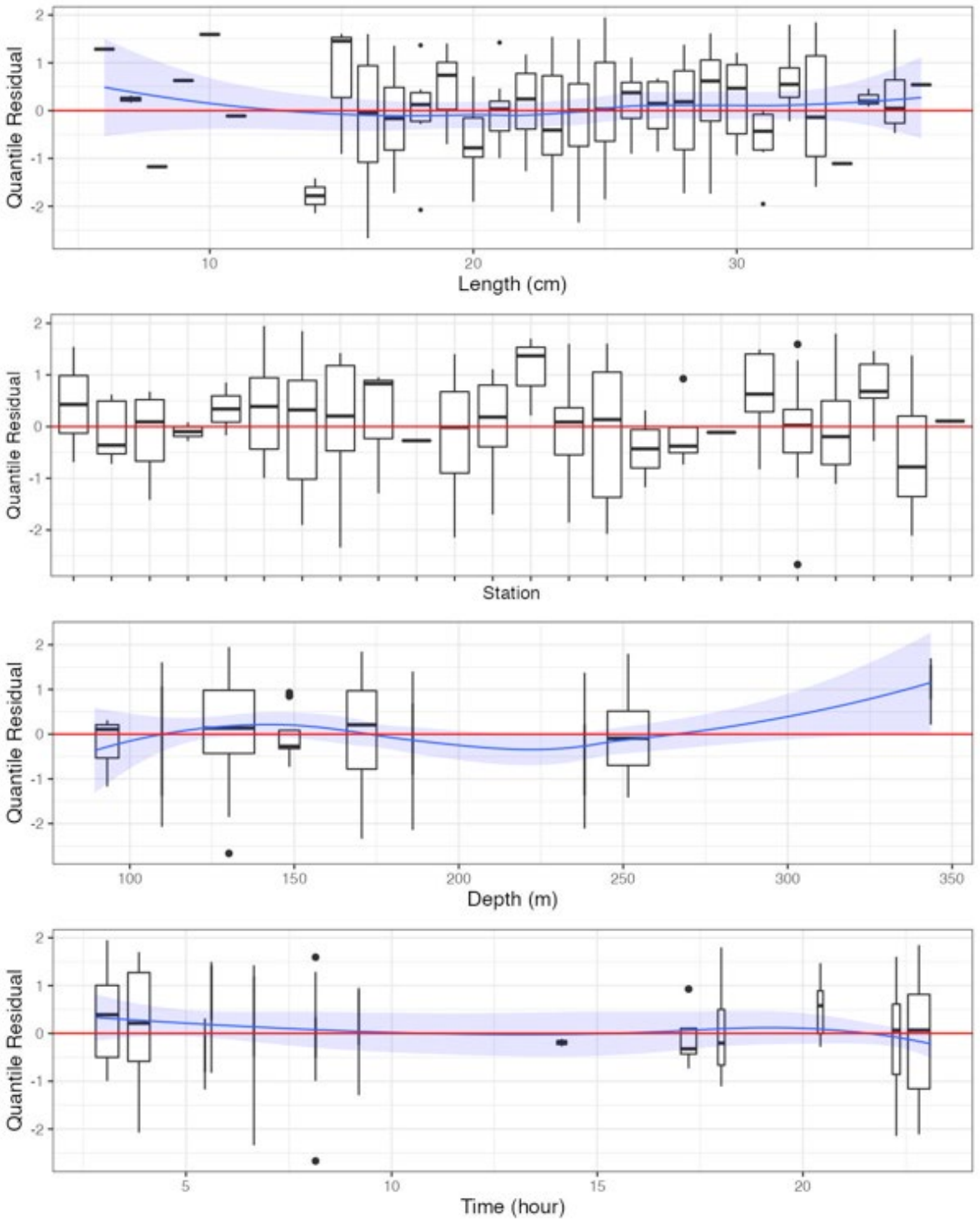

Figure 27c. Randomized and normalized quantile residuals for the selected model for Urophycis chesteri (112).

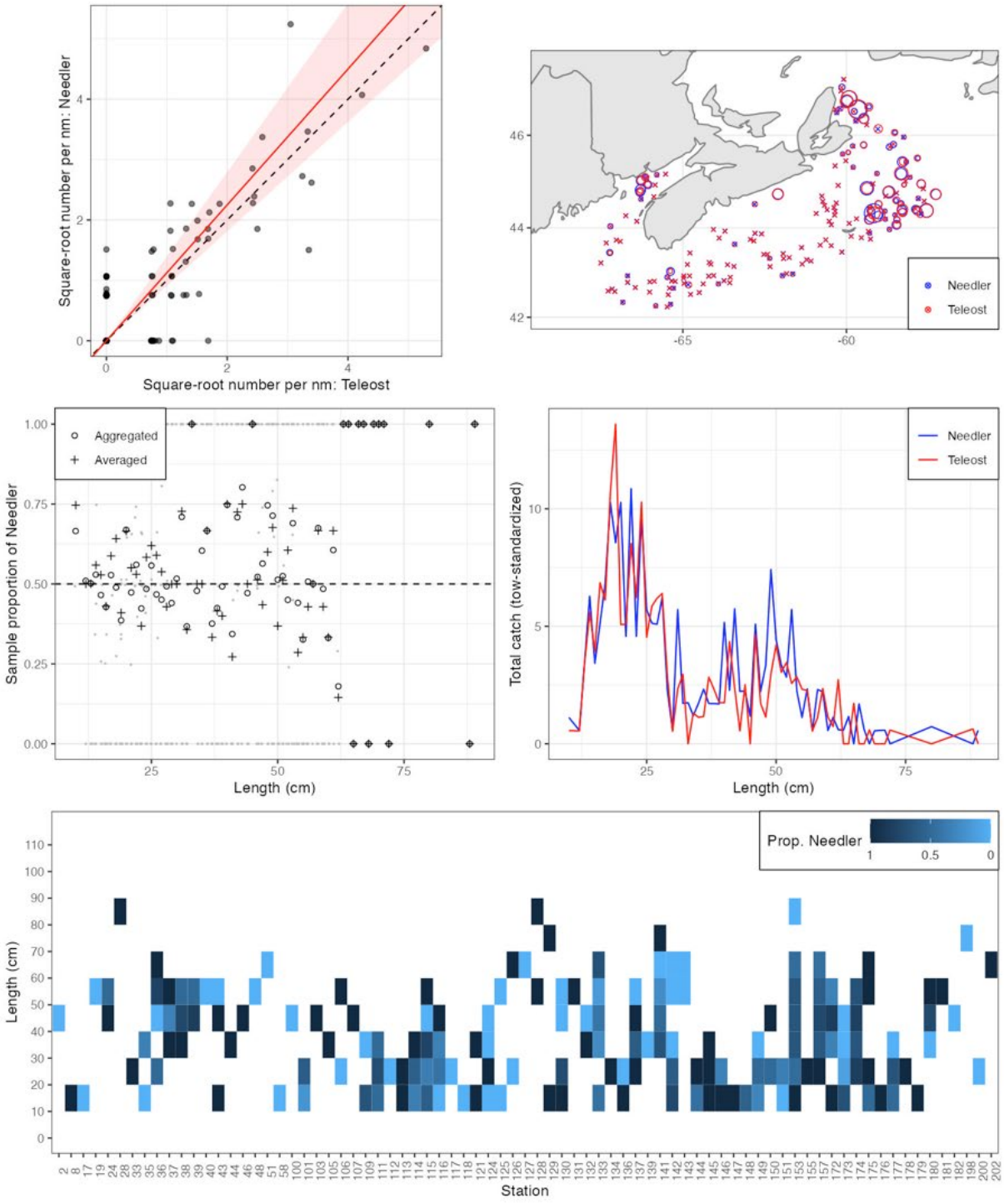

Figure 28a. Visualisation of comparative fishing data and size-aggregated model fit for Amblyraja radiata (201).

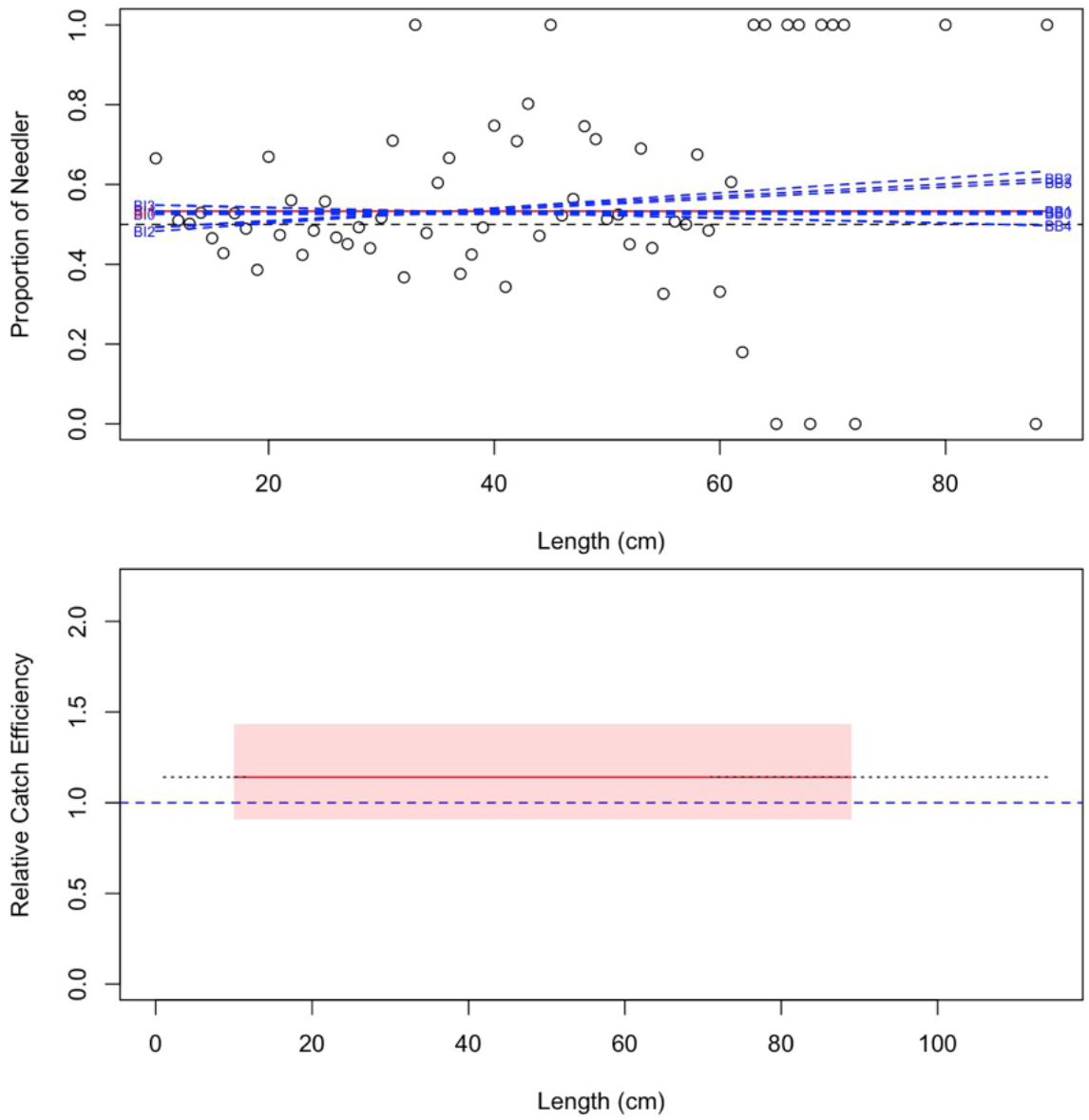

Figure 28b. Model fits and the selected length-based calibration for Amblyraja radiata (201).

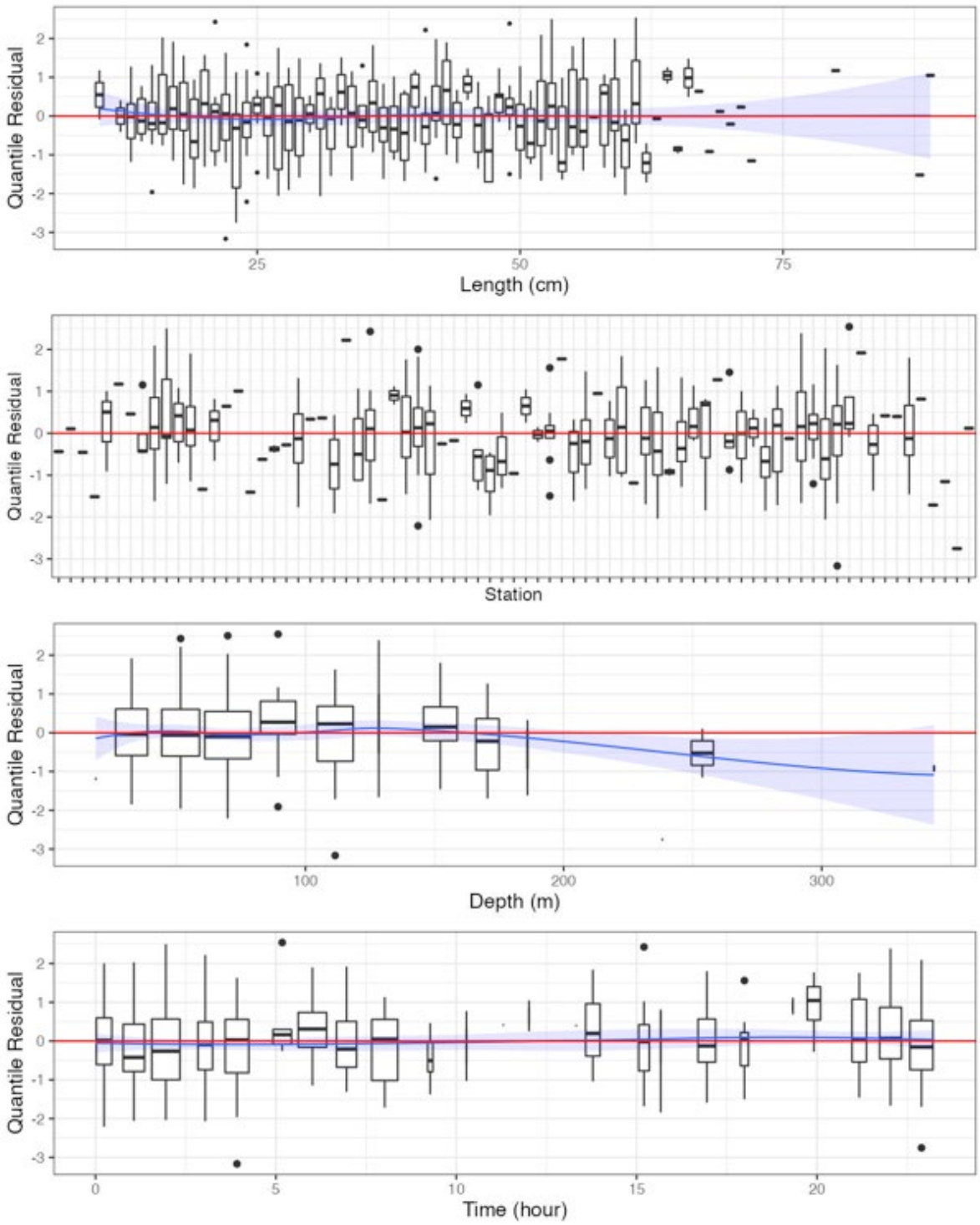

Figure 28c. Randomized and normalized quantile residuals for the selected model for Amblyraja radiata (201).

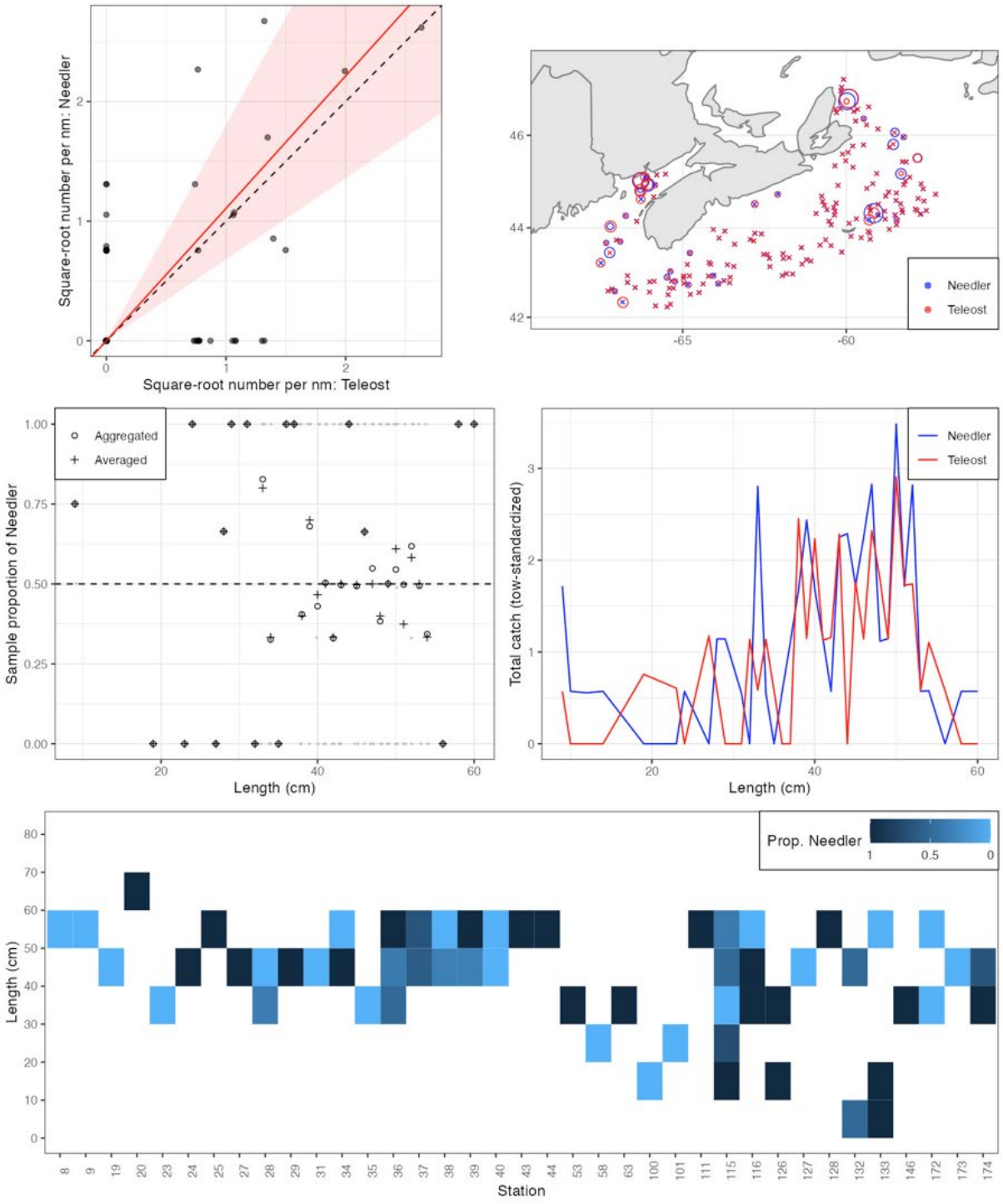

Figure 29a. Visualisation of comparative fishing data and size-aggregated model fit for Malacoraja senta (202).

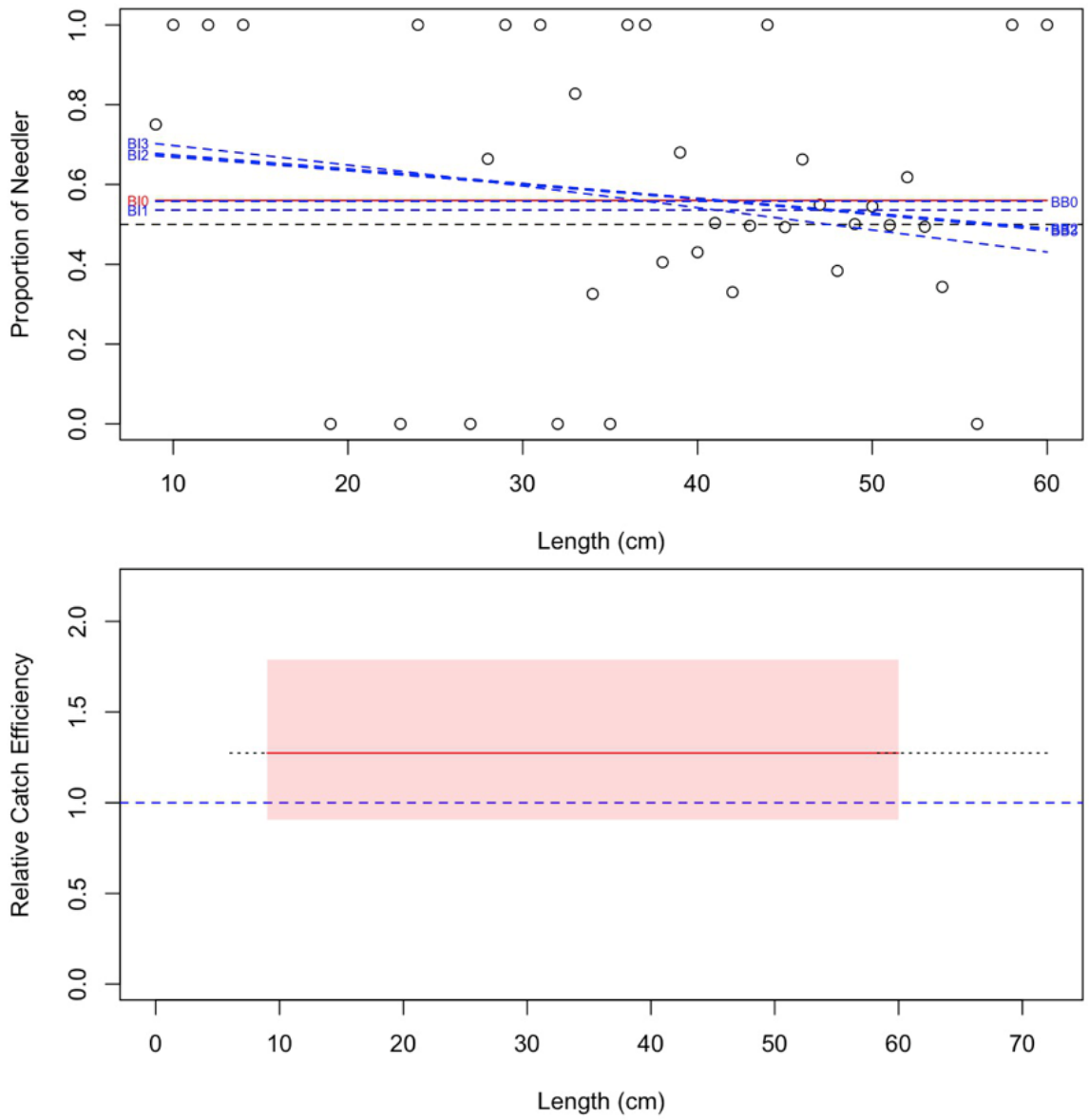

Figure 29b. Model fits and the selected length-based calibration for Malacoraja senta (202).

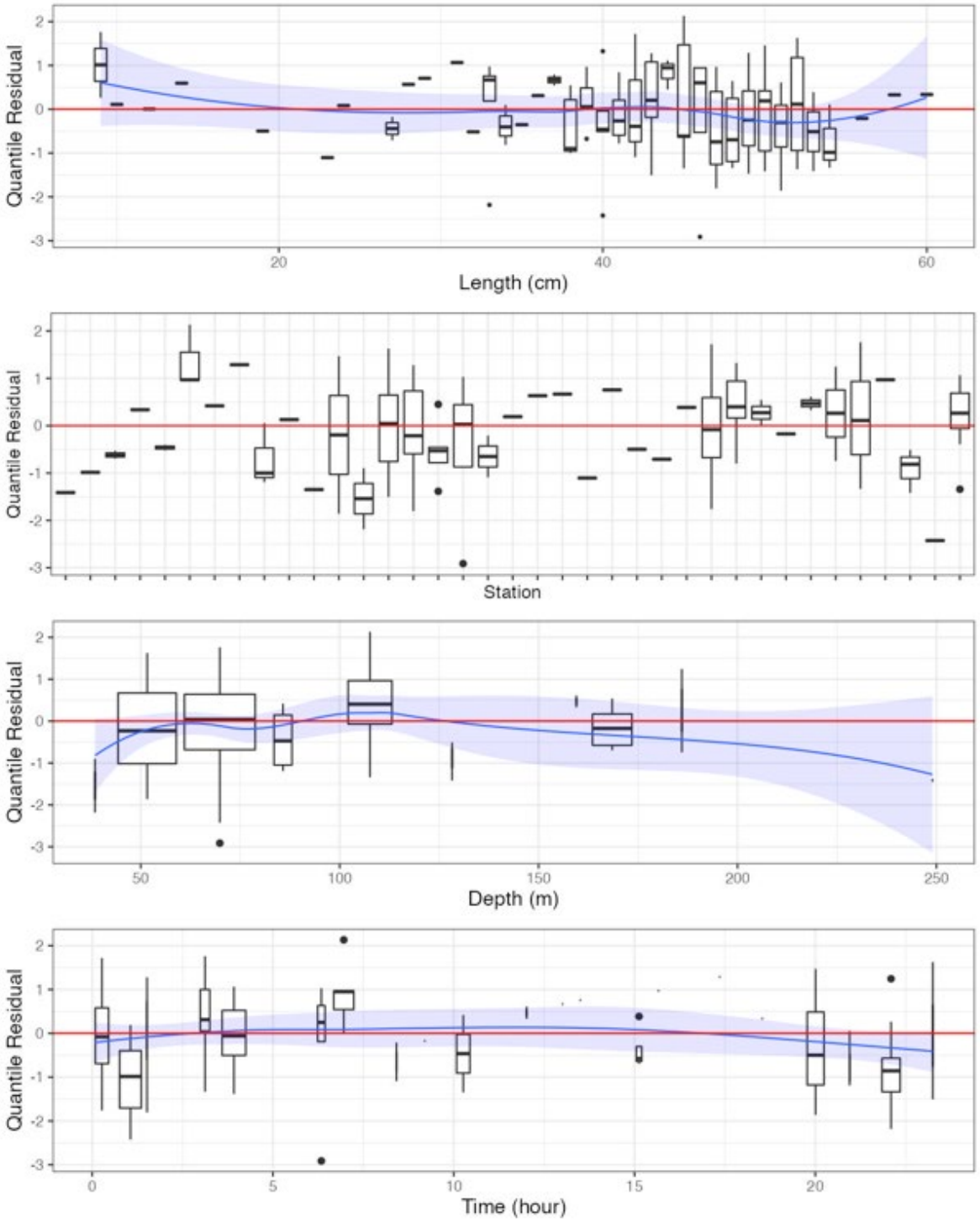

Figure 29c. Randomized and normalized quantile residuals for the selected model for Malacoraja senta (202).

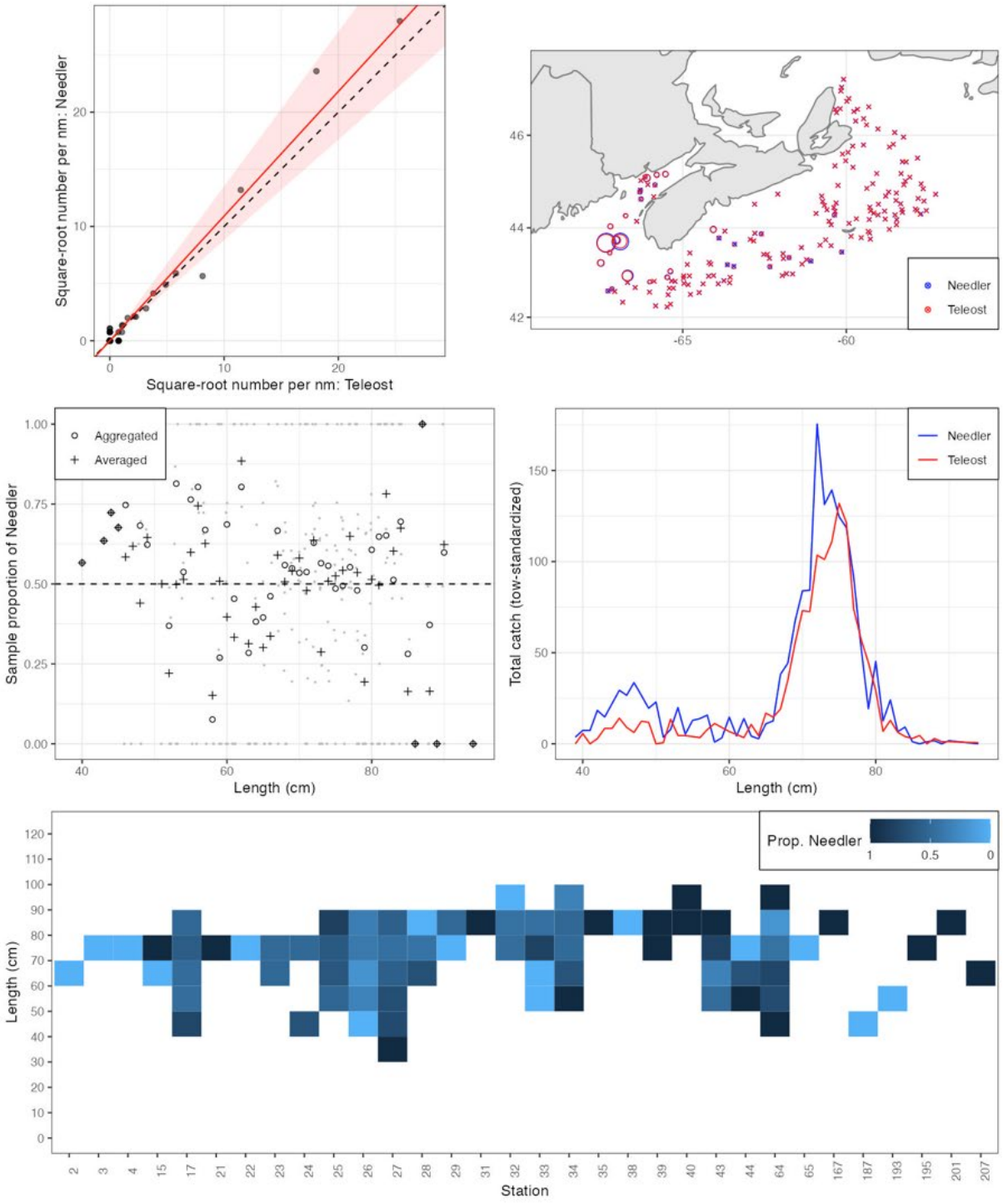

Figure 30a. Visualisation of comparative fishing data and size-aggregated model fit for Squalus acanthias (220).

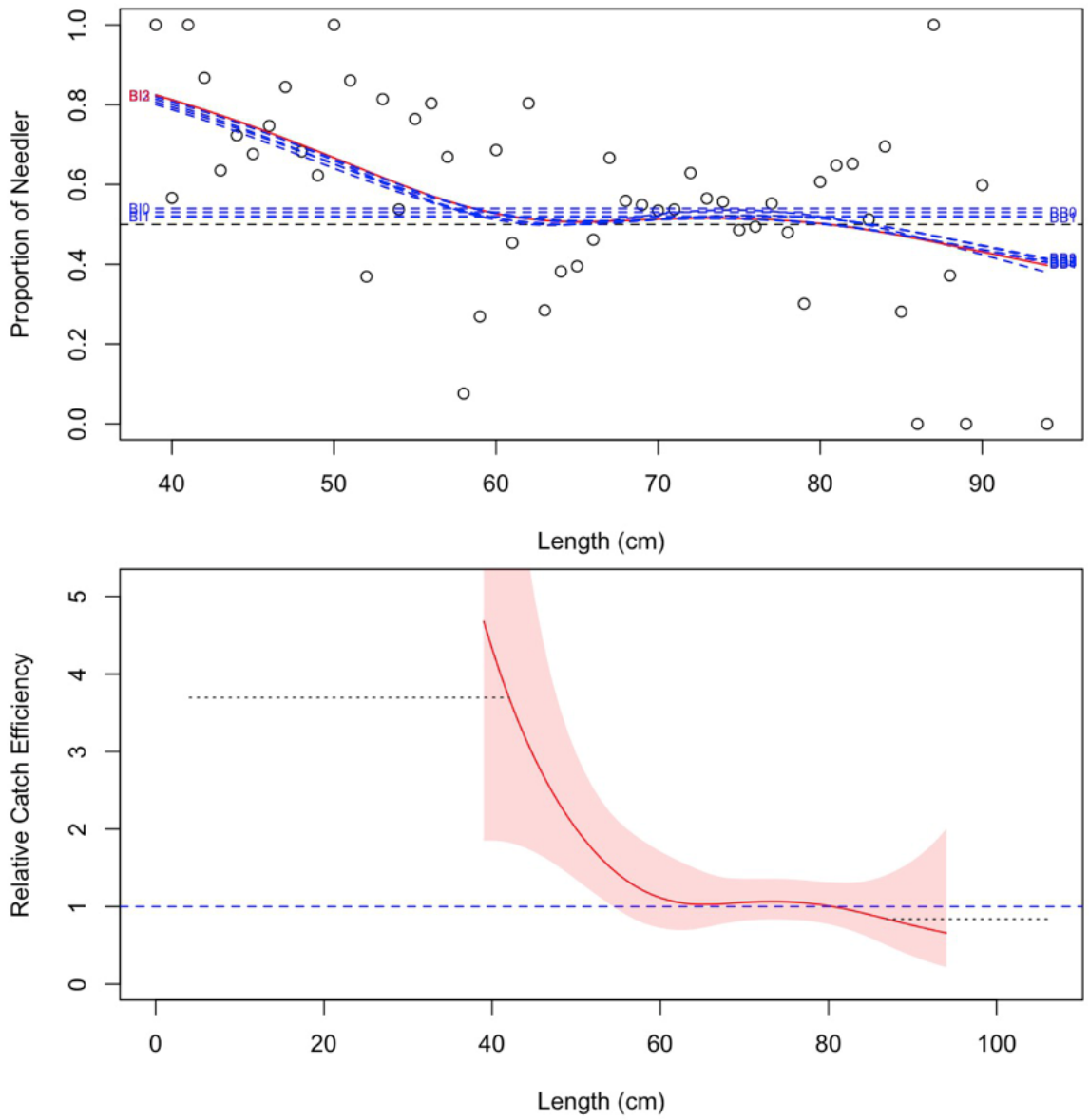

Figure 30b. Model fits and the selected length-based calibration for Squalus acanthias (220).

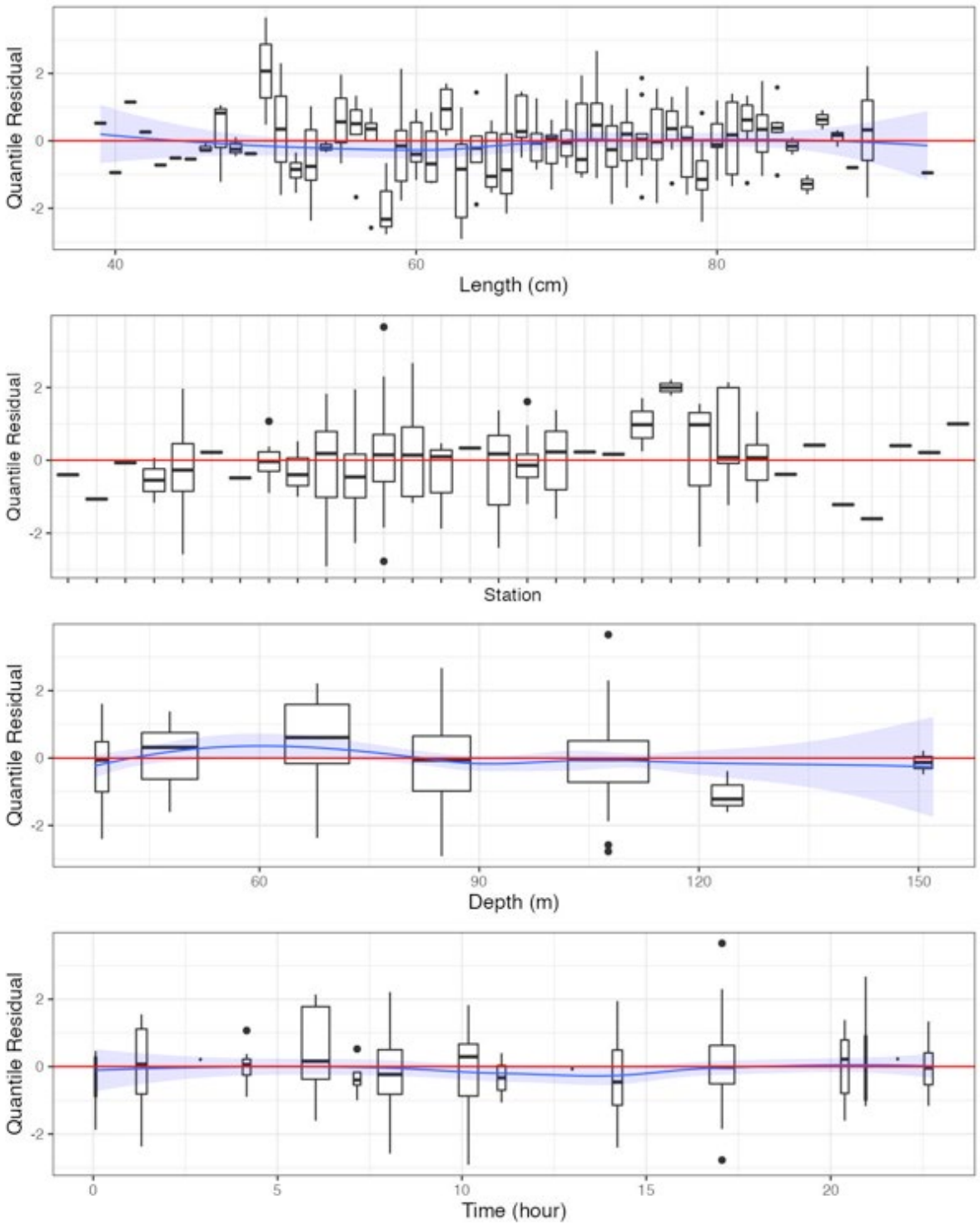

Figure 30c. Randomized and normalized quantile residuals for the selected model for Squalus acanthias (220).

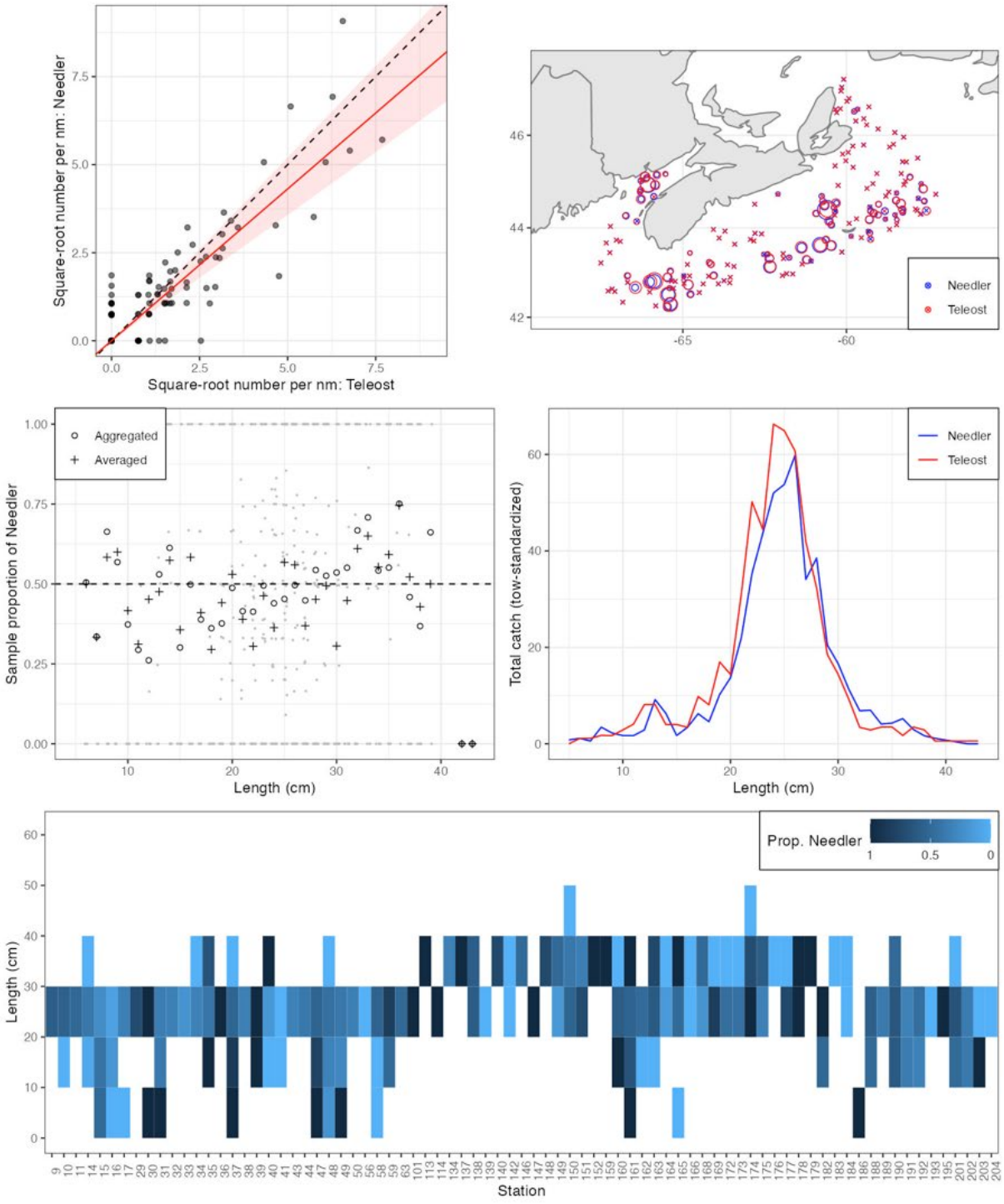

Figure 31a. Visualisation of comparative fishing data and size-aggregated model fit for Myoxocephalus octodecemspinosus (300).

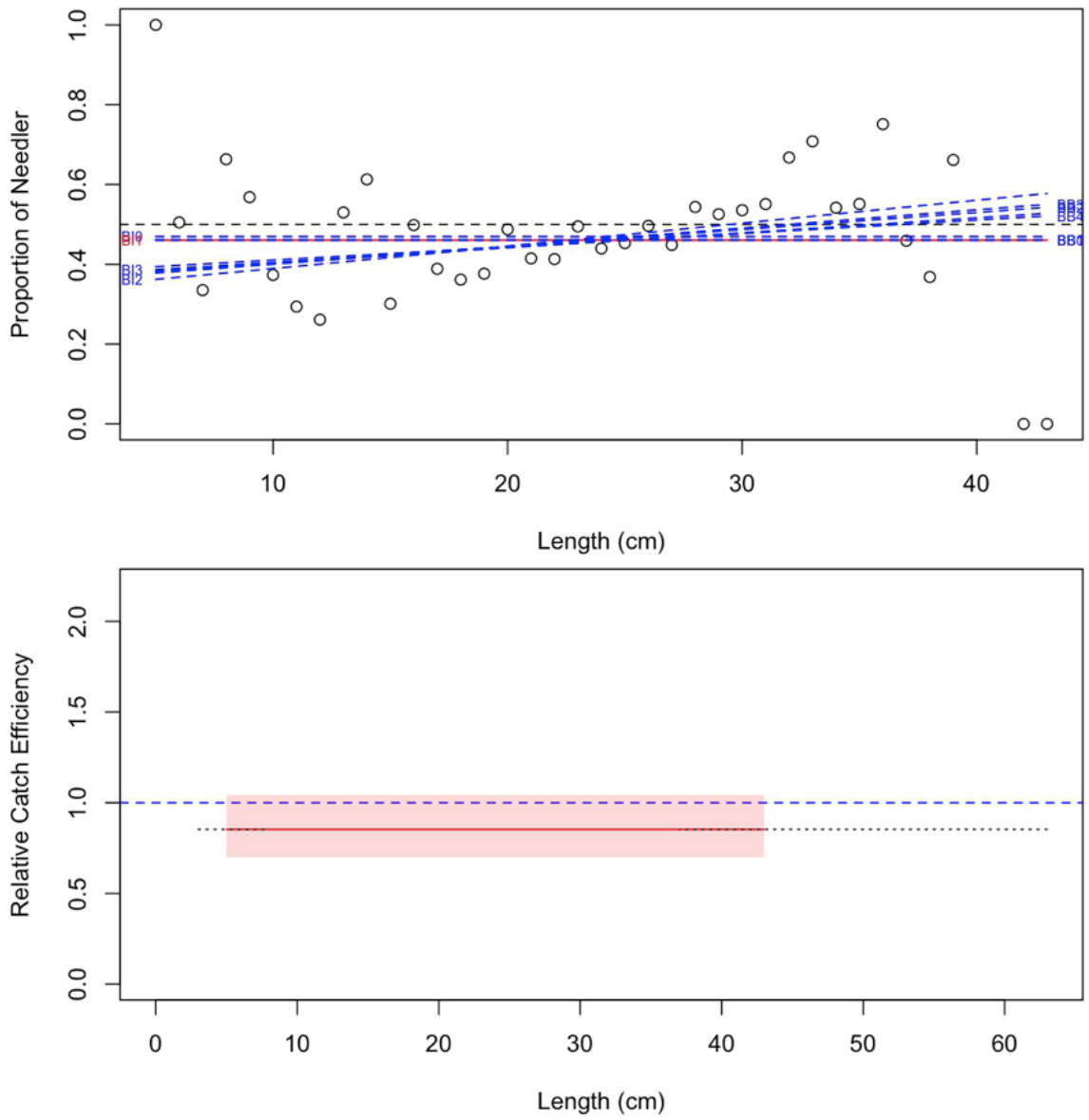

Figure 31b. Model fits and the selected length-based calibration for Myoxocephalus octodecemspinosus (300).

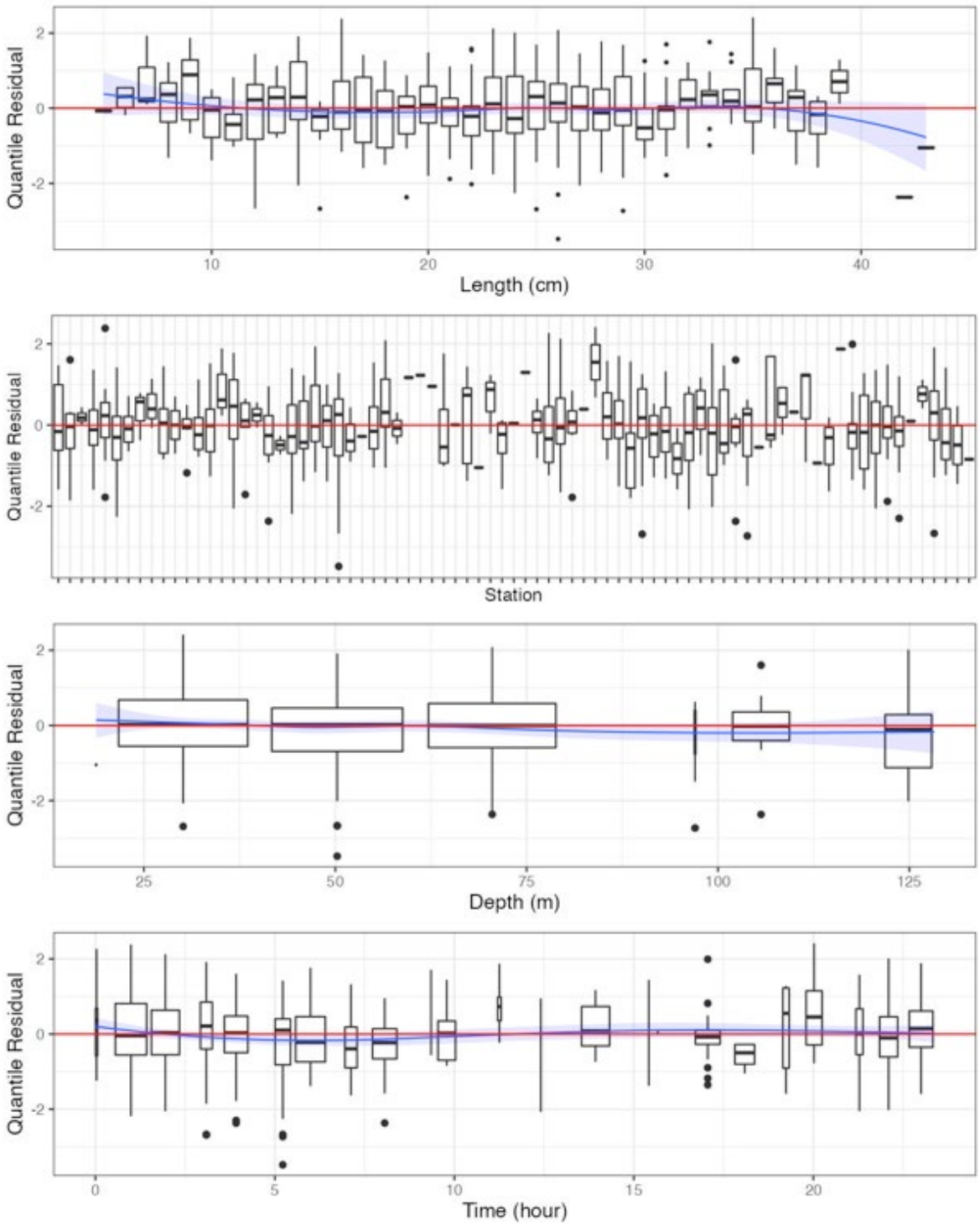

Figure 31c. Randomized and normalized quantile residuals for the selected model for Myoxocephalus octodecemspinosus (300).

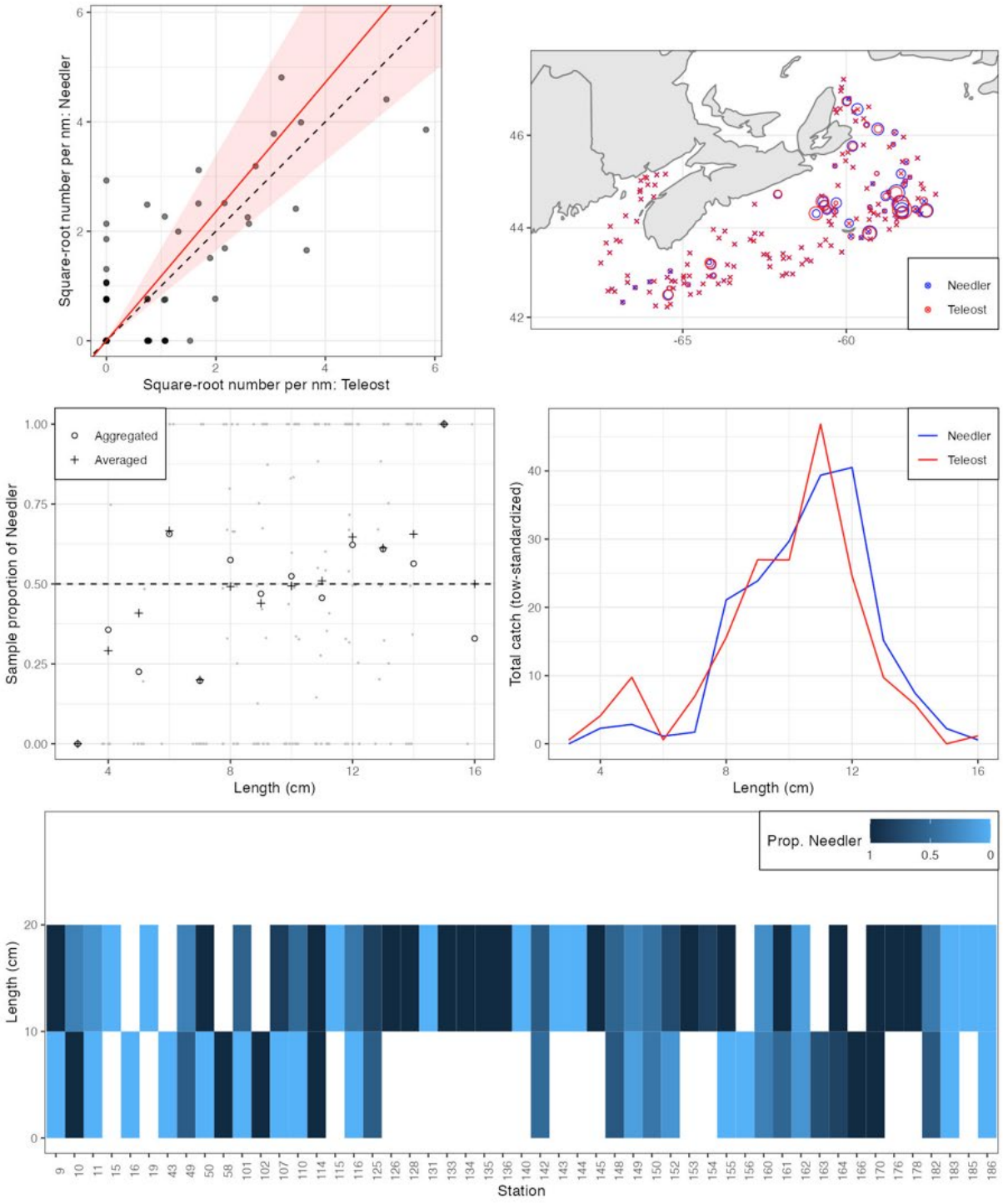

Figure 32a. Visualisation of comparative fishing data and size-aggregated model fit for Triglops murrayi (304).

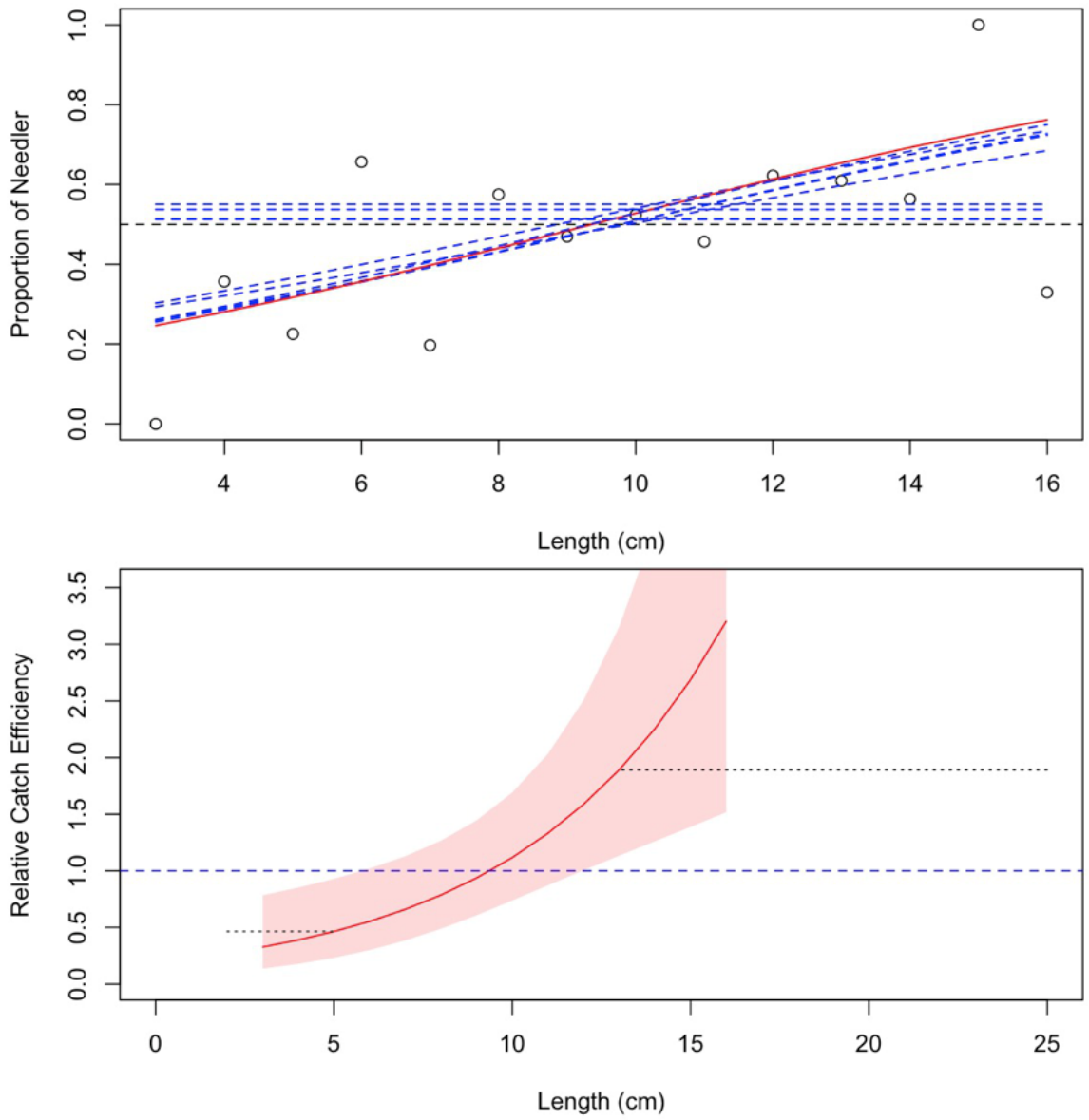

Figure 32b. Model fits and the selected length-based calibration for Triglops murrayi (304).

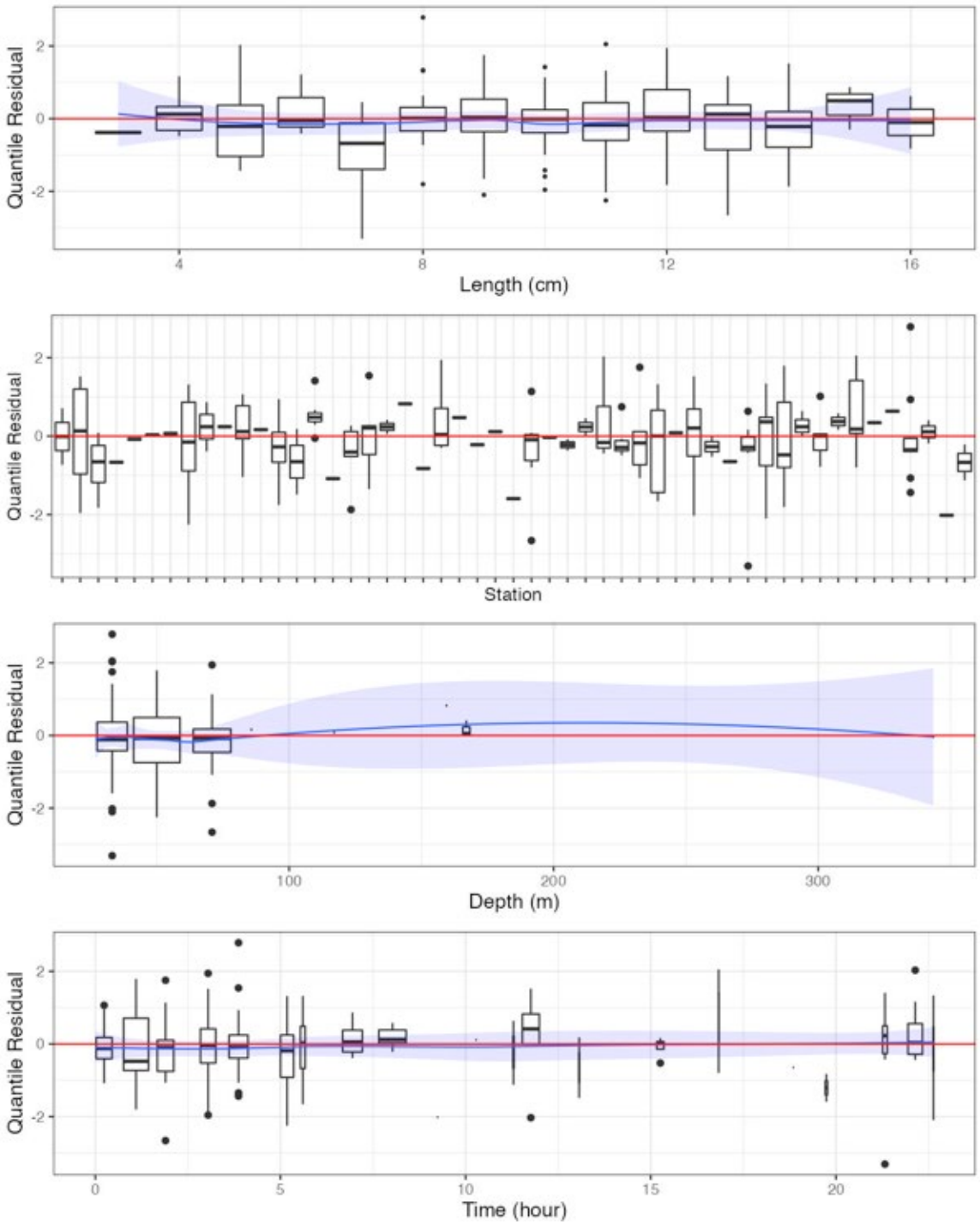

Figure 32c. Randomized and normalized quantile residuals for the selected model for Triglops murrayi (304).

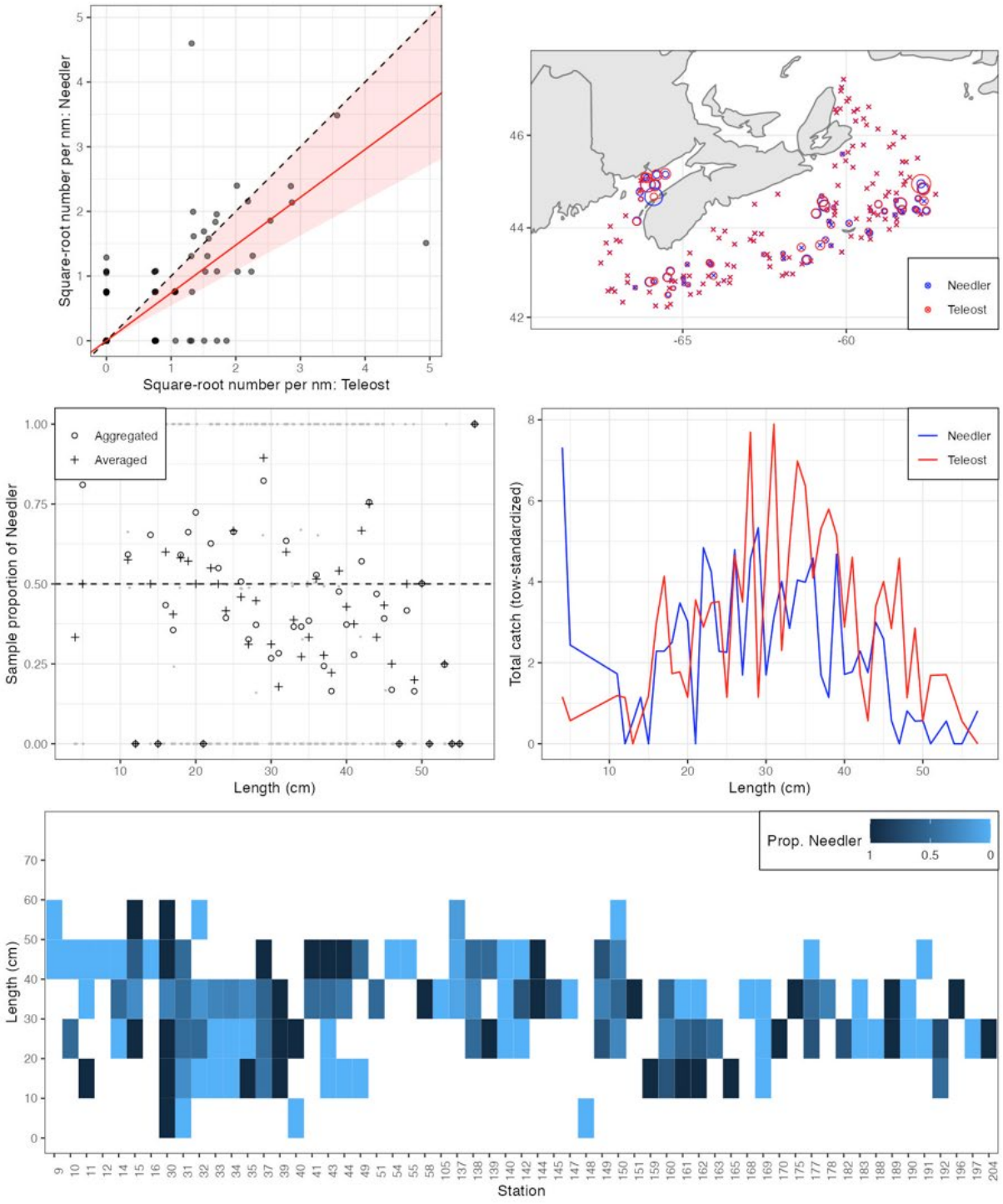

Figure 33a. Visualisation of comparative fishing data and size-aggregated model fit for Hemitripterus americanus (320).

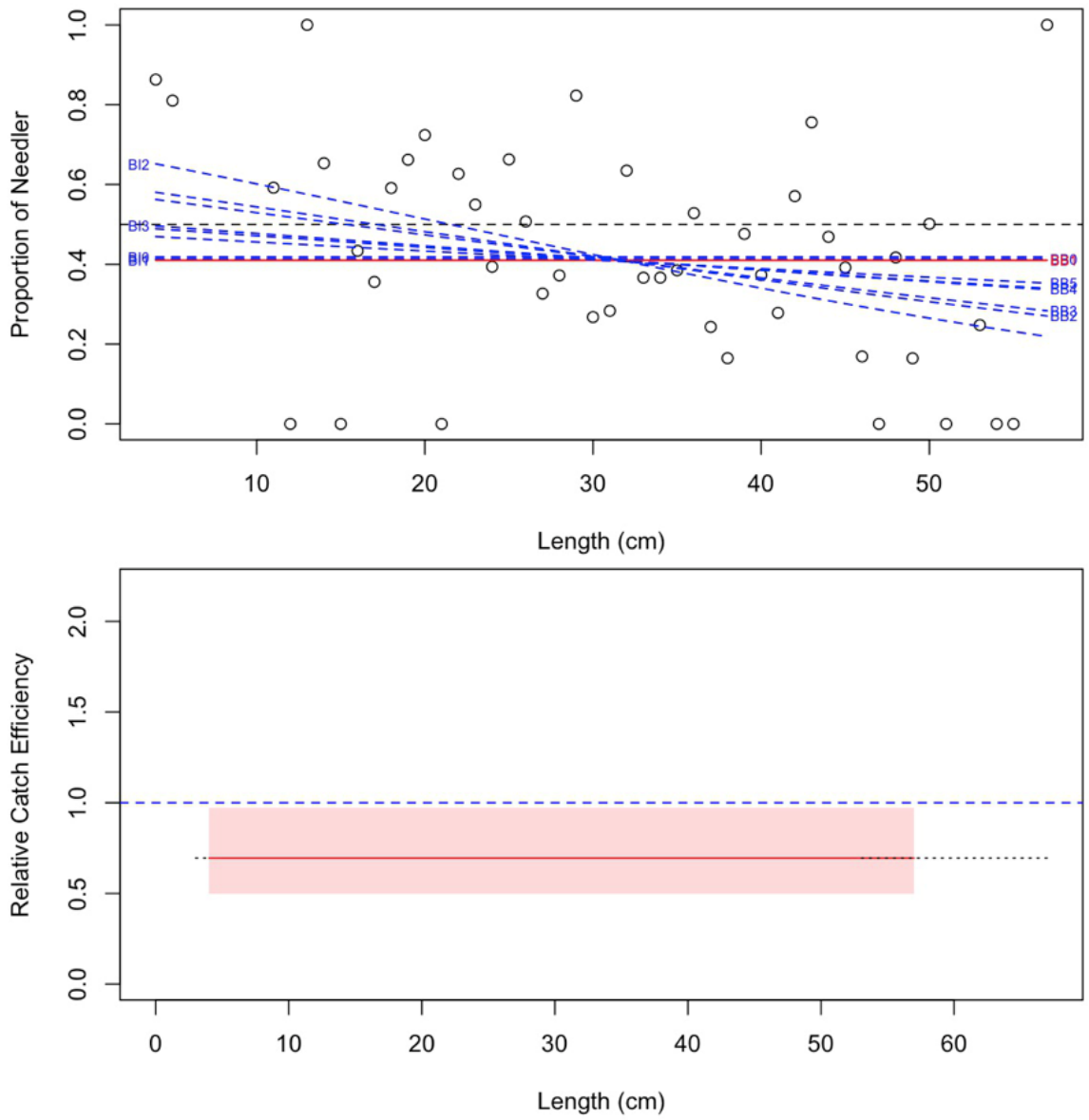

Figure 33b. Model fits and the selected length-based calibration for Hemitripterus americanus (320).

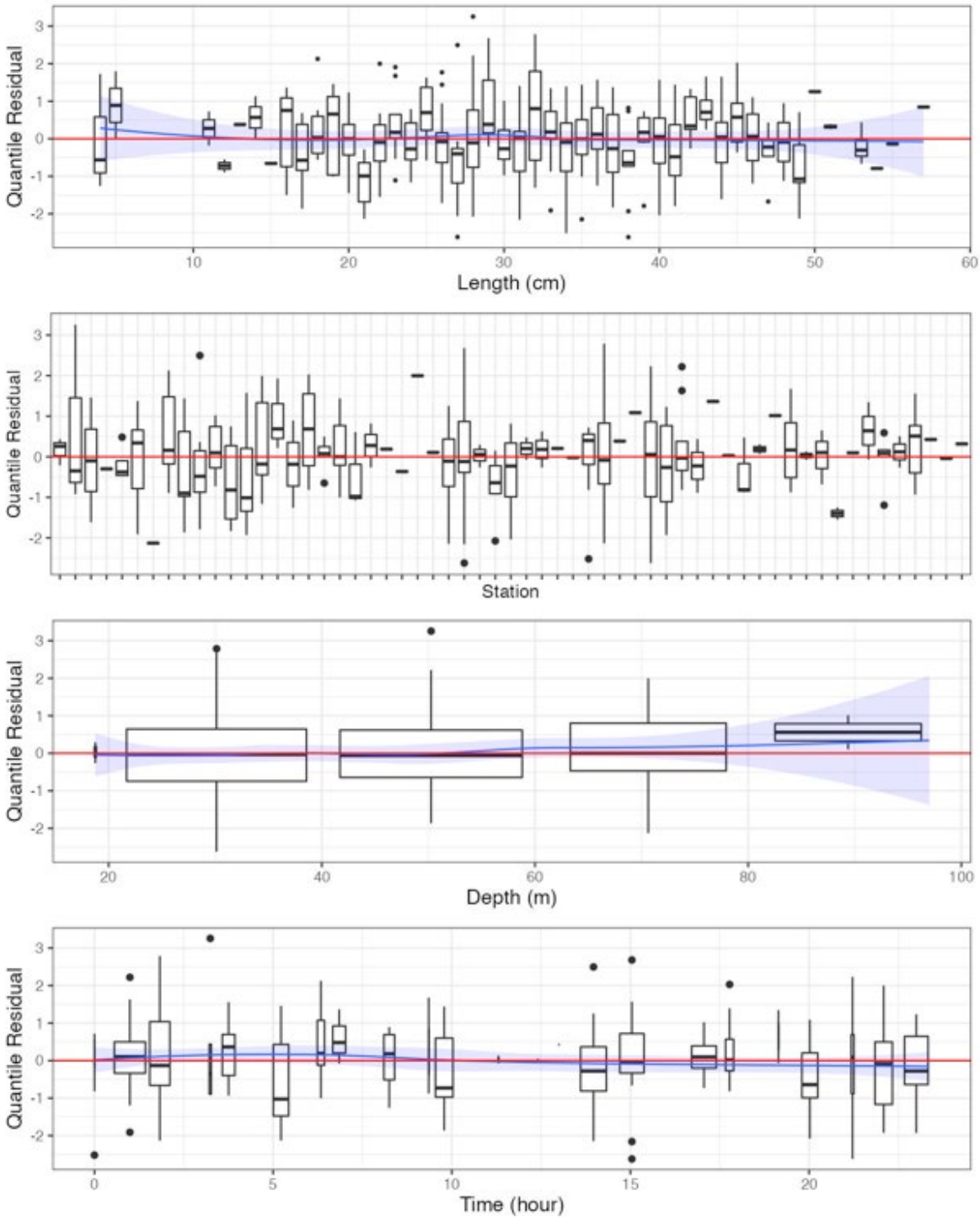

Figure 33c. Randomized and normalized quantile residuals for the selected model for Hemitripterus americanus (320).

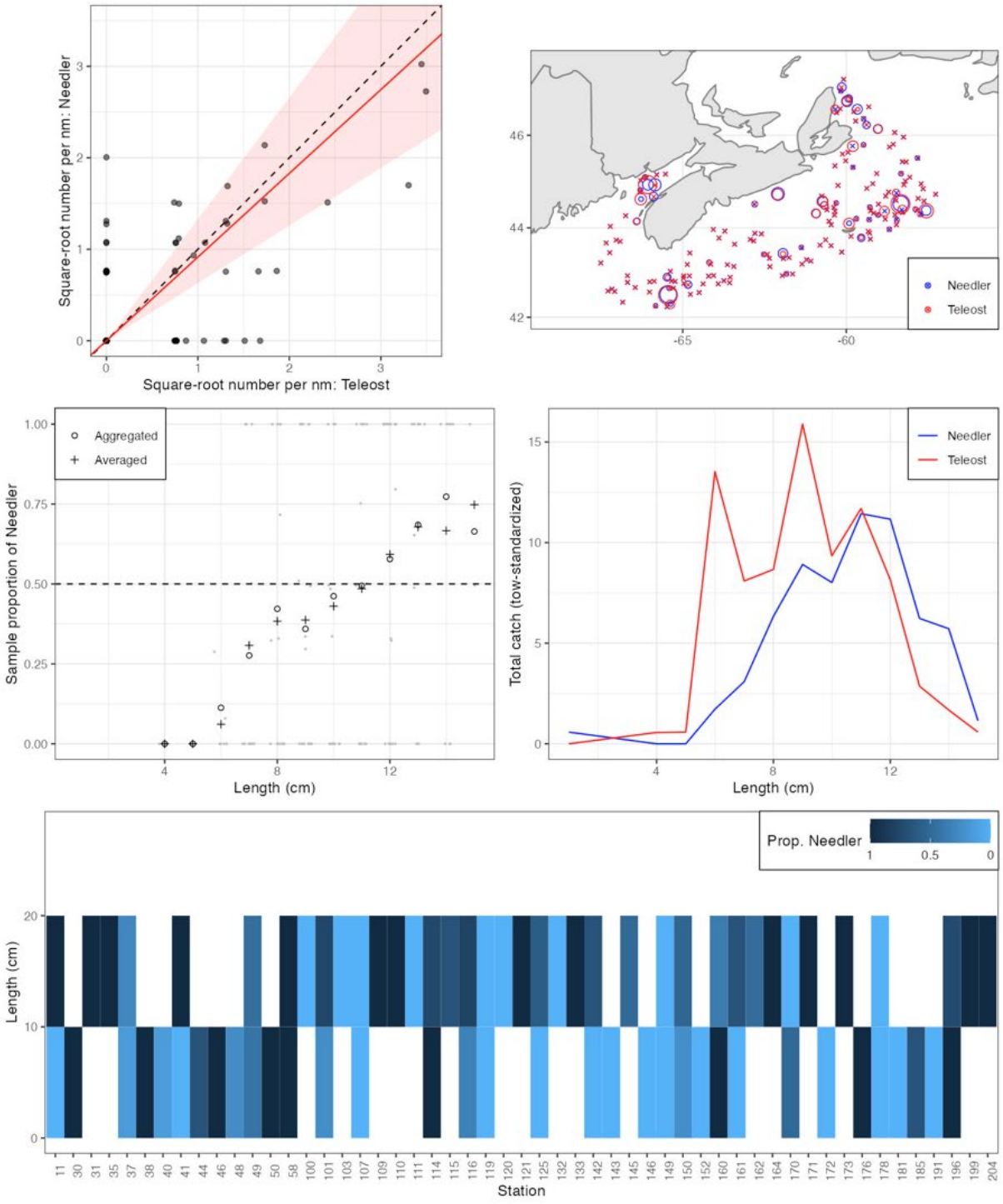

Figure 34a. Visualisation of comparative fishing data and size-aggregated model fit for Aspidophoroides monopterygius (340).

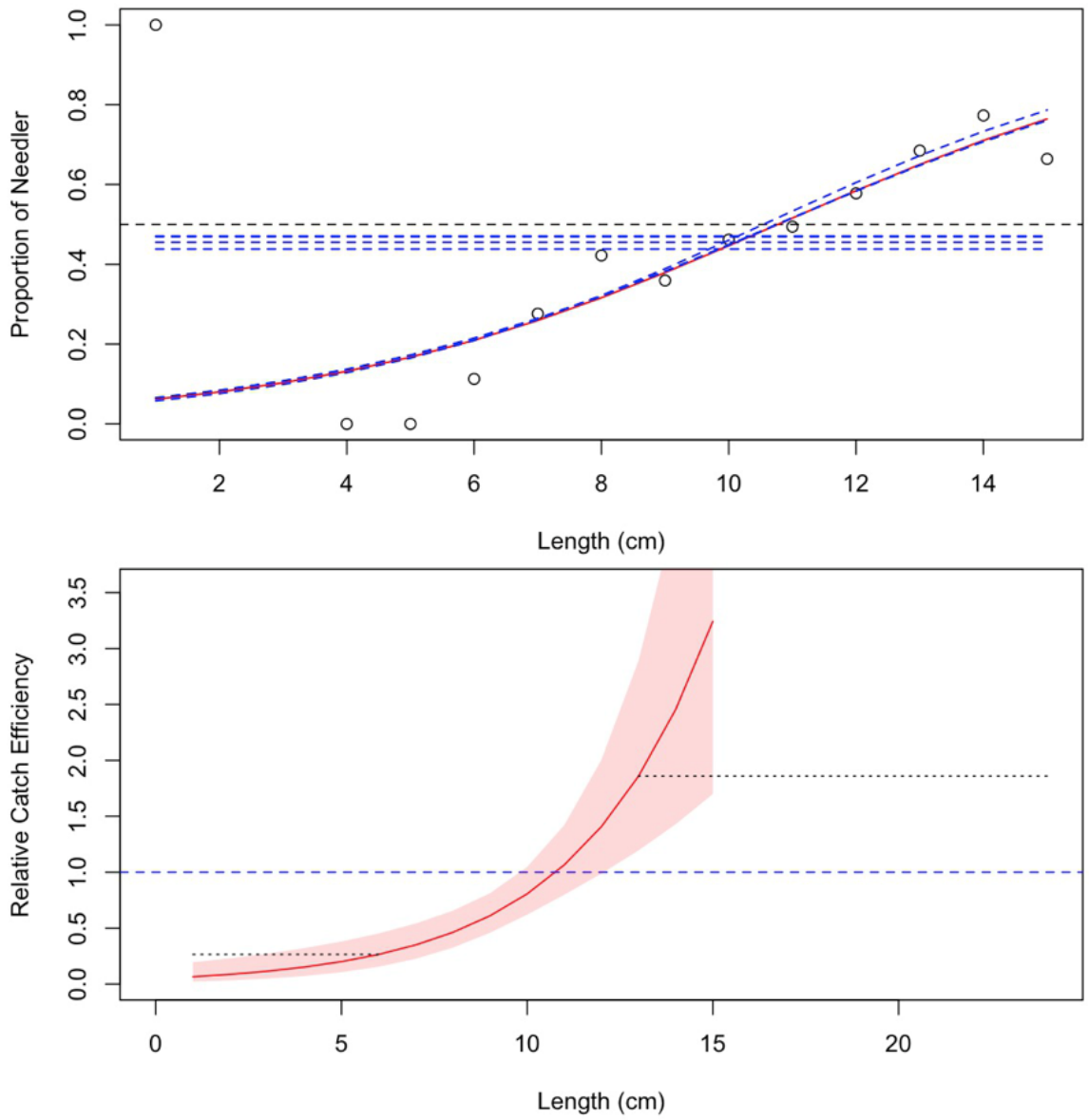

Figure 34b. Model fits and the selected length-based calibration for Aspidophoroides monopterygius (340).

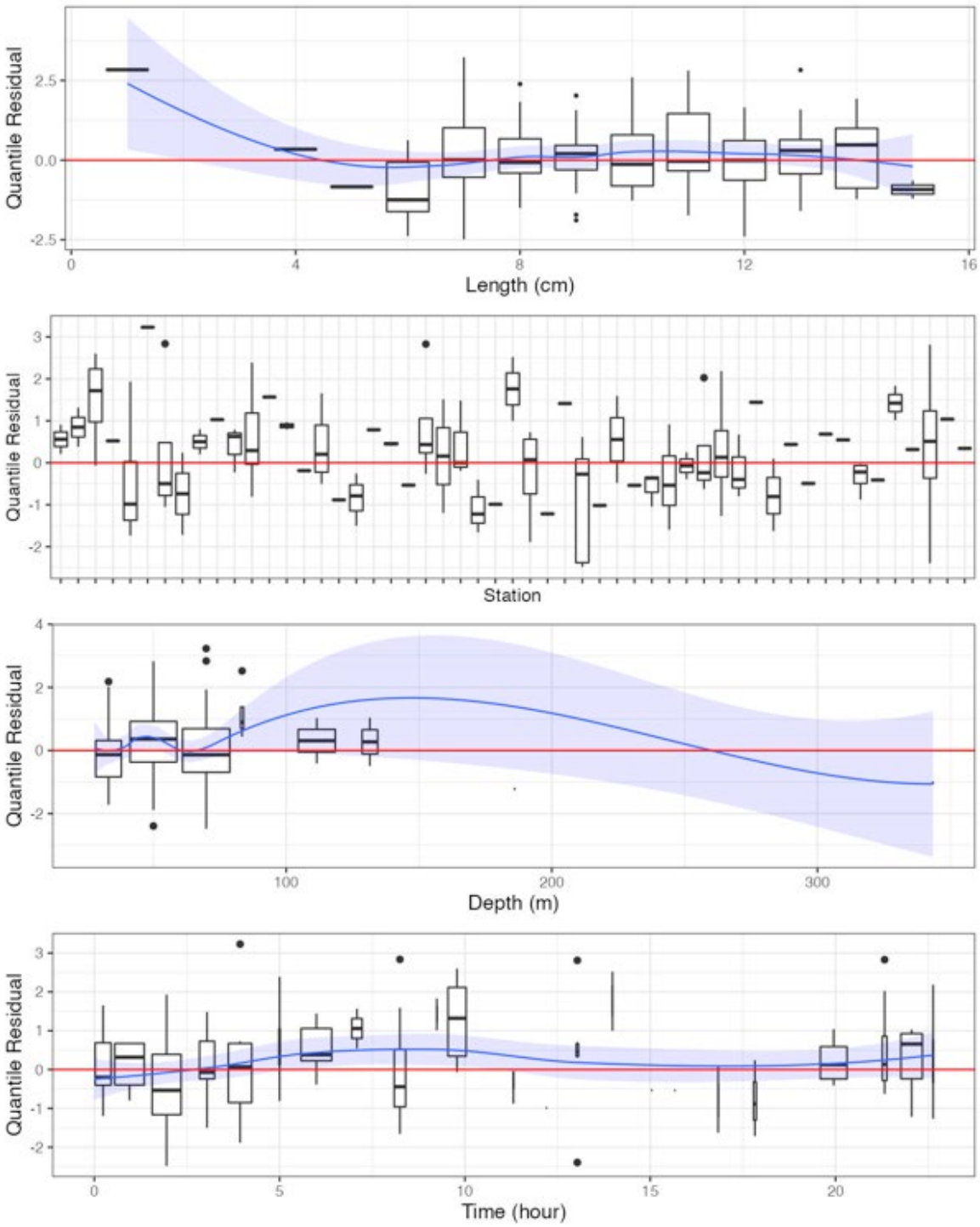

Figure 34c. Randomized and normalized quantile residuals for the selected model for Aspidophoroides monopterygius (340).

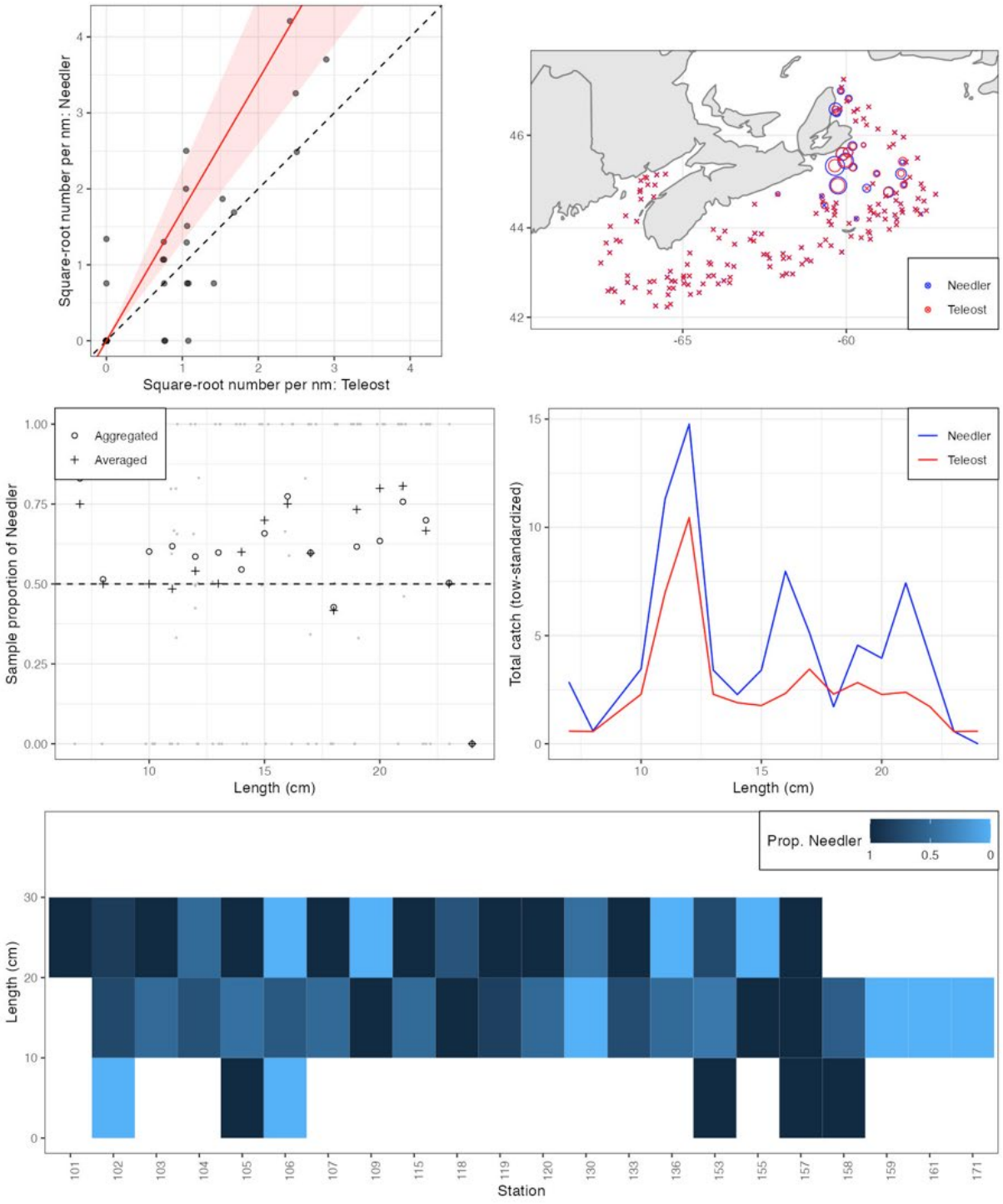

Figure 35a. Visualisation of comparative fishing data and size-aggregated model fit for Leptagonus decagonus (350).

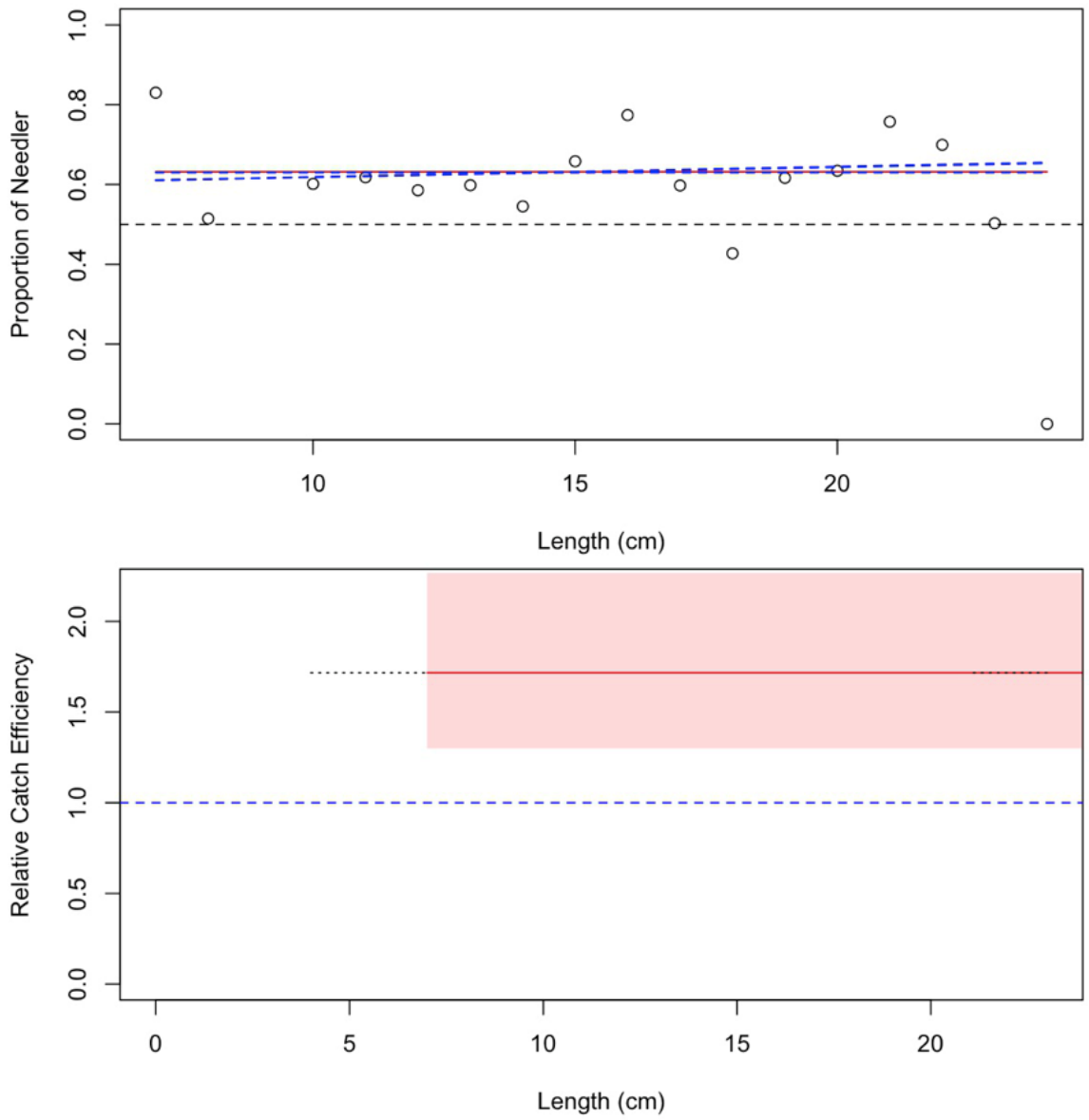

Figure 35b. Model fits and the selected length-based calibration for Leptagonus decagonus (350).

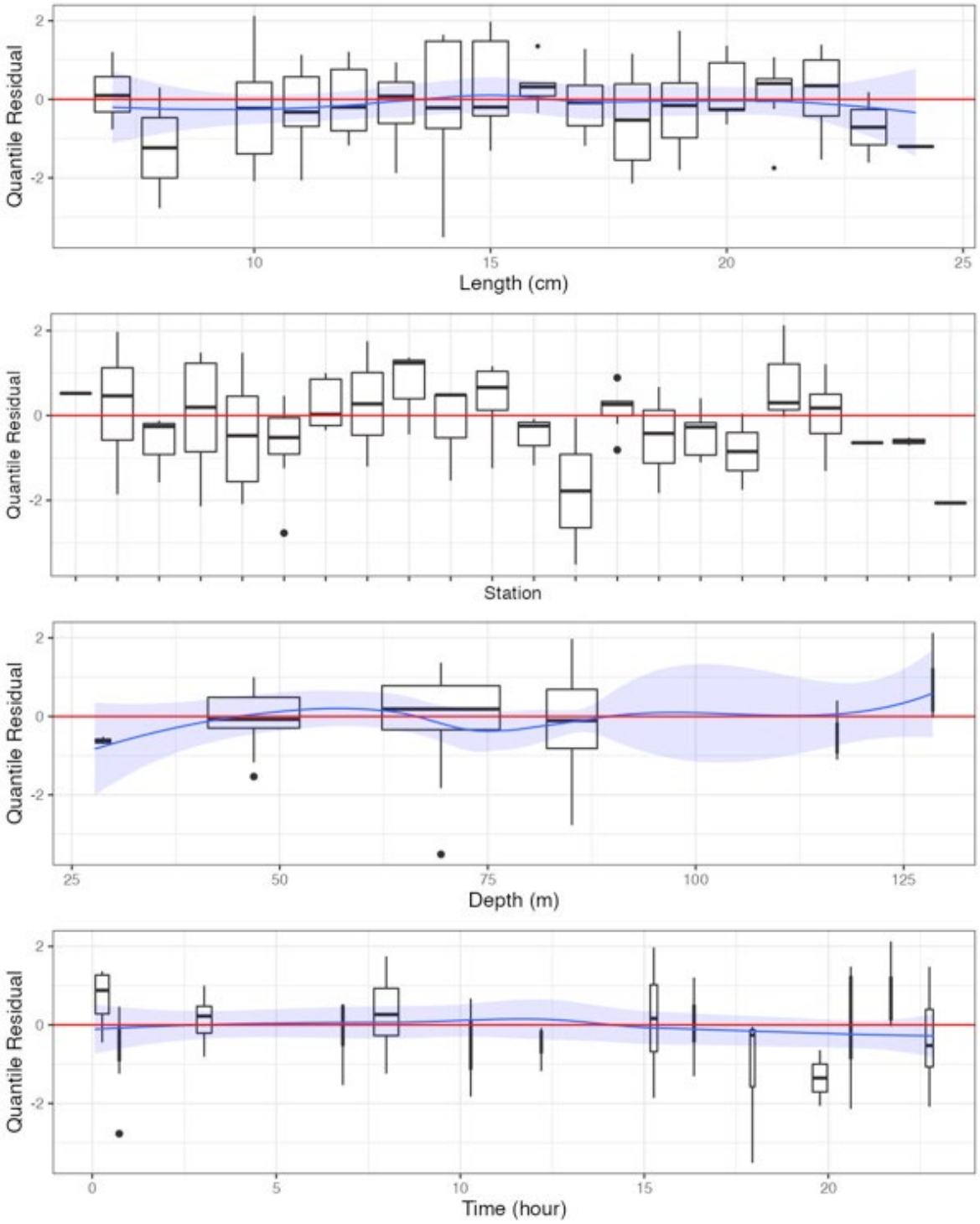

Figure 35c. Randomized and normalized quantile residuals for the selected model for Leptagonus decagonus (350).

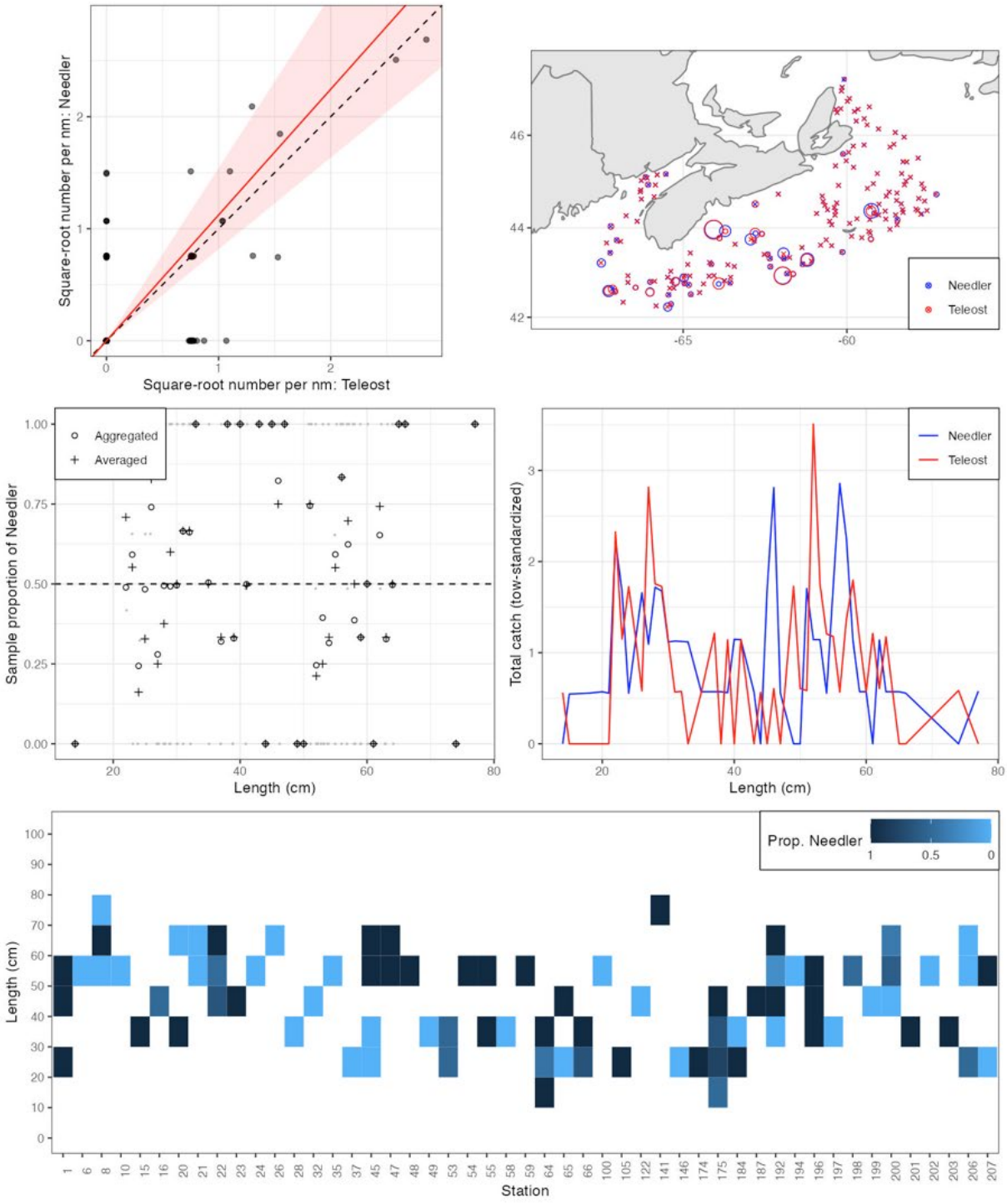

Figure 36a. Visualisation of comparative fishing data and size-aggregated model fit for Lophius americanus (400).

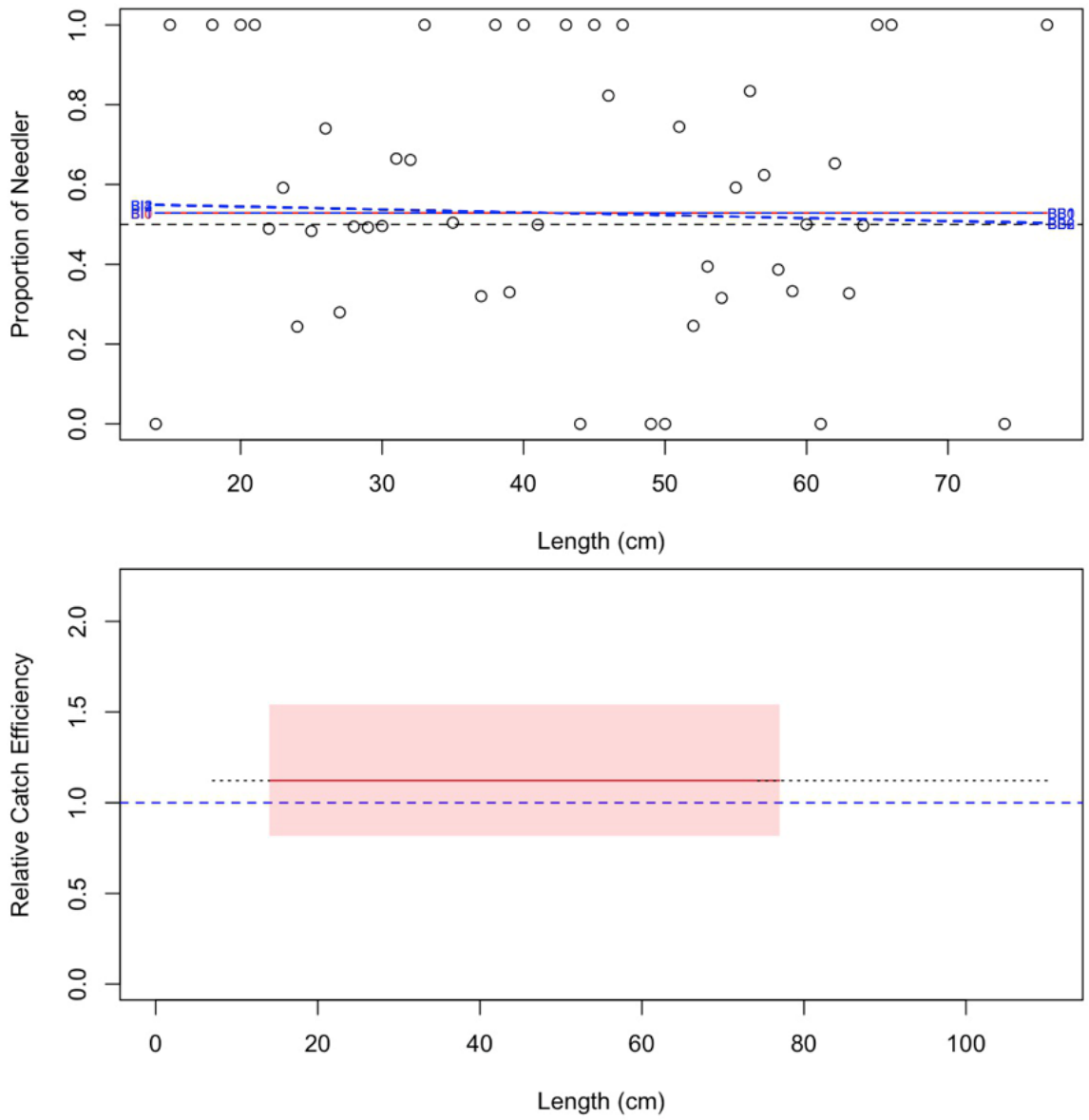

Figure 36b. Model fits and the selected length-based calibration for Lophius americanus (400).

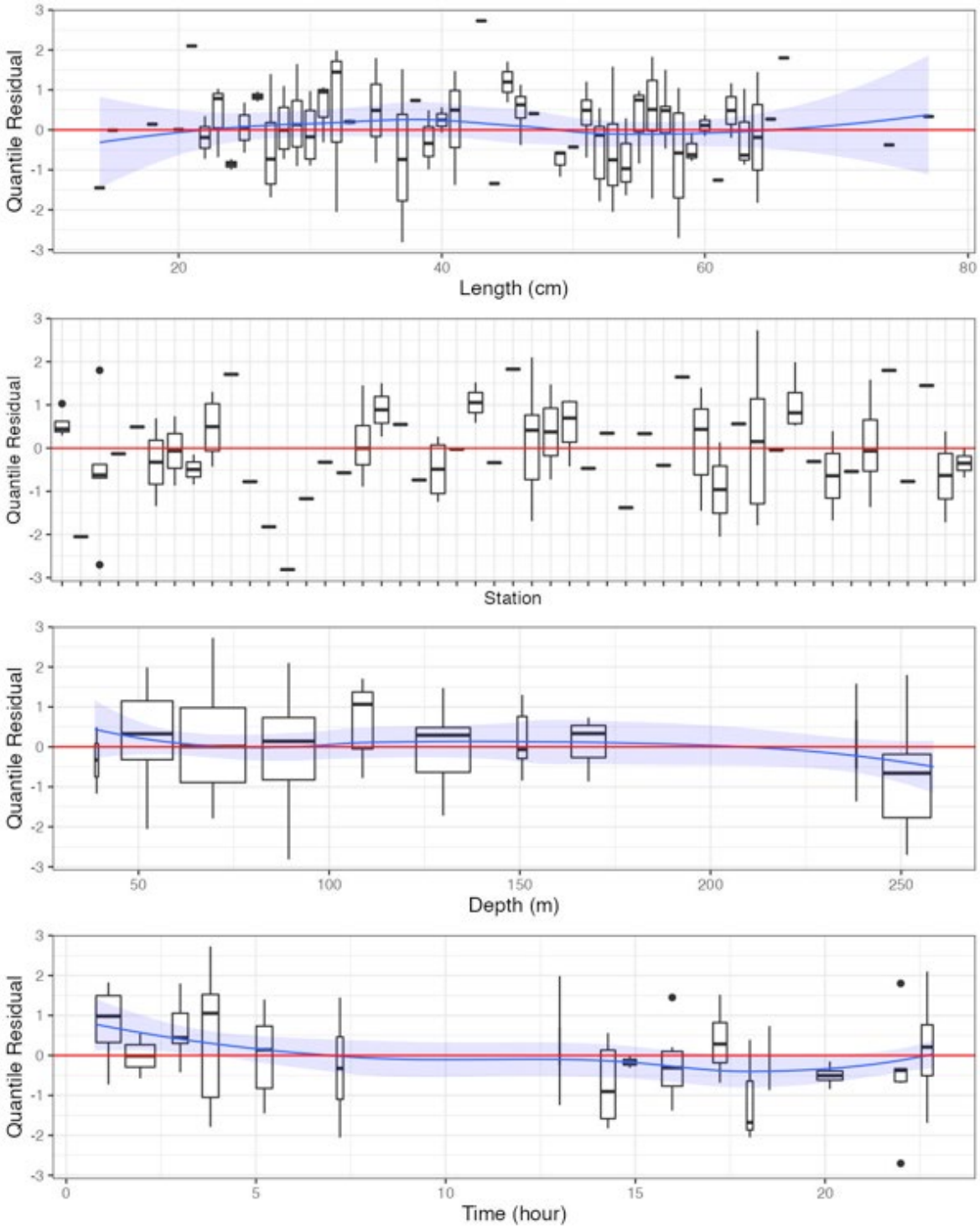

Figure 36c. Randomized and normalized quantile residuals for the selected model for Lophius americanus (400).

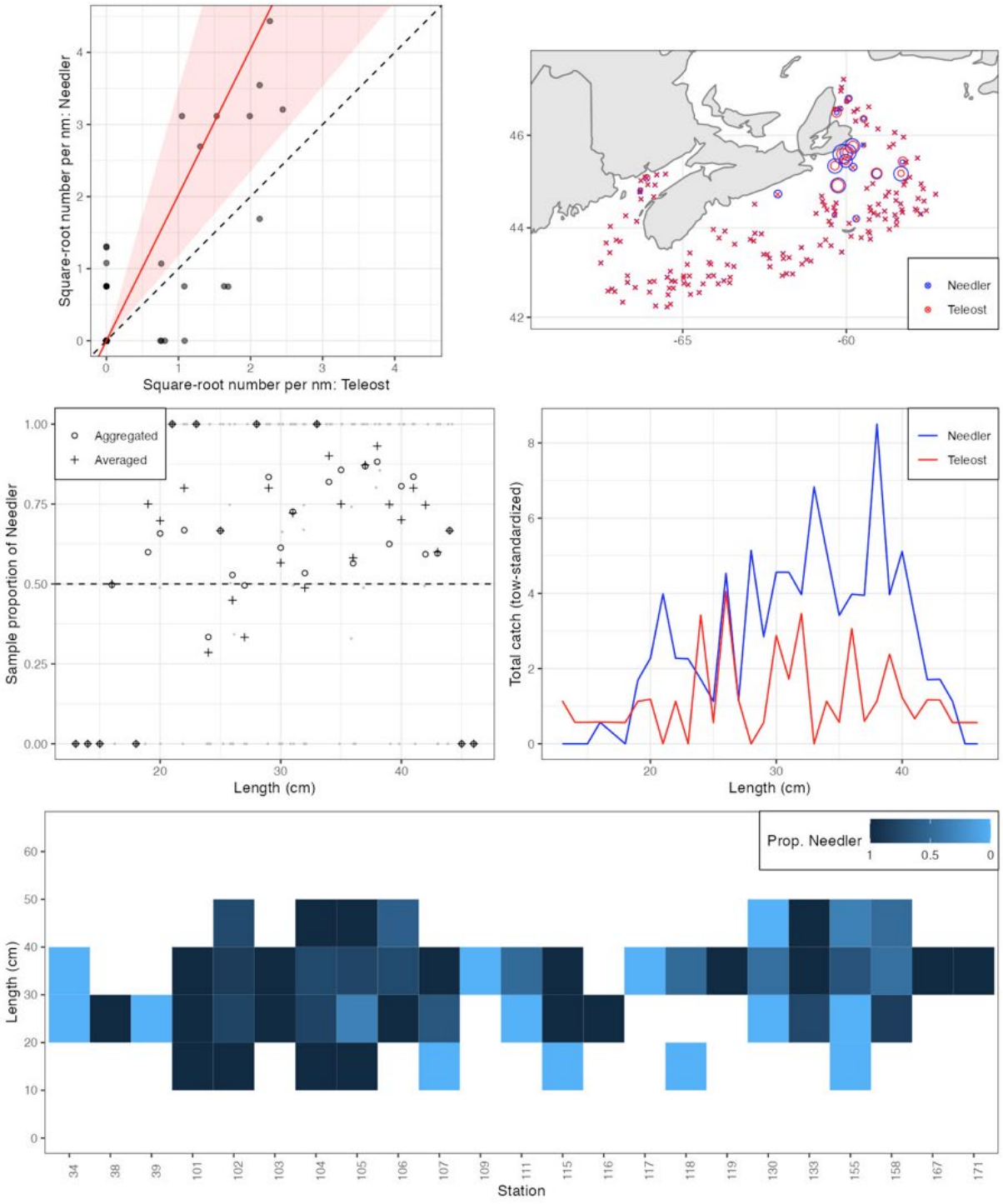

Figure 37a. Visualisation of comparative fishing data and size-aggregated model fit for Lumpenus lumpretaeformis (622).

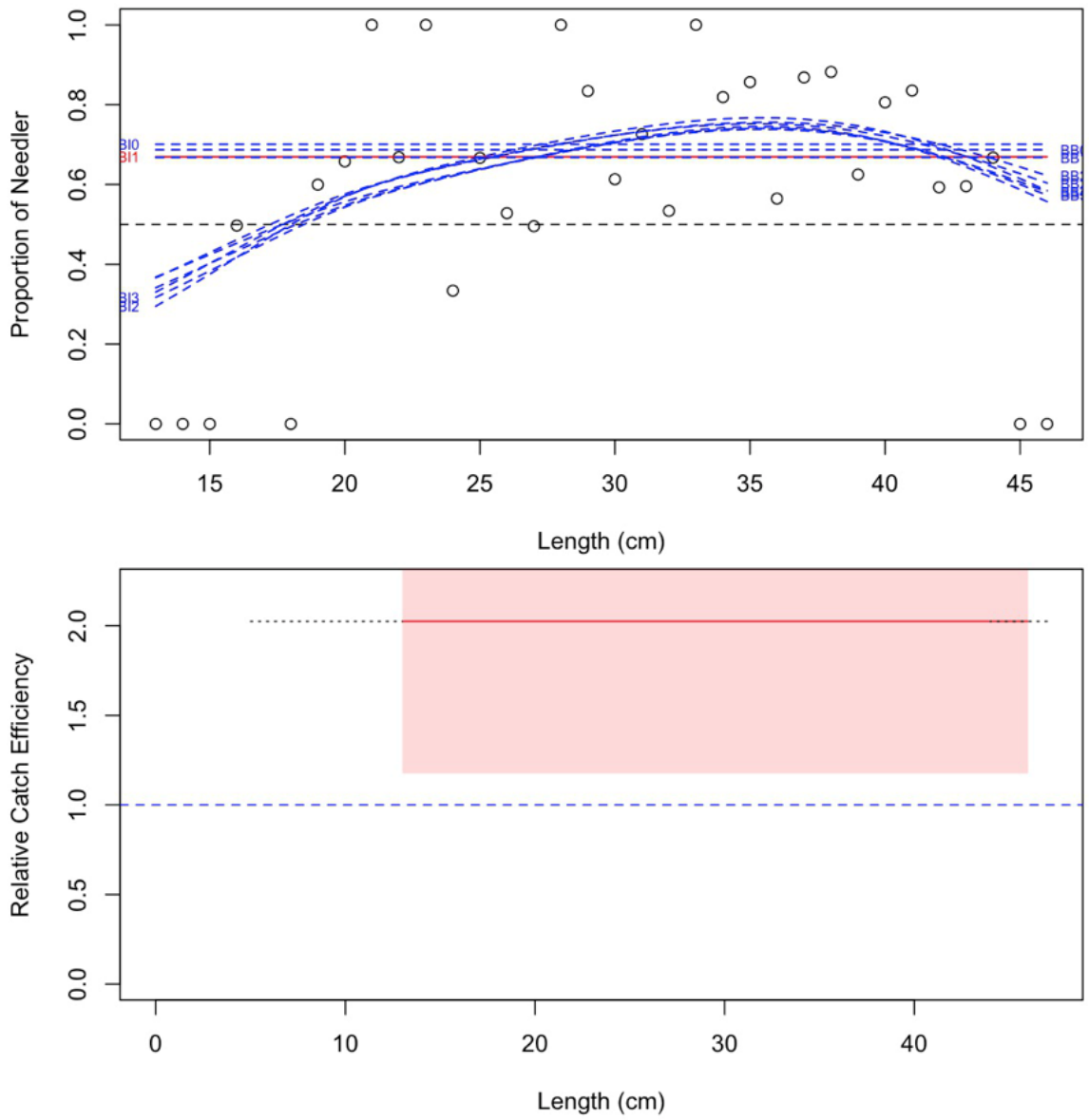

Figure 37b. Model fits and the selected length-based calibration for Lumpenus lumpretaeformis (622).

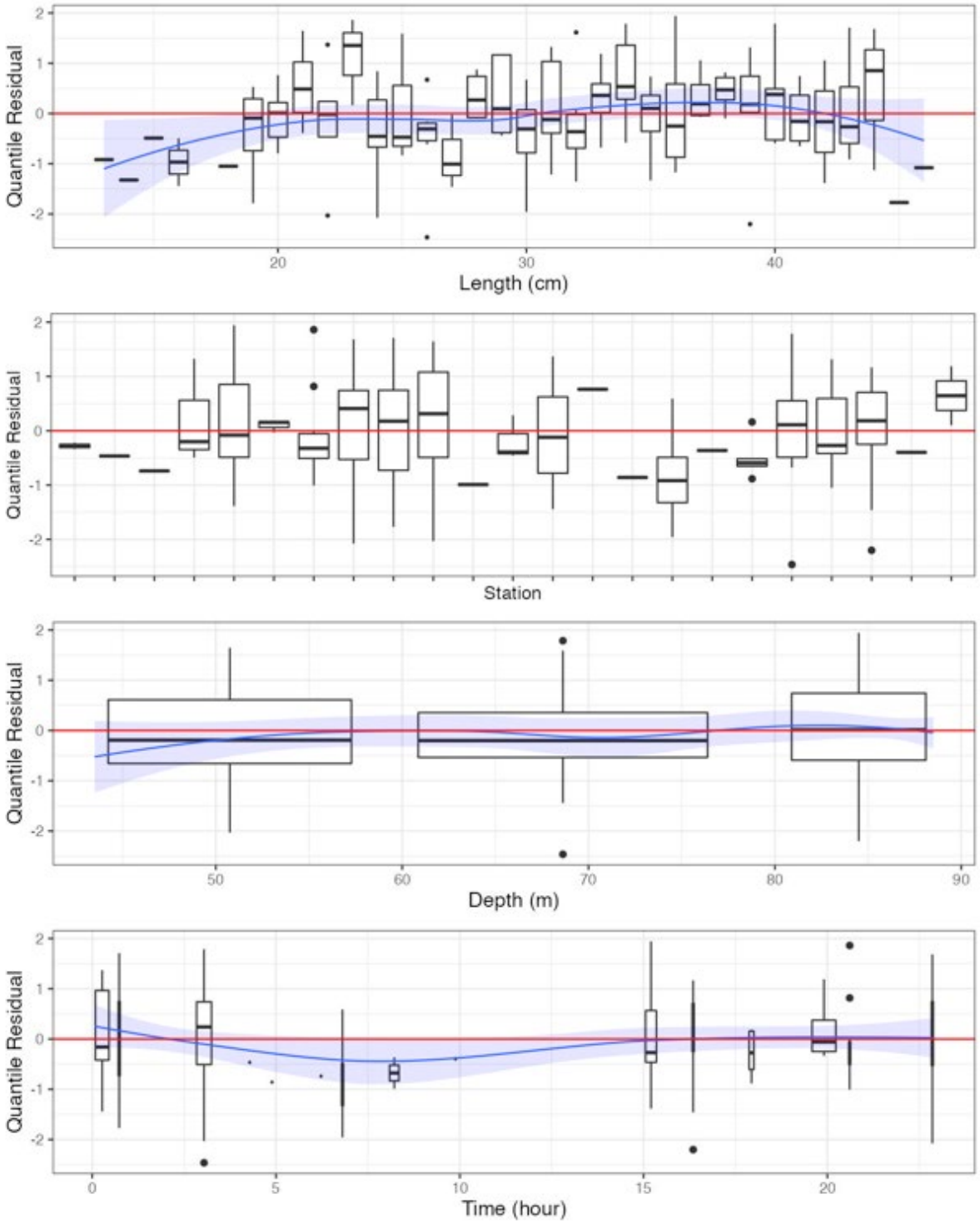

Figure 37c. Randomized and normalized quantile residuals for the selected model for Lumpenus lumpretaeformis (622).

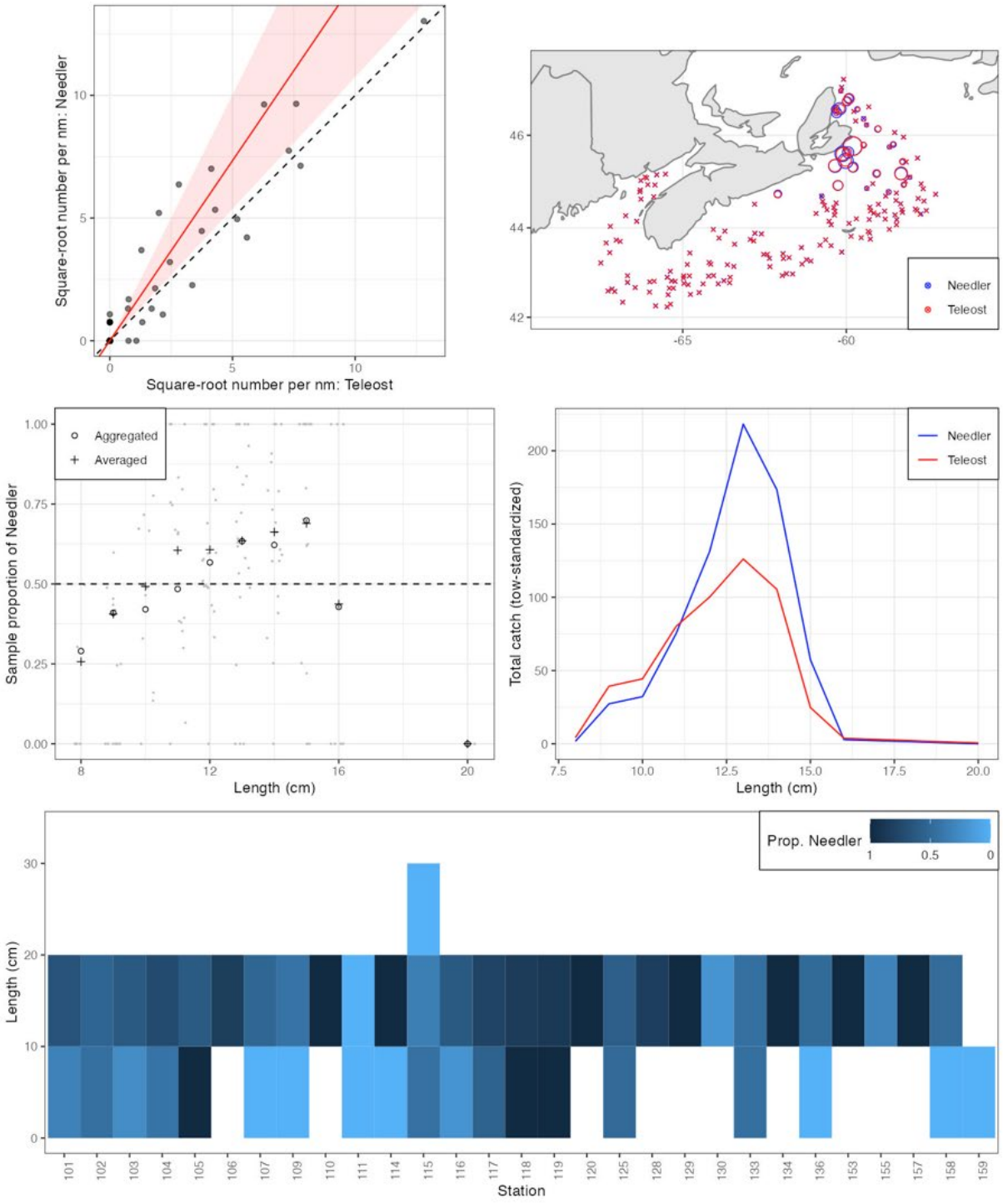

Figure 38a. Visualisation of comparative fishing data and size-aggregated model fit for Lumpenus maculatus (623).

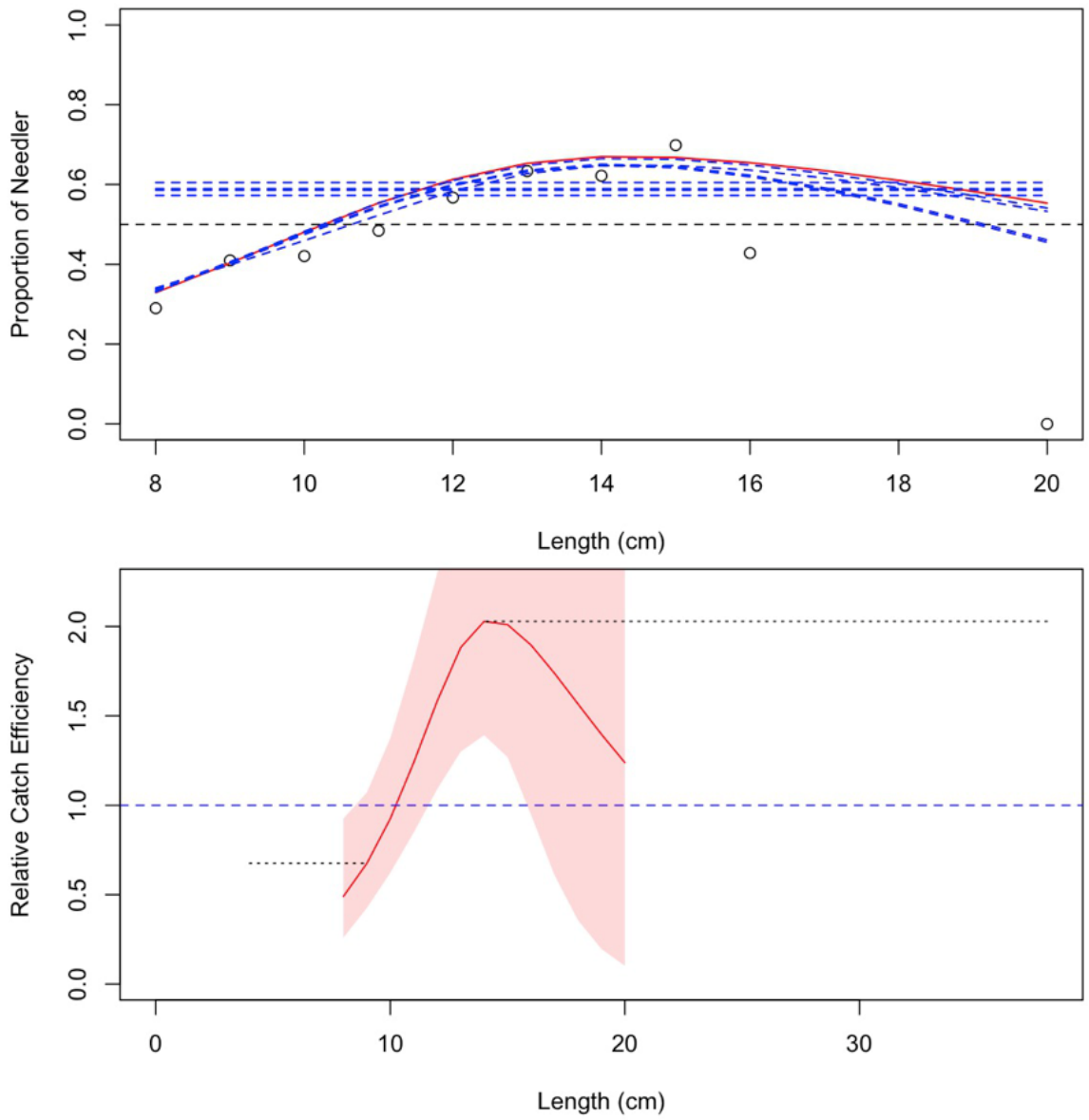

Figure 38b. Model fits and the selected length-based calibration for Lumpenus maculatus (623).

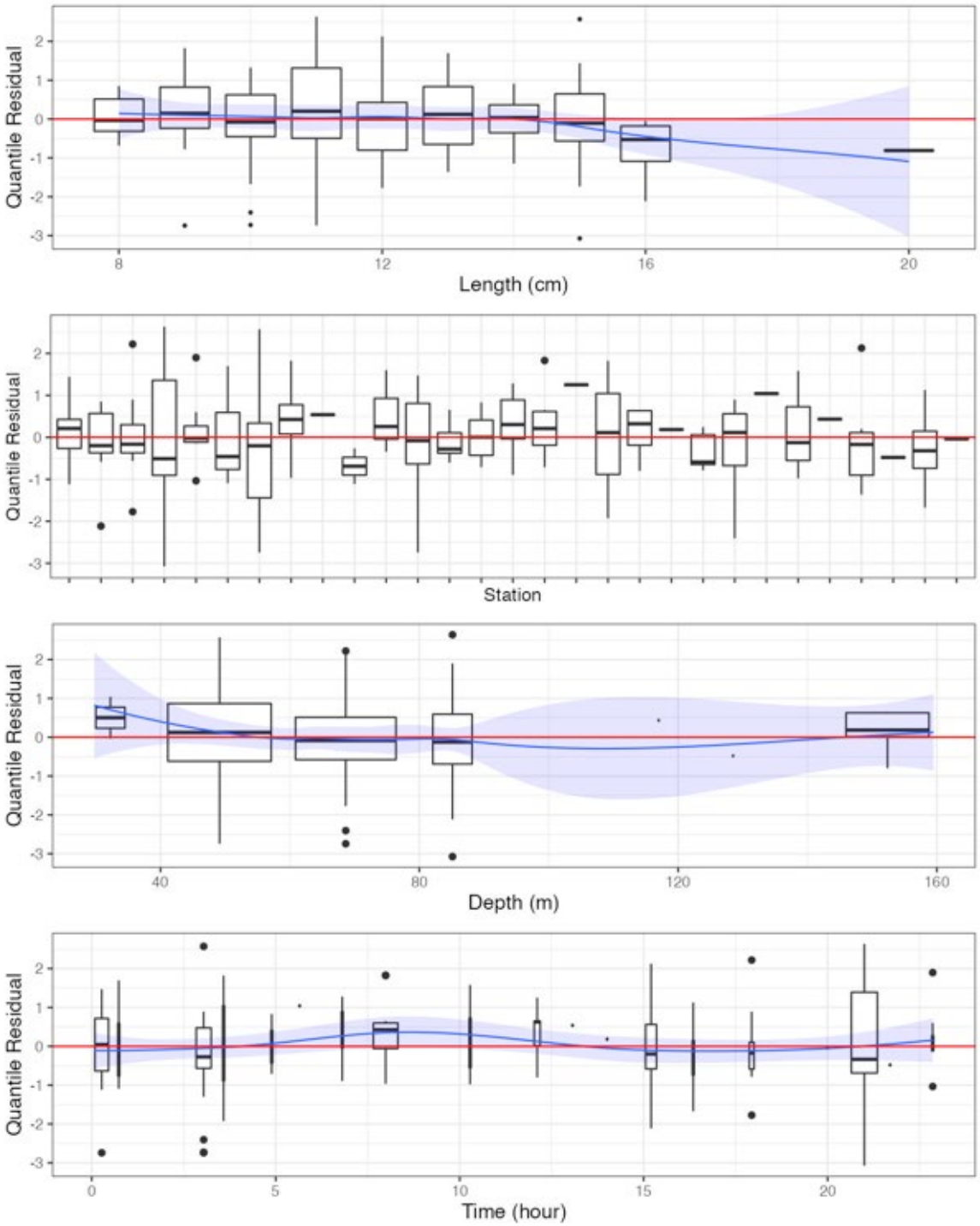

Figure 38c. Randomized and normalized quantile residuals for the selected model for Lumpenus maculatus (623).

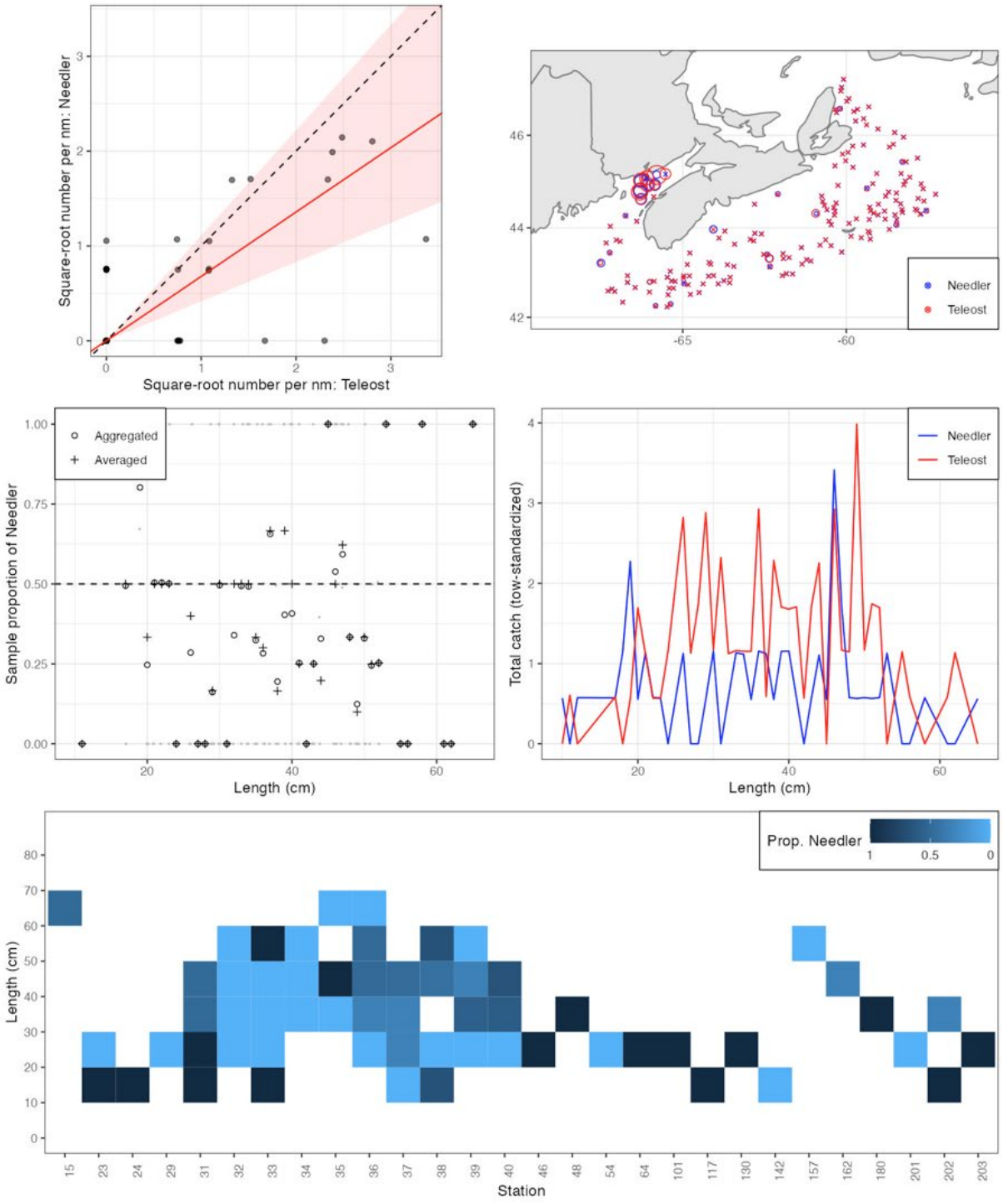

Figure 39a. Visualisation of comparative fishing data and size-aggregated model fit for Zoarces americanus (640).

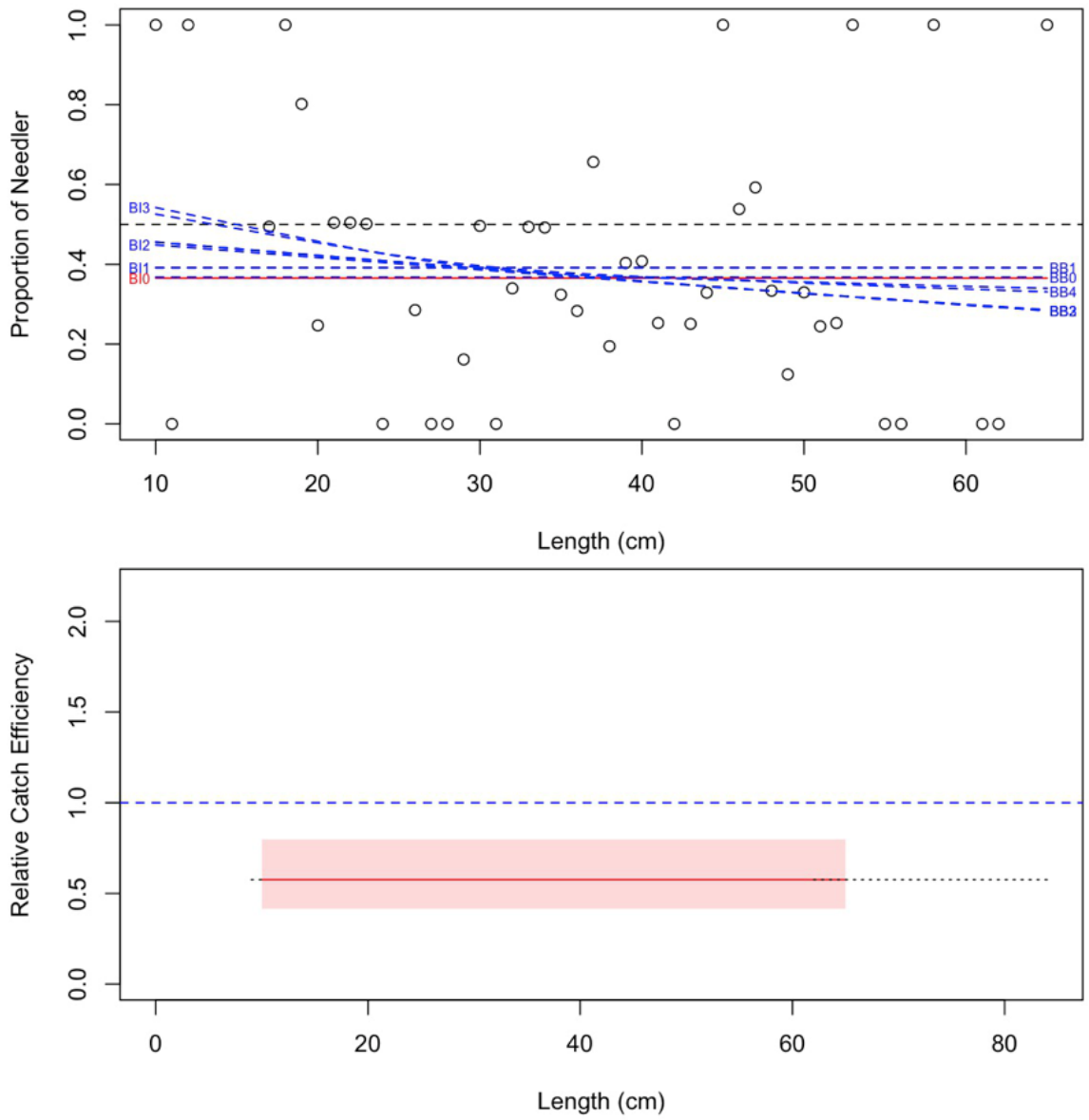

Figure 39b. Model fits and the selected length-based calibration for Zoarces americanus (640).

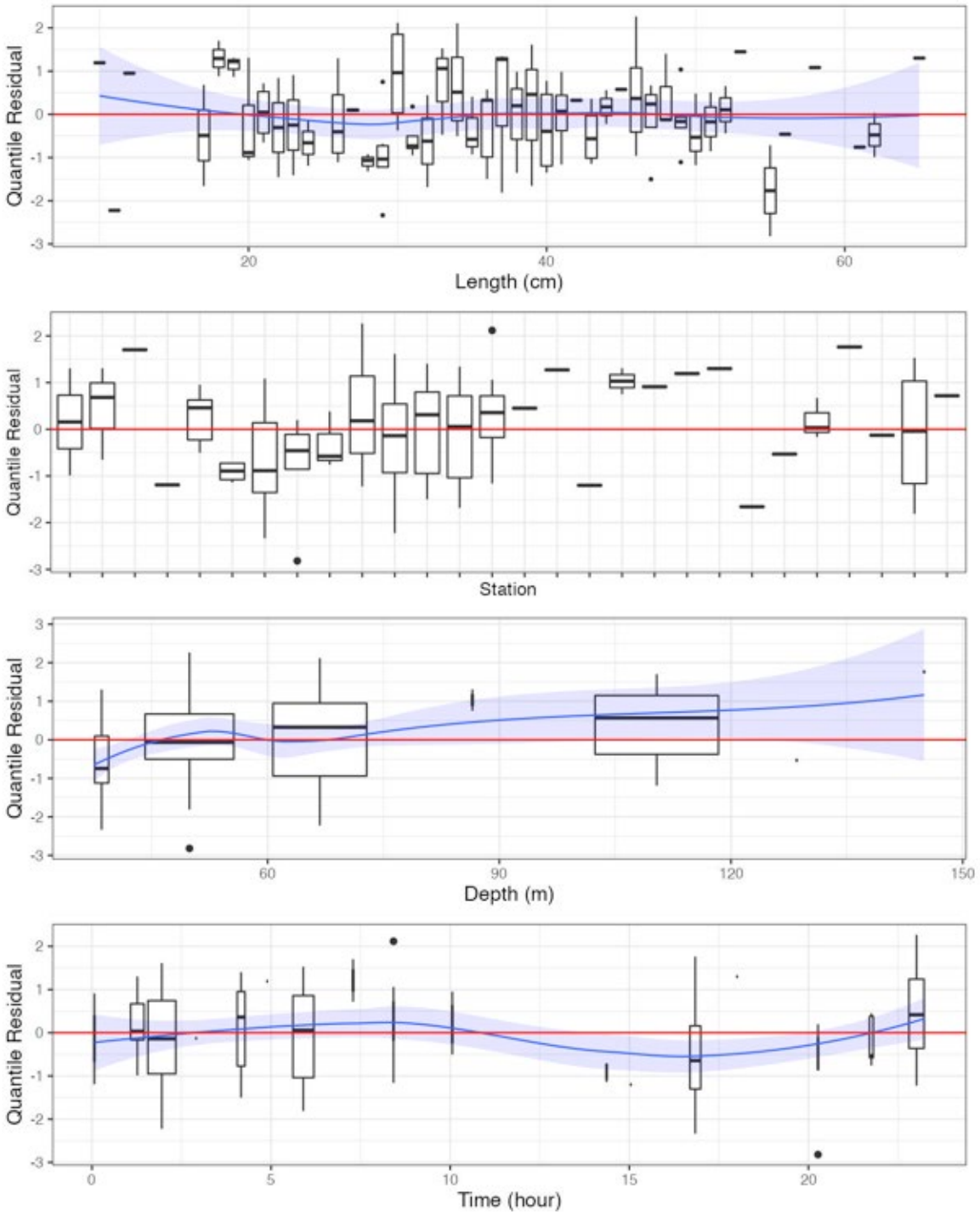

Figure 39c. Randomized and normalized quantile residuals for the selected model for Zoarces americanus (640).

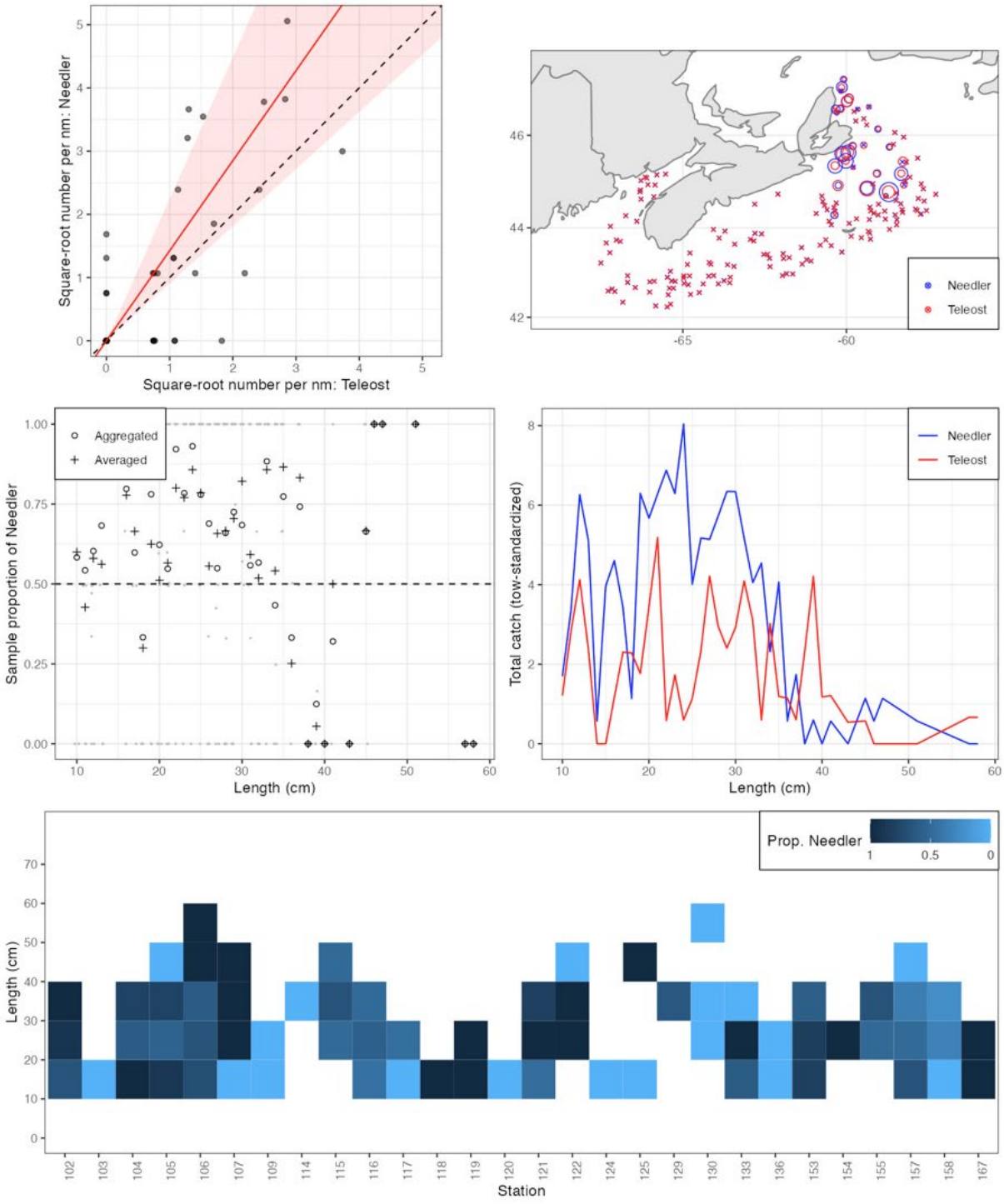

Figure 40a. Visualisation of comparative fishing data and size-aggregated model fit for Lycodes vahlii (647).

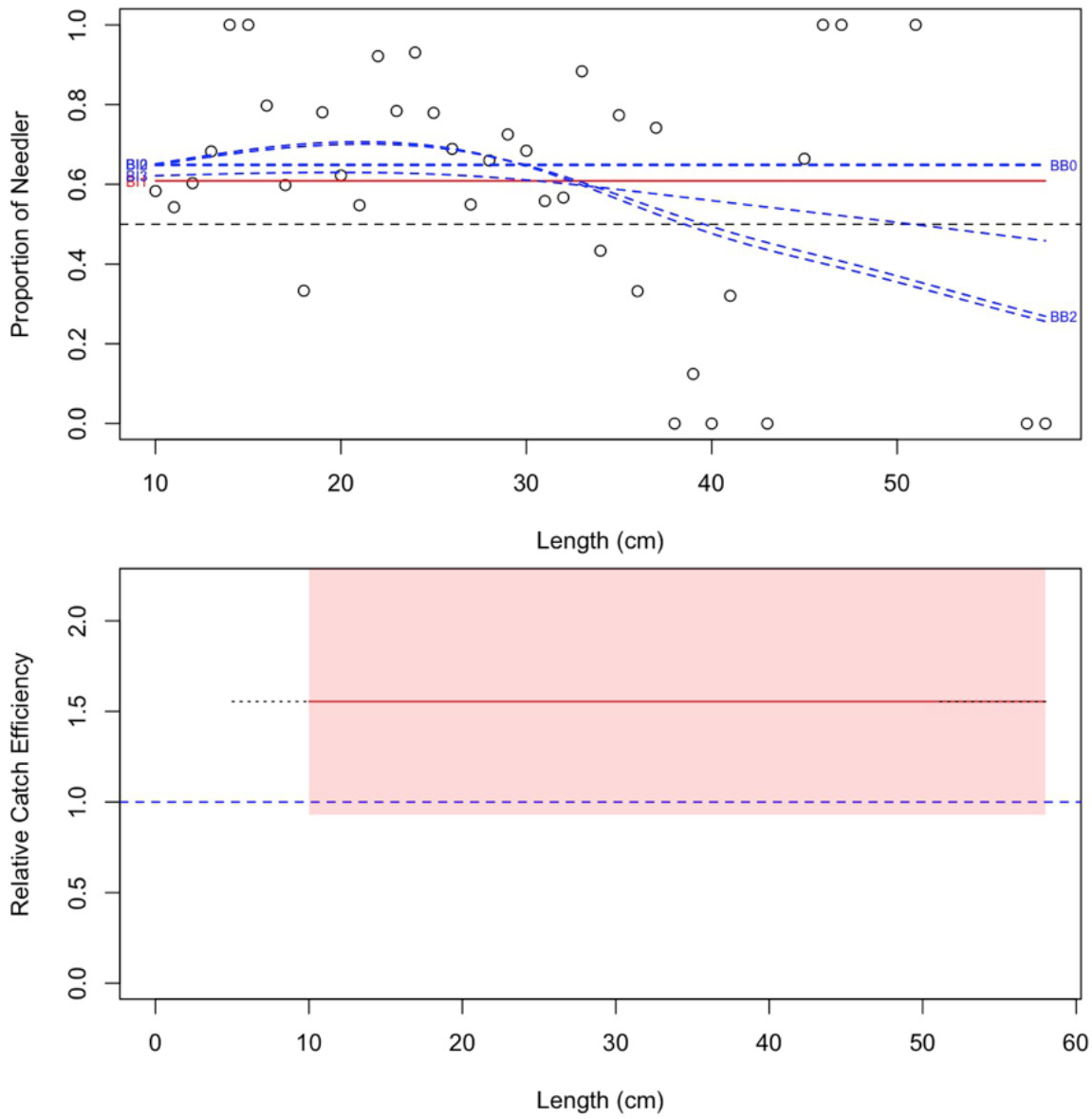

Figure 40b. Model fits and the selected length-based calibration for Lycodes vahlii (647).

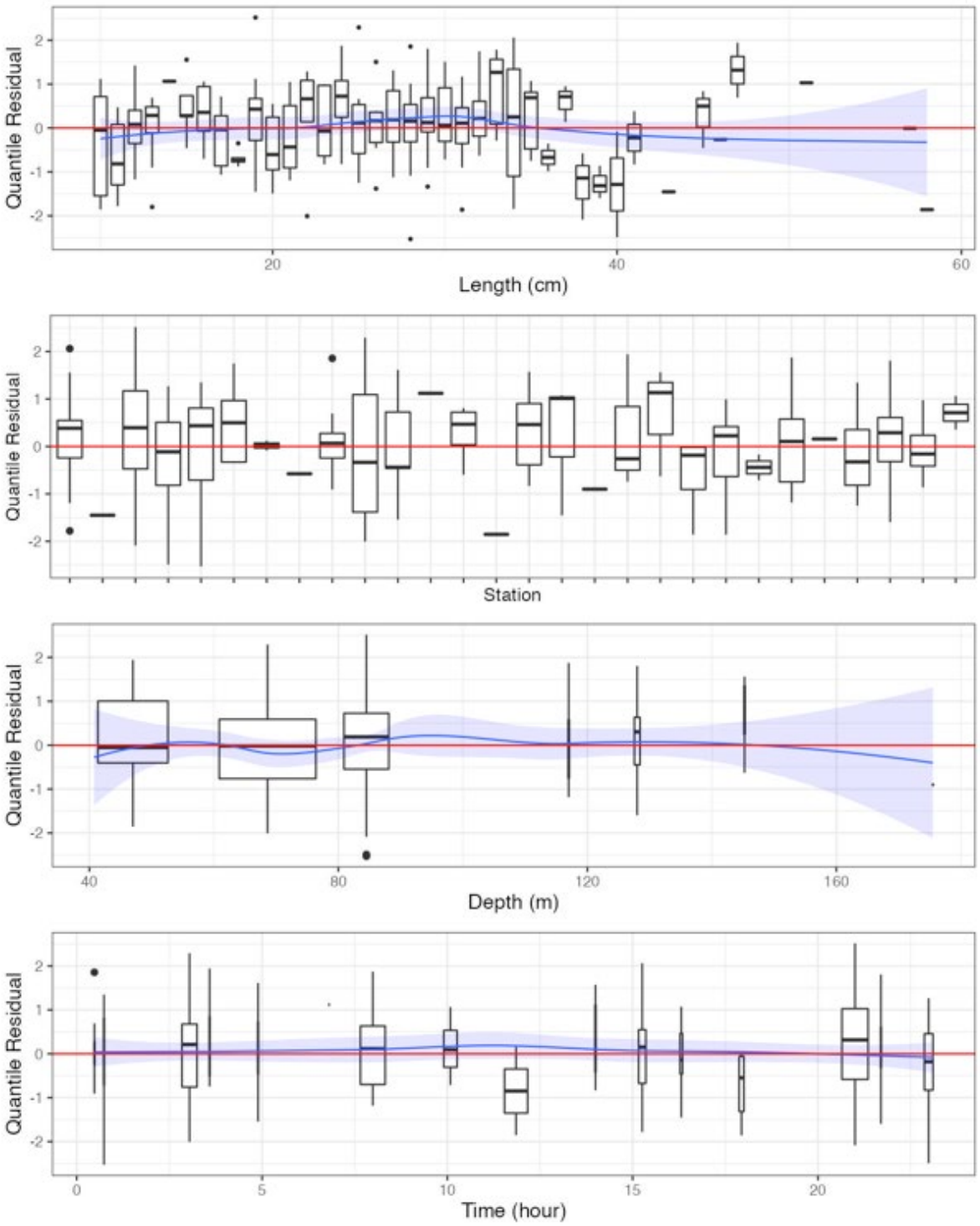

Figure 40c. Randomized and normalized quantile residuals for the selected model for Lycodes vahlii (647).

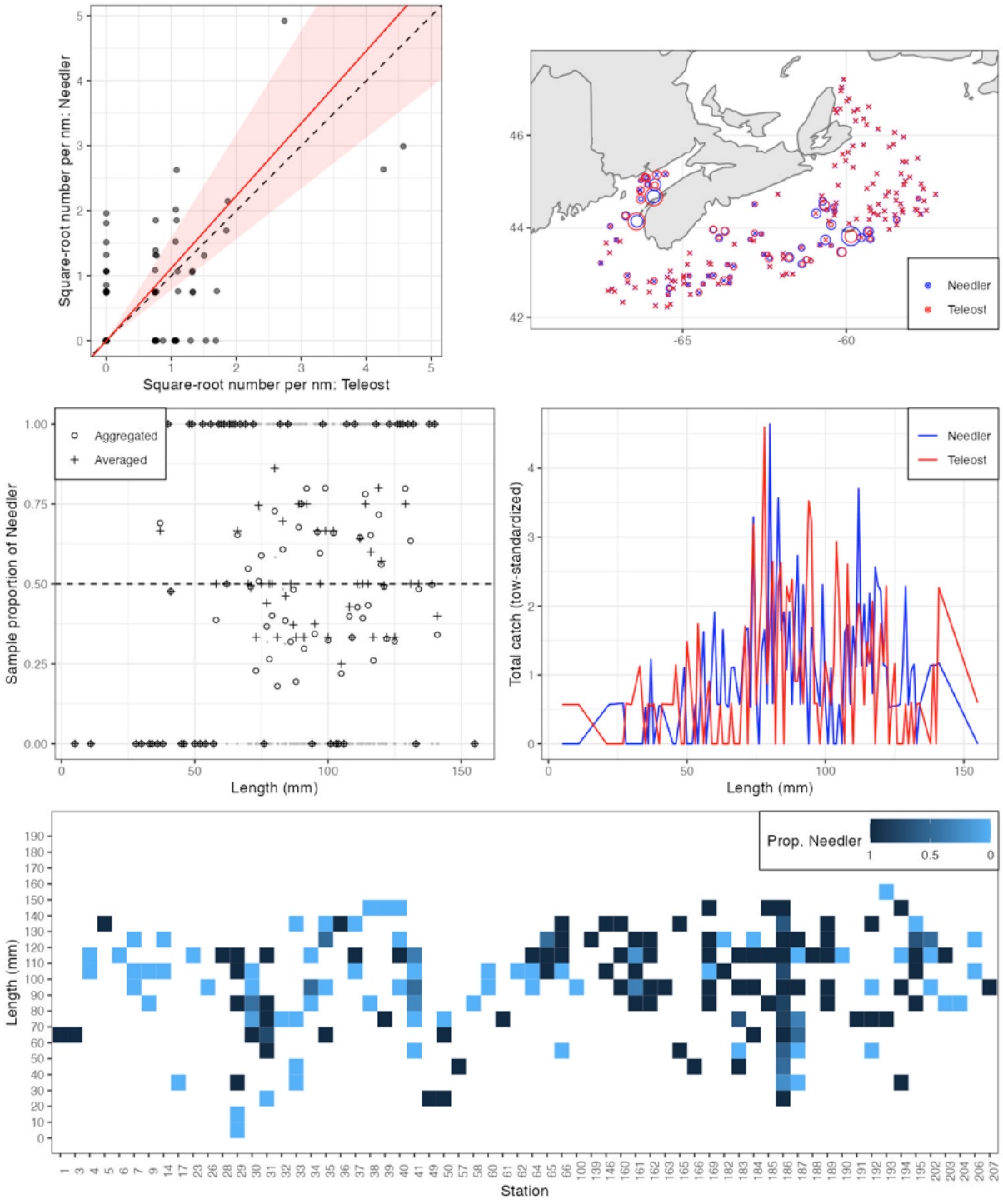

Figure 41a. Visualisation of comparative fishing data and size-aggregated model fit for Cancer borealis (2511).

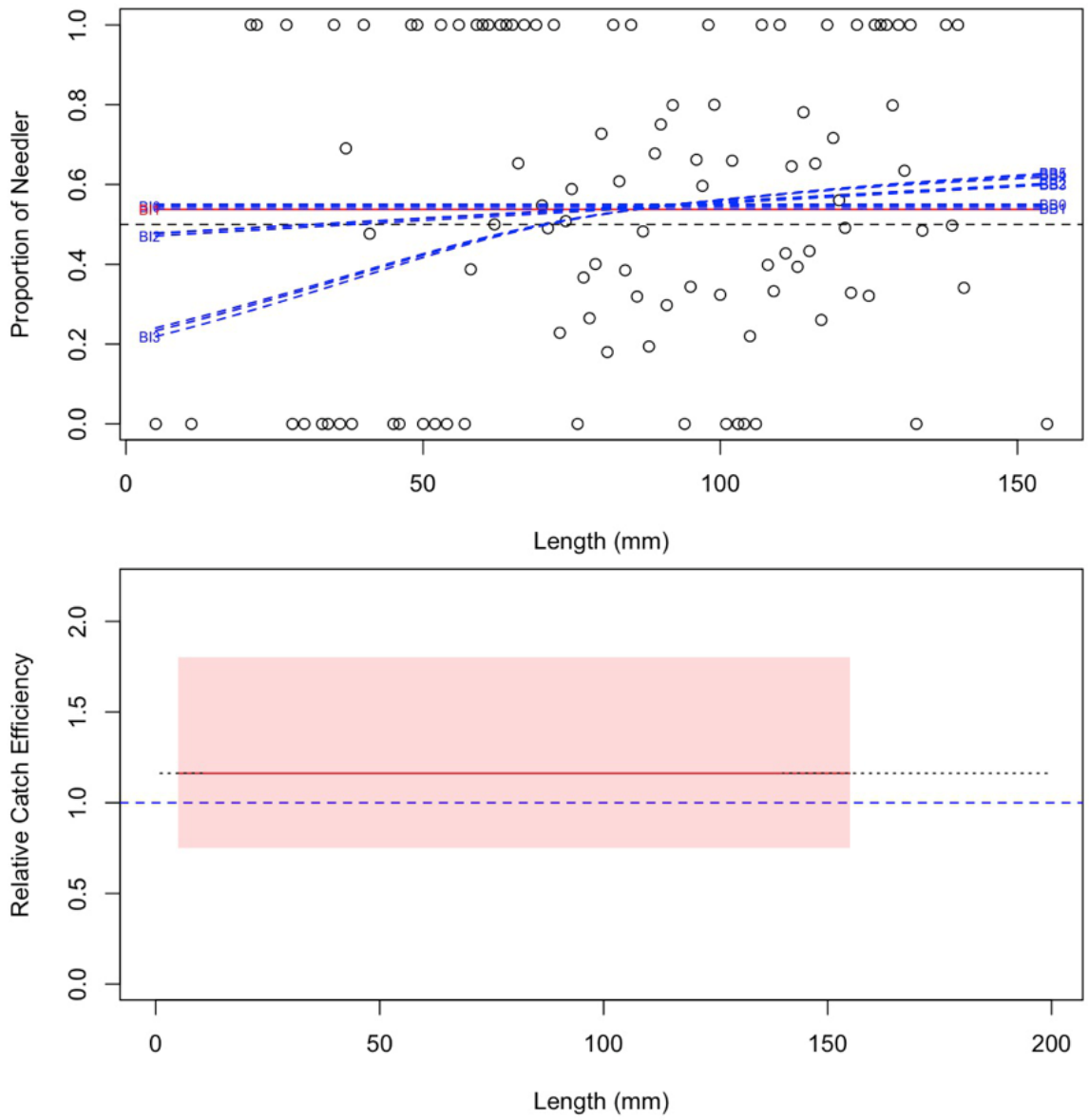

Figure 41b. Model fits and the selected length-based calibration for Cancer borealis (2511).

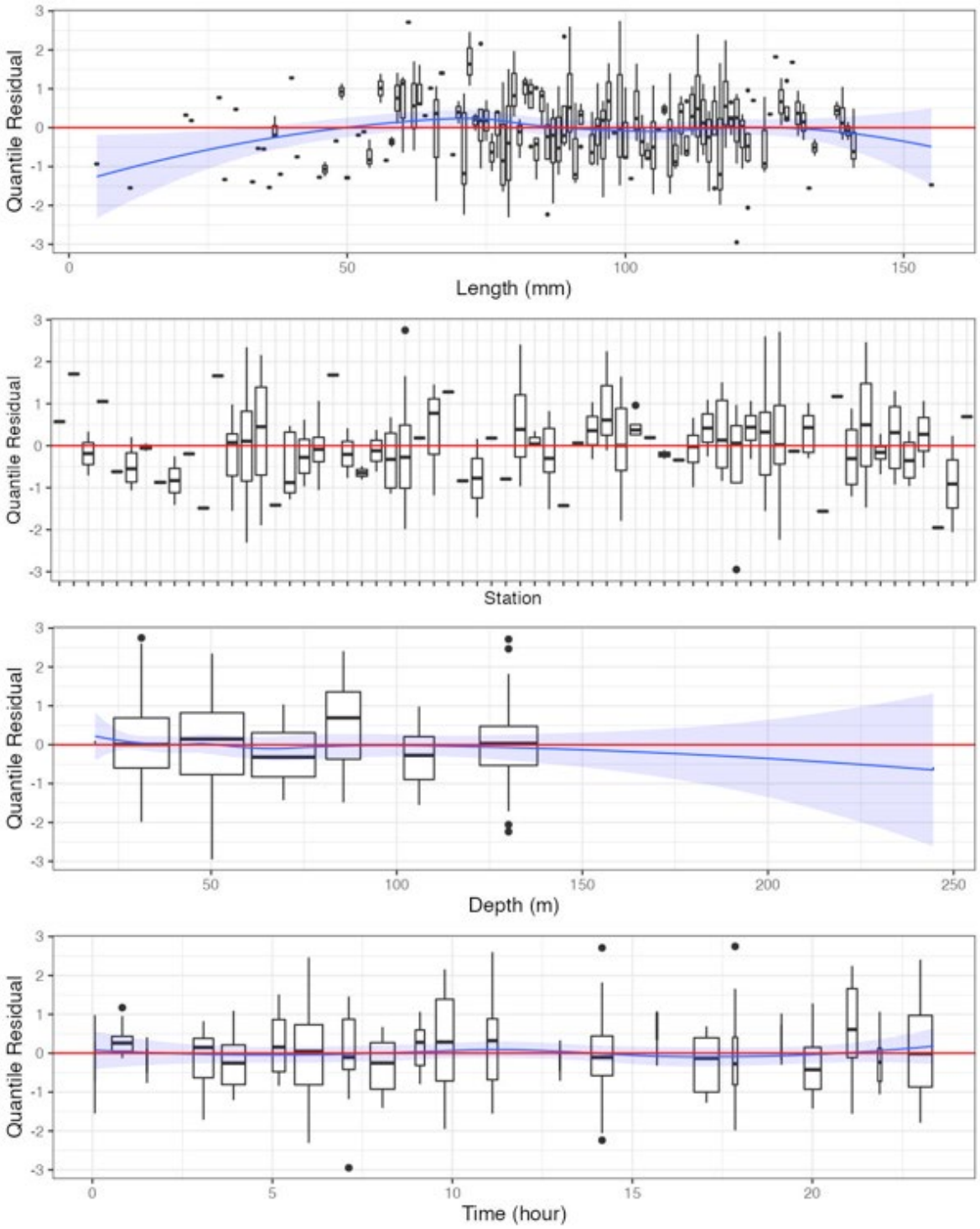

Figure 41c. Randomized and normalized quantile residuals for the selected model for Cancer borealis (2511).

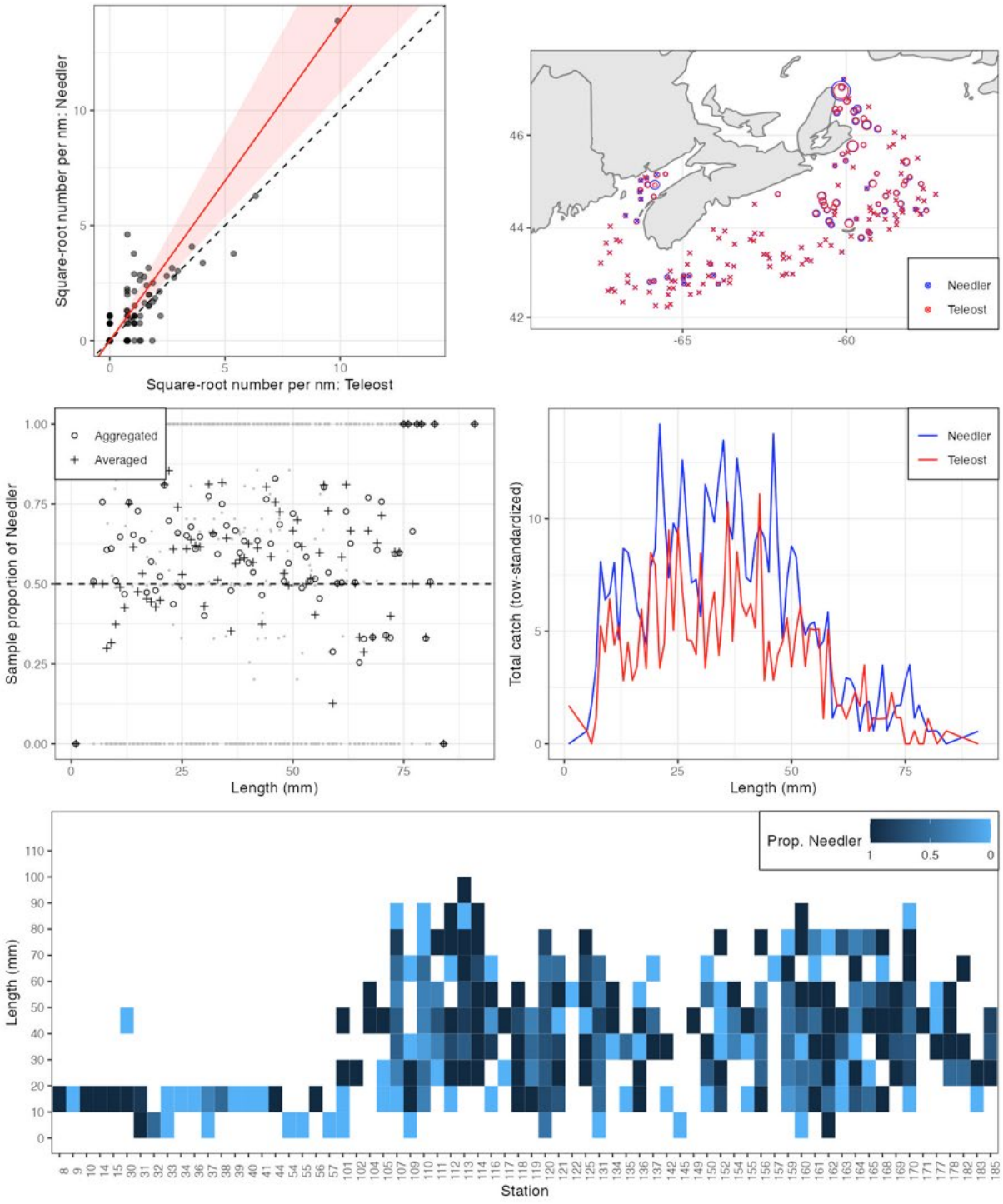

Figure 42a. Visualisation of comparative fishing data and size-aggregated model fit for Hyas sp. (2520).

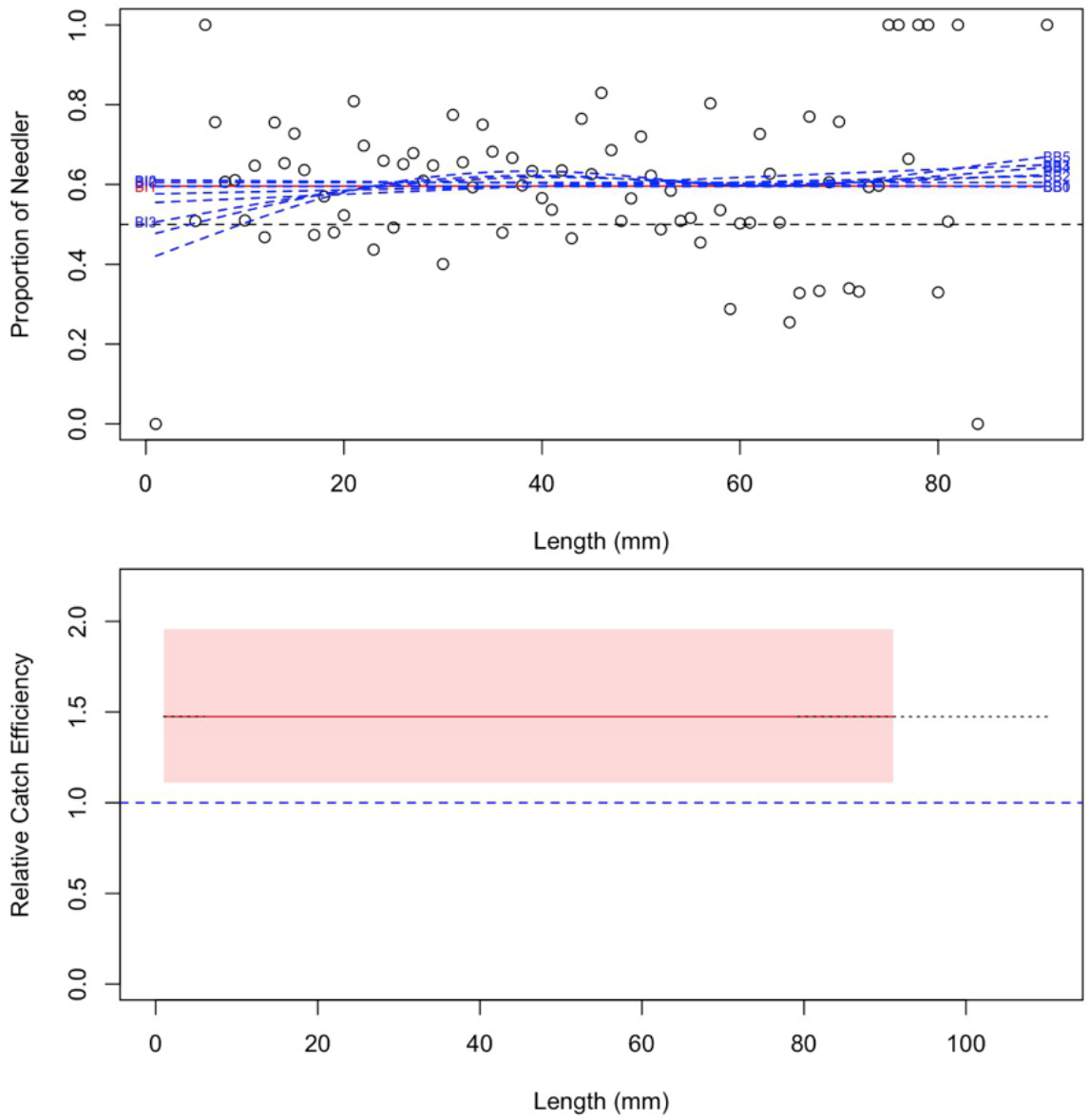

Figure 42b. Model fits and the selected length-based calibration for Hyas sp. (2520).

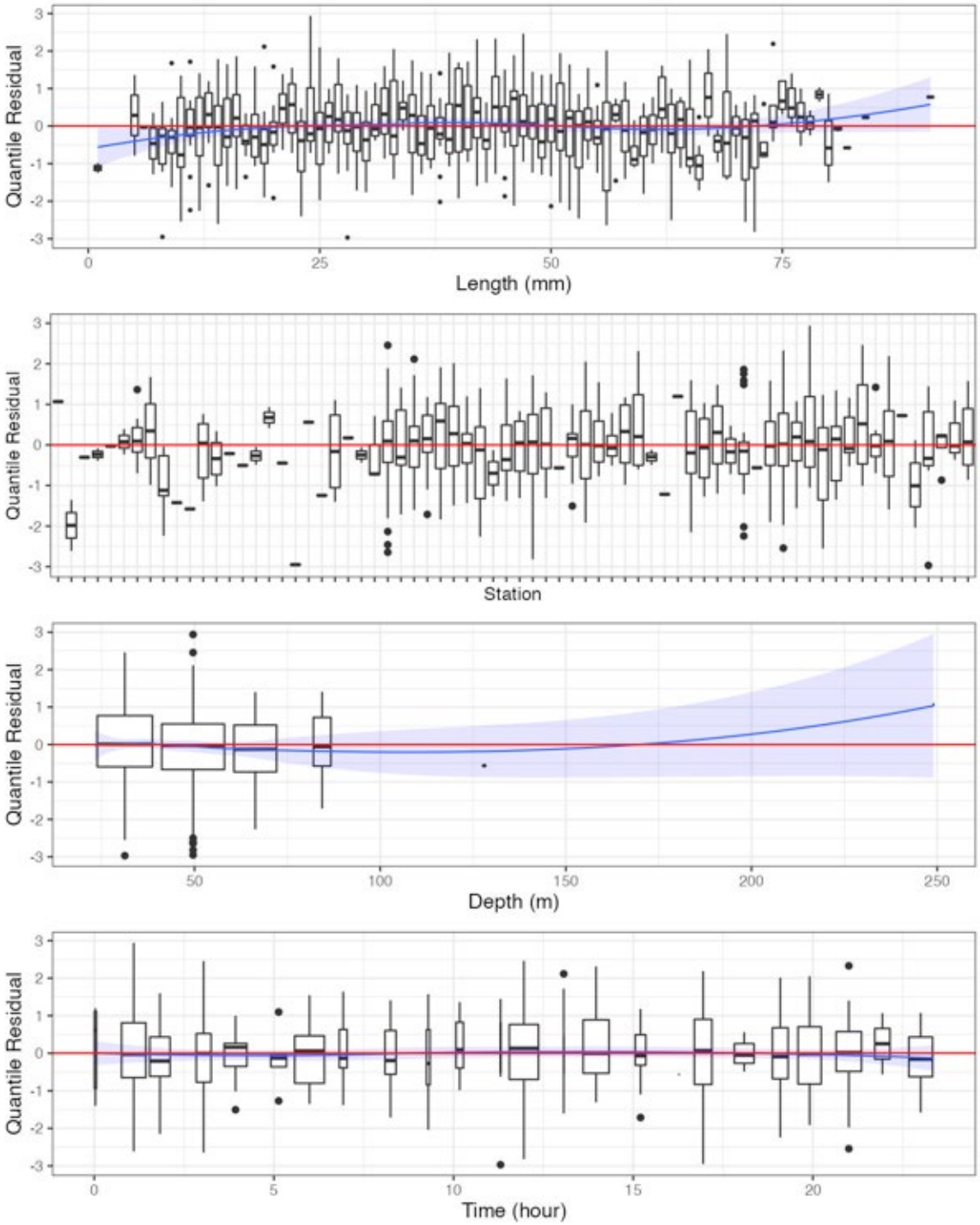

Figure 42c. Randomized and normalized quantile residuals for the selected model for Hyas sp. (2520).

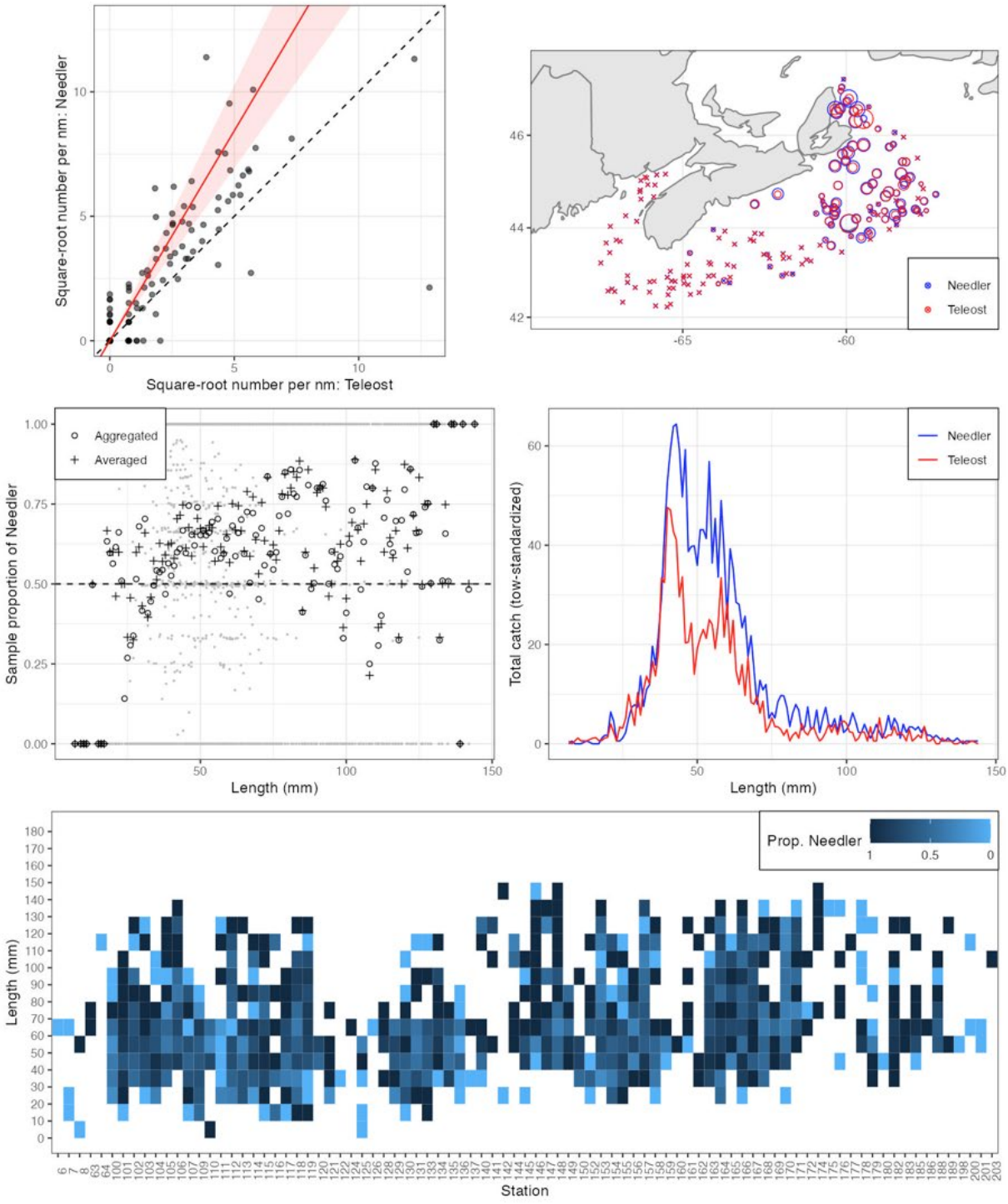

Figure 43a. Visualisation of comparative fishing data and size-aggregated model fit for Chionoecetes opilio (2526).

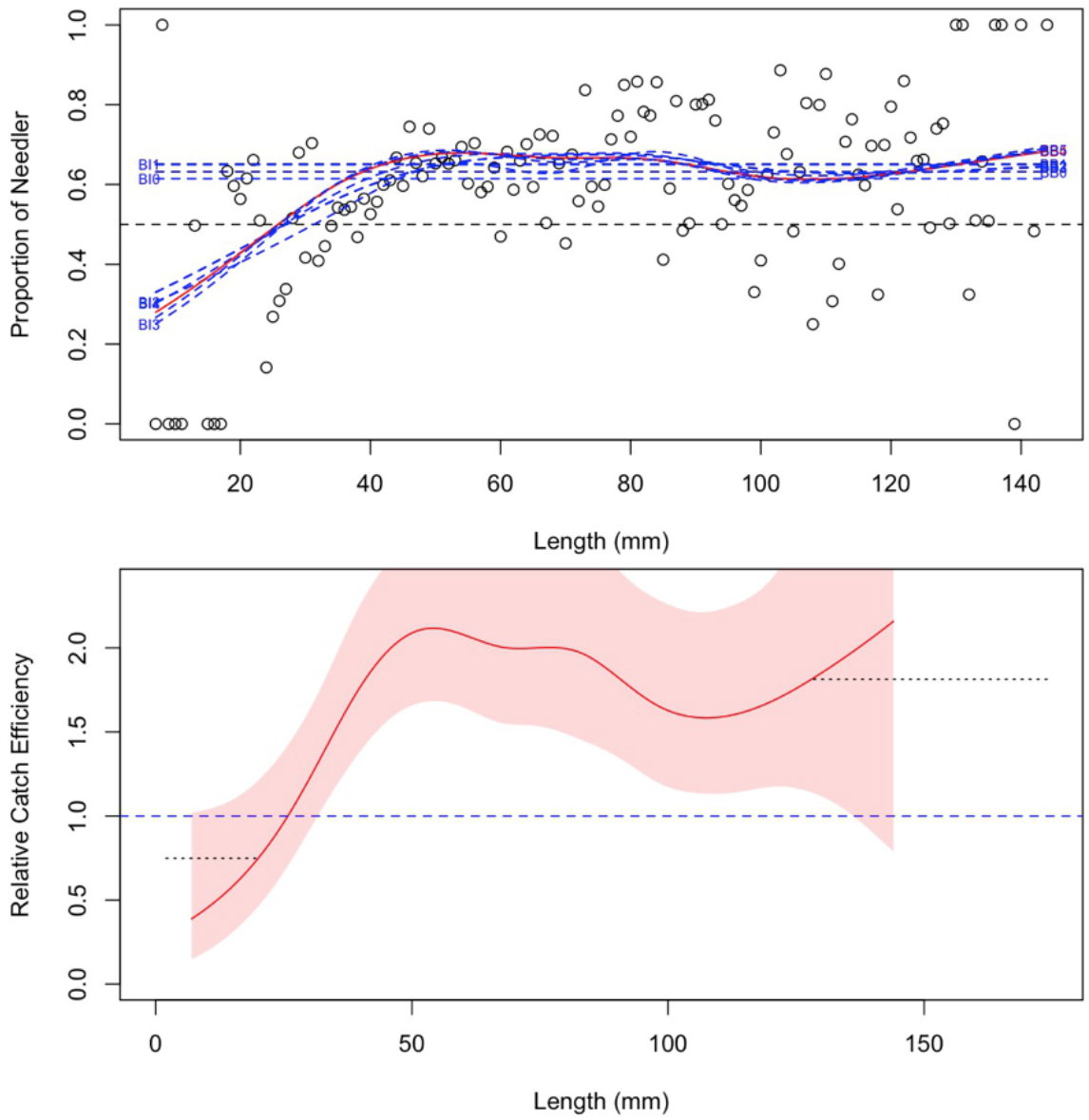

Figure 43b. Model fits and the selected length-based calibration for Chionoecetes opilio (2526).

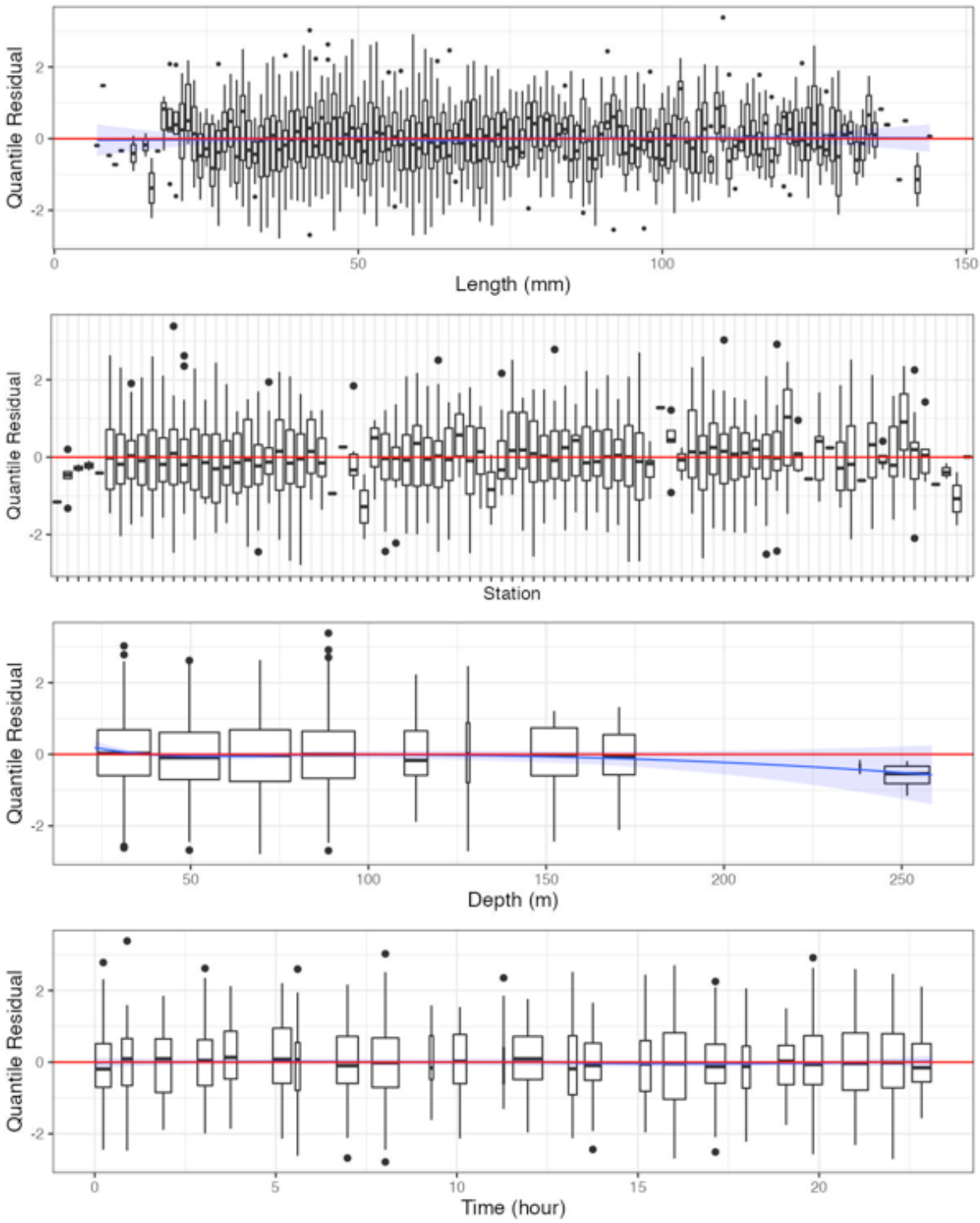

Figure 43c. Randomized and normalized quantile residuals for the selected model for Chionoecetes opilio (2526).

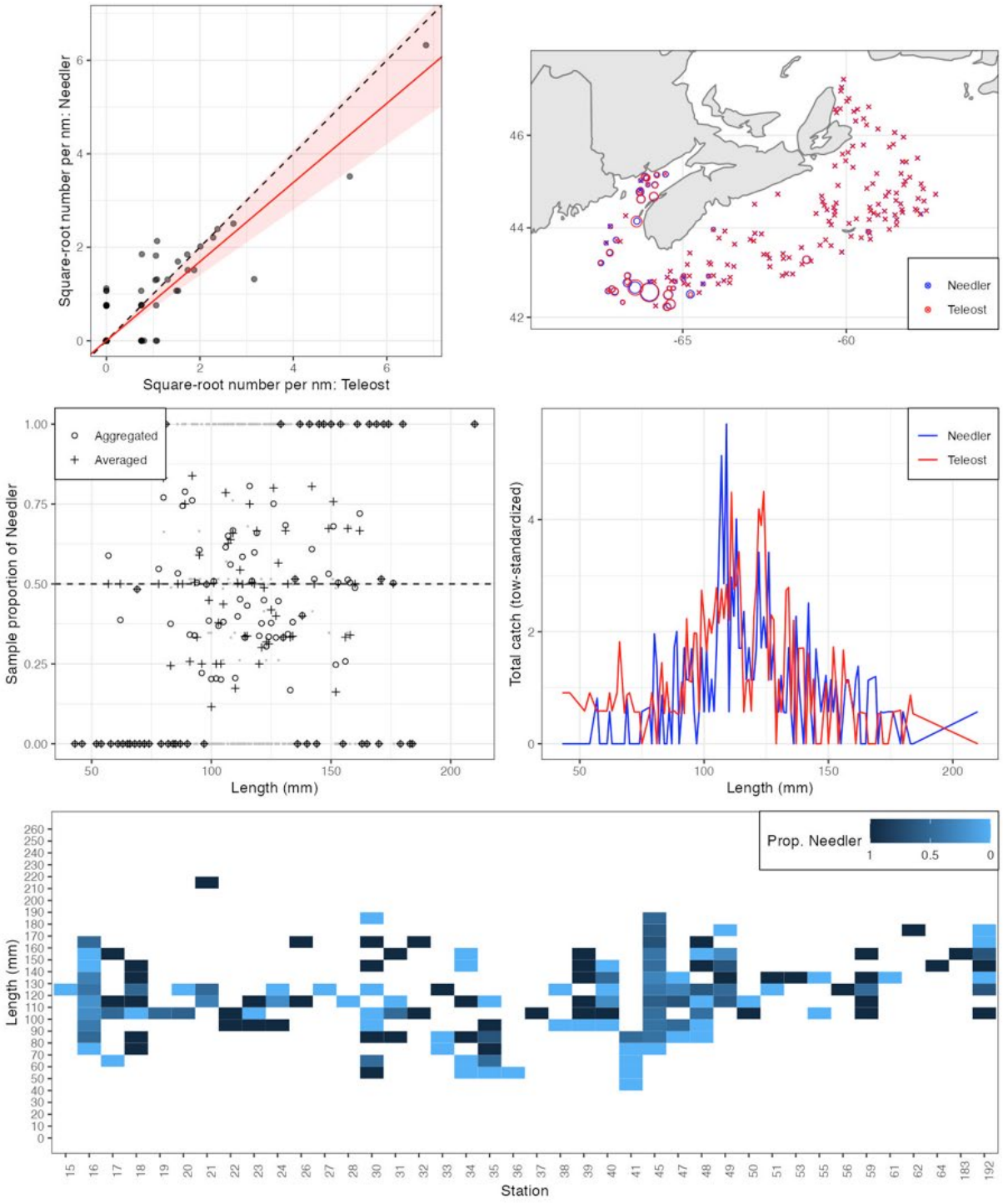

Figure 44a. Visualisation of comparative fishing data and size-aggregated model fit for Homarus americanus (2550).

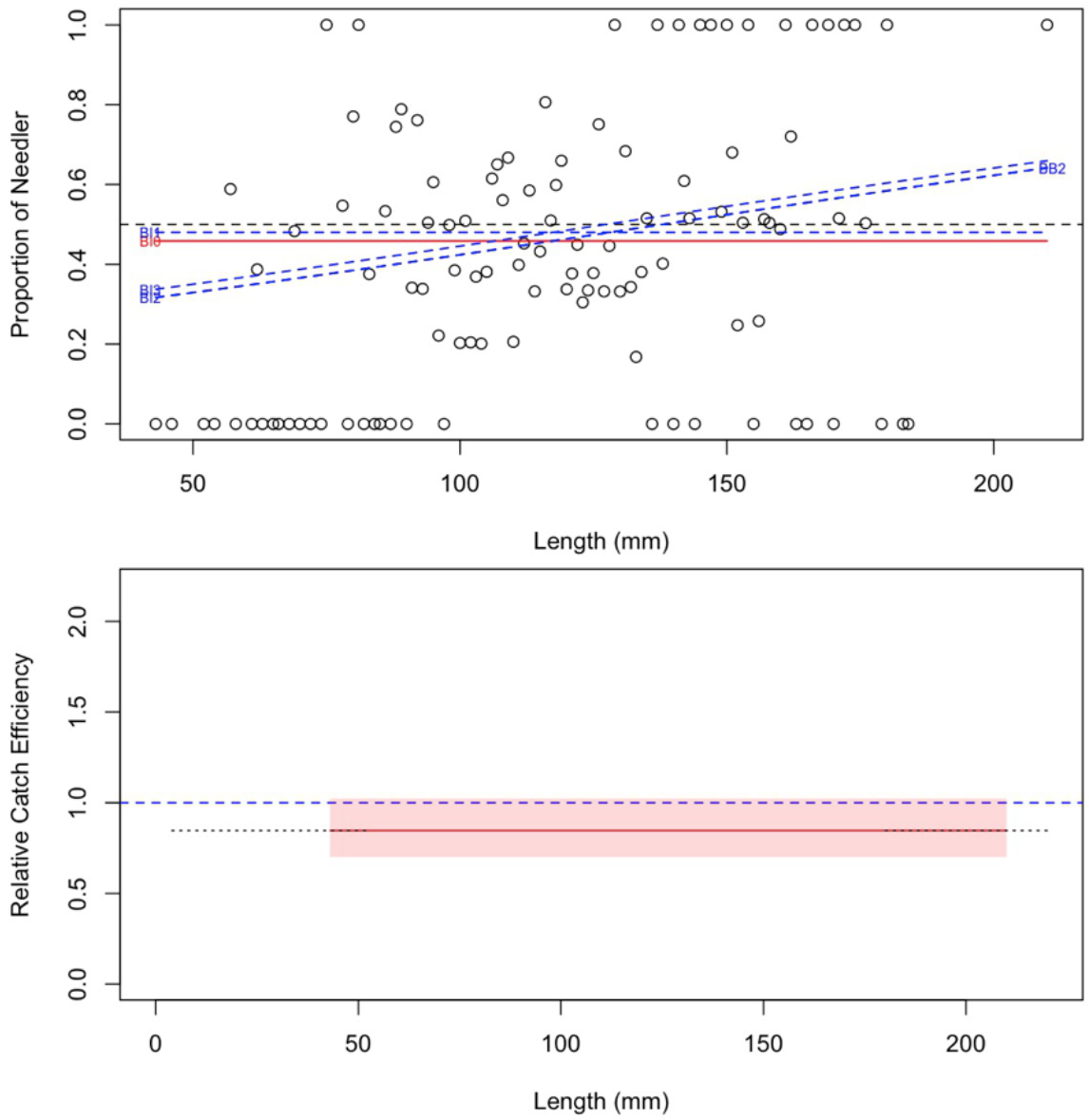

Figure 44b. Model fits and the selected length-based calibration for Homarus americanus (2550).

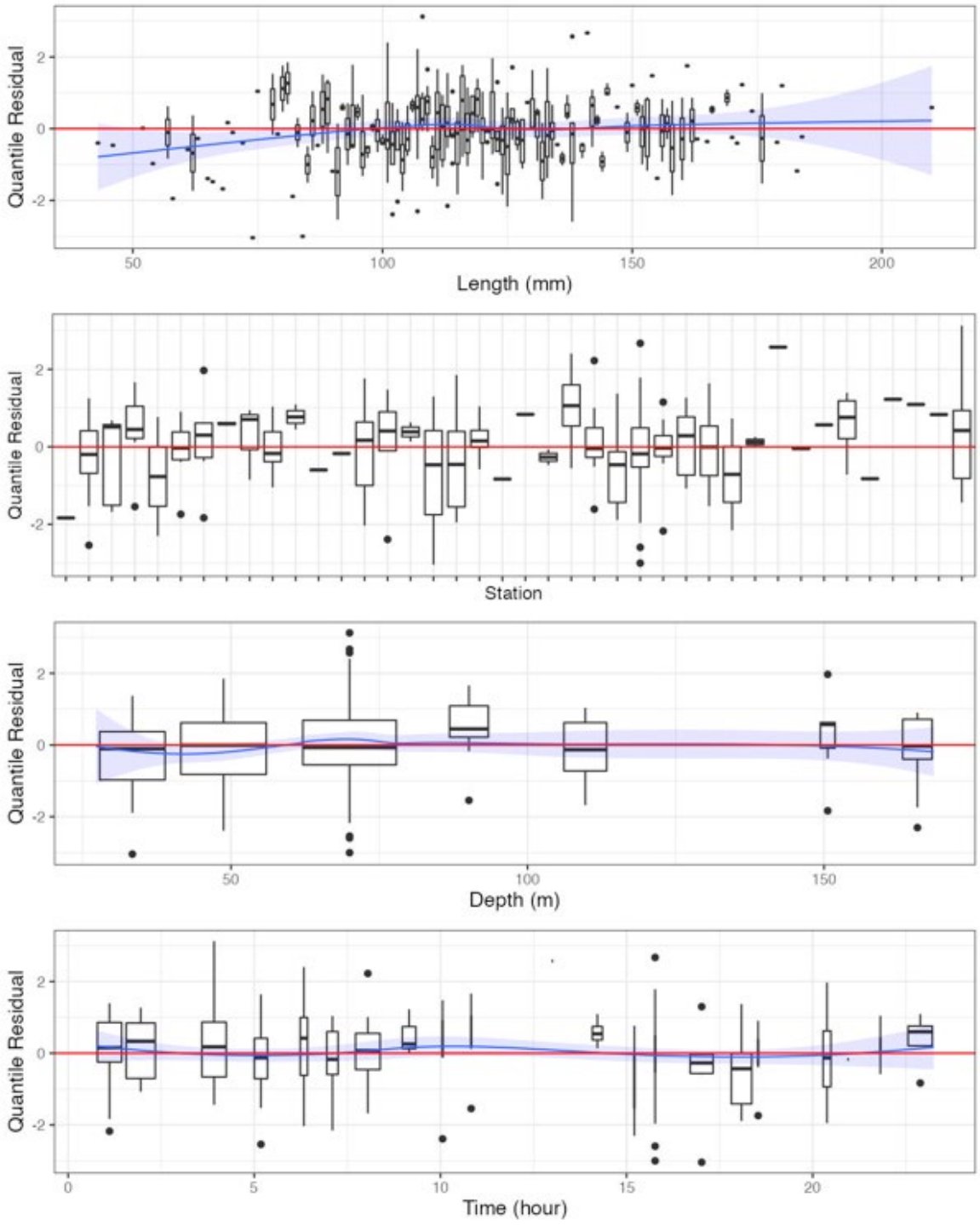

Figure 44c. Randomized and normalized quantile residuals for the selected model for Homarus americanus (2550).

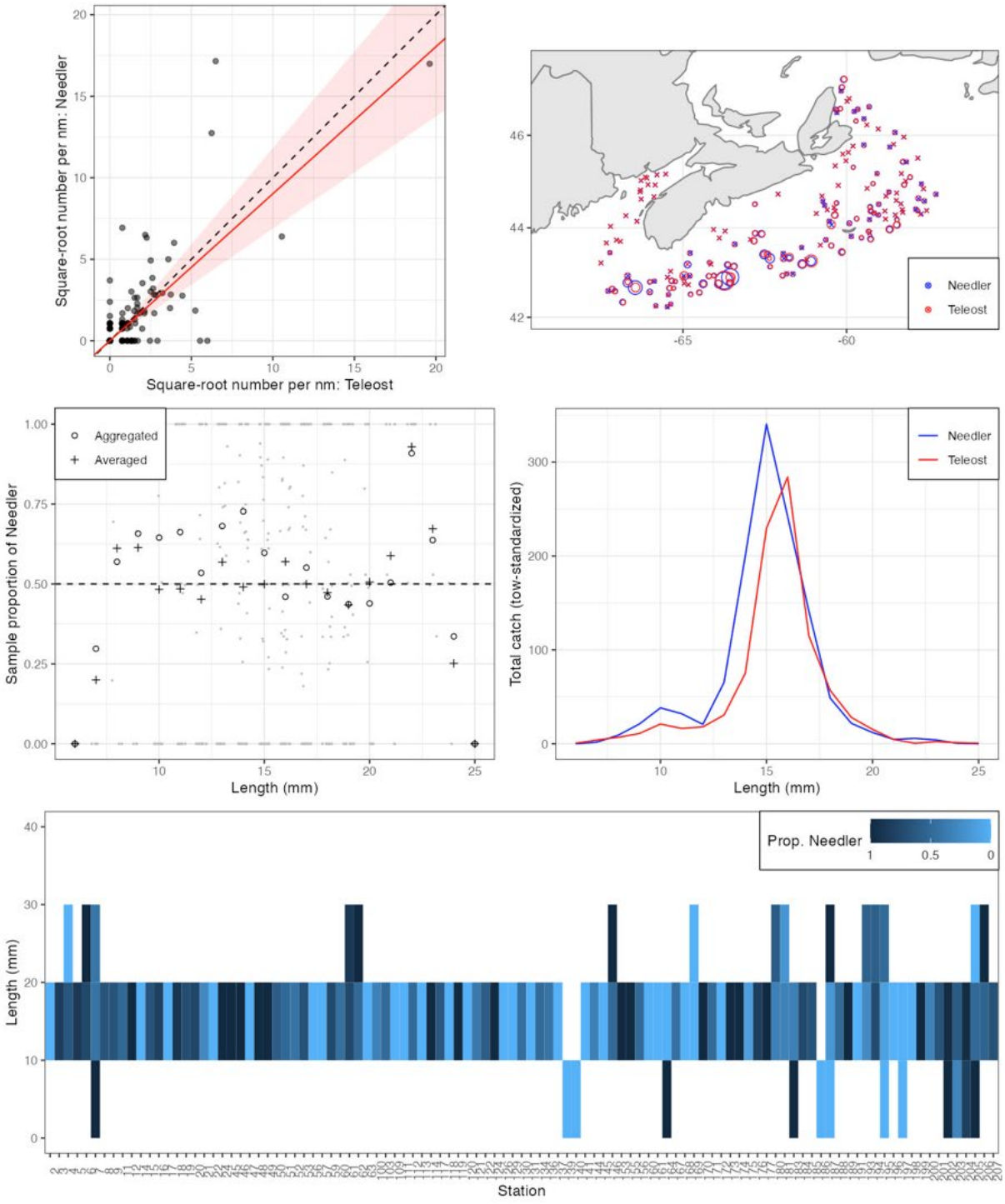

Figure 45a. Visualisation of comparative fishing data and size-aggregated model fit for Illex illecebrosus (4511).

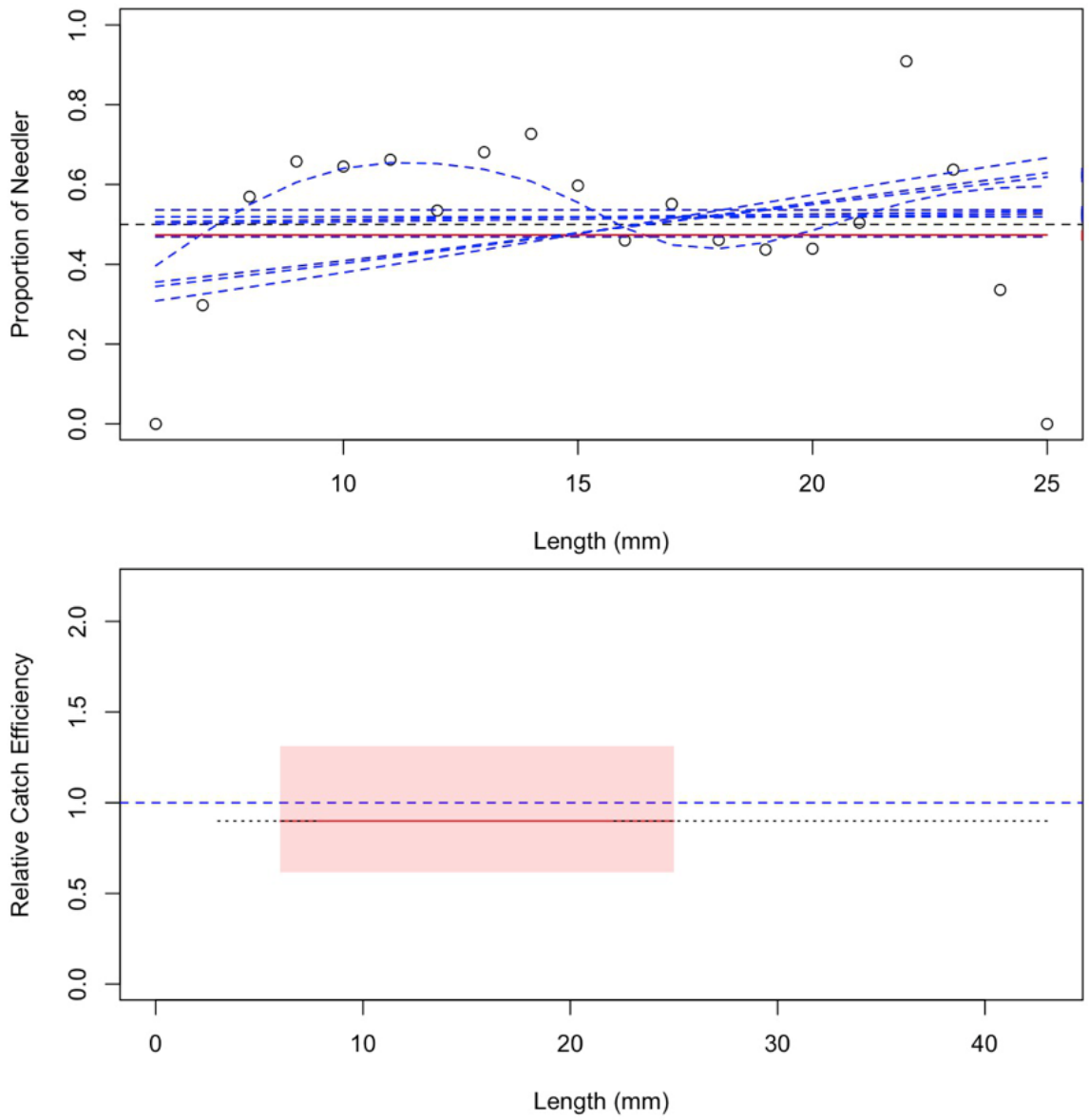

Figure 45b. Model fits and the selected length-based calibration for Illex illecebrosus (4511).

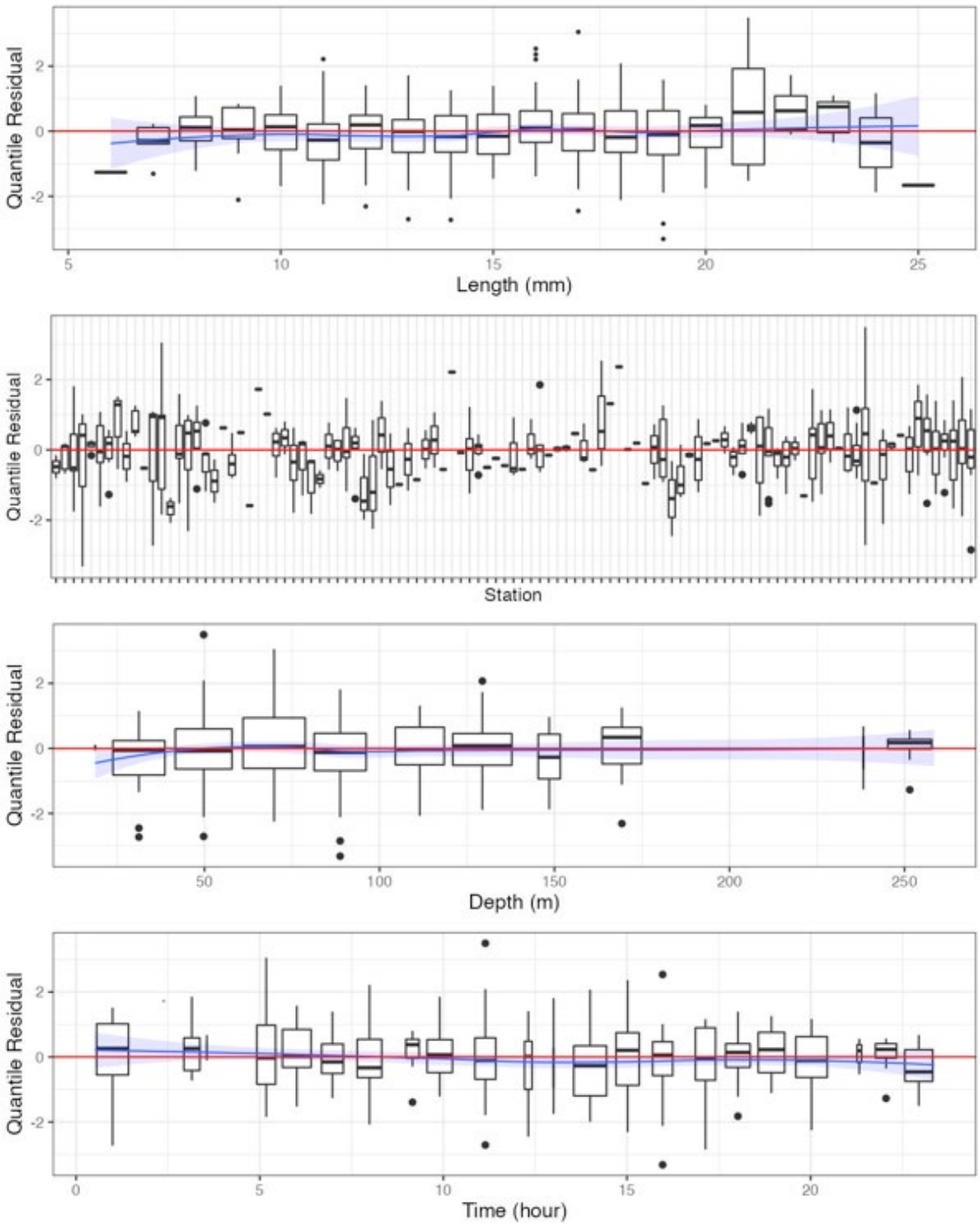

Figure 45c. Randomized and normalized quantile residuals for the selected model for Illex illecebrosus (4511).

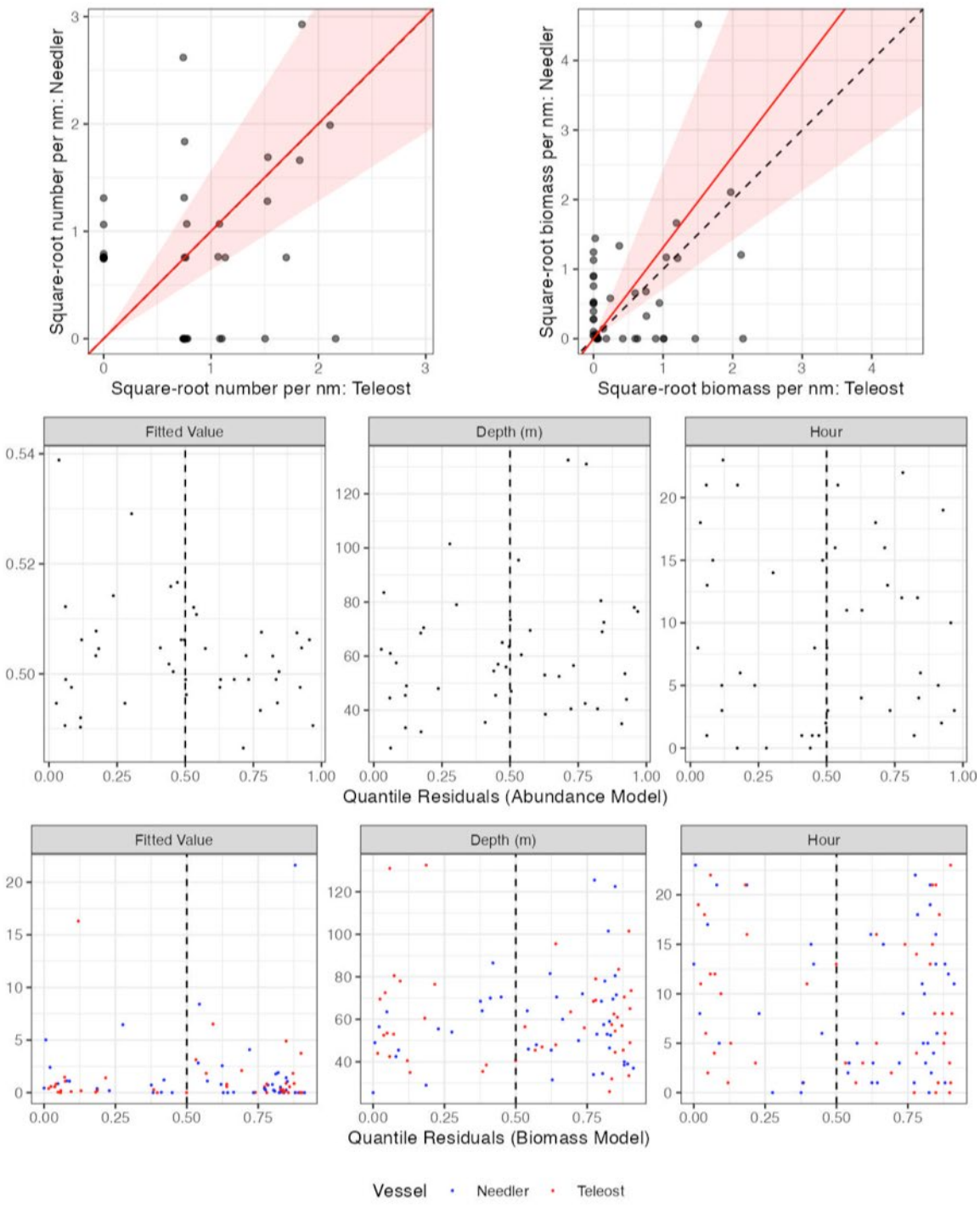

Figure 46. Visualisation of comparative fishing data, size-aggregated model predictions and residual diagnostics plots for Anarhichas lupus (50).

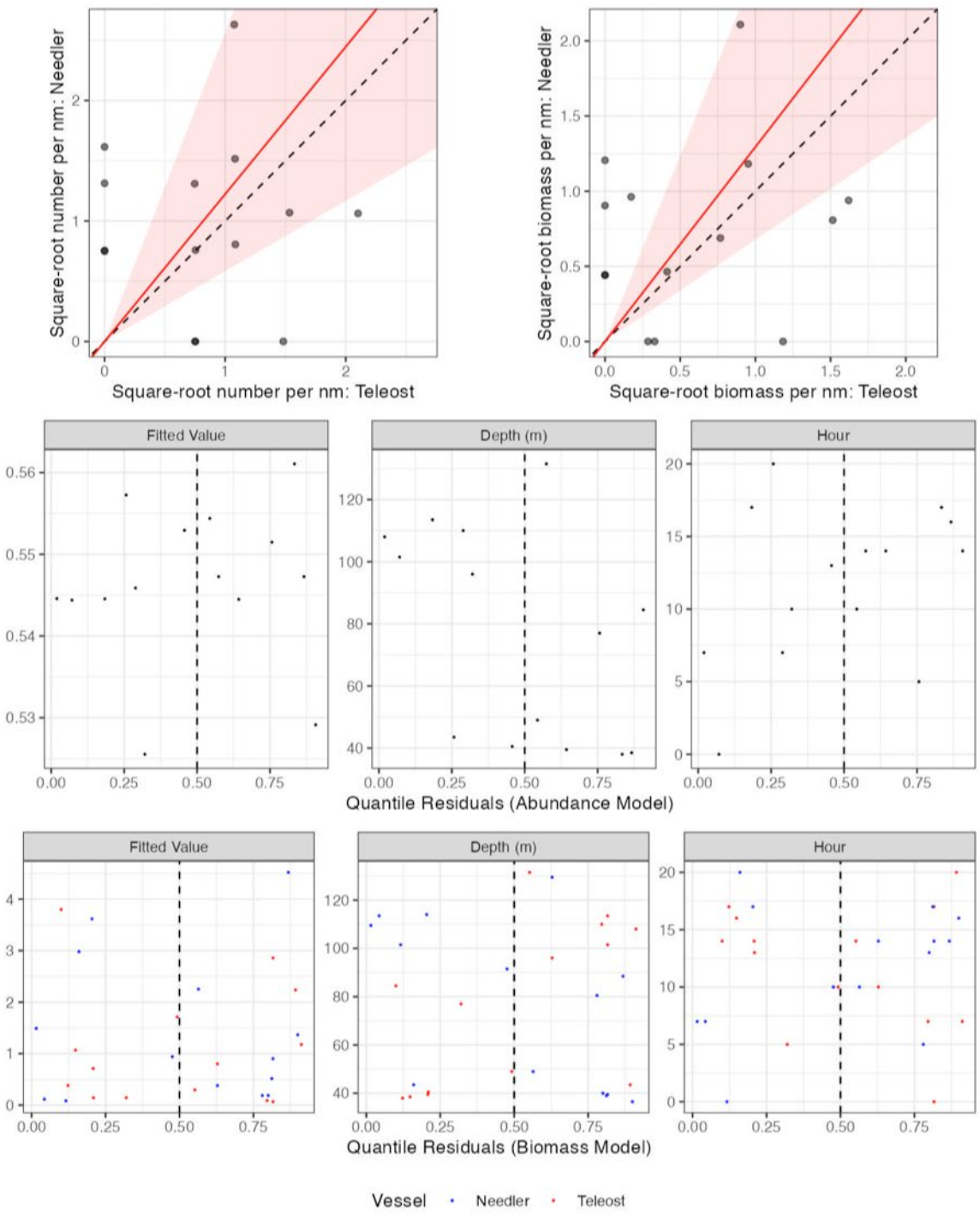

Figure 47. Visualisation of comparative fishing data, size-aggregated model predictions and residual diagnostics plots for Alosa sapidissima (61).

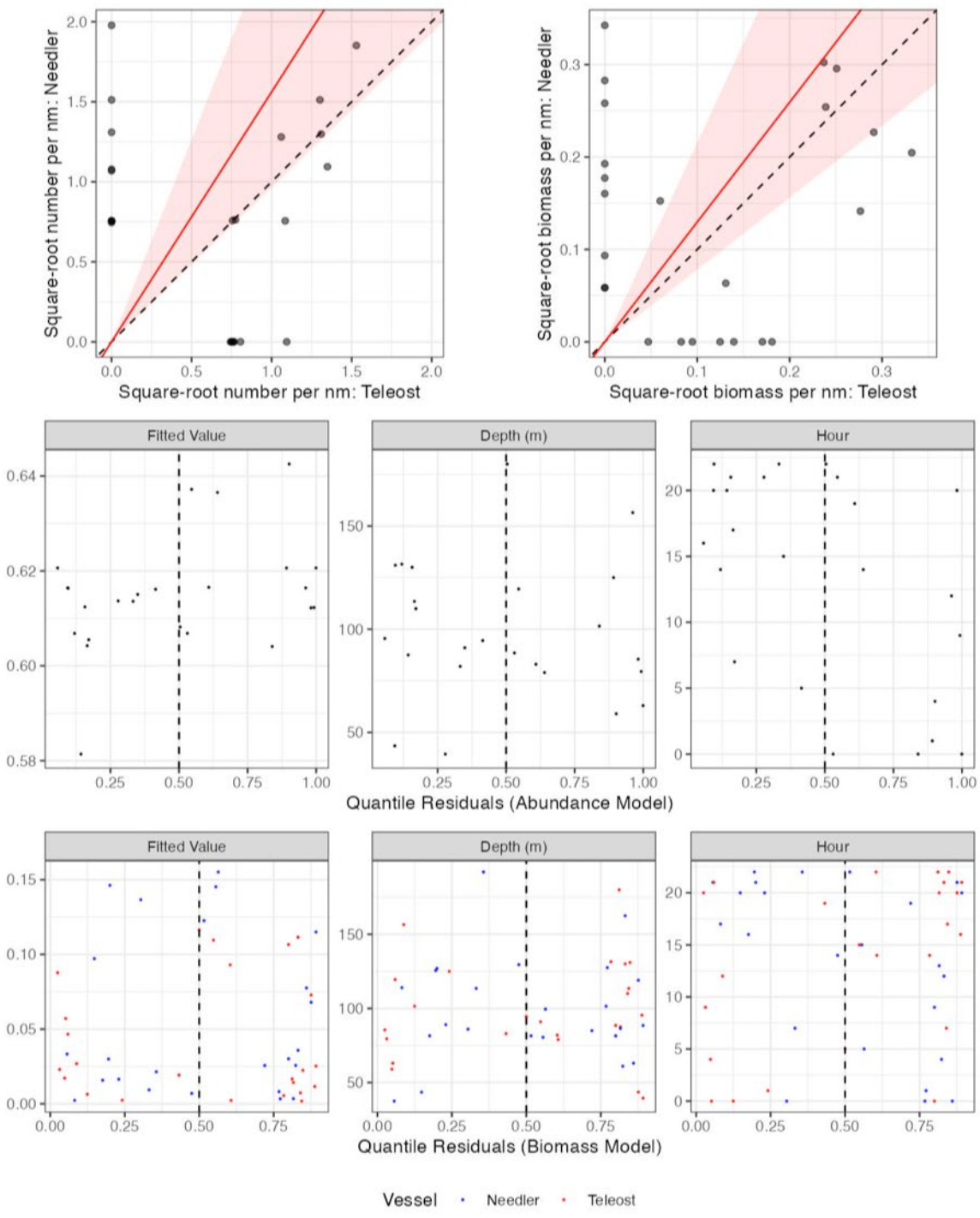

Figure 48. Visualisation of comparative fishing data, size-aggregated model predictions and residual diagnostics plots for Enchelyopus cimbrius (114).

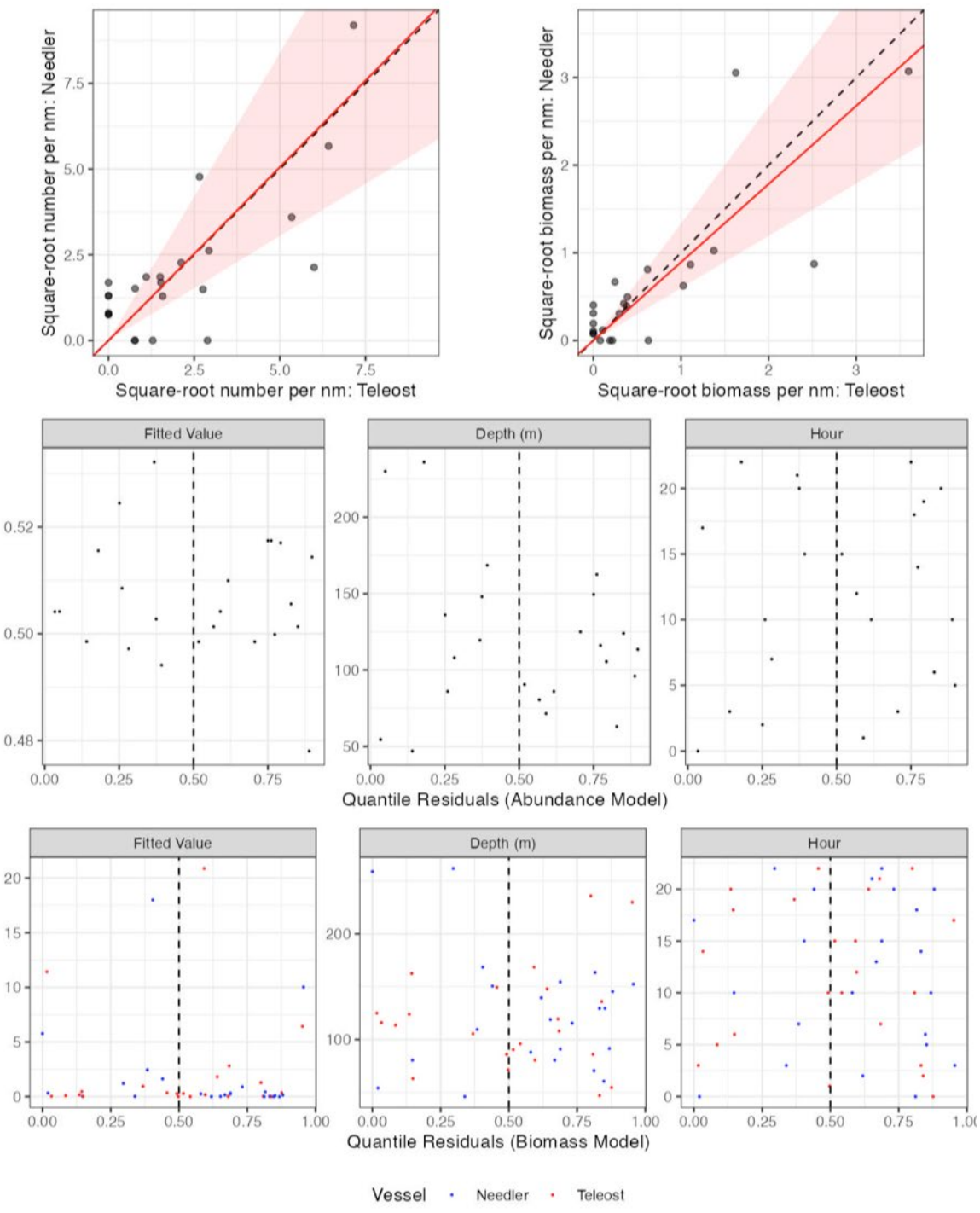

Figure 49. Visualisation of comparative fishing data, size-aggregated model predictions and residual diagnostics plots for Helicolenus dactylopterus (123).

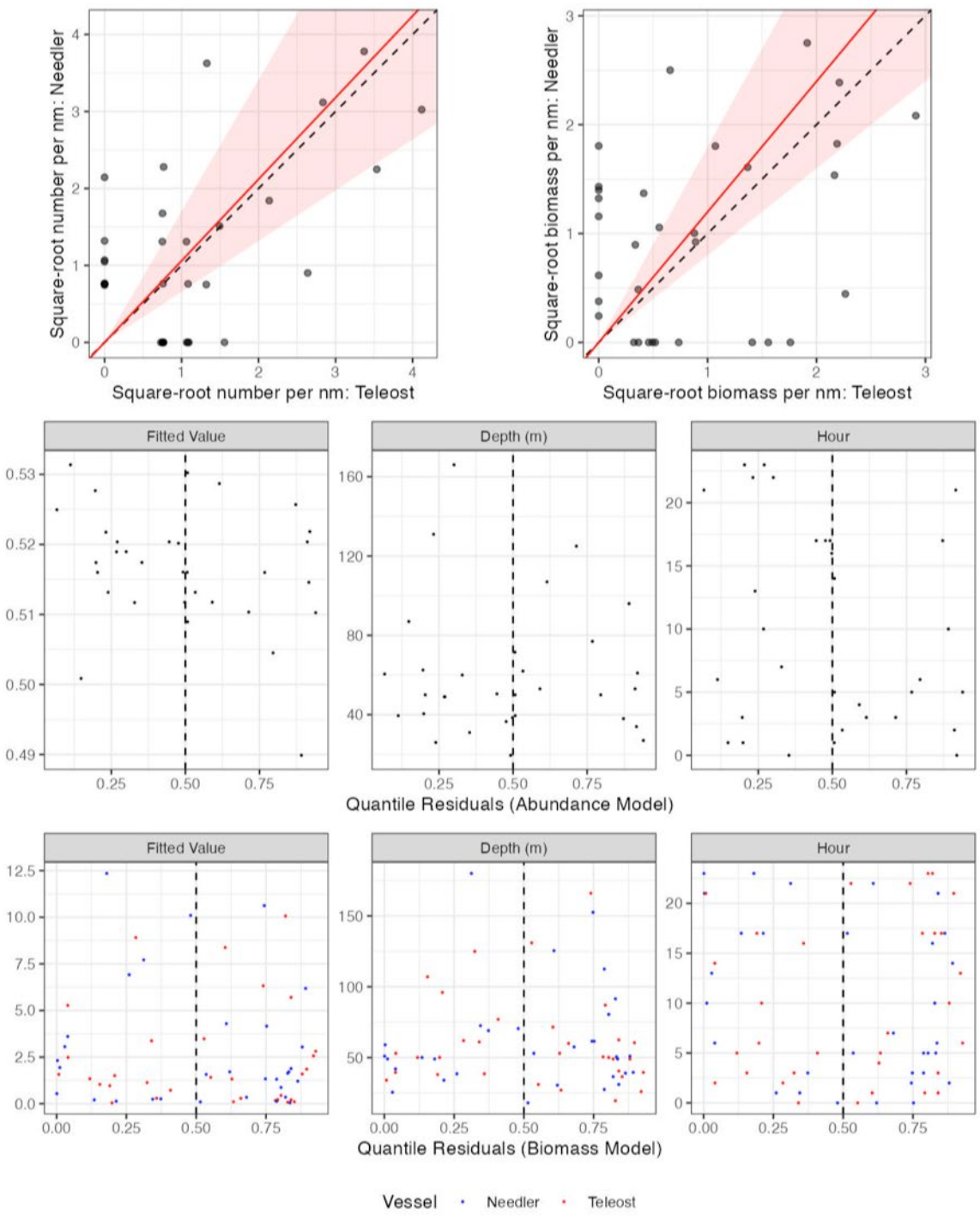

Figure 50. Visualisation of comparative fishing data, size-aggregated model predictions and residual diagnostics plots for Leucoraja erinacea (203).

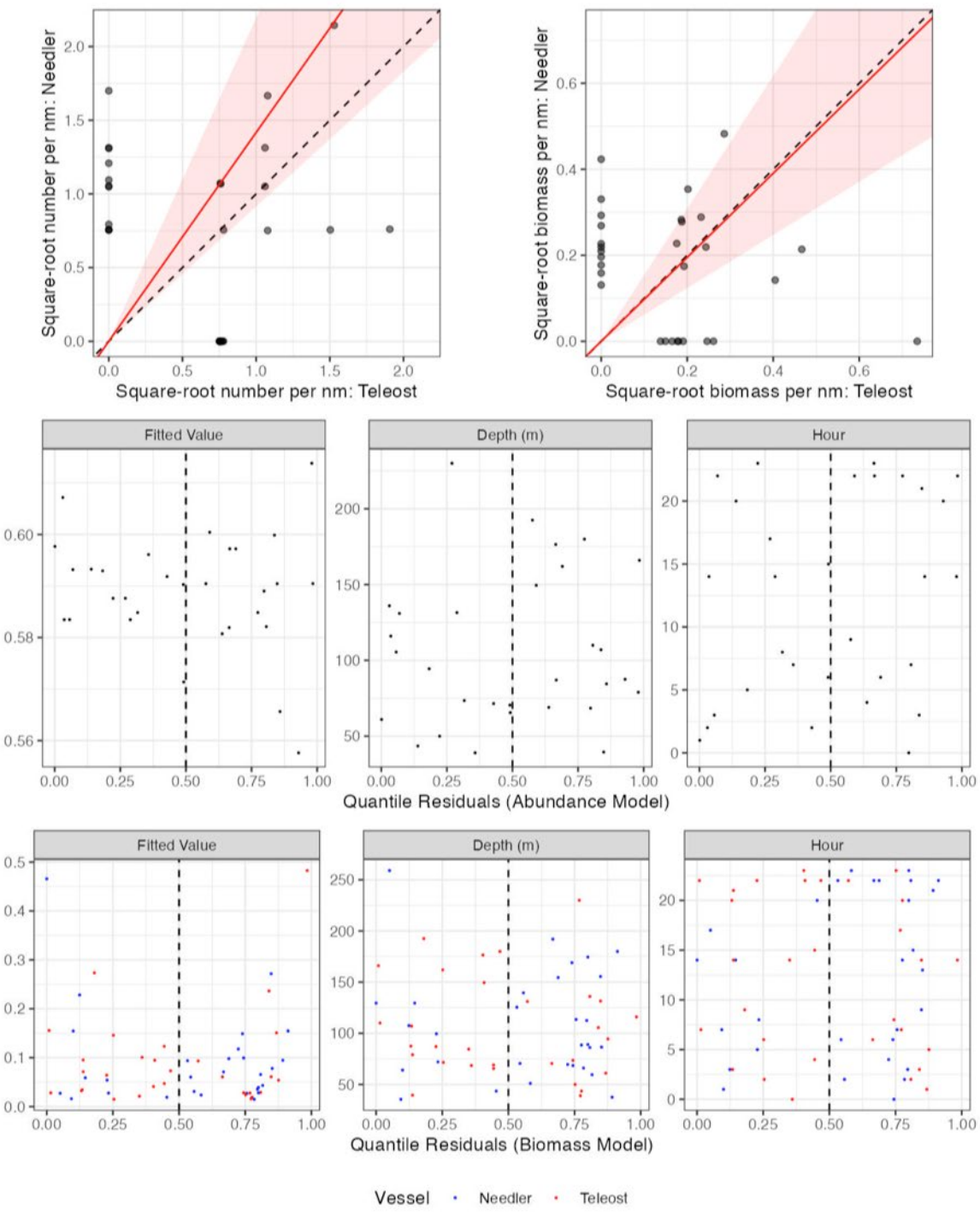

Figure 51. Visualisation of comparative fishing data, size-aggregated model predictions and residual diagnostics plots for Myxine glutinosa (241).

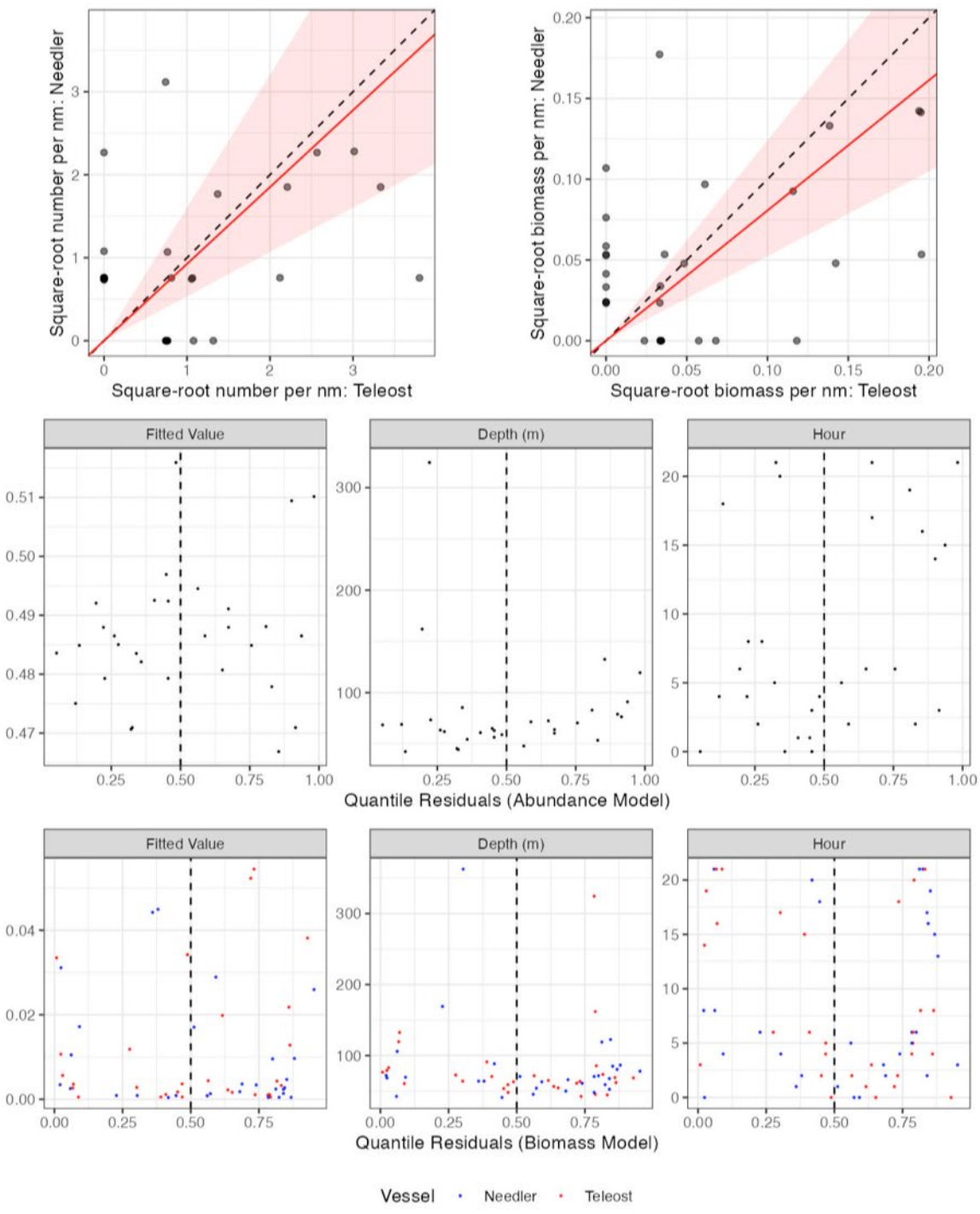

Figure 52. Visualisation of comparative fishing data, size-aggregated model predictions and residual diagnostics plots for Artediellus sp. (323).

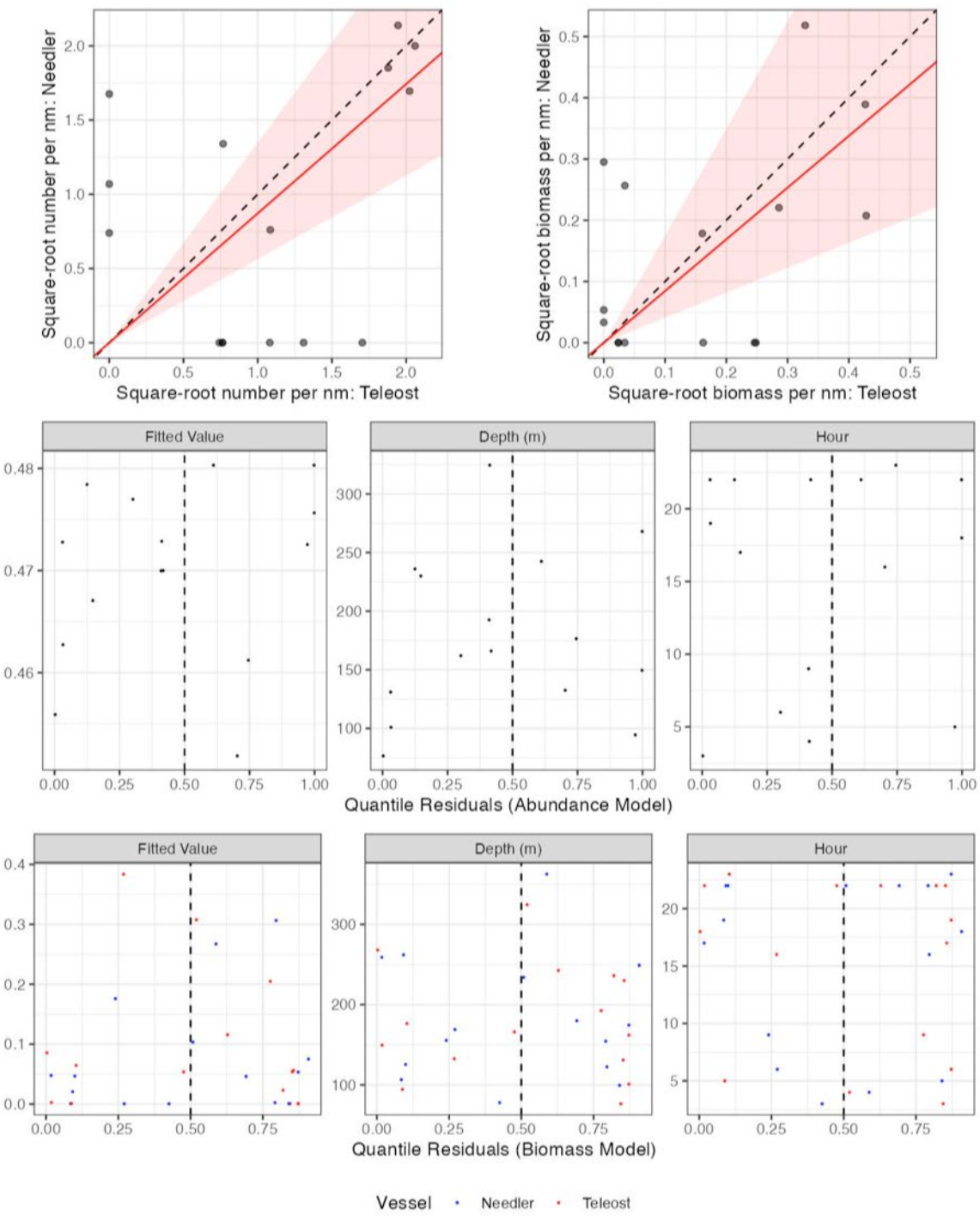

Figure 53. Visualisation of comparative fishing data, size-aggregated model predictions and residual diagnostics plots for Nezumia bairdii (410).

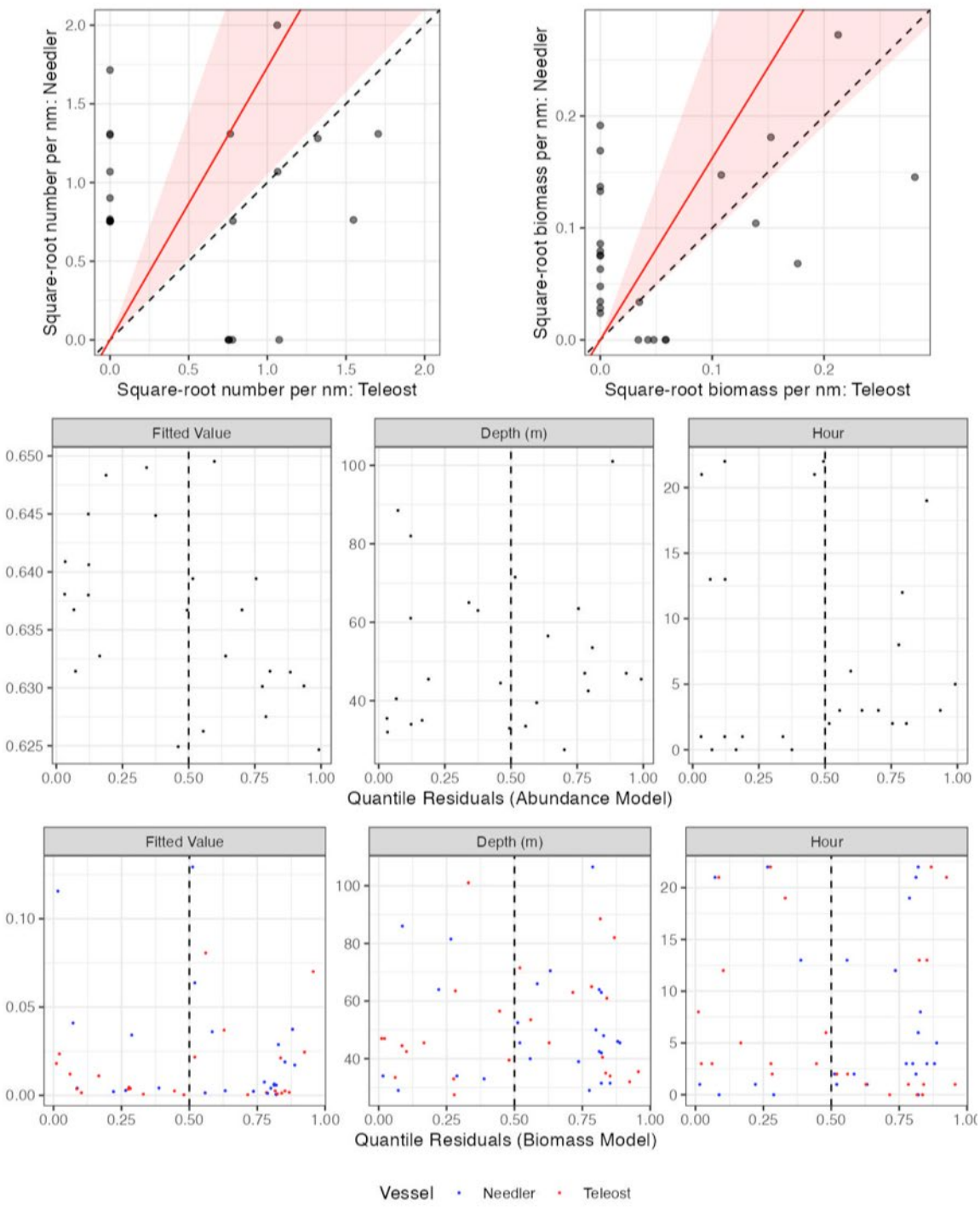

Figure 54. Visualisation of comparative fishing data, size-aggregated model predictions and residual diagnostics plots for Eumicrotremus spinosus (502).

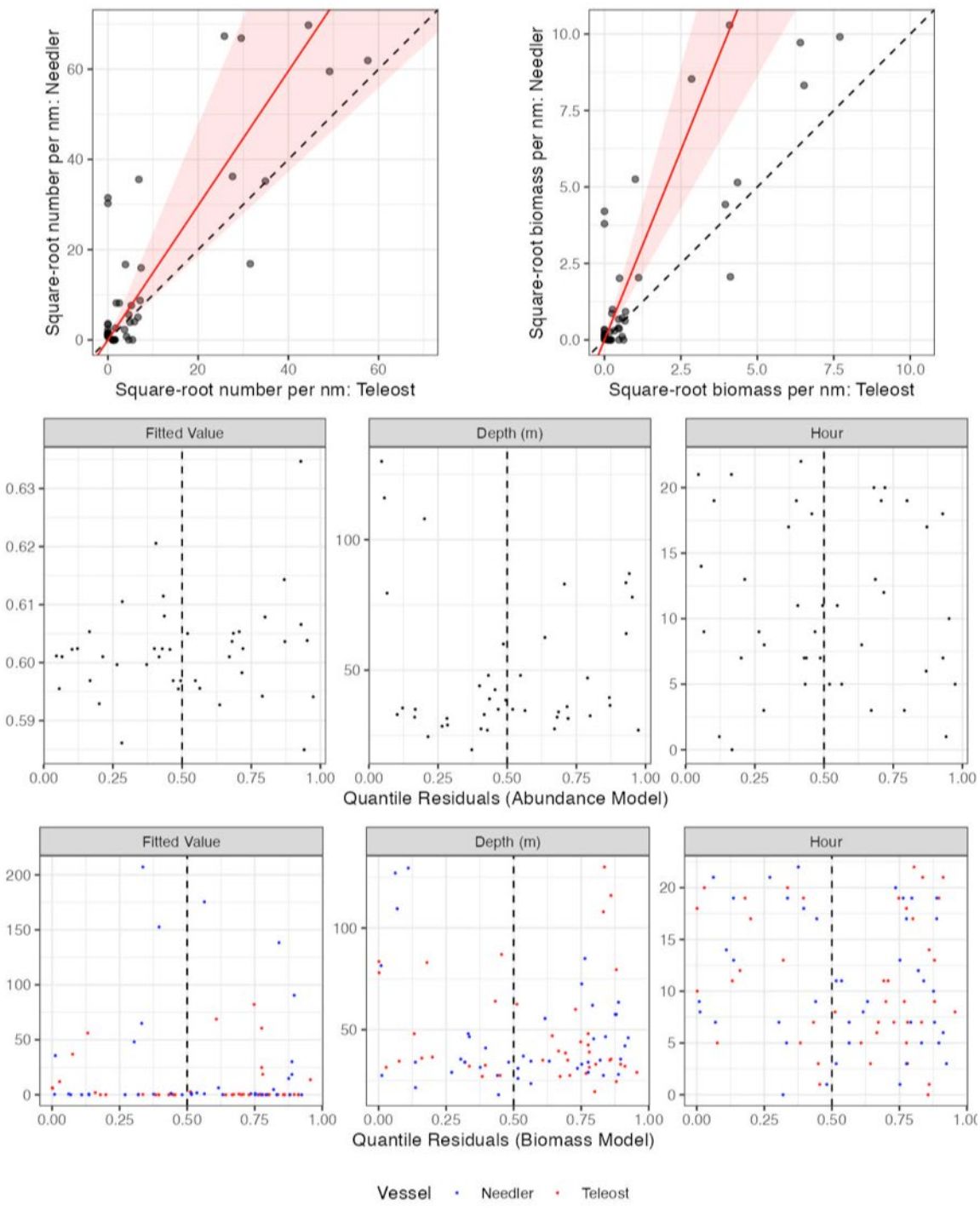

Figure 55. Visualisation of comparative fishing data, size-aggregated model predictions and residual diagnostics plots for Ammodytes dubius (610).

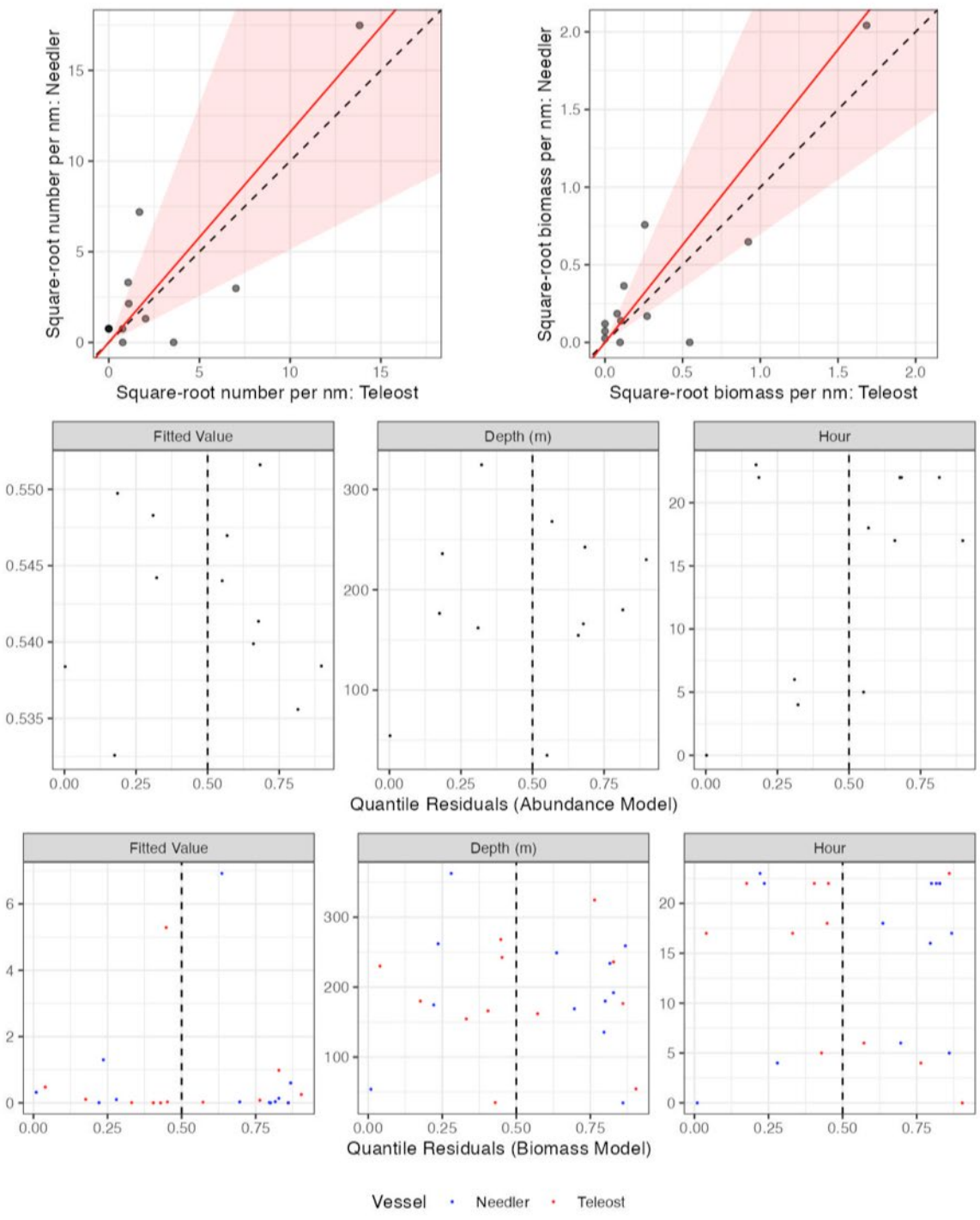

Figure 56. Visualisation of comparative fishing data, size-aggregated model predictions and residual diagnostics plots for Notolepis rissoi (712).

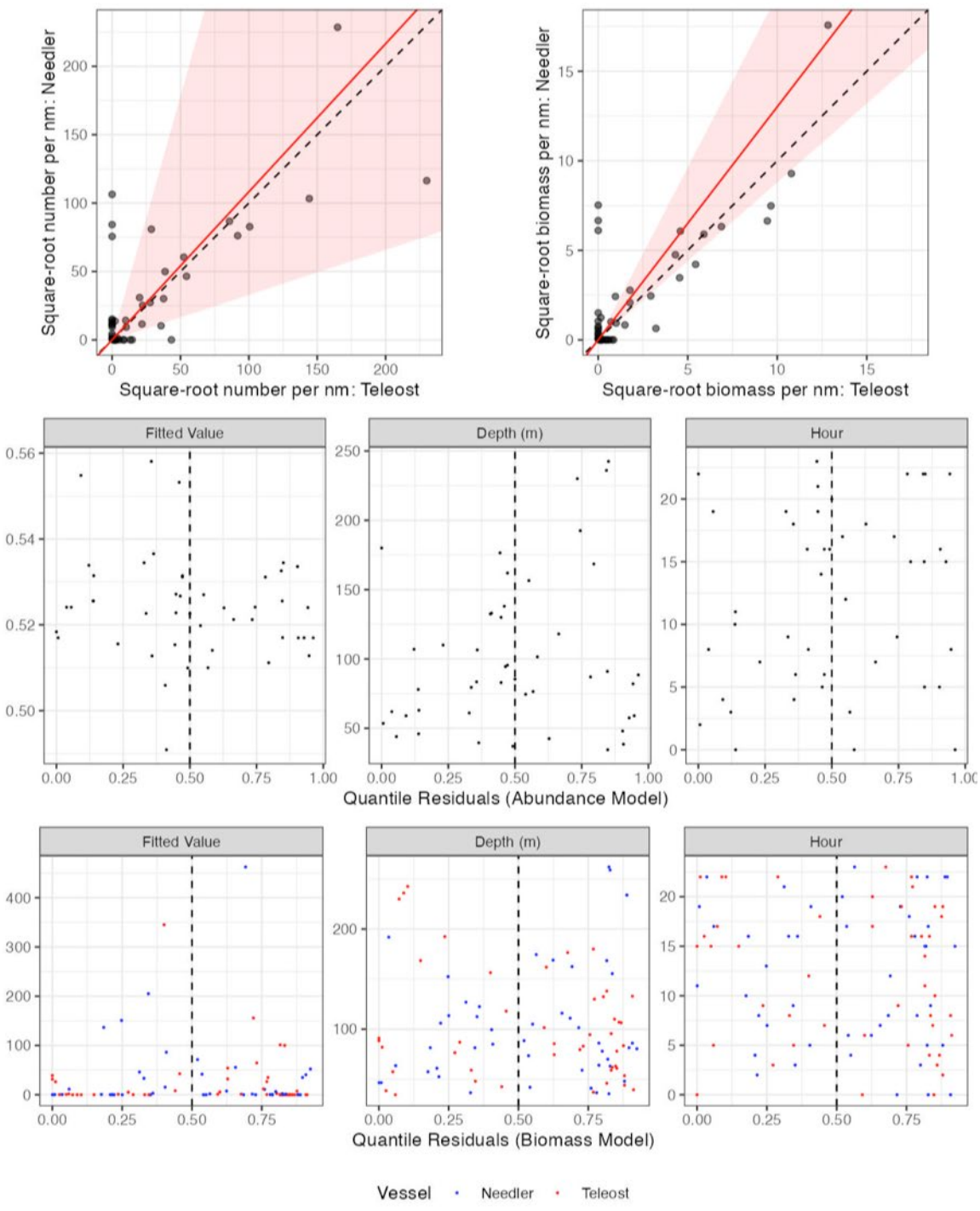

Figure 57. Visualisation of comparative fishing data, size-aggregated model predictions and residual diagnostics plots for Pandalus borealis (2211).

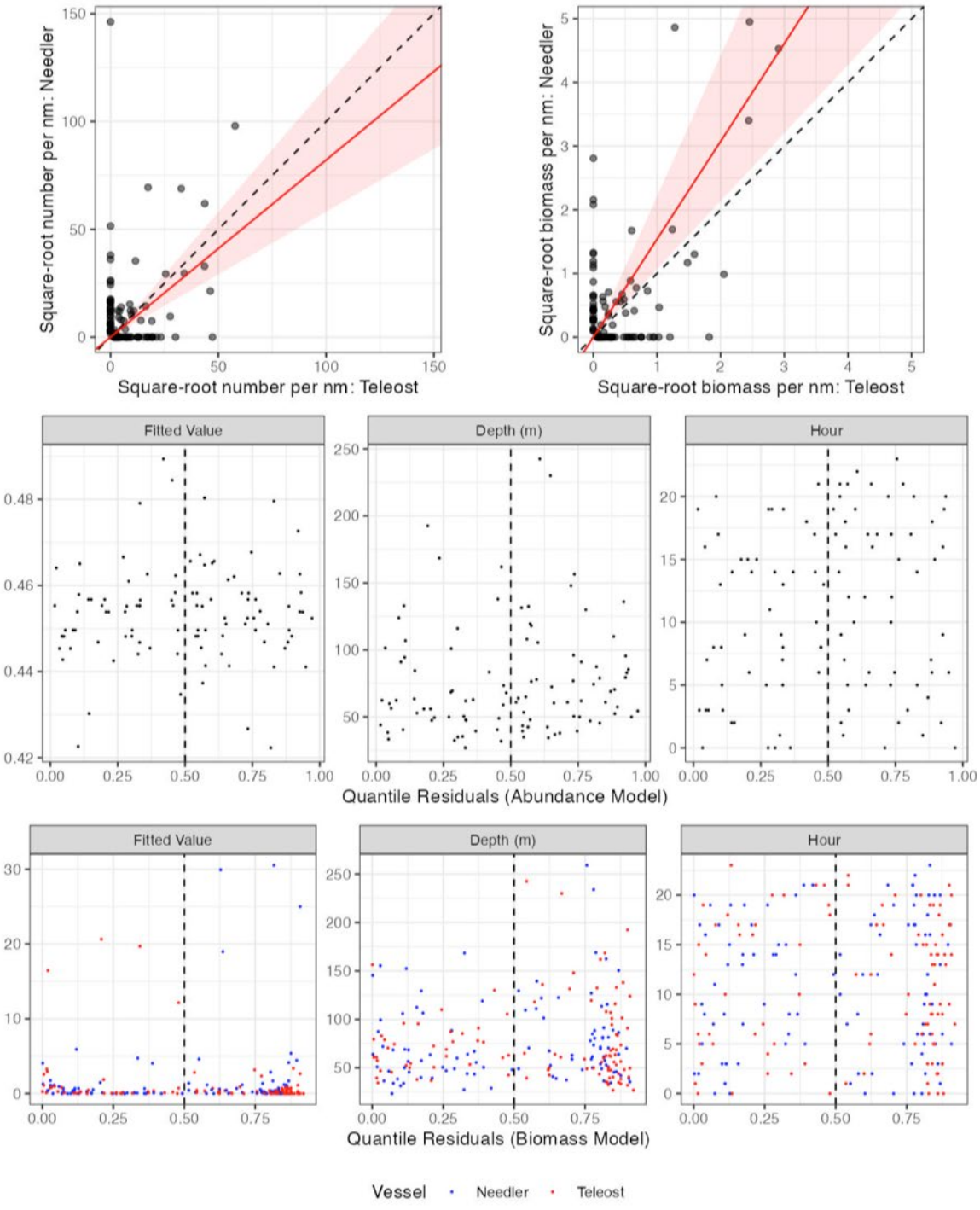

Figure 58. Visualisation of comparative fishing data, size-aggregated model predictions and residual diagnostics plots for Pandalus montagui (2212).

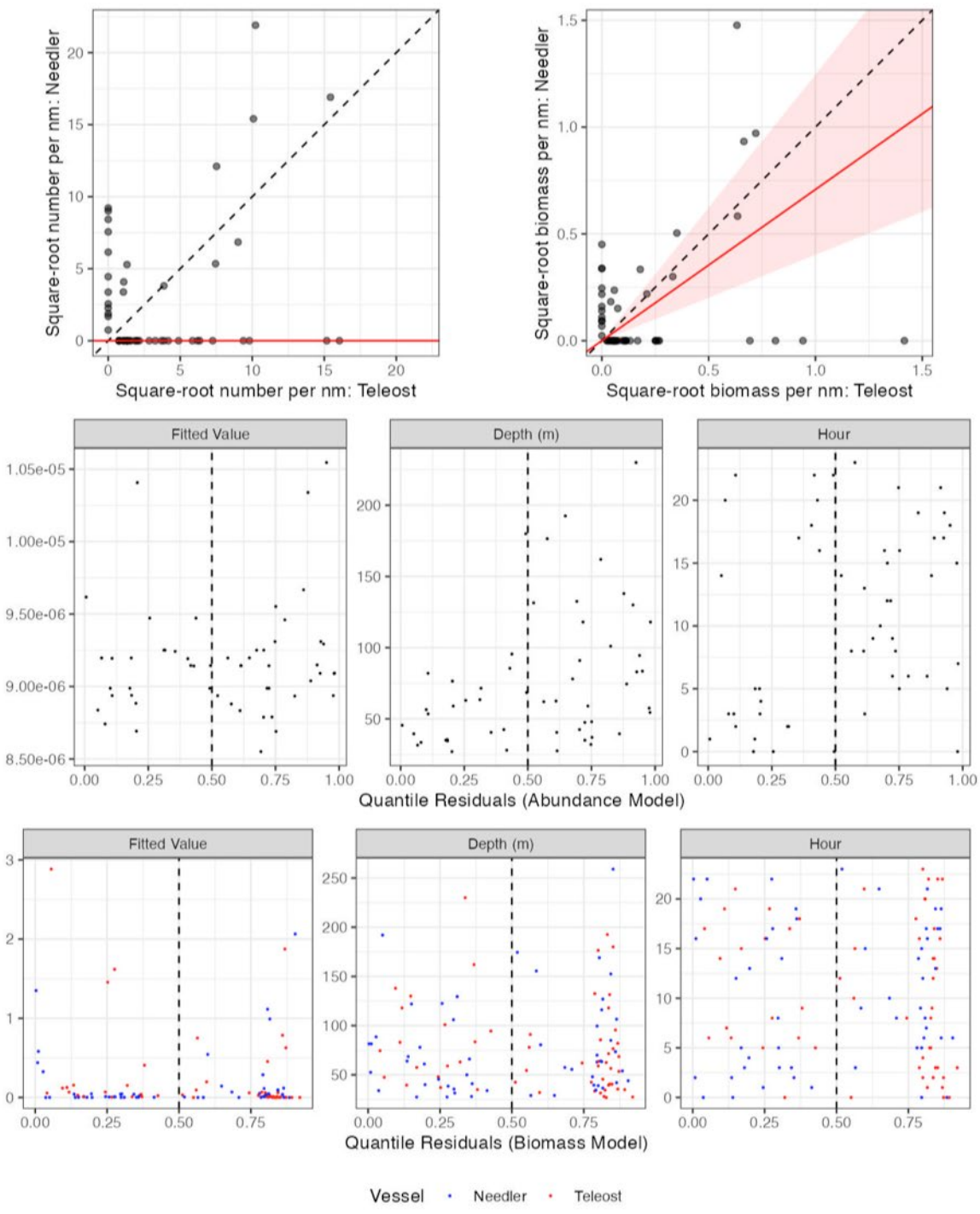

Figure 59. Visualisation of comparative fishing data, size-aggregated model predictions and residual diagnostics plots for Crangon sp. (2416).

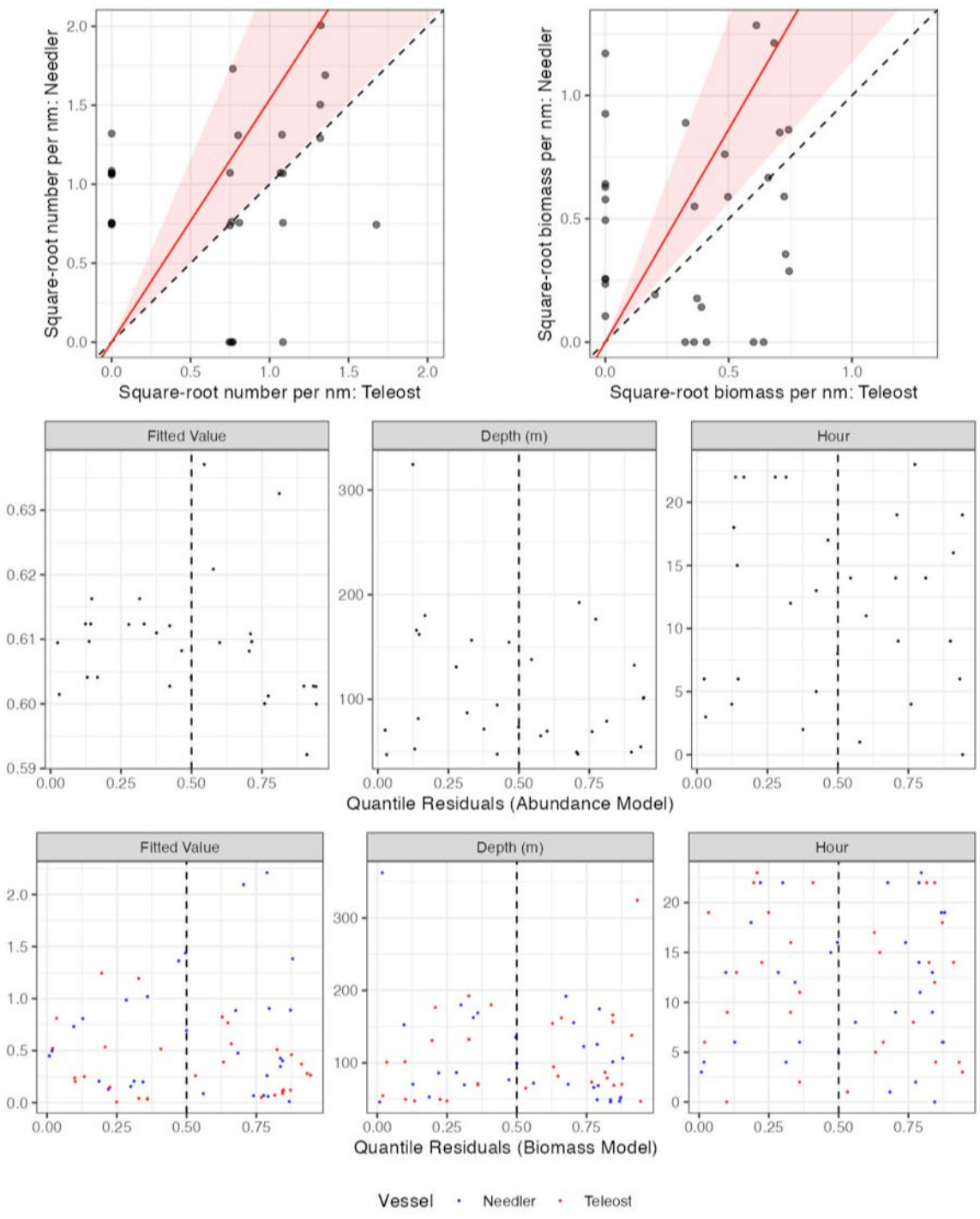

Figure 60. Visualisation of comparative fishing data, size-aggregated model predictions and residual diagnostics plots for Lithodes maja (2523).

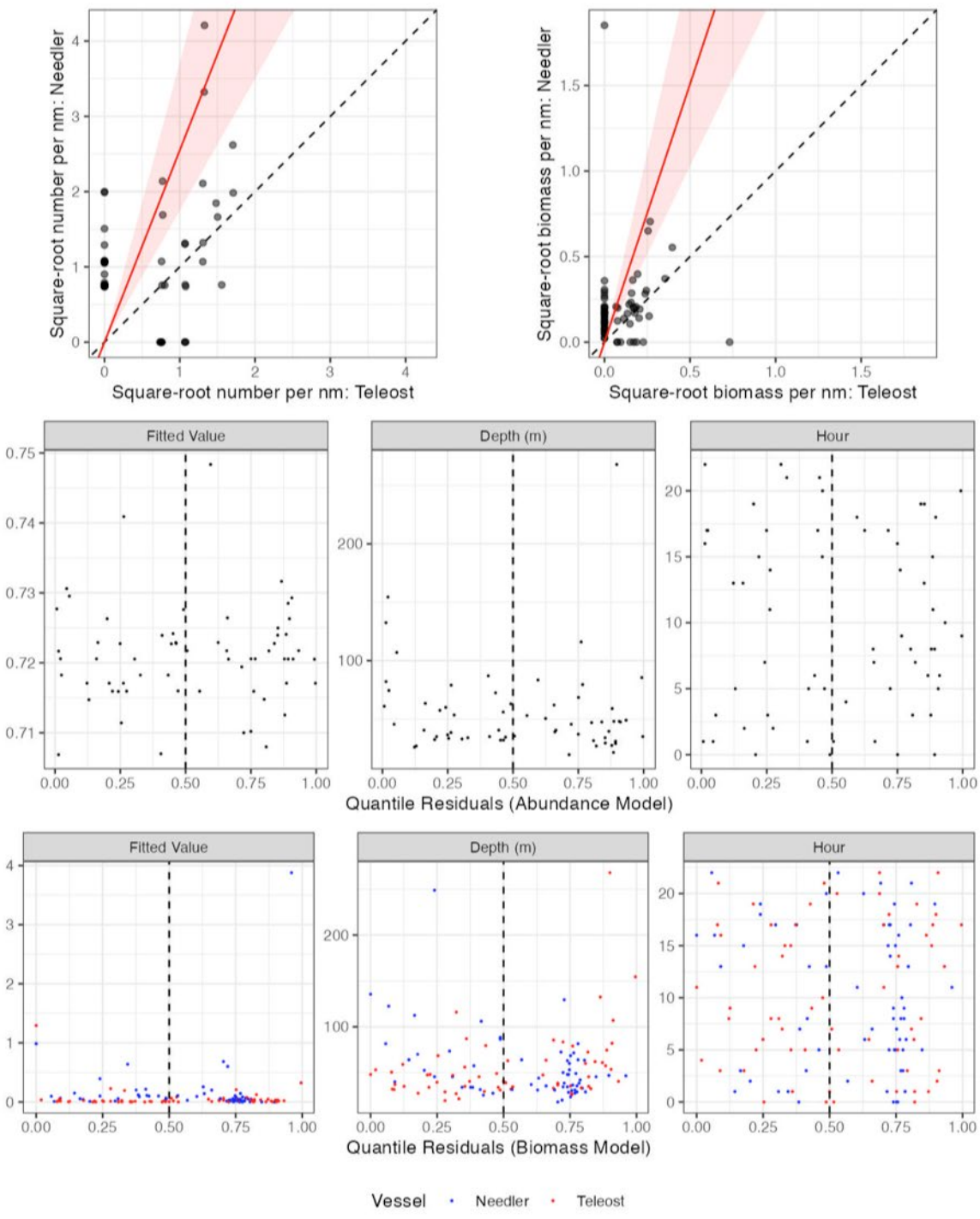

Figure 61. Visualisation of comparative fishing data, size-aggregated model predictions and residual diagnostics plots for Paguridae f. (2559).

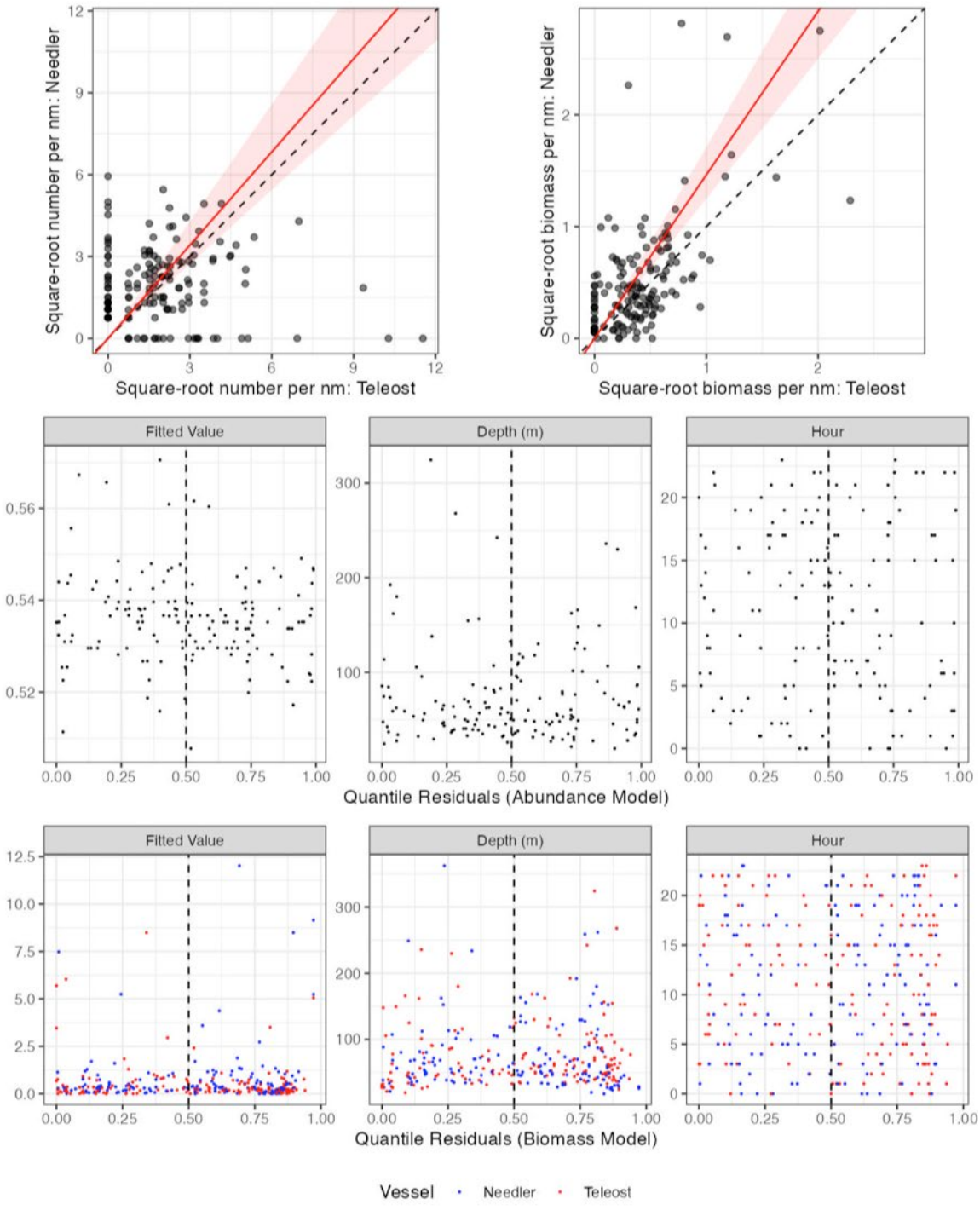

Figure 62. Visualisation of comparative fishing data, size-aggregated model predictions and residual diagnostics plots for Asteroidea s.c. (6100).

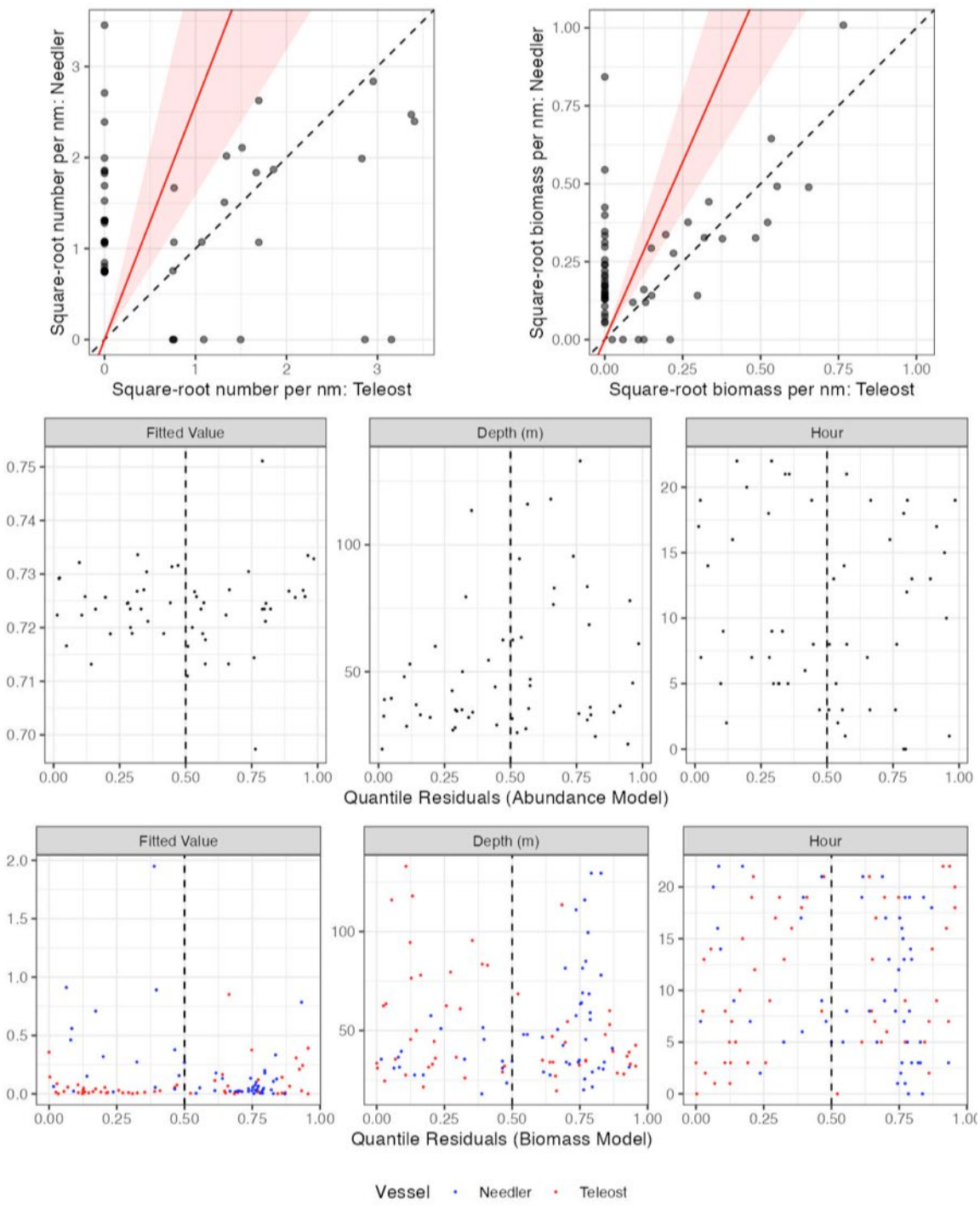

Figure 63. Visualisation of comparative fishing data, size-aggregated model predictions and residual diagnostics plots for Clypeasteroida o. (6500).

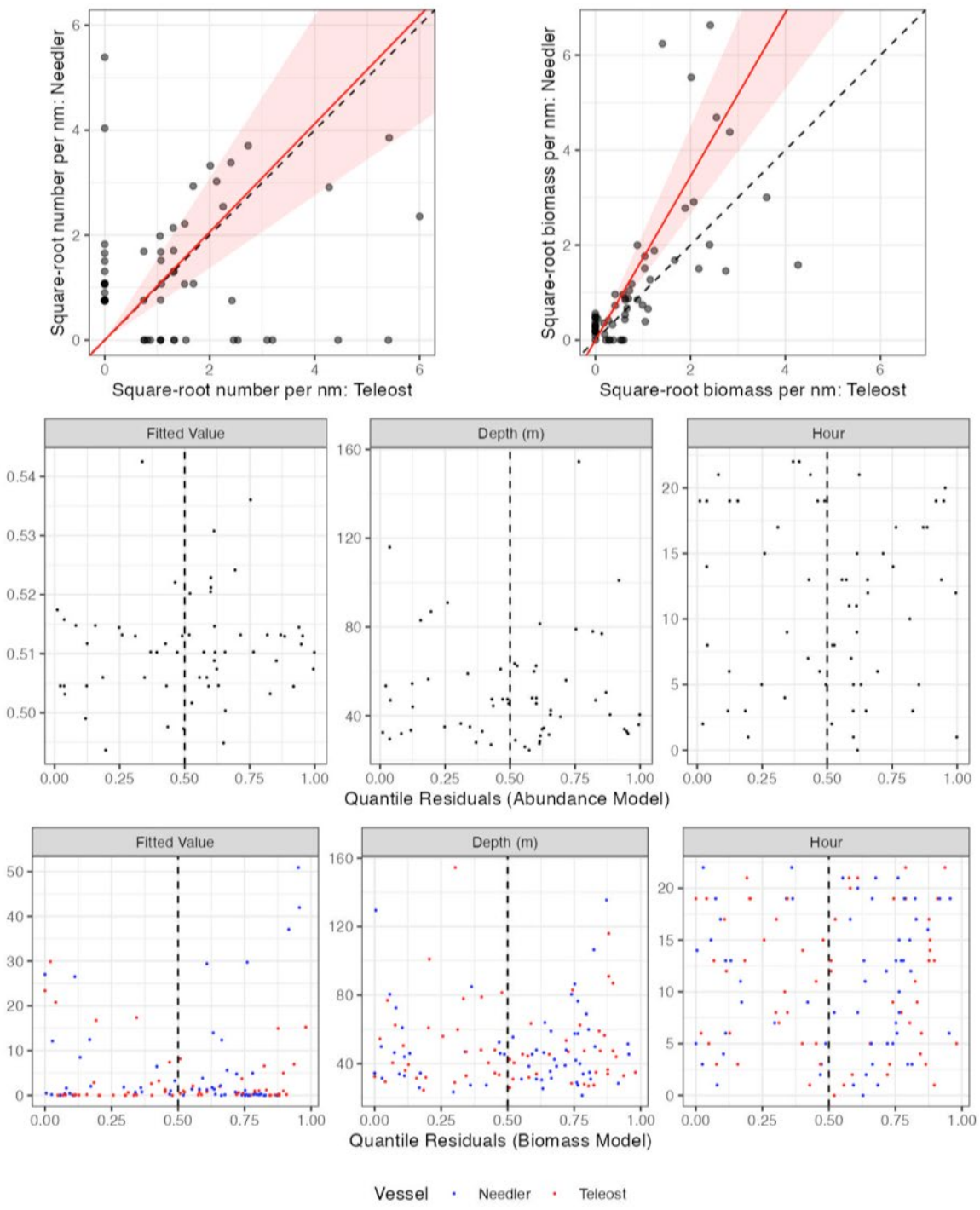

Figure 64. Visualisation of comparative fishing data, size-aggregated model predictions and residual diagnostics plots for Holothuroidea c. (6600).